UNIVERSITÀ DI PARMA

UNIVERSITÀ DEGLI STUDI DI PARMA

DOTTORATO DI RICERCA IN
"MEDICINA MOLECOLARE"

CICLO XXXIV

Morphofunctional analysis and identification of novel diagnostic and prognostic biomarkers of acute myocardial infarction and primary myelofibrosis

Coordinatore:
Chiar.mo Prof. Prisco Mirandola

Tutore:
Chiar.mo Prof. Marco Vitale

Dottorando: Giulia Pozzi

Anni Accademici 2018/2019 – 2020/2021

Table of contents

Abstract

During my PhD at the Laboratory of Human Anatomy and Biology applied to the hematopoietic system (SSD: BIO/16), I investigated the role and the diagnostic accuracy of platelet-based biomarkers in acute myocardial infarction, and the biological role and prognostic value of the rs1024611 SNP of *CCL2* and the chemokine system CCL2/CCR2 in primary myelofibrosis.

Acute myocardial infarction (AMI) represents one of the leading causes of morbidity and mortality worldwide. The main AMI clinical manifestation is chest pain, but often this symptom can be associated to different underlying pathological conditions other than AMI and only the 15% of chest pain patients generally receive a final diagnosis of AMI. Therefore, a timely diagnosis in chest pain patients, as well as a prompt and accurate risk stratification in patients with coronary disorders, represent an urgent and relevant clinical priority in both emergency and outpatient setting. Currently, the differential diagnosis of AMI is mainly based on a composite evaluation of patient medical history, physical examination, ECG, and biomarkers of myocardium necrosis. However, these biomarkers are detectable only after the acute event and are affected by several clinical factors.

Here, I propose two different approaches, both based on platelets, to investigate the diagnostic performance of pre-existing biomarkers in blood circulation before the acute events or in the "peri-infarctual" period. Platelets are anucleate cells that play a key role in the initiation of atherosclerosis as well as in the final step of thrombus formation, considered the main biological processes underlying AMI. PKCε is a serine/threonine kinase exclusively expressed in platelets of AMI patients, in occurrence of the acute event.

Here, I demonstrate that the evaluation of PKCε-expressing platelets by flow cytometry could be used in combination with the well established hs-cardiac troponin (cTn) to the diagnosis of AMI in patients with chest pain.

Moreover, I evaluated platelet gene expression profile by microarray assay to identify a platelet gene signature specific for AMI. Indeed, platelets have a unique mRNA signature, mainly derived from their hematopoietic precursors. Therefore, gene expression profiling at the time of an AMI provides information concerning the platelet gene expression preceding the coronary event. Platelet transcriptome analysis using microarray identified five differentially expressed genes (DEGs) including *FKBP5, S100P, SAMSN1, CLEC4E* and *S100A12*. The logistic regression model based on these five DEGs show a very good diagnostic performance in discriminating ST-segment elevation myocardial infarction (STEMI) patients from both sCAD (patients with stable coronary artery disease) and healthy subjects, configuring the combination of these five DEGS as a promising biomarker for the diagnosis of STEMI.

During my PhD, I also studied the functional role of the rs1024611 polymorphism of *CCL2* and the chemokine system CCL2/CCR2 in primary myelofibrosis. Primary myelofibrosis (PMF) is the most aggressive myeloproliferative neoplasm (MPN), representing the paradigm of onco-inflammation. Indeed, chronic inflammation, fuelled by neoplastic clone, contributes to several changes at both local (bone marrow fibrosis) and systemic levels (constitutional symptoms, pro-thrombotic state, second cancers). Inflammation in turn supports the expansion and evolution of the neoplastic clone, in a self-perpetuating vicious cycle.

Cytokines are key mediators of this detrimental crosstalk between the neoplastic clone (primarily the megakaryocytic clone) and the bone marrow microenvironment. Among various cytokines, CCL2 is one of the most potent immune-modulatory and pro-fibrotic cytokines known to be elevated in PMF. CCL2 exerts its biological effects by preferentially binding to its receptor CCR2 and activating a downstream signaling which includes G-proteins, MAPK/ERK, PI3K/Akt and JAK/STAT pathways. *CCL2* gene is highly polymorphic and SNPs in the regulatory regions of *CCL2* account for the great inter-individual variability in CCL2 expression levels.

Here, I demonstrate that male subjects homozygous (G/G) for the rs1024611 SNP of *CCL2* have an increased risk of developing PMF and that, among patients with PMF, the G/G genotype is an independent prognostic factor for reduced overall survival. Concerning the functional role the SNP and the CCL2/CCR2 axis in PMF, I demonstrate that i) homozygous PMF patients are the highest CCL2 producers as compared to the other genotypes; ii) hemotopoietic progenitors ($CD34^+$ cells) of PMF patients are a selective target of CCL2, since they uniquely express CCR2 (CCL2 receptor); iii) CCR2 expression correlates with bone marrow fibrosis in PMF, iv) the CCL2/CCR2 chemokine system boosts pro-survival signals via Akt phosphorylation; v) ruxolitinib effectively turns-off CCL2/CCR2 axis in PMF cells. Finally, the peculiar expression of CCR2 in $CD34^+$ cells of PMF represents a promising diagnostic biomarker to discriminate patients with trueET and prePMF, as well as between prePMF and overtPMF.

All the data reported in this thesis have been published on peer reviewed international scientific journals.

Part I

Novel diagnostic biomarkers of AMI

Introduction

1. Acute myocardial infarction and chest pain

Acute myocardial infarction (AMI) is one of the major causes of death and disability worldwide and, given its unpredictability, it represents a leading health problem in the world. Approximately 550,000 first episodes and 200,000 recurrent episodes of AMI occur per year in the USA (Mozaffarian et al., 2016). In European countries, the incidence rate of AMI ranges from 43 to 144 per 100 000 per year (Widimsky et al., 2010).

AMI is defined as an event of myocardial necrosis caused by an unstable ischemic syndrome (Thygensen et al., 2012). Myocardial necrosis results from acute obstruction of a coronary artery which induces a sudden and prolonged ischaemia. The initiating mechanism for AMI is the rupture or erosion of a vulnerable atherosclerotic coronary plaque, that leads to the exposure of highly thrombogenic core and matrix materials to circulating blood (see the dedicated chapter) (Libby et al., 2013). Several factors are involved in the formation of thrombus that could be totally or partially occluding but could also occur in the presence of collateral circulation, resulting in different type of acute coronary syndrome (ACS). AMI with ST-segment elevation (STEMI) is the most severe form of AMI and it is generally due to a totally occluding thombus (Anderson and Morrow, 2017).

The prolonged ischemia, induced by thrombus, causes dysfunction and subsequent necrosis of the myocardial tissue, which loses its contractile properties.

Morphological alterations of myocardial tissue have been identified by histological postmortem evaluation of infarted heart and are listed in the table below (Table 1).

Myocardial histologic parameters (HE staining)	Earliest manifestation	Full development	Decrease/disappearance
Streched/wavy fibres	1–2 h		
Coagulative necrosis: 'hypereosinophilia'	1–3 h	1–3 days; hyper-eosinophilia and loss of striations	> 3 days: disintegration
Interstitial oedema	4–12 h		
Coagulative necrosis: 'nuclear changes'	12–24 (pyknosis, karyorrhexis)	1–3 days (loss of nuclei)	Depends on size of infarction
PMN infiltration	12–24 h	1–3 days	5–7 days
PMN karyorrhexis	1.5–2 days	3–5 days	
Macrophages and lymphocytes	3–5 days	5–10 days (including 'siderophages')	10 days to 2 months
Vessel/endothelial sprouts*	5–10 days	10 days–4 weeks	4 weeks: disappearance of capillaries; some large dilated vessels persist
Fibroblast and young collagen*	5–10 days	2–4 weeks	After 4 weeks; depends on size of infarction;
Dense fibrosis	4 weeks	2–3 months	No

*Some authors summarize the vascular and early fibrotic changes as 'granulation tissue', which is maximal at 2–3 weeks

Table 1. Histological features of AMI. (Michaud et al., 2020).

The morphological features in AMI vary with time after the onset of the acute event (Figure 1). After few minutes from ischemia, cardiomyocyte coagulative necrosis starts and results into

mitochondrial swelling and sarcolemmal disruptions, denaturation of structural proteins and loss of contractile properties. Within the first 1–2h from the onset of ischemia, “wavy myocardial fibers” (Figure 1, panel A) can be oserved especially when associated with focal oedema (Figure 1, panels B, C) (Eichbaum, 1975; Jennings et al., 1975; Reimer and Jennings, 1979).

This peculiar alteration is probably induced by the increased hydrostatic pressure of interstitial oedema, which deforms and stretches the surrounding fibers, and by the stretching of dead non-contractile myocytes induced by adjacent functional myocardium during the cardiac cycle (Fishbein et al.,1978). Contraction band necrosis (CBN) of myocytes consists of thick eosinophilic bands in the cytoplasm of cardiomyocytes due to clustering of hypercontracted contractile proteins.
After 12 hours, coagulative necrosis evolves with loss of the nuclei (days 1–3), infiltration of neutrophils at borders and further at the central core of AMI (early days 1–3) (Figure 1, panel D), myocyte fragmentation (days 3–7) and early phagocytosis at the border of the infarcted area (days 3–7). The formation of granulation tissue at the margins occurs after 2 weeks, and it is associated with the presence of newly formed microvessels and persistent inflammatory cell infiltrate, including lymphocytes and macrophages (Figure 1, panels E, F). During the late fibrotic stage, the granulation tissue is gradually replaced by dense collagen and hypocellular and acontractile scar takes about 1-2 months to completely form (Figure 1, panels G, H) (Michaud et al., 2020).

AMI symptoms are highly variable and can be confused with other less severe pathological conditions. Patients with AMI may present with typical ischemic-type chest pain or with dyspnea, nausea, weakness, or a combination of these symptoms. Chest pain (CP) is one of the most common complaints for which patients seek medical evaluation at the hospital's emergency department (ED) and only the 10-15% of them receive a final diagnosis of AMI.
Chest pain accounts for about the 10% of the whole non- injury-related ED admittance, yearly (Mockel et al., 2013). The incidence of the admittance ED for chest pain ranges 8–19 per 1000 person-years (Goodacre et al., 2005; Ekelund et al., 2012) and it is higher in urban than in rural hospitals. The mean age is about 52–61 years, and the 49–57% of patients are men (Mockel et al., 2013).

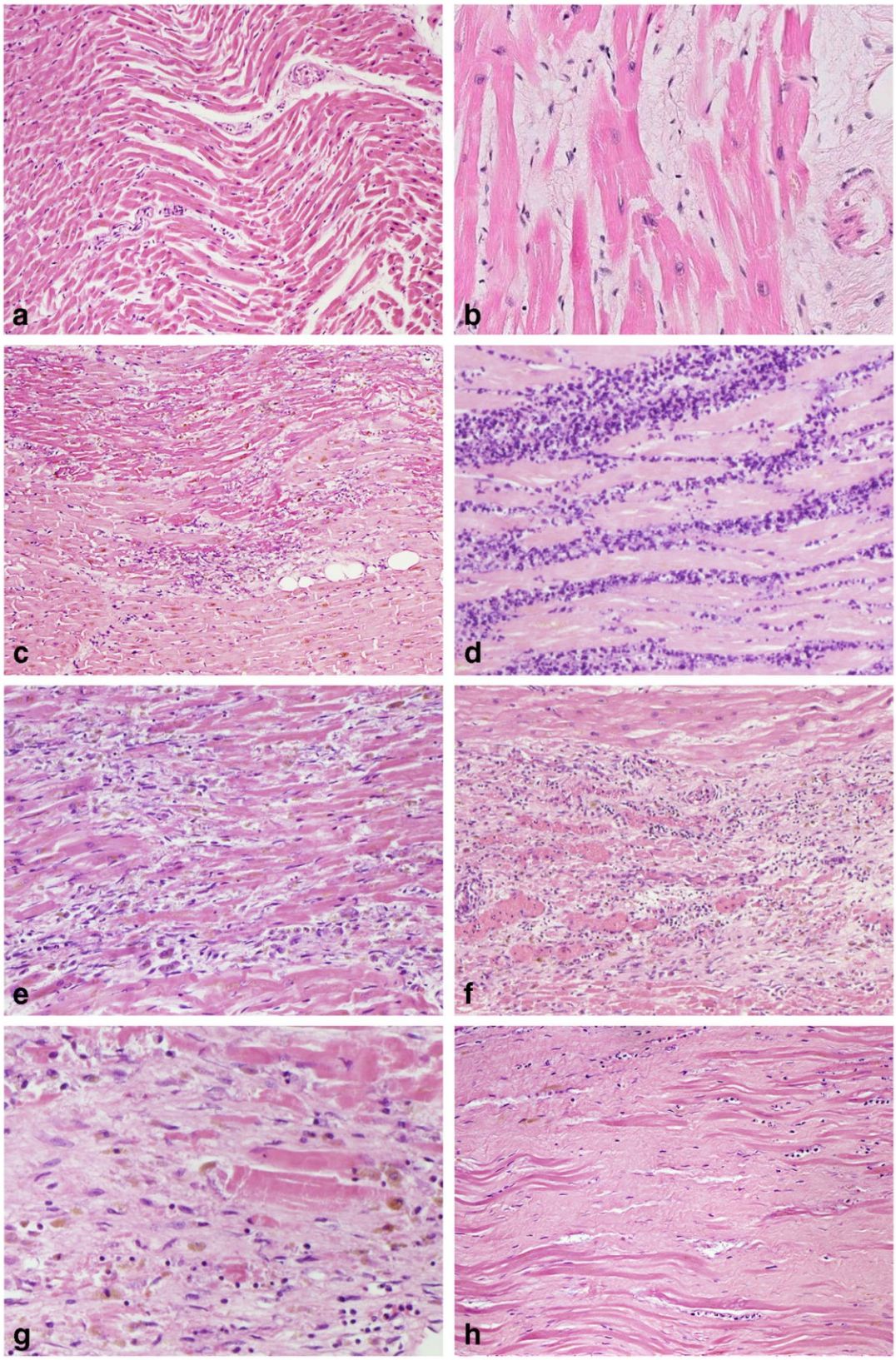

Figure 1. Evolution of the histological featurs of AMI. Representative myocardial sections, stained with haematoxylin and eosin, showing: A) myofiber waviness; B) interstitial oedema; C) hypereosinophilia and coagulative necrosis of cardiomyocytes; D) heavy granulocyte infiltration; E) macrophage and lymphocyte infiltration for the early removal of necrotic debris; F) granulation tissue with formation of microvessels; G) fibroblast proliferation and early collagen deposition; H) dense fibrotic scar replacing myocyte loss. (Michaud et al., 2020).

Acute chest pain is conventionally defined as “the perception of non-traumatic pain or other thoracic discomfort occurring within the preceding 24 hours, localised anteriorly, between the base of the nose and the umbilicus and, posteriorly, between the occiput and the 12th vertebra” (Fallon, 1997; Stepinska et al., 2020). Symptoms could appear in many forms, and it makes the correct diagnosis challenging. Patients with chest pain often describe pressure, tightness, squeezing, heaviness, or burning sensation, or a pain that ranges from a sharp twinge to a dull ache. In some cases, the pain reaches the neck, the jaw, and then spreads to the back or down one or both arms.

Primary cardiovascular	Primary non-cardiovascular
Acute coronary syndromes	Oesophageal spasm, oesophagitis, gastroesophageal reflux (GER)
• ST-segment elevation myocardial infarction (STEMI)	Peptic ulcer disease, cholecystitis, pancreatitis
• Non-ST elevation ACS (NSTE-ACS)	Pneumonia, bronchitis, acute asthma
◦ Non-ST-segment elevation myocardial infarction	Pleuritis, pleural effusion, pneumothorax
◦ Unstable angina	Pulmonary embolism, severe pulmonary hypertension
Acute pericarditis, pericardial effusion	Thoracic trauma
Acute myocarditis	Costochondritis, rib fracture
Severe hypertensive crisis	Cervical/thoracic vertebral or discal damage
Stress cardiomyopathy (Takotsubo syndrome)	Herpes zoster
Tachyarrhytmias	Psychogenic
Hypertrophic cardiomyopathy, aortic stenosis	
Severe acute heart failure	
Acute aortic syndrome (dissection, haematoma)	
Pulmonary embolism, pulmonary infarction	
Cardiac contusion	

Table 2. Causes of chest pain (Gulati et al., 2021).

Chest pain can be due to an extensive variety of disorders (Table 2) ranging from life-threatening syndromes of cardiac origin such as ACSs, acute aortic diseases, and pulmonary embolism (PE) (Ibanez et al., 2018; Roffi et al., 2016; Konstantinides et al., 2015; Erbel et al., 2014) to conditions of non-cardiac origin that are relatively harmless (Gulati et al., 2021).

Therefore, an early and accurate differential diagnosis is a major need in the ED; physicians and all triage personnel must quickly distinguish between those who require urgent management, and those, with more benign entities, who do not require admission to the ED, but can be transferred to an outpatient setting.

Approximately, the 50% of patients with chest pain can be discharged without hospitalisation from the ED. Most of these patients received a final diagnosis of non- cardiac origin chest pain; chest pain of unknown origin was documented in 48% of these patients and non-cardiac origin in a about 35% of cases. Non–cardiac causes include musculoskeletal conditions (chest sprain or strain), indigestion or gastrointestinal diseases, chest infection or pneumonia, and panic disorders or other psychiatric conditions (Cayley, 2005). Of patients who need further monitoring, only the 25% have a final diagnosis of acute coronary syndrome (ACS), and the other 25% are discharged with a final

diagnosis of stable angina (3.5–6.6%) or non-ischaemic cardiac problem (10-19%). AMI accounts only for a very small percentage of chest pain patients, approximately the 10-19% (Goodacre et al., 2005; Carlton et al., 2015), and it results fatal in one third of these patients, with about half of the deaths occurring within one hour of the acute event.

The percentage of chest pain patients with an ACS who are erroneously discharged from the ED is around 2%; unfortunately, these patients show a twofold-increased probability of morbidity and mortality in the following 30 days (Pope et al., 2000). Indeed, the absence of typical symptoms of chest pain could not exclude an ACS; in this group of patients, AMI was diagnosed in the 1.6% of cases (Möckel et al., 2013). Moreover, chest pain of both origins, cardiac and non-cardiac, could be documented in the same patient (Lenfant, 2010). Psychological and psychiatric factors also play a critical role in the perception of pain and could mask the severity of chest pain.

Chest pain due to cardiac disorders could be associated to coronary artery disease (CAD), as stable angina; or acute coronary syndrome (ACS) including unstable angina, ST-segment elevation AMI (STEMI) and non-ST-segment elevation (NSTEMI).
Patients undergoing coronary angiography for stable angina usually show a “normal” or mildly diseased epicardial coronary tree, and absence of a luminal diameter reduction of ≥50% (Montalescot et al., 2013). Indeed, it has been defined angina with “normal” coronary arteries or angina in the absence of obstructive CAD. Incidence of stable angina increases with age (Kennel et al., 1972; Mittelmark et al., 1993); and it is more common in women as an initial presentation of coronary disease, however a higher overall prevalence of coronary disease has been observed in men than in women (Shaw et al., 2008; Sharaf et al., 2001).

Although stable angina was considered until a few years ago as a benign and relatively harmless form of coronary disease, only recently different research groups have demonstrated that it is associated to an elevated risk of acute cardiovascular events (Shaw et al., 2008; Jespersen et al., 2012). Jespersen and colleagues investigated the prognostic relevance of cardiac symptoms of stable angina pectoris in a cohort of 11,223 patients, enrolled from 1998 to 2002, comparing to patients with obstructive CAD and healthy subjects. Stable angina with normal coronary arteries and diffuse non-obstructive CAD was associated with 52 and 85% increased risk of future MACE (cardiovascular mortality, hospitalization for AMI, heart failure, or stroke) and with 29 and 52% increased risk of mortality, respectively, with no gender differences (Jespersen et al., 2012).

Concerning ACS, it includes ST-elevation myocardial infarction (STEMI), non-ST-elevation myocardial infarction (NSTEMI) and unstable angina (UA). Since these latter two pathological conditions share a wide spectrum of clinical and biological characteristics and have

undistinguishable ECG features, they are considered similar and thus are grouped together in the patient management guidelines (Roffi et al., 2016).
Nevertheless, a recent large prospective multicentre study of patients with acute chest pain, by Puelacher et al., highlighted the substantial differences between UA and NSTEMI, proving that (i) UA incidence was substantially lower than AMI (<10% of overall cases); (ii) UA patients usually had a previous history of cardiovascular events (as AMI and prior coronary revascularisation) than NSTEMI; (iii) mortality was significantly lower in UA than NSTEMI at 30 days and 1 year (probably because of the higher use of aspirin and statins); (iv) the 82% of patients with UA did not exhibit relevant changes in high-sensitivity cardiac troponin (hs-cTnT) after 1 or 2 hours, excluding acute heart injury after the ischaemic episode (Puelacher et al., 2019).
Moreover, patients with a history UA as well as stable angina, show usually endothelial dysfunction and relative elevated local inflammation. However, UA patients were demonstrated to have a higher risk, almost twofold, of occurring in a fatal or non-fatal AMI per year as compared to patients with stable angina (Morrow et al., 2010), suggesting different prognostic implications.

In the most severe case, chest pain is one of the main manifestations of a concomitant AMI. According to the World Health Organization, the European Society of Cardiology (ESC), the American College of Cardiology (ACC), the American Heart Association (AHA) and the World Heart Federation (WHF), the diagnosis of AMI requires “detection of rise and/or fall of cardiac biomarkers (preferably troponin) with at least one value above the 99th percentile of the upper reference limit (URL) together with evidence of myocardial ischaemia with at least one of the following criteria: symptoms of ischemia, ECG changes indicative of new ischaemia (new ST-T changes or new left bundle branch block (LBBB), development of pathological Q waves in the ECG, imaging evidence of new loss of viable myocardium or new regional wall motion abnormality” (Thygesen et al., 2007) (Figure 2). Myocardial infarction diagnosis is constantly evolving, and diagnostic criteria are continuously updated based on the discovery of new biomarkers or the development of new diagnostic techniques.
Chest pain due to AMI is often not localized but diffuse, not positional, not affected by movement of the region; and it may be accompanied by diaphoresis, dyspnoea, nausea, or syncope. Usually, it lasts at least 20 minutes (Thygesen et al., 2007). Advanced age is associated with an increased in AMI incidence and mortality, but a relevant number of cases has been documented in subjects <45 years (Mehta et al., 2001; Canto et al., 2012; Sagris et al., 2021). Considering gender disparities, AMI is significantly more frequent in male patients than female ones, and men tend to have AMI earlier in life than women (Millet et al., 2018). However, after the age of 75, women represent the majority of patients, usually with the poorer outcome (Metha et al., 2016).

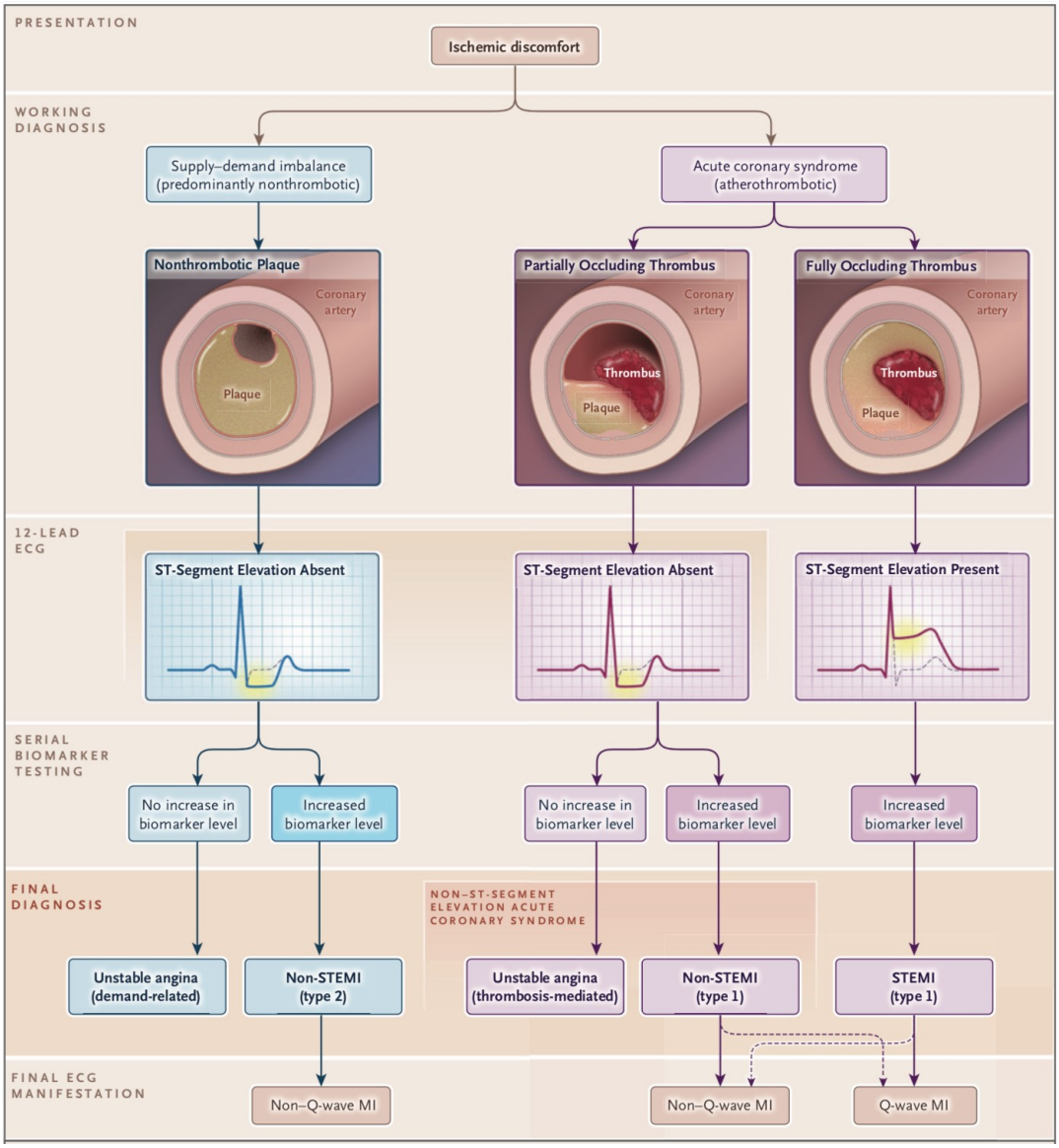

Figure 2. Clinical workup of ST-Segment Elevation Acute Myocardial Infarction (STEMI) and Non-STEMI Acute Coronary Syndromes (Anderson and Morrow, 2017).

The main risk factors include hyperlipidemia, obesity, smoking history, substance abuse, thrombophilia, and sedentary lifestyle (Vernon et al., 2019).

A myocardial infarction may occur as the first manifestation of coronary artery disease, or as a repeated event in patients with established chronic coronary disorders. The outcome is also extremely variable, AMI may represent a minor event, sometimes it is not even detected, but it can be associated to severe haemodynamic deterioration and even fatal outcome.

Consequently, AMI can be clinically classified into 5 different types, and based on the presence of significant alterations of the T- and ST- segment of the ECG into:

- **AMI with ST-segment elevation (STEMI).** It generally reflects an acute, complete, and prolonged occlusion of an epicardial coronary blood vessel. The ECG usually detects a persistent ST-segment elevation. The therapeutic approaches have the goal to achieve rapid and complete, reperfusion by fibrinolytic therapy or primary angioplasty (Antman et al., 2004).

- **AMI without persistent ST-segment elevation (NSTEMI).** It results from severe coronary artery narrowing, transient occlusion, or microembolization of thrombus and/or atheromatous material. It is usually associated to elevated myocardial necrosis biomarkers, but no ECG changes at the onset of symptoms or absence or transient ST-segment depression or T-wave inversion, or pseudo-normalization of T-waves (Roffi et al., 2016).

STEMI and NSTEMI have also been associated to a different prognostic relevance; indeed, STEMI patients have significantly higher in-hospital rate mortality as compared to NSTEMI (Vernon et al., 2019).

2. From atherosclerosis to AMI

Chest pain, due to cardiac ischemia, may result from different types of functional disease involving the epicardial coronary arteries, the coronary microcirculation, or both (Radico et al., 2014). Whatever the cause, when myocardial oxygen demand transiently exceeds the myocardial oxygen supply, myocardial ischemia occurs with an oxygen supply-demand mismatch. Myocardial ischemia stimulates chemosensitive and mechanosensitive receptors within cardiac muscle fibres and surrounding coronary vessels. The activation of these receptors triggers impulses through the sympathetic afferent pathways from the heart to the cervical and thoracic spine, in a specific dermatome. The discomfort described by the patient often coincides with a specific dermatome pattern (Foreman, 1999).

In most cases, myocardial ischemia is triggered by coronary atherosclerosis, of which stable angina and acute myocardial infarction are the main manifestations. Atherosclerosis has been considered for years a cholesterol storage disease, characterized by the progressive accumulation of cholesterol and thrombotic debris in cells of subendothelial intima and the formation of foam cells (Tabas et al., 2007).

Currently, atherosclerosis is recognized as a chronic inflammatory disorder, associated to the complex interaction of artery endothelial cells, immune cells, and pro-inflammatory mediators (Libby, 2002). Atherosclerosis occurs predominantly at sites of disturbed laminar flow, notably, arterial branch points and bifurcations (Moore and Tabas, 2011).

In dyslipidemia, hypertension, hyperglycemia, or hypercholesterolemia conditions, lipoproteins progressively accumulate into the subendothelial layer of arterial wall. Consequently, endothelial cells undergo inflammatory activation and increase the expression of adhesion molecules on their membranes, as vascular cell adhesion molecule-1 (VCAM-1) (Cybulsky and Gimbrone, 1991). In addition to VCAM-1, P- and E-selectin and chemokines also contribute to leukocyte recruitment and directional migration in atherosclerosis-susceptible mice (Dong et al., 1998).

The transcriptional activation of the *VCAM-1* gene is activated by nuclear factor-κβ (NF-κβ) in response to modified lipoprotein particles, as oxidized phospholipids and short-chain aldehydes, and pro-inflammatory cytokines, such as interleukin IL-1β or tumour-necrosis factor-α (TNF-α) (Collins and Cybulsky, 2001). P-selectin and VCAM-1 promote the adhesion of blood leukocytes, including monocytes and T lymphocytes, to the inner surface of the arterial wall. Monocytes begin rolling on endothelial cells through the interaction of monocyte P-selectin glycoprotein ligand-1 (PSGL-1) with endothelial selectins (Mestas and Ley, 2008). Some monocytes then firmly adhere to injured endothelial cells through the interaction of monocyte integrins with endothelial cell ligands, including integrins VLA-4 (very late antigen-4) and LFA-1 (lymphocyte function-associated

antigen 1) and their respective endothelial cell ligands, VCAM-1 (vascular cell adhesion molecule) and ICAM-1 (intercellular adhesion molecule-1). After adhesion to activated endothelial cells, monocytes penetrate the tunica intima (diapedesis) (Kamei and Carman, 2010). Within the intima, the monocytes differentiate into tissue macrophage, and they start to internalize modified lipoprotein particles (through phagocytosis of matrix-retained and aggregated LPs and pinocytosis non-retained native LDL) and oxidized low-density lipoproteins (oxLDL), giving rise to the arterial foam cell, a hallmark of the arterial lesion (Figure 3).

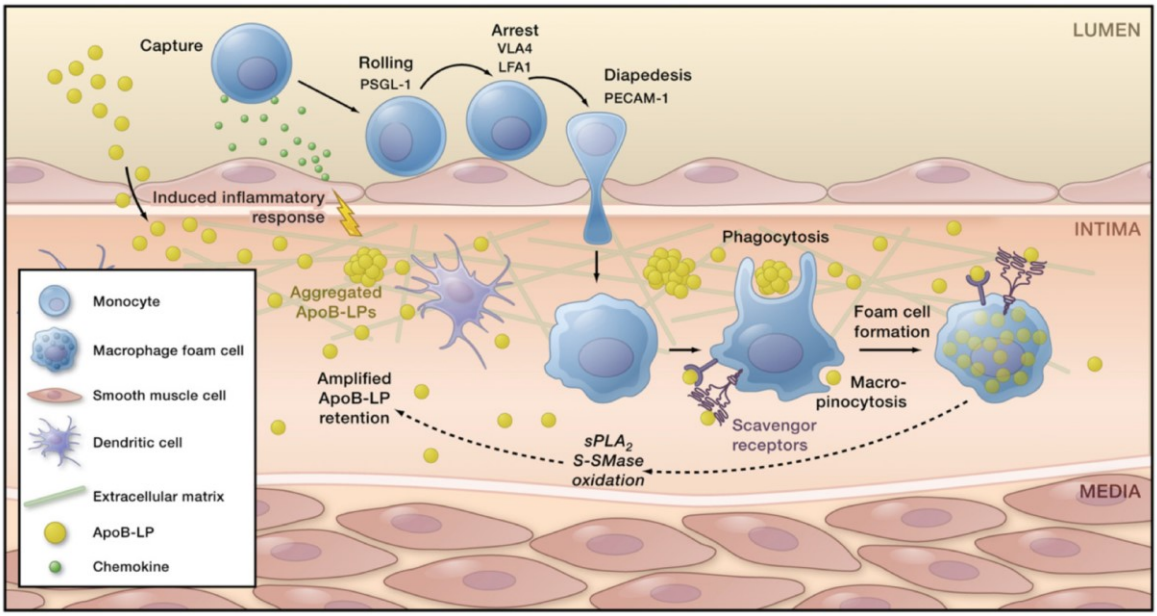

Figure 3. Lipoprotein retention promotes monocyte recruitment and subsequent foam cell formation. Lipoproteins in particular apolipoprotein B-containing (apoB-LPs), enter the intima, bind to proteoglycans, and undergo various modifications, including oxidation and hydrolysis by secretory phospholipase A2 (sPLA2) and secretory sphingomyelinase (S-SMase). These modifications trigger an inflammatory response characterized by chemokine secretion and altered expression of adhesion molecules by the overlying endothelial cells. The inflammatory signals lead to monocyte diapedesis into the intima, in which they differentiate into macrophages and internalize native and modified lipoproteins, resulting in foam cell formation (Moore and Tabas, 2011).

Foam cell secretes pro-inflammatory cytokines and reactive oxygen species (ROS) that amplify local inflammatory response within the lesion. Foam cells show impaired migratory capacity and thus remain trapped within the plaque, where they die and form the necrotic core of the atherosclerotic lesion (Pagler et al., 2011).

In addition, T-cells migrate into subendothelial layer, recognise local antigens, and secrete pro-inflammatory cytokines, boosting local inflammation and contributing to the growth of the atherosclerotic plaques.

The connective tissue of atherosclerotic lesions is initially that of a normal arterial intima or adaptive intimal thickening, but progressively this loose fibrocellular tissue is replaced by collagen-rich fibrous tissue, which become the predominant component of the plaque. Thus, the tissue

between the necrotic core and the luminal surface of the plaque, is defined fibrous cap and contains a high content of type I collagen (Kragel et al., 1989).

According to their microscopic morphology, atherosclerotic lesions have been classified by Stary's research group and subsequently by Virmani and colleagues, (Stary et al., 1994; Virmani et al., 2000) in two main categories: "non-atherosclerotic intimal lesions", including intimal thickening and intimal xanthoma, characterized by focal accumulations of fat-laden macrophages in absence of necrotic core; and "progressive atherosclerotic lesions", which include all different phases of atherosclerosis development from pathological intimal thickening, to fibroatheroma, plaque rupture and fibrocalcific plaque (Figure 4).

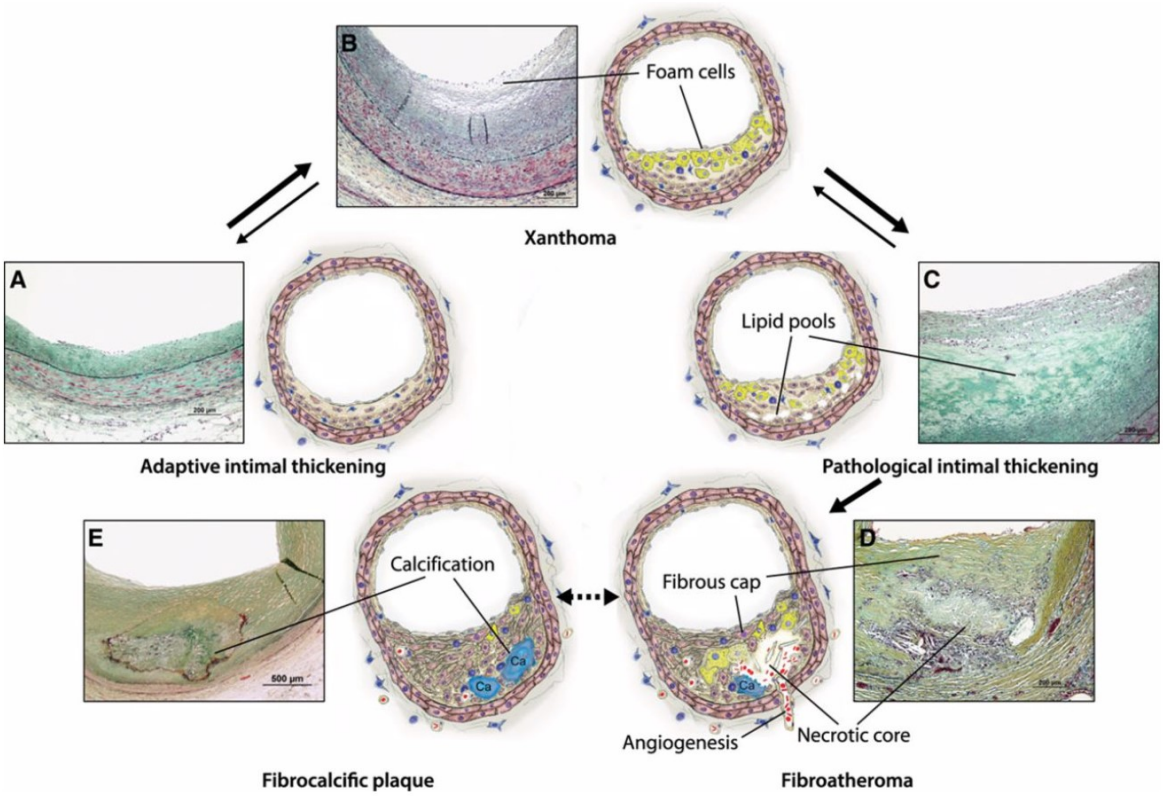

Figure 4. Lesion types of atherosclerosis according to AHA classification and a proposed sequence of their development. A) Adaptive intimal thickening characterized by smooth muscle cell accumulation within the intima. B) Intimal xanthoma with accumulation of foam cell macrophages in absence of necrosis. C) Pathological intimal thickening with consistent lipid pool in the absence of apparent necrosis. D) Fibroatheroma, in the presence of a necrotic core. E) fibrocalcific plaque with calcified necrotic core. Movat pentachrome stain (Bentzon et al., 2014).

Monocytes continue to enter the plaque and differentiate into macrophages during the atherosclerotic lesion evolution. Of note, macrophages contribute to the thinning of the fibrous cap, through the continuous production of pro-inflammatory cytokines and matrix metalloproteinases (MMPs) (Moore and Tbas, 2011).

Therefore, the ‘‘vulnerable’’ plaque or the “thin-cap fibroatheroma” (TCFA) have been defined as the precursor lesions of plaque rupture, and the high risk factors for thrombus formation (Virmani et al 2002). TCFAs are mostly found in the proximal left anterior descending coronary arteries and less commonly in the proximal right or the proximal left circumflex coronary arteries (Bentzon et al., 2014). In TCFAs, the large necrotic core has often a mean length of 8 mm (range 2–17 mm) and an area of ≤3 mm^2, and it is covered by thin (<65-μm) fibrous cap, infiltrated by activated macrophages. The atherosclerotic plaque induces a cross-sectional luminal narrowing in over 75% of cases, with a decrease of the lumen diameter of < 75% (< 50% diameter stenosis) (Virmani et al., 2002). Rarely, the necrotic core can undergo a process of stabilization and calcification, leading to the formation of a fibrocalcific plaque, which occupies almost all the plaque volume (Stary, 2000).

Most of the atherosclerotic plaques remain clinically asymptomatic, but some of them (defined stable plaques) gradually become obstructive manifesting with stable angina; whereas only few become thrombosis-prone (defined vulnerable plaques), leading to acute coronary syndrome (ACS).

Plaque rupture occurs when the fibrous cap loses its structural integrity, and the highly thrombogenic core is exposed to the flowing blood. The rupture site is often located to the side (shoulder) of raised lesions, in close proximity to the necrotic area (Bentzon et al., 2014).

Rupture of the plaque thin cap and subsequent thrombus formation may occur spontaneously, but also emotional or physical stress, as physical activity, anger, anxiety, work stress, earthquakes, war and terror attacks, temperature changes, infections, and cocaine abuse may favor this process (Muller et al., 1985). All these factors are involved in the activation of the sympathetic nervous system, resulting in increased heart rate, blood pressure, coagulability and platelet reactivity (Chen at al., 2016). Plaque erosion, instead, is caused by endothelial damage in the absence of frank cap rupture (Figure 5).

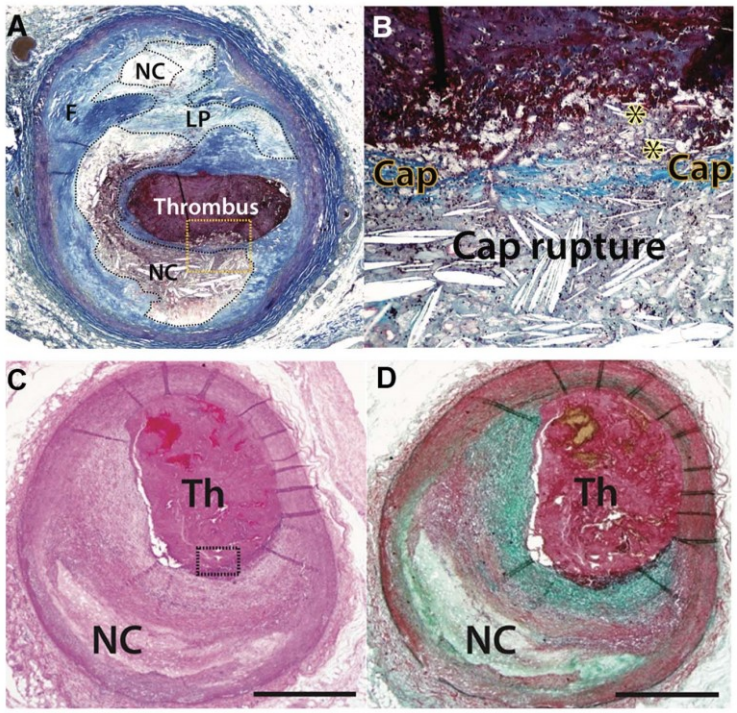

Figure 5. Plaque rupture and erosion. A) representative image of coronary artery plaque rupture (yellow rectangle) showing a fibroatheroma with fibrotic tissue (F), areas enriched in extracellular lipid pools (LP), and necrotic cores (NC). B) Large magnification of the yellow rectangle in A. The thin and inflamed fibrous cap covering the necrotic core is broken and core materials, including cholesterol crystals (*), are released into the vessel lumen, where the thrombus is developing. Elastin–trichrome stain (collagen blue). C, D) Plaque erosion with fibroatheroma with early necrotic core (NC) and occlusive luminal thrombus (Th). Hematoxylin–eosin (C) and Movat pentachrome stains (D). (Scale bars = 1 mm (adapted from Kramer et al., 2010; Bentzon et al., 2014).

The magnitude of the thrombotic response upon plaque rupture or erosion and the timing of symptoms onset are extremely variable. Moreover, the possibility of thrombus formation is unpredictable, and only occasionally it turns into a critical stenosis and, therefore, to acute coronary event. Microscopic examination in an autopsy study shown that the 8.7-16.7% of patients, who die suddenly of non-cardiac causes, presents both thrombotic and non-thrombotic ruptured plaques. Therefore, it has hypothesized that vulnerable plaques undergo reparative processes after rupture (Bentzon et al., 2014), indeed an average of 7.5 plaque ruptures per year occurs in absence of any cardiovascular event.

In this scenario, plaque rupture with local thrombin activation and subsequent healing process might represent different phases of atherosclerotic disease progression, and rupture may improve plaque growth. Therefore, acute coronary syndromes probably depend on the imbalance between instability (“activation”) and healing (“passivation”) of the atherosclerotic plaque (Vergallo and Crea, 2020) (Figure 6).

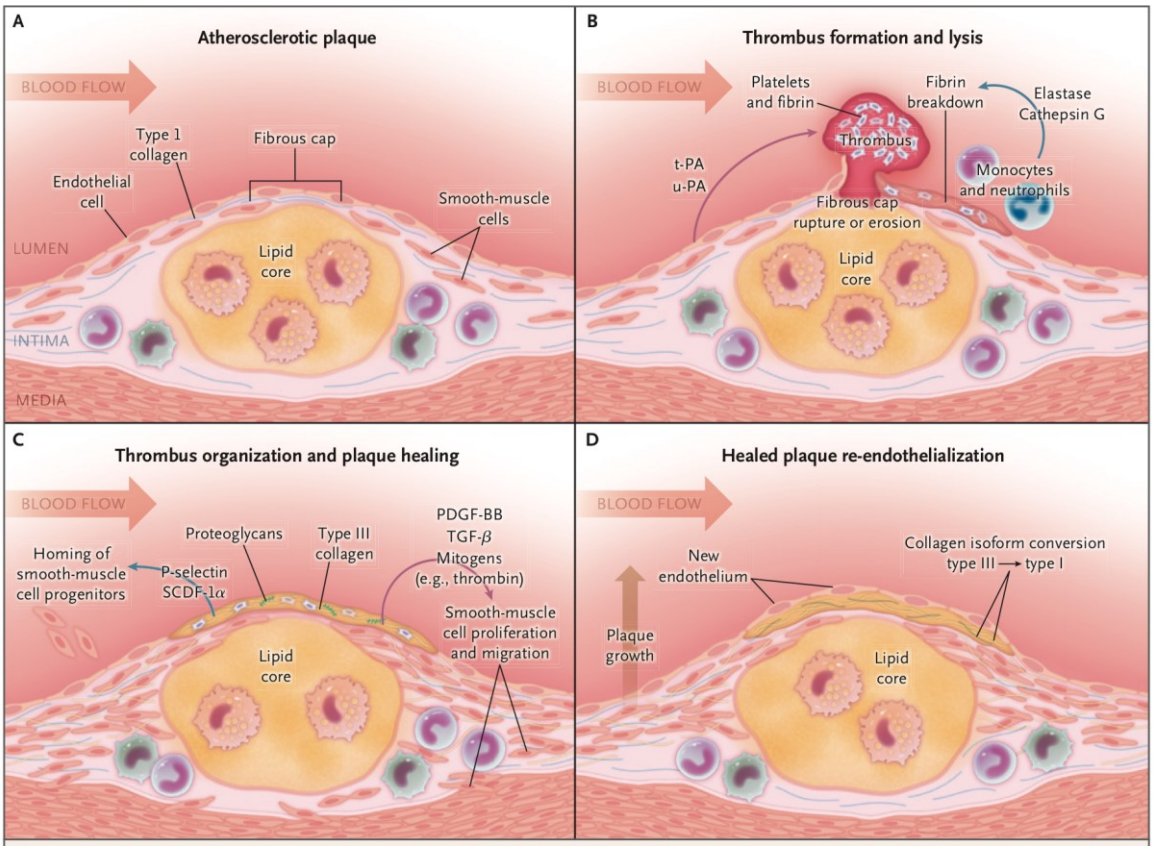

Figure 6. Mechanisms of Atherosclerotic Plaque Healing. Different phases of atherosclerotic plaque: plaque rupture, thrombus formation and lysis, thrombus reorganization and plaque healing and re-endothelialisation (Vergallo and Crea, 2020).

Plaque healing begins after the disruption of the plaque to prevent the formation of a thrombus, promote plaque repair, and restore vessel integrity. After plaque rupture or erosion, the exposure of thrombogenic plaque components provides a potent stimulus for platelet activation and aggregation, leading to thrombus formation (Bentzon et al., 2007). Simultaneously, plaque rupture or erosion triggers endogenous fibrinolysis to preserve vessel physiologically functionality (Okafor and Gorog, 2015) and activates smooth muscle cells migration and proliferation within the intima (Basatemur et a., 2019). The final step of plaque healing is represented by re-endothelialization of the plaque surface with creation of a neointima (Lev at al., 2019).

According to the “double hit” theory of atherosclerosis, acute coronary syndrome will develop after repeated cycles of rupture and healing, with gradually alteration of healing capacity and progressive luminal loss. Patients with impaired healing capacity will develop occlusive or sub-occlusive thrombosis and acute coronary syndrome; while patients with an effective healing system, will develop a more fibrous, and stable plaque and, therefore, a stable angina (Vergallo et al., 2019). Thrombogenicity of the exposed plaque material, local flow disturbances, and systemic thrombotic predisposition, defined as “the classic triad of Virchow”, represent the main risk factors for thrombosis (Virchow, 1849; Lip and Gibbs, 1999).

ACS, and especially STEMI and NSTEMI, are nearly always caused by plaque rupture, and less frequently by a plaque erosion or a sudden plaque haemorrhage, accompanied by the subsequent formation of an occlusive thrombus. The thrombus can block blood flow and deprive the myocardium of oxygen. Prolonged deprivation of oxygen supply can lead to myocardial cell death and compromised heart functionality. Myocardial cell necrosis, but also apoptosis and autophagy, are mainly involved in this process (Konstantinidis et al 2012).

Gross examination (during postmortem autopsies) usually shows dark, mottled area corresponds to a 12 to 24 hours old MI, and the yellow, softened lesion with red-tan borders consistents with a 10 to 14 days old MI (Figure 7, panels A and B, respectively). At this stage, necrotic myocardium is weak and vulnerable to septal, papillary muscle or free wall ruptures in case of transmural infarctions, all associated with high mortality (Ghafoor et al., 2020).

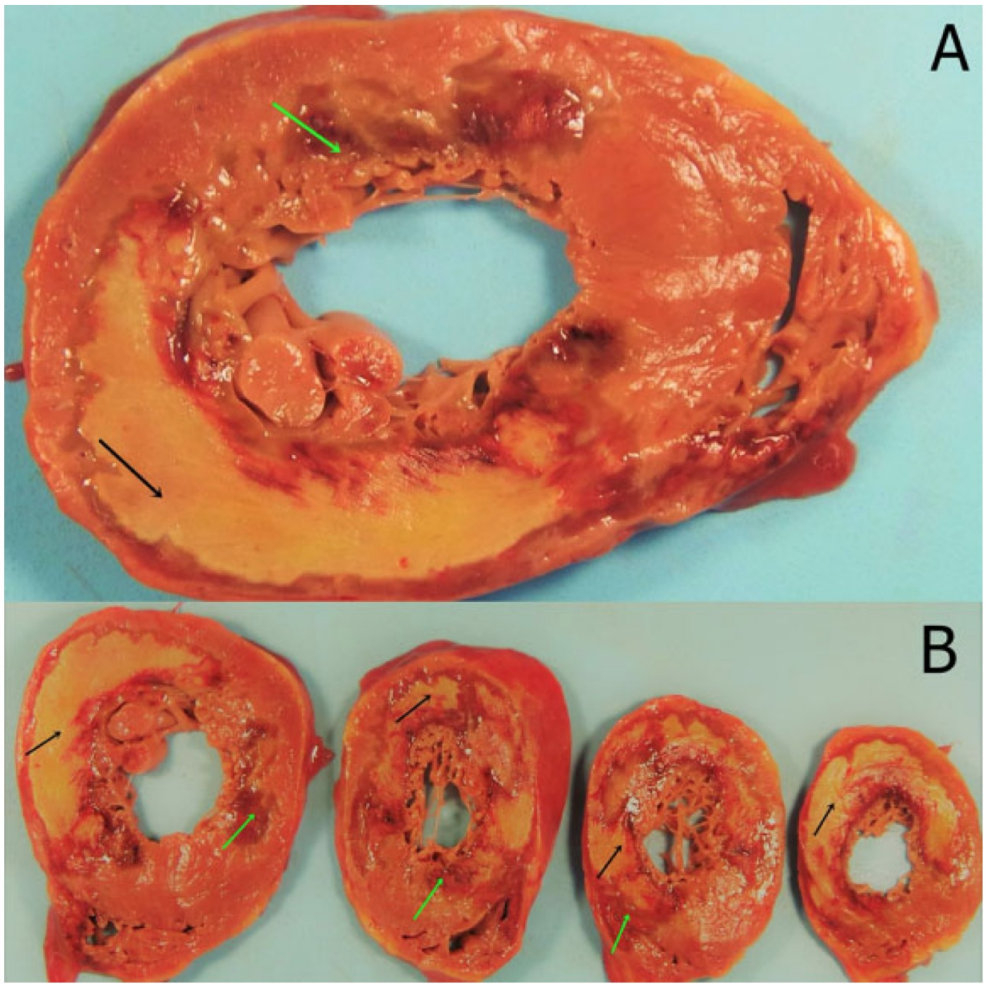

Figure 7. Necrotic myocardium after AMI. A, B) On gross examination, two lesions of the myocardium and the papillary muscles. Green arrows indicate cyanoyic tissue, and the black arrows indicate a yellow, softened lesion with red-tan borders corresponding to a myocardial infarction after 12-24 hours and 10-14 days, respectively (Ghafoor et al., 2020).

The ultrastructural changes, that can be observed 10–15 min after the onset of ischaemia, are glycogen depletion, myofibril relaxation, sarcolemma disruption, and mitochondrial abnormalities by electron microscopy (Thygesen et al., 2018). Complete necrosis of cardiomyocytes within the infarct area requires at least 2–4 h or longer according to several factors as persistent or intermittent coronary arterial occlusion, the presence of collateral circulation to the ischaemic zone, myocyte sensitivity to ischaemia, pre-conditioning, and/or, finally, individual demand for myocardial oxygen and nutrients.

Myocardial infarction can be classified region involved (topoghraphic distribution) in regional transmural or subendocardial, circumferential or diffuse multifocal infarction, or according to the myocardial size in “microscopic (focal necrosis), small (<10% of the LV myocardium), moderate (10–30% of the LV myocardium), and large (>30% of the LV myocardium)” (Thygesen et al., 2007). Moreover, myocardial necrosis can evolve in a wave front-like pattern over several hours from the endocardium to the epicardium, resulting in a transmural MI. Indeed, MI affects predominantly the left ventricle (LV), but the loss of viable cardiomyocytes may also extend into the right ventricle (RV) or the atria.

Furthermore, AMI can be classified, according to the phase of lesion development and to nature of immune cell infiltrate in evolving (<6 h), acute (6 h–7 days), healing (7–28 days), and healed (29 days and beyond).

Indeed, after the ischaemic event cardiomyocyte death triggers an inflammatory response, whose intensity determines patient's outcome. Indeed, the injured tissue releases danger-associated molecular patterns (DAMPs), that attract and activate circulating immune cells, as granulocytes and monocytes, through the binding to their pattern recognition receptors (PRRs). DAMPs also induce endothelial activation, up-regulating the expression of cellular adhesion molecules, such as P- and E-selectin, which are involved in leukocyte adhesion and diapedesis. Neutrophils are the first immune cell to infiltrate the infarcted area, reaching a peak at ~24 h post-AMI. Together with neutrophils, also monocytes are recruited in the myocardial lesion, and monocyte infiltration peaks ~3 days after the acute episode. Neutrophils and monocytes are the main actors of the immune system-mediated tissue repair and myocardium reperfusion, regulating the phagocytosis of necrotic debris, the release of proteolytic enzymes, and the production of reactive oxygen species (ROS) (Timmers et al., 2012). However, excessive or prolonged immune cell activity can exert direct cytotoxic effects on the surrounding viable myocytes and blood vessels, inducing microvascular dysfunction or plugging (namely the “no-flow” phenomenon), compromising the complete reperfusion and exacerbating ischemic injury (Heusch, 2016). Myocardial necrosis could be detected hours after the acute event, and indirectly measuring levels of several biochemical markers in peripheral blood including creatine kinase (CK-MB), myoglobin, troponins T and I (cTnT), and lactate dehydrogenase (LDH) (see dedicated chapter). The inflammatory phase is

then following by the proliferative phase, in which inflammatory response is resolved, regulatory T cell are recruited, tissue macrophages polarize towards a reparative phenotype, myofibroblasts start to proliferate and secrete pro-fibrotic cytokines and collagen to favour scar formation. Finally, myocardial scar undergoes a maturation process often accompanied by alterations in cardiac structure and functionality to compensate the loss of contractile activity of the infarct area (Frangogiannis, 2012). The remodelling process affects both the infarct area and the non-infarct surrounding tissue of the ventricle, leading to myocardial hypertrophy, increased chamber dilation and sphericity and worsened cardiac function. Post-infarction remodelling depends on the size of the infarcted area and on the quality of cardiac repairing process (White et al., 1987). In this context, a finely tuned inflammatory response and heart remodelling are essential for a favourable prognosis. Indeed, impaired tissue repair and altered remodelling have been associated to heart failure and poor prognosis in patients surviving an AMI (Westman et al., 2016; Aimo et al., 2019).

3. Chest pain clinical evaluation and AMI biomarkers

A rapid and accurate differential diagnosis and risk stratification of patients presenting with chest pain to the ED, represent a relevant clinical issue; indeed, emergency physicians have to identify the small group of patients with chest pain of cardiac origin who require hospitalisation for acute management, from the majority of patients with a more harmless chest pain who can be safely discharged from the ED. As previously mentioned, the three potential life-threatening causes of chest pain are pulmonary embolism, aortic dissection, and acute coronary syndrome (ACS).

In addition to the direct consequences on patient health, a fast rule-in or rule-out of chest pain patients engraves also on cost-effectiveness of patient management. Indeed, the shared approach remains primarily precautionary/inclusive; patients must be observed and monitored for a prolonged period (1-3 hours) to avoid inadvertent early discharge.
Clinical strategies for the diagnosis of chest pain have been frequently update based on the progresses that have been made in diagnostic techniques and the development of new decision algorithms.
Currently, the triage of chest pain patients in the ED is based on the evaluation of patient medical history, physical examination, recording and interpretation of a 12-lead ECG within 10 minutes of arrival and measurement of cardiac biomarkers (Thygesen et al., 2018). However, these parameters are essential tools for initial management and risk stratification of patients, but each of them suffers from poor sensitivity and specificity and are often not sufficient to reliably detect or rule out an ACS, in particular AMI.

Concerning ECG, only a small number of patients with acute chest pain shows a typical STEMI ECG pattern at the presentation to the ED. The majority has instead a completely normal ECG (40–60%) or nonspecific initial ECG parameters (Welch et al., 2001; Knolman et al., 2017). ECG evaluation shows some limitations, for instance ST elevation may be observed in other cardiac conditions such as acute pericarditis, LV hypertrophy, LBBB, Brugada syndrome, and early repolarization patterns. Furthermore, Q-waves changes may occur due to myocardial fibrosis in the absence of coronary artery disease including cardiomyopathy (Wang et al., 2003).
Moreover, computed tomography angiography (CTA) and ultrasonography and echocardiography, have allowed the non-invasive evaluation of coronary arteries in patients with suspected unstable angina, acute aortic diseases, or PE (Stepinska et al., 2020).

Over the years, the accuracy of AMI diagnosis has improved with the availability of more specific biomarkers of myocardial necrosis, that allow the detection of ever smaller amounts of myocardial necrotic tissue. Myocardial cell death can be detected by the measurement levels of several proteins released into the peripheral blood from the damaged myocytes. These cardiac biomarkers include serum glutamic oxalacetic transaminase (SGOT), lactic dehydrogenase (LDH) and myoglobin that have been used for years and then have been replaced by recent creatinine kinase (CPK), LDH isoenzymes, creatinine kinase-MB (CPK-MB), and troponin (Jaffe and Babui, 2006). Cardiac biomarkers have been introduced sequentially to diagnose AMI and have been then incorporated into international guidelines for the diagnosis of AMI (Thygesen et al., 2018). Myocardium necrosis biomarkers show different release kinetics after the acute event, reported in figure 8.

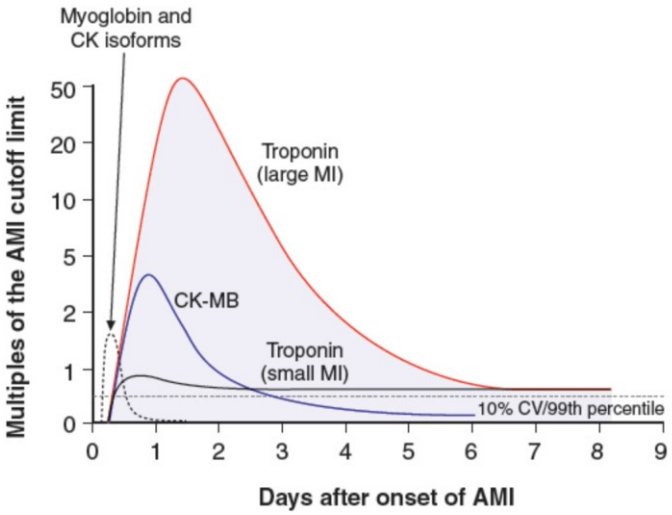

Figure 8. The release kinetics of myocardium necrosis biomarkers (adapted from Jaffe, 2006).

Among these cardiac biomarkers, in particular the cardiac troponin I and T (cTnI and cTnT) represent the biomarkers of choice for the diagnosis of myocardial necrosis because of their high sensitivity and specificity and are considered the “gold standard” for AMI (Babui and Jaffe, 2005). Cardiac troponins are structural proteins, almost exclusively expressed by heart tissue. cTnT and cTnI are immobilised on thin filaments and unbound in the cytosol, as “cytosolic pool”. They mediate the interaction between actin and myosin filaments and thereby regulate contraction and relaxation coupling in cardiomyocytes (Katrukha, 2013; Jaffe, 2006). After AMI, cTnI and cTnT are released as intact proteins or degradation products from necrotic myocardium (Mair et al., 2018).

An increased value for cTn is defined as “a measurement exceeding the 99th percentile of a normal reference population (defined as upper reference limit, URL). Detection of a rise and/or fall of cTn levels is essential to the diagnosis of AMI” (Jaffe, 2006; Thygesen et al., 2018). The heart injury may be acute, when peak of cTn is detected with a dynamic rising and/or falling pattern of values

above the 99th percentile URL; or chronic, with persistently elevated cTn levels.

Current guidelines recommend two serial measurements of cTn, 6 - 9 hours after patient's arrival to the to the ED (Thygesen et al., 2007). This requires a prolonged assessment before safe patient discharge. Sometimes patients may require an additional blood sampling between 12 and 24 hours, in the case of previous cTn levels are not elevated but the clinical suspicion of AMI is high (Macrae et al., 2006). Indeed, the increase of cTn levels is closely associated to the timing of symptom onset, and myocardium necrosis could be detectable only hours after the acute event. Diagnostic protocols become faster with the introduction of high-sensitivity cTn (hs-cTn) assay, which requires two serial cTn evaluations and reduces testing time to 3-6 hours after patient's admission to the ED (Twerenbold et al., 2017).

Recently, several risk score systems and diagnostic protocols based on a single hs-cTn assay have been suggested to reduce the time of patients permanence in the ED, ensuring at the same time diagnostic accuracy. The History, ECG, Age, Risk Factors and Troponin (HEART) score have been recently designed by Backus and colleagues, incorporating data from patient clinical history, ECG, clinical assessment and single hs-cTn assay to identify both low and high-risk chest pain patients with AMI and consequently safely discharged or transferred to out-patients setting the patients with chest pain due to non-cardiac origin or more benign causes (Backus et al., 2013). Furthermore, diagnostic accuracy of a novel accelerated diagnostic protocol (ADP) for suspected chest pain due to ACS, namely Triage Rule-out Using high-Sensitivity Troponin (TRUST), was recently tested by Carlton and colleagues. The TRUST ADP, which combines clinical risk-assessment and hs-cTnT assay, turned out to be extremely useful, allowing early discharge of the 40% of all chest pain patients, identified as low-risk patients after just a single hs-cTnT at presentation to the ED, with a NPV of >99.5% (Carlton et al., 2019).

Although cTnT is considered organ/tissue specific, its detection has been suggested to be also associated to tissue other than myocardium, as injured skeletal muscle in particular pathological conditions (Bodor et al., 1997). Moreover, cTnT and cTnI are not disease-specific markers; although elevated cTn values reflect myocardial necrosis, they give no information on the underlying pathological mechanisms and can increase following a mechanical stretch or physiological stresses in otherwise normal hearts. The mechanisms accounting for the release of cTn into the circulation may include normal turnover of myocardial cells, apoptosis, increased cellular wall permeability, the formation and release of membranous blebs (Garg et al., 2017). In addition, cTn plasma levels were increased in many cardiovascular diseases other than AMI, including acute or aortic dissection, atrial fibrillation, chronic heart failure, myocarditis, Takotsubo cardiomyopathy, and stroke (Eggers and Lindahl, 2017). Moreover, Eggers and Lindahl have

recently highlighted the differences in terms of hs-cTn concentration according patients' gender. Indeed, male patients usually have higher hs-cTn plasma levels as compared to women (Eggers and Lindahl, 2017).

Since it is not clinically possible to identify the underlying pathological mechanism, a single hs-cTn assay alone has no real diagnostic utility and it should always be considered in combination with clinical assessment of other clinical parameters or scoring systems (Twerenbold et al., 2017; Ibanez et al., 2018; Thygesen et al., 2018). Therefore, new diagnostic tools are urgently required to improve the clinical algorithm for chest pain diagnosis and the efficiency in terms of costs and time of ED management.

4. Platelets

Platelets are anucleate blood cells, with discoid shape, a diameter of 2 to 5μm and a thickness of 0.5 μm (Machlus and Italiano, 2013). Platelets are formed and released into the bloodstream by megakaryocytes (MKs), which reside within the bone marrow (Paese, 1956). Thrombopoiesis is the physiological mechanism of platelet formation.

MKs are rare myeloid cells, accounting for the 0.01% of nucleated bone marrow cells (Nakeff and Maat, 1974). MKs develop from haematopoietic stem cells (HSC) that reside mainly in the bone marrow, but are also found in lung, peripheral blood and second site of hematopoiesis as the yolk sac, fetal liver, and spleen in early fetal development (Long et al., 1982).

During their differentiation, MKs adapt their cytoplasm and membrane systems for platelet biogenesis (Long et al., 1982). They increase in size, become polyploid through repeated cycle of endomitosis, a thrombopoietin (TPO)-dependent process in which DNA replication occurs without cytokinesis, resulting in DNA content of 4N, 8N, 16N in a single polylobulated nucleus (Patel et al., 2005). Polyploidization is essential for supporting organelle synthesis, cytoplasmic maturation and expansion, and efficient platelet production. Moreover, ribosomes and granules production increase to facilitate the synthesis of platelet-specific proteins and mRNAs. MKs develop also a highly invaginated and interconnected membranous system of cisternae and tubules, namely demarcation membrane system (DMS) (Zimmet and Ravid, 2000). MKs contain α granules, which are spherical shaped with a typically 200 to 500 nm diameter, and a dark central core. The α granules content depends on the endogenous protein synthesis and on the uptake and packaging of plasma proteins by receptor-mediated endocytosis and pinocytosis (Handagama et al. 1987). Some of the proteins stored in α granules, including von Willebrand factor (vWF), integrin αIIbβ3, platelet factor 4, P-selectin (CD62P), and CD36, play a key role in platelets function. MKs also contain dense granules (250 nm in size), which represent a reservoir of hemostatically active substances released upon platelet activation, as serotonin, catecholamines, ADP, adenosine 5'-triphosphate (ATP), and calcium (Youssefian and Cramer, 2000).

Currently, the most accredited theory for platelet formation is the "proplatelet model" (Patel et al., 2005) (Figure 9).

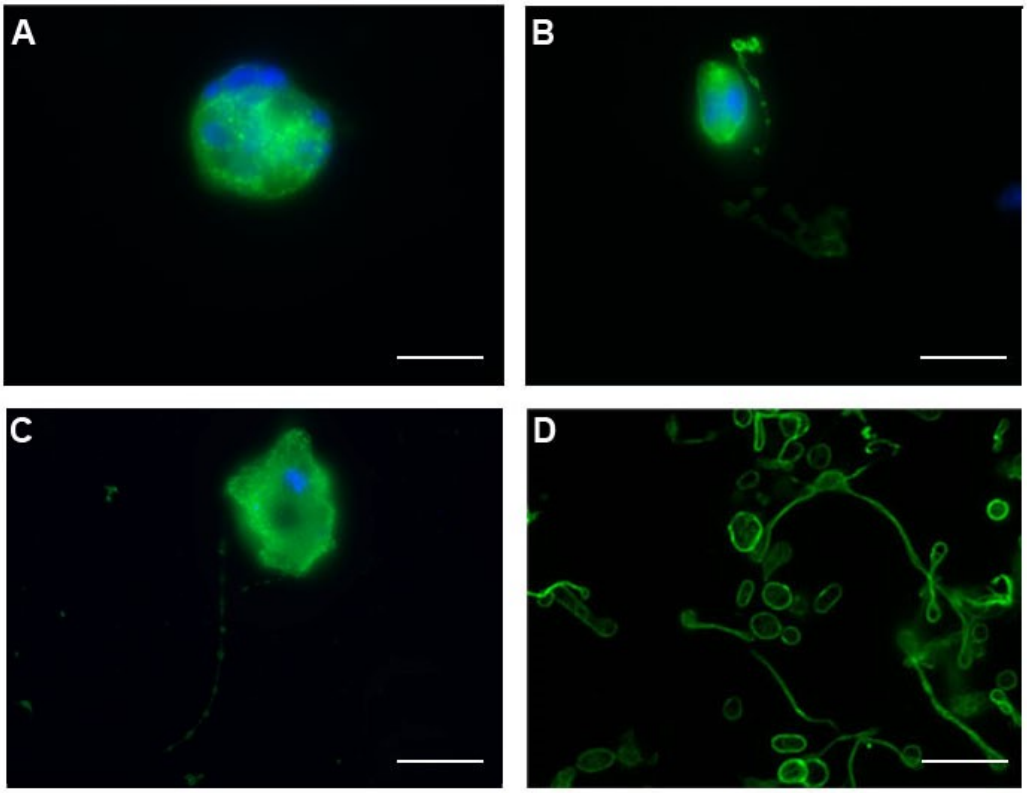

Figure 9. Thrombopoiesis. Representative IF images showing different phases of thrombopoietic process: a mature polyploid megakaryocyte (A), a megakaryocyte with initial proplatelet filaments (B), a megakaryocyte with a long proplatelet filament (C) and released proplatelets (D). (Nuclei are shown in blue and α-tubulin in green; A, B, C magnification= 40x; D magnification 100X) (from Prof. Gobbi's lab).

According to this model, MKs undergo a maturation process and releases platelets through the extension of long, cytoplasmic branching processes, defined proplatelets, into the circulation. The process starts usually at one single site of the MK, and a single MK can extend 10-20 proplatelets into the sinusoidal blood vessels of bone marrow. Proplatelets, which have a pseudopod form, elongate until forming thin tubules of 2–4μm diameter, called the proplatelet shafts. Proplatelets show platelet-sized swellings connected by thin bridges of rich cytoplasmic microtubules.

Some authors have hypothesized that proplatelets, extending into the lumen, acts as "blood receptor" to monitor circulating protein levels, such as TPO, or even platelet numbers. In this way, they regulate MK protein translation, granule packaging and their own production (Machlus and Italiano, 2013).

During proplatelets elongation, megakaryocyte undergoes a structural reorganization, cytoplasm is entirely transformed into a complex system of interconnected proplatelets. The polylobulated nucleus is compressed into a central mass with little cytoplasm and it may be extruded and degraded, whereas the MK cytoplasmatic content as proteins, organelles, granules, and mitochondria, is transported towards proplatelet terminal and packaged into proplatelets bulges (Italiano et al., 1999). Indeed, platelets also inherit a specific set of megakaryocyte-derived mRNAs and are capable of *de novo* protein synthesis.

In vivo MKs take about 5 days to complete the final steps of their maturation and be able of releasing platelets (Machlus and Italiano, 2013).

The last step of thrombopoiesis is the breaking of the bridges between proplatelets and preplatelet release in the bloodstream (Machlus and Italiano, 2013). Successively, proplatelets circulating fragments, also defined as preplatelets, form single platelets thanks to the hydrodynamic forces that promote and accelerate their cleavage in sinusoids (Junt et al., 2007).

Each MK releases hundreds of virtually identical-sized platelets into the circulation, and platelets count ranges from 150 to 400 × 10^9 platelets/L of blood. Since platelet lifespan is relatively short, only 8–10 days until clearance by liver and spleen, 100 billion new platelets are produced daily from bone marrow megakaryocytes to maintain normal platelet count (Kaushansky, 2006). Under inflammatory conditions or acute platelet demand, MKs increase the basal platelet production more than 10-fold to maintain the homeostasis. In these conditions, platelet release also occurs via direct rupture of the mature MK membrane (Nishimura et al., 2015).

Physiologically, platelets circulate in their quiescent form (non-adherent “resting” state), with a typical flat, discoid shape. Upon stimulation, platelets undergo a rapid morphological change and cytoskeletal reorganization, as they convert from their resting discoid shape to rounded or spheroid form with finger-like filopodia and pseudopods (Figure 10).

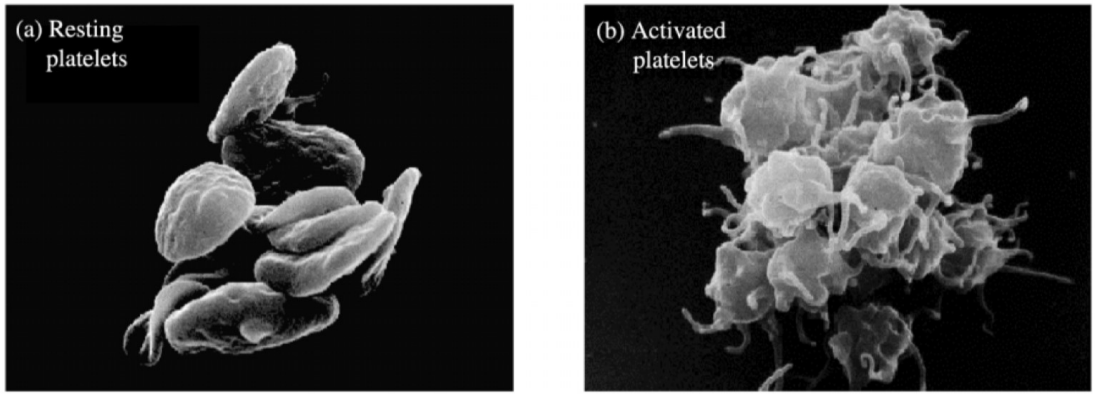

Figure 10. Platelet activation induces morphological changes. A) Resting discoid platelets, B) Activated spherical platelets with several pseudopods (Willoughby et al., 2002).

Given their peculiar structure, platelets play an essential role in haemostasis, regulating the formation of a plug at the site of vascular lesion to prevent bleeding. Platelets are also involved in inflammation, immune response, and tissue repair (Machlus and Italiano, 2013). Impaired platelet production or functional deregulation have been observed in several pathological contexts, indeed, excessive platelet release (defined thrombocytosis) or activation (platelet hyperreactivity) are usually associated with a higher thrombotic risk (Lippi et al., 2011); while reduced platelet count (thrombocytopenia) and altered platelets function, due to acquired or inherited defects (Carubbi et al., 2014), might compromise wound healing, resulting in an increased risk of bleeding and haemorrhagic disorders (Vinholt et al., 2019).

4.1 Platelets functions and their role in Functional aspects and role of platelets in atherosclerosis

The most relevant physiological role of platelets is primary haemostasis. Upon vascular injury, platelets response can be subdivided into three closely related steps: adhesion, activation, and aggregation (Nieswandt et al., 2011). Single platelets circulate at high-shear rates and are activated following binding through specific membrane receptors to cellular and extracellular matrix constituents exposed towards the vessel lumen after vascular injury. Platelet adhesion is mediated by the interaction between platelet glycoprotein GPIbα and GPVI, with von VWR and collagen, respectively (Polanowska-Grabowska et al., 1999; Moroi et al., 1996; Xu et al., 2016). The GPIb/vWF binding is not sufficient to mediate stable adhesion but it allows the close contact between platelets and endothelium. During this "rolling," platelets may bind other thrombogenic ECM proteins, as collagen, through GPVI. Stable adhesion triggers platelet activation, typified by a series of events as membrane and cytoskeleton rearrangements, shape changing, calcium mobilization, activation of integrin αIIbβIIIa (GPIIb–IIIa) (Li et al., 2010), and phosphatidylserine (PS) externalization (Lentz, 2003). GPVI binding to collagen results in activation of several intracellular signalling cascade, including PI3K/PLCγ2-IP3/PKCs, PI3K/AKT and G protein–mediated signaling pathways, which are involved in platelet degranulation and aggregation (Varga-Szabo et al., 2008). The activation of intracellular signals induces conformational changes of platelet integrins ("inside-out" activation), as αIIbβIIIa, leading to a high-affinity state and promoting the secretion of secondary mediators as adenosine diphosphate (ADP) and thromboxane A2 (TXA2), previously packaged in platelet granules (Jin et al., 2002). ADP and TXA2, together with locally produced thrombin, contribute to platelet aggregation and amplify platelet pro-coagulant activity. In this context, ROS have been widely studied, highlighting their double role as product of activated platelets and triggers of platelet activation (Masselli et al., 2020). Consequently, additional platelets and other immune cells are recruited in correspondence of vascular injury to promote the formation of a plug and to inhibit bleeding. Platelet-leukocyte aggregates (PLAs) (including platelet-neutrophil, platelet-lymphocyte, and platelet-monocyte aggregates) are considered as one of the most sensitive markers related to platelet activation and are associated to several cardiovascular diseases (Gremmel et al., 2016).

Newly formed platelet aggregates are stabilised by fibrinogen and fibrin, the end-products of the coagulation cascade. The aggregation of adjacent platelets involves multiple platelet receptors, such as αIIbβIIIa and the C-type lectin-like receptor 2 (CLEC-2) (Lisman et al., 2005; May et al., 2009).

Platelet-mediated plug formation is crucial to prevent post-traumatic blood loss and to ensure primary haemostasis. However, the entire process has to be finely tuned, since abnormal platelet

activation and uncontrolled thrombus formation in injured vessels could have life-threatening consequences, resulting in vascular occlusion, ischemia and infarction of vital organs.

Indeed, platelets are critically involved in the onset and progression of atherosclerosis, exerting a plethora of pro-atherogenic activities, and representing an interface between haemostasis, inflammation, and innate immunity (Figure 11).

Platelet adhesion to the exposed matrix in correspondence of plaque rupture is considered the initial step in thrombus formation. Thrombus growth is finely regulated to repair the vascular damage, without obstructing blood flow. However, prolonged and abnormal activation of platelets and other immune cells may induce the development of an occluding thrombus.

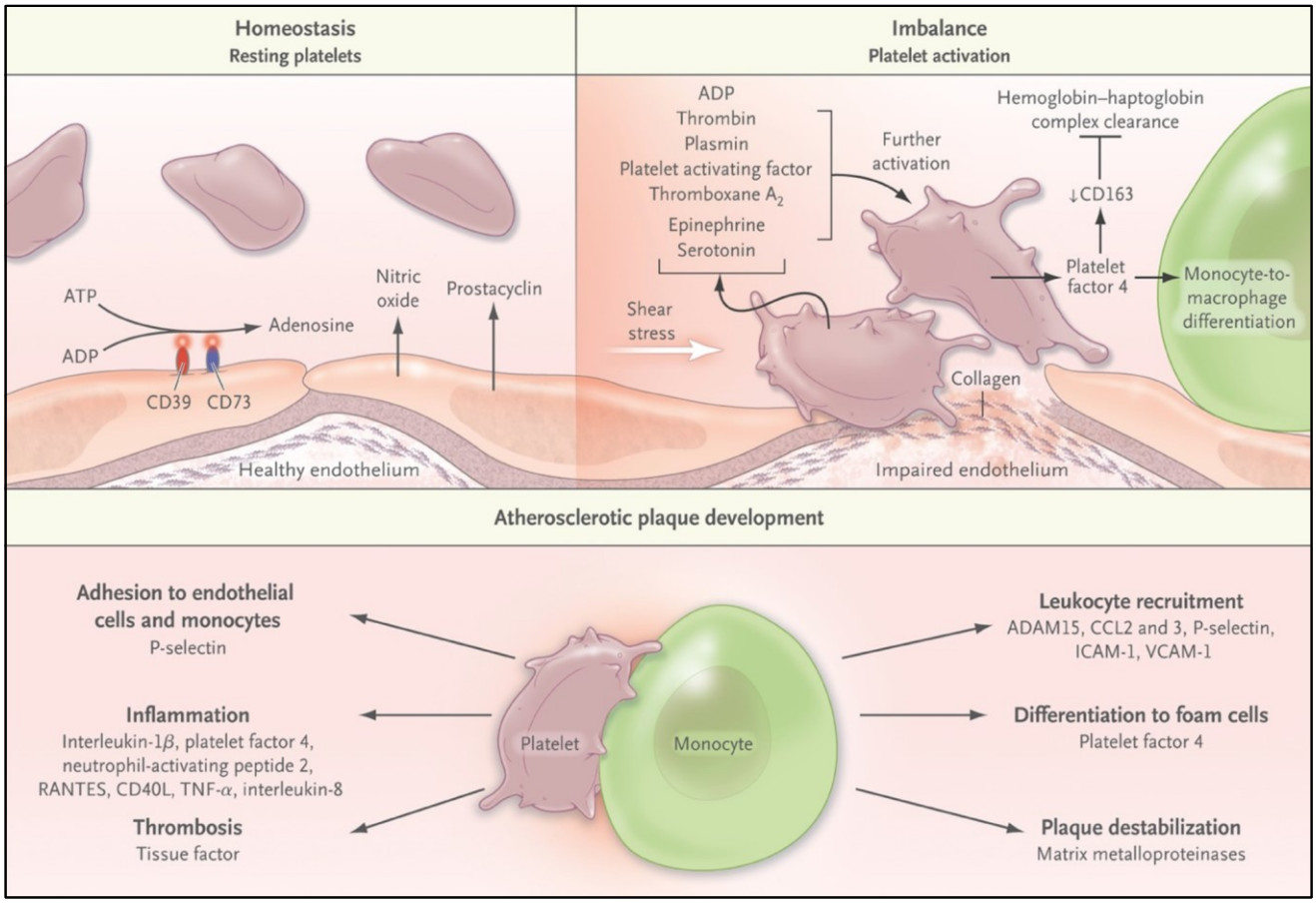

Figure 11. Platelets as key actors in atherosclerosis. Intact endothelium normally expresses CD39 and CD73, to convert the prothrombotic adenosine 5′-triphosphate (ATP) and adenosine diphosphate (ADP) into the largely anti-inflammatory adenosine, preventing platelet activation and aggregation. Healthy endothelium also secretes vasodilators, such as prostacyclin and NO, which have potent anti-adhesive and antiaggregating effects. Upon plaque rupture, prothrombogenic components of the necrotic core, are exposed toward blood vessel lumen, and promote platelets interaction with endothelial cells, and the subsequent platelet activation and aggregation. Platelet release proinflammatory mediators and chemokines to recruit additional platelets and leukocytes to the plaque to support thrombus formation and growth (Borissoff et al., 2011).

Endothelial cells normally control platelet reactivity through inhibitory mechanisms including CD39 (ecto-ATPase) and CD73 (ecto-5′-nucleotidase) Cox-2, PGI2, or prostacyclin systems, but upon inflammation, endothelial cells become more adhesive for platelets. Of note, under pathological conditions, platelets can also adhere to the intact activated vascular endothelium (Varga-Szabo et al., 2008) and contribute to inflammatory processes by facilitating endothelial cell activation and the subsequent leukocyte recruitment (Lindemann et al., 2007). Plaque rupture triggers platelet activation and the release of a great variety of potent inflammatory and mitogenic molecules into the surrounding microenvironment, which in turn enhance the adhesive, chemotactic, and proteolytic properties of endothelial cells (Gawaz, 2004), amplifying inflammatory response and immune cell recruitment. IL-1β is secreted by platelets during degranulation and acts on endothelial cells to induce a further release of inflammatory mediators as IL-6, IL-8 (Kaplanski et al., 1994), and chemokines CCL2 (Gawaz et al., 2000). Moreover, platelet-derived platelet activating factor (PAF), RANTES and macrophage inflammatory protein (MIP-1α) promote chemiotaxis of leukocytes, while TGF1β and platelet derived growth factor (PDGF) favour smooth muscle cell proliferation within the plaque. Besides interleukins and chemokines release, the only deposition of platelets on endothelial walls, even a single layer of platelets, acts as a stimulus for smooth muscle cell proliferation and fibrotic tissue component production within the plaque (Jawien et al., 1992). Furthermore, platelet factor 4 (PF4), the most abundant platelet secreted protein, acts as a chemoattractant for monocyte, and polarizing factor for macrophages (Gleissner, 2012). Moreover, PF4 promotes the retention of lipoproteins in the endothelium. Indeed, PF4 may support the retention of LDL on endothelial cell surface by inhibiting its degradation and enhancing esterification of oxidized-LDLs (oxLDL), well known pro-thrombogenic factors (Sachais et al., 2002). In transgenic mice lacking PF4, a significantly reduction of vulnerable plaque was observed, suggesting the pro-atherogenic property of platelet products (Eslin et al., 2004).

In addition to the abnormal production of pro-inflammatory factors, others platelet alterations have been observed in atherosclerosis, ACS and AMI. Several studies have reported that AMI patients usually show higher circulating platelet count and larger platelets. Higher platelet count has been associated with higher risk in thrombotic events and higher rate of adverse clinical outcome in STEMI patients, including arrhythmia, heart failure, and death (Paul et al., 2010). In addition, circulating platelets are heterogeneous in size, density, and reactivity. Mean platelet volume (MPV) is the most widely measure used to assess platelet size. Of note, newly produced platelets or immature platelets usually show elevated MPV. Tong and colleagues demonstrated that platelets produced under conditions of forced platelet production (defined as “stress platelets”) showed an increased MPV as compared to normal circulating platelets (Tong et al., 1987). Moreover, larger platelets were found to be metabolically and enzymatically more active (Karpatkin et al., 1969), and to display a pro-thrombotic phenotype (Kamath et al., 2001). The elevated MPV has been

associated with other markers of platelet reactivity, as the increased expression of adhesion molecules, platelet aggregation, thromboxane synthesis and β-thromboglobulin release (Kamath et al., 2001). In cross-sectional studies involving 2,809 patients with chest pain, Chu and co-workers observed that MPV was significantly higher in those with AMI than those without AMI, and elevated MPV was associated to poor outcome and higher rate of mortality following the acute event (Chu et al., 2009). This correlation suggests an alteration of platelet production from megakaryocyte, which probably occurs a few days before the acute event. Furthermore, platelet hyperreactivity has been associated to a high predisposition to thrombotic events. Indeed, patients with STEMI have significantly enhanced platelet function when measured under high shear rates by PFA-100, and platelet hyperreactivity appears to correlate to cTnT and CK-MB, and thus to myocardial necrosis (Frossard et al., 2004). Biomarkers of platelet activation, as CD62p, CD63 and PAC1, as well as platelet capacity to form aggregates with leukocytes, were found elevated in thrombotic disorders and in many pathological conditions, associated to cardiovascular events, such as diabetes mellitus, smoking, hypertension, hypercholesterolemia (Willoughby et al. 2002; Ferroni et al., 2004; Gkaliagkousi et al., 2010; Wang and Tall, 2016).

Further evidence of platelet role in atherosclerosis, from the plug development to the thrombus formation, are provided by the ability of antiplatelet and anticoagulant drugs in reducing cardiovascular events (Meadows et al., 2007). Indeed, clinical trials on various antiplatelet drugs, as aspirin, glycoprotein GPIIb/IIIa inhibitors (Roffi et al., 2001) and clopidogrel (Yusul et al., 2003) demonstrated substantial therapeutic efficiency in patients with ACSs.

4.2 Platelet gene expression profile

Human platelets are anucleate blood cells and are therefore unable to translate DNA. Platelets inherit a specific set of mRNAs from their MK progenitors and maintain functionally intact machinery for protein synthesis including rough endoplasmic reticulum and polyribosomes translational capabilities. Thereby, platelet transcripts are largely produced in MK precursor, but they are physiologically active in platelets, which may translate RNAs, regulating protein/RNA levels (Weyrich et al., 2004). It has been suggested that each platelet contains just 0.002fg mRNA (~12,500-fold less than a nucleated cell) (Fink et al., 2003). Besides mRNA, platelets inherit also long-noncoding RNA (lncRNA) and micro-RNA (miRNA), which are non-encoding transcripts of about 200 and 22 nucleotides, known to regulate several cell functions.

Bugert and colleagues provided a complete mRNA profile of human platelets in physiological conditions using microarray hybridization. More than 10,000 transcripts, which are expressed in MKs, have also been detected in platelets (Bugert et al., 2003). Microarray analysis of gene expression profile of isolated platelets allows to identify transcripts that encode for surface receptors and glycoproteins, as well as proteins involved in metabolism, signalling, inflammation, and immunity (Gnatenko et al., 2003).

Since changes in mRNA in platelets mirror what occurs in MKs, platelet transcriptome profiling has been suggested of potential utility as a diagnostic, prognostic, or even therapeutic strategy in clinical setting. Indeed, gene expression profiling by microarray technologies has been successfully applied to study the transcriptional changes that occur in tissues as blood cells, endothelial cells, and heart to unravel the complex gene expression pictures underlying pathological conditions (Nanni et al., 2006).

Concerning platelets, resting platelets are generally characterized by a minimal translational activity. However, platelet activation can induce protein synthesis of various platelet proteins (Weyrich et al., 1998). Furthermore, reticulated platelets have been found to retain larger amounts of mRNA and to show a greater capacity for protein synthesis. Since reticulated platelet production has been associated to higher thrombotic risk, it has been suggested that the increase in mRNA content correlates with a more pro-thrombotic platelet phenotype (Rinder et al., 1998). In a recent study by Bongiovanni and co-workers, 1,744 differentially expressed genes (DEGs) (1,074 upregulated and 670 downregulated) have been found in reticulated platelets as compared to mature platelets. The most abundant transcripts were those that account for the collagen receptor *GP6*, thromboxane receptor A2 (*TBXA2R*), thrombin receptor *PAR4* (*F2RL3*), and adenosine triphosphate receptors involved in calcium signalling (*P2RX1*, *ORAI2*, and *STIM1)*, suggesting a more pro-thrombotic phenotype in newly formed platelets (Bongiovanni et al., 2019).

More recently, several studies have suggested that platelet gene expression profile might also be indicative of platelet state or platelet function alterations (Gnatenko et al., 2009; Nagalla et al., 2011).

Platelets participate in different phases of atherosclerosis development and mainly in the events that immediately precede the thrombotic events; thereby the idea of investigating platelet transcriptome to identify the differentially expressed gene (DEG) that typified ACSs as STEMI and NSTEMI, and stable angina has emerged. Currently, few studies are available. Microarray analysis of platelets transcripts on 14 patients with stable angina and 15 NSTEMI, identified 45 DEGs. Of these, only 3 genes, *BAIAP2*, *CLTA*, and *GP1BB,* were significantly more expressed at both mRNA and protein levels in NSTEMI as compared to stable angina (Colombo et al., 2011). Healy et al., demonstrated that platelets isolated from STEMI and coronary artery disease patients contained 54 DEGs, with *CD69* and *MRP-14* as the strongest discriminators. Plasma levels of MRP-14 were also increased in STEMI patients and represented an independent predictive factor for future cardiovascular events (Healy et al., 2006). Moreover, a recent work by Eicher and colleagues, detected 9,565 expressed transcripts in platelets of AMI patients using transcriptome sequencing (RNAseq). Most of them were involved in platelet-related pathways, including wound response, haemostasis, and platelet activation, and actin-related processes. Among these platelet transcripts, *FBXL4, ECHDC3, KCNE1, TAOK2, AURKB*, *ERG*, and *FKBP5* were significantly higher, *MIAT, PVRL3, and PZP* lower expressed in STEMI platelets as compared to NSTEMI (Eicher et al., 2016).

However, an AMI-specific platelet mRNA pattern has not yet been found. Furthermore, the mechanisms underlying the altered gene expression profile or selected modifications in discrete subsets of platelet mRNA during rapid platelet turnover or in pathological conditions remain unknown.

Therefore, further studies are needed to demonstrate that platelet gene expression profile can be a predictive marker of cardiovascular risk.

5. Flow cytometry in the study of platelet biological functions

Flow cytometry (FCM) is a rapid and effective technique for studying platelets. Indeed, FCM allows a rapid analysis of platelet turnover and count as well as structure parameters, antigen expression, activation state, interaction with other blood components, and response to agonists. FCM platelet analysis is widely used in both experimental and clinical settings, for the diagnosis of cases of suspected thrombocytopenia and thrombocytopathies. It is also a relevant tool for the evaluation of the effects of antiplatelet drugs and of circulating platelets number or activation in pathological conditions associated to high risk of thrombotic events.

FCM is a versatile and reliable tool for the study of cell phenotype, based on its ability to rapidly acquire numerous events in a few seconds. Information on cell dimension and complexity can be easily obtained evaluating forward and side light scatter (FSC and SSC) properties of the population of interest. Furthermore, a wide range of antibodies or cell-permeable fluorescent dyes are now commercially available to study cell immunophenotype, cell activation, cell–cell interaction, and apoptosis.

Considering platelets, FCM represents a non-invasive technique that requires an extremely reduced volume of blood sample. Since platelet concentration in human peripheral blood ranges from 150 to 400×10^9/L, and acquisition of 5,000 to 10,000 events is recommended in FCM, only 5 µL of peripheral blood is generally sufficient for an adequate analysis.

The starting material for platelet study by FCM is represented by either whole blood, platelet-rich plasma (PRP), or washed platelets. In order to maintain their physiological environment, limit operator handling and prevent *ex-vivo* artefacts, whole blood is highly recommended as the main platelet source. In addition, other advantages of FCM technique are represented by rapid acquisition of large datasets and sample processing, and the possibility to integrate complementary information (Carubbi et al. 2014).

One of the main applications of FCM concerns the evaluation of platelet markers of activation at basal state or after stimulation with platelet agonists. Upon activation, platelets undergo morphological changes that can be identified in FSC/SSC morphological plot; and alterations in surface antigen expression and granule release (Figure 12). Many biomarkers of platelet activation can be evaluated by FCM and they can be classified into **surface markers** (including P-selectin, the activated form of αIIbβIIIa, lysosomal integral membrane protein, GPIV) and **intracellular markers** (including serotonin and vasodilator-stimulated phosphoprotein-VASP). The two mainly studied surface antigens that reflect platelet activation are P-selectin (or CD62P) and the αIIbβ3 complex (Shattil et al. 1987; Stenberg et al. 1985). CD62P is contained in the α granules of resting

platelets but is expressed on platelets membrane after degranulation to mediate neutrophils and monocytes adhesion. The αIIbβ3 complex is receptor that mediates the binding with fibrinogen, vWF and fibronectin upon activation it undergoes a conformational change that allows its recognition by the monoclonal antibody PAC1 (Carubbi et al. 2017). FCM evaluation of platelet activation markers can be applied to monitor patient outcome or response to anti-platelet or anti-coagulant therapies.

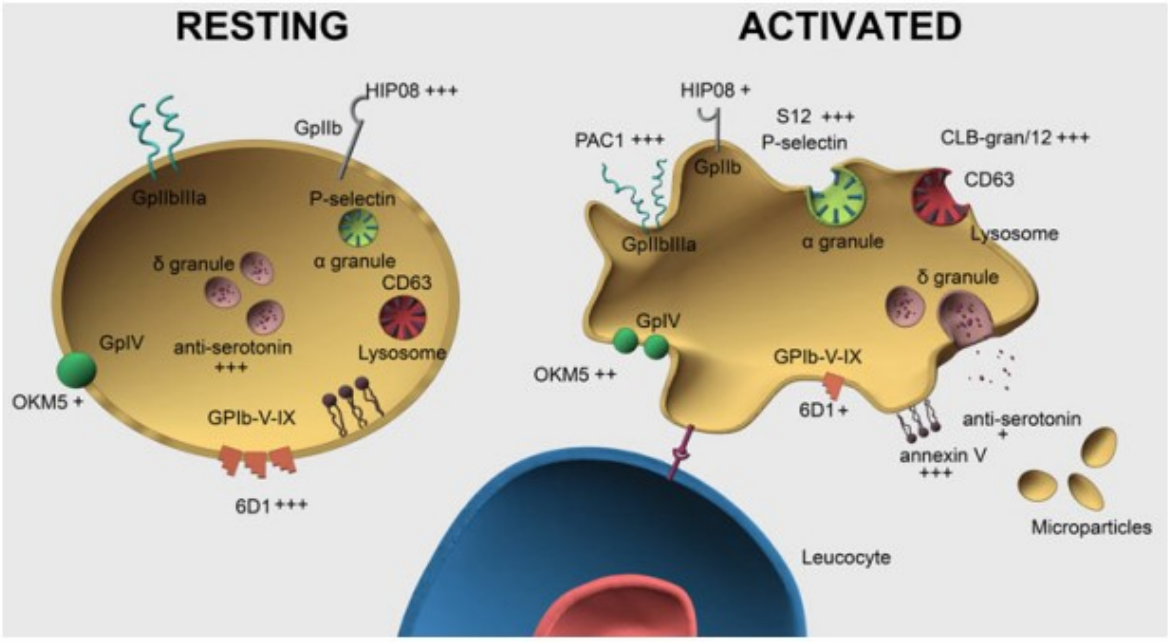

Figure 12. Biomarkers in resting and activated platelets (Carubbi et al, 2017).

FCM can also be used to evaluate intracellular markers, as specific δ-granule components (serotonin and adenine nucleotides) and specific protein or phosphoproteins.

In addition, the FCM is used to assess platelets aggregability, identifying aggregates platelets/leucocytes aggregates (PLA) and platelet microvesicles (MVs) or microparticles (MPs), which are consider both markers of platelet activation (Italiano et al., 2010). An increased level of circulating PLAs has been reported in pathological conditions and it is considered a biomarker for microvascular damage in ischemic stroke, diabetes mellitus (Elalamy et al. 2008) and coronary artery disease (Furman MI et al. 1998). FCM detection of PLAs is based on the combination of platelet markers as CD41, CD42 and/or CD61; and monocyte-specific antibody able to recognize CD19; or leukocyte-specific antibody, which recognizes CD45 (lymphocytes), CD3 (T-lymphocytes), and CD19 (B-lymphocytes).

The FCM is also used to discriminate between “young” and “older” platelets, based on their mRNA content. Platelet mRNA, inherited from their progenitor cells, is high unstable, and progressively denatures during platelet lifetime. The analysis of the thiazole orange (TO) uptake is widely used to identify newly released platelets from bone marrow, namely reticulated platelets (Kienast and Schmitz, 1990). TO is a fluorescent dye, which intercalates nucleic acids, and thus stains platelet mRNA.

FCM evaluation of platelet activation markers can also be applied to monitor patient outcome or response to anti-platelet or anti-coagulant therapies.

6. PKCε: structure and functions

Protein kinase C epsilon (PKCε) is a novel PKC, a family of closely related serine/threonine kinases involved in a variety of biological physiological and pathological processes as cell growth, differentiation, cell cycle, apoptosis, migration, inflammation, immune response, and oncogenesis (Akita, 2002; Mackay and Twelves, 2007).

PKC family members are generally composed of a N-terminal regulatory domain and a C-terminal catalytic domain. According to the structural differences within the regulatory domain and to different cofactors required for their activation, PKC isoforms are conventionally divided into three categories (Cameron AJ, Parker PJ. 2010): conventional isoforms, cPKCs (α, βI, βII and γ), novel isoforms, nPKCs (δ, ε, θ and η) and the atypical ones, aPKCs (ζ and λ (murine)/ι (human)).

PKCε is the first discovered and described isoform among the novel PKCs, and it is expressed by several tissues and cells, mainly neuronal, hormonal, and immune cells (Ono et al., 1988; Nishizuka et al., 1988; Schaap and Parker, 1990).

PRKCE gene is mapped on chromosome 2p21, its sequence is highly conserved and encoded for a protein of 737 amino acids (Schaap and Parker, 1990).

Primary protein structure shares many structural features with the other members of the PKC family. PKCε is a single polypeptide, it is composed by an N-terminal regulatory region (approximately 20-40 kDa) and a C-terminal catalytic region (approximately 45 kDa) separated by a hinge region. The C-terminal catalytic domain contains the ATP-binding site (C3 domain), enriched in purines, the substrate-binding site (C4 domain) and three key phosphorylation sites that are indispensable for PKC functions. The N-terminal regulatory domain contains a C2-like phospholipid binding domain, a C1 domain containing two cysteine-rich motifs that bind diacylglycerol (DAG) and others phorbol esters. The C1 and C2-like domains show an opposite order as compared to the others PKC isoforms (Figure 13).

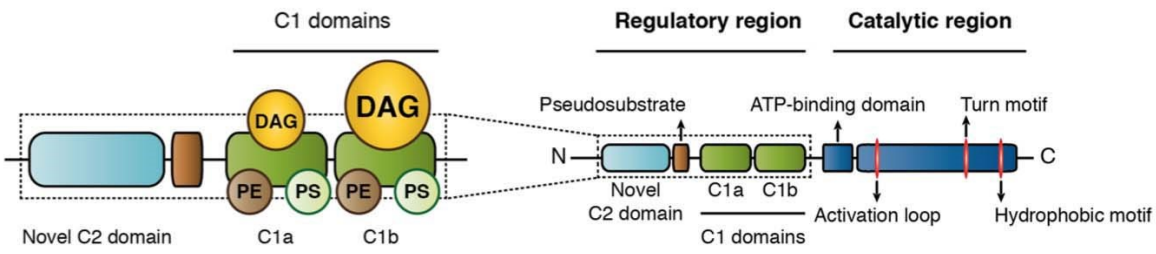

Figure 13. Representative primary structure of PKCε (adapted from Merida et al., 2019).

In addition, nPKC C2-like domain lacks the residues that mediate Ca^{2+} binding, thus it prevents Ca^{2+}-dependent activation of this subfamily of PKC (Giorgione et al., 2006). The N-terminal domain has a dual function: it regulates the kinase activity by an auto-inhibitory sequence and drives the kinase to the appropriate cellular compartment (Newton, 1995).

As other PKC isozymes, PKCε requires a process of priming to display full enzymatic activity and respond to allosteric second regulators. Priming of PKCε occurs through the phosphorylation of three conserved sites: Thr-566 in the activation loop, Ser-729 in the C-terminal hydrophobic site, and Thr-710 in the turn motif. Phospholipid-dependent kinase 1 (PDK1) generally phosphorylates Thr-566, whereas Ser-729 and Thr-710 are autophosphorylated in PKCε (Takahashi et al., 2000). However, experimental evidence indicates that mammalian target of rapamycin complex 2 (mTORC2) may trans-phosphorylates these latter sites (Facchinetti et al., 2008).
Three additional residues (Ser-234, Ser-316, and Ser-368) have been identified in PKCε sequence, which undergoes auto-phosphorylation *in vitro*; however, in viable cells, these residues are trans-phosphorylated by conventional PKC isozymes (Durgan et al., 2008).
PKCε immature forms (non- or hypo-phosphorylated) are associated directly with anchoring proteins such as CG-NAP (centrosome and Golgi localized PKN-associated protein) that localizes PKCε to the Golgi/centrosome area, and the phosphorylation of Thr-566 and Ser-729 residues seems to occur in these compartments (Takahashi et al., 2000).

Priming of PKCε increases the affinity for cell membrane, and induces the release of the pseudosubstrate, allowing PKCε to translocate from the cytosol to the plasma membranes or to other subcellular compartments, where the kinase can interact with its receptors for activated C-kinase (RACK) (Schechtman and Mochly-Rosen, 2001). Bound to RACK, mature PKCε (fully phosphorylated) may be subsequently activated by several different second messengers, including DAG, phosphatidylinositol 3,4,5-trisphosphate (PIP3) and fatty acids as platelet-derived growth factor (PDGF) and bradykinin (Moriya et al., 1996; Graness et al., 1998). According to the second messenger that binds the kinase, activated PKCε translocates then to different specific subcellular compartments. PKCε translocates to Golgi-networks in response to linoleic and arachidonic (AA) acids, while it translocates to the plasma membrane and/or cytoskeleton in response to DAG and tridecanoic acid (Shirai et al., 1998).

PKCε has been widely investigated for its relevant role in physiological cell functions and pathological conditions, regulating cell cycle, proliferation, differentiation in various cellular models (Saurin et al., 2009; Galli et al., 2012; Gobbi et al., 2012; Di Marcantonio et al., 2015; Martini et al., 2018).

Among the other isoforms of the PKC family members, PKCε is considered an oncogene and a tumoral biomarker (Gorin and Pan, 2009; Parker at al., 2020). Indeed, it has been found overexpressed in several types of tumoral cell lines and primary neoplastic cells isolated from bladder, brain, breast, head lung and prostate (Gorin and Pan, 2009), in which PKCε manifests its tumorigenic potential, boosting clone proliferation, expansion and promoting metastasis formation (Griner and Kazanietz, 2007; Parker et al., 2020).

7. PKCε in megakaryocytopoiesis and its ectopic expression in platelets of AMI patients

The members of PKC family have been also investigated in hematopoiesis. The expression of PKC isoforms during hematopoiesis appears to be lineage-specific and partially related to the growth factor response (Bassini et al., 1999).

PKCε has found to play a key role in megakaryocytopoiesis in both normal and pathological conditions. In Dami cells, a human megakaryocytic cell line obtained from a patient with megakaryoblastic leukemia, the expression of PKC isoforms alpha, beta, delta, epsilon, eta, theta, and zeta were detected. Moreover, stimulation of Dami cells with phorbol 12-myristate 13-acetate (PMA), was found to sustain endomitosis and differentiation, regulating the expression of platelet-related proteins, including vWF and glycoprotein GpIb, in a signalling pathway mediated by PKCε (Ballen et al., 1996). Furthermore, Goldfarb and colleagues demonstrated that PKCε cooperates with GATA-1 to promote MK lineage commitment in K562 cell line, a human immortalised myeloid leukemia cell line (Goldfarb et al., 2001). In MK differentiation, PKCε has a precise timing and pattern of expression. Indeed, in *in vitro* culture of primary human CD34+ cells, PKCε expression is induced by TPO at the beginning of MK differentiation, its levels increase until day 6 and then are markedly reduced in the advanced phase of differentiation. The forced expression of PKCε significantly impairs MK differentiation through Bcl-xL modulation, as demonstrating by the down-modulation of MK-specific markers expression and platelet production observed in human CD34+ that overexpressed PKCε (Gobbi et al., 2007).

A prolonged expression of PKCε is instead observed in mature MKs from patients with primary myelofibrosis (PMF). PMF is a Philadelphia chromosome-negative myeloproliferative neoplasm, characterised by impaired MK differentiation and platelet production. Bone marrow MKs from PMF patients are usually hyperplastic, and show typical morphological abnormalities such as reduced size, hypolobated nuclei, and tendency to form tight clusters. Of note, mature MKs, obtained *in vitro* from PMF CD34+, show high levels of PKCε as compared to those of healthy subjects. This exclusive PKCε expression in MKs correlates to impaired platelet production and disease severity.

The inhibition of kinase functions, using siRNA or translocation inhibitors, restores MK *in vitro* differentiation from PMF hematopoietic progenitor cells (Masselli et al., 2015).

Focusing on platelets, PKC family members are involved in several aspects of platelets biology since they regulate platelet production, activation, and degranulation. PKC isoforms are found to exert distinct functions, sometimes opposite functions (Harper and Poole, 2010). Human and mouse platelets predominantly express the conventional PKC isoforms α and β and the novel isoforms δ and θ. In addition, mouse platelets express PKCε, which is virtually absent in human platelets (Pears et al., 2008). PKC activation occurs upon platelet activation and Ca^{2+} mobilization, and their function has been elucidated in murine knockout models. PKCα and PKC β regulates the secretion of dense and α-granules following platelet stimulation with collagen and thrombin, via phospholipase C (PLC) (Konopatskaya et al. 2011; Yoshioka et al., 2001). Indeed, secretion of dense granules and α-granules by collagen and thrombin was almost completely abolished in PKCα$^{-/-}$ murine platelets (Yoshioka et al., 2001). Moreover, PKCθ seems to indirectly promote TxA2 synthesis via regulation of ERK2 (Nagy et al., 2009).
Regarding platelet aggregation, PKC-mediated protein phosphorylation also induces the conformational change of integrin αIIbβIII, which is indispensable for fibrinogen binding. This alternative pathway involves PKC and a guanine nucleotide exchange factor, namely CalDAG-GEFI. However, the exact molecular mechanism is still unclear, since PKC inhibitors also abolish other signalling pathways, known to be involved in αIIbβIII activation (Cifuni et al., 2008). Data on PKCε functions in mouse platelets are instead contradictory. Pears and co-workers observed a drastic reduction in dense granule secretion in response to collagen or collagen-related peptide, in PKCε$^{-/-}$ mouse platelets (Pears et al., 2008). By contrast, Bynagari-Settipalli has reported an increase in ADP-induced thromboxane production, calcium mobilization and ERK phosphorylation, in platelets from PKCε null mice, suggesting a role for murine PKCε in platelet aggregation and thombus formation (Bynagari-Settipalli et al., 2012).
Although data on murine models describe a role for PKC in platelets biology, human platelets lack of PKCε. In addition, PKC isoforms, PKCε and PKCδ, appear to exert antithetical functions in mouse and human model (Pears et al., 2008; Carubbi et al., 2012).

An ectopic expression of PKCε in human platelets has been observed in pathological disorders.
As mentioned above, MKs from PMF patients show elevated level of PKCε even in the final step of differentiation, and they correlate with impair MK differentiation, represented by altered morphology small cell size, reduced expression of megakaryocytic surface markers and markedly impaired or absent proplatelet formation (Masselli et al., 2015). Our research group demonstrated that circulating platelets from patients with primary myelofibrosis displayed elevated levels of activation

markers and the same aberrant expression of PKCε as their precursors. Since platelets are anucleate cells and inherit their mRNA and proteins from their progenitor cells, platelets may inherit the elevated levels of the kinase from MKs in PMF. The results, obtained from 9 PMF and 10 healthy subjects (HD), showed significantly higher mRNA and protein levels of PKCε in PMF platelets, as compared to HD. Of note, patients with at least one previous major cardiovascular event showed significantly higher PKCε levels than those with no previous history of thrombotic events, suggesting the association between higher level of PKCε and the increased platelet reactivity that typified PMF (Masselli et al., 2017).

Moreover, an abnormal PKCε expression was also found in platelets from patients with acute myocardial infarction (AMI). Indeed, Carubbi and colleagues investigated the expression of this kinase in platelets of AMI patients as compared to patients with stable coronary artery disease (sCAD) and healthy controls (HD), demonstrating that only platelets from AMI patients showed significantly higher leves of PKCε. Furthermore, PKCε expression correlates with platelet activation levels: PKCε-expressing platelets display higher levels of CD62p, a well-known marker of platelet activation, upon stimulation with ADP; and enhanced adhesion to sub-endothelial collagen. Thereby these results suggest that higher levels of this kinase account for an increased platelet reactivity. In addition, the forced *ex vivo* overexpression of PKCε in platelets from healthy subjects, mimics what was previously observed in platelets from AMI patients, in particular an improvement of platelet adhesion properties to collagen-coated surfaces under physiologically elevated shear forces.
Interestingly, PKCε expressing platelets are produced *de novo* in patients with AMI, probably concurrently with the acute event, and the ectopic expression of the kinase returns negative after 15 days after the acute events, suggesting PKCε as a predictive marker of AMI (Carrubbi et al., 2012).

Aim

Acute myocardial infarction (AMI) is a leading cause of morbidity and mortality, accounting for around 8% of deaths in the population aged 35-74 years in Italy. Chest pain is AMI most frequent manifestation but also one of the most common causes of emergency department (ED) admittances, but only ~20% of patients receive a final diagnosis of AMI. Indeed, chest pain may be due to several non-cardiac and often “benign” disorders.

Currently, diagnosis of AMI primarily relies on cardiac troponin (cTn) plasma levels, as biomarker of myocardium necrosis. However, cTn assay, even the newly introduced hs-cTnT, has been associated to cardiovascular disorders other than AMI, and it can be influenced by other clinical factors. Moreover, myocardium necrosis is detectable only after the acute events, and therefore patient diagnosis requires prolonged monitoring and serial sampling with indirect consequences on the ED management.

The identification of biomarkers whose levels increase during the whole “peri-infarction” timeframe and not only after myocardial necrosis and that could possibly be informative in a “single-shot rule-in/rule-out asset” is of strategic relevance for a rapid and accurate differential diagnosis of chest pain patients. At the same time, another challenging goal in this field concerns the risk stratification of AMI patients at the initial presentation and the prediction of the acute event, to identify those patients with stable or unstable angina who have a higher risk of AMI and poorer outcome. Several predictive factors have been proposed, but their role and contribution to risk stratification remains to be fully determined. Therefore, a timely diagnosis in chest pain patients, as well as an accurate risk stratification in patients with coronary disorders represent an urgent and relevant clinical priority in both emergency and outpatient setting.

Platelets play a key role in the initiation of atherosclerosis as well as in the final step of thrombus formation. As anucleate cells, they inherit a specific mRNA set from their progenitor cells and they retain the capacity to synthesise protein. Moreover, an increase of platelet turnover and reactivity has been observed in concomitance with the acute events.

Given this background, the aim of my PhD research project is to validate two different approaches for the diagnosis of AMI both based on platelets.

The first one is based on a fast FCM assay to detect intracellular PKCε expression in platelets from chest pain patients. PKCε is virtually absent in normal human platelets, but the ectopic expression of the kinase has been found in platelets of AMI patients, in which it correlates with platelet reactivity.

The second aim is based on the analysis of platelet transcriptome in AMI, sCAD and healthy subjects using microarray technology. Given the peculiar characteristics of platelet mRNA, we hypothesise that platelet gene expression profile could represent a valued predictive biomarker of AMI.

Materials and Methods

Materials and Methods I: PKCε-expressing platelets in chest pain

1 Study population

This study was carried out in collaboration with the Emergency Department (ED) and the Diagnostic Department of Parma University Hospital. The study was approved by the Ethical Committee of Parma University Hospital (Prot. no. 5344), and it was performed according to the Declaration of Helsinki. Each patient was made to sign a written informed consent and was subjected to a peripheral venous blood sampling (10ml in tubes containing 3.8% sodium citrate). Exclusion criteria included age <18 years and the inability to sign a written informed consent. Immediately after sampling, a progressive code number was assigned to each patient for their identification. Patient clinical information and diagnosis were retrospectively collected from patients' medical records. According to the European Society of Cardiology (ESC) Guidelines for the management of acute coronary syndrome (Roffi et al., 2016), the diagnostic workup was performed by the emergency physicians. Final diagnosis of acute myocardial infarction (AMI), ST-segment elevation myocardial infarction (STEMI) or non-ST-segment elevation myocardial infarction (NSTEMI) was confirmed by a cardiologist in accordance with the international clinical guidelines and clinical parameters (Roffi et al., 2016; Ibanez et al., 2018).

2 Routine laboratory analysis

All patients were subjected to clinical examination, electrocardiogram (ECG), chest X-ray, pulse oximetry and routine laboratory tests analysis. At the same time, only 5µL of whole blood was used for flow cytometry (FCM) analysis. Clinical parameters, including red blood cell distribution width (RDW), mean platelet volume (MPV) and C-reactive protein were immediately evaluated after blood sampling, by standardized methods by the Laboratory of Clinical Chemistry and Hematology of Parma Hospital.

Specifically, concentration of serum cardiac troponin I (cTnI) was assessed at the first admission at the ED (T0) and after 3 and 6 to 9 hours, according to the clinical protocols. Serum cTnI levels were measured by Beckman Coulter Access Accu-TnI+3 immunoassay using the UniCel DxI 800 platform (Beckman Coulter, Brea, CA, USA). The limit of detection (LoD) and the limit of quantitation (LoQ) at 20% CV are <10ng/L and 20ng/L respectively, as reported by the manufacturer for this chemiluminescent immunoassay. Serum cTnI diagnostic cut-off is 0.06µg/L.

3 Evaluation of PKCε-expressing platelet by flow cytometry

Platelet PKCε expression was evaluated by flow cytometry without centrifugation, which could artificially activate platelets. FCM assay was performed using residual whole blood from patients' samples in 3.8% sodium citrate tube. All samples were processed in blind and, only after FCM data analysis, the final diagnoses were revealed.

For FCM analysis, 5µL of whole blood, diluted 1:20 in PBS (Phosphate-Buffered Saline, Euroclone, Milan, Italy), were labelled with 5µL of anti-human CD3-PECy5 monoclonal antibody (Beckman Coulter, Brea, CA, USA) and 5µL of anti-human CD61-PE monoclonal antibody (Beckman Coulter, Brea, CA, USA) for 15 minutes in the dark at room temperature (RT). After incubation, samples were fixed adding 400µL of Fixation Buffer (BioLegend, San Diego, CA, USA) for 15 minutes at RT, and then permeabilized with 500µL of Permeabilization Buffer (BioLegend, San Diego, CA, USA) for 15 minutes at RT. Finally, samples were labelled with 10µL of anti-human PKCε-FITC rabbit monoclonal antibody (code: NBP2–21823, Novus Biologicals, Centennial, CO, USA). After 30 minutes of incubation, samples were analysed by FC500 flow cytometer and analysed by the Expo ADC software (Beckman Coulter Brea, CA, USA). As isotype controls, samples were stained with mouse IgG-PeCy5, mouse IgG1-PE, and rabbit IgG-FITC.

All samples were stained with anti-human CD61-PE and anti-human PKCε-FITC monoclonal antibodies, and PKCε-expressing platelets (PKCε-expressing PLTs) were identified as $CD61^{+}PKC\varepsilon^{+}$ cells. For each sample, the percentage of $CD61^{+}PKC\varepsilon^{+}$ cells was normalized to the entire platelet population ($CD61^{+}$ cells). On a subset of 53 patients, a triple staining was performed with anti-human CD3-PECy5, anti-human CD61-PE, and anti-human PKCε-FITC monoclonal antibodies. In order to exclude lymphocytes, we labelled samples with anti-human CD3 monoclonal antibody, widely used as T cells marker. The gating strategy was based on the exclusion of the CD3 positive population, and the detection of $CD61^{+}PKC\varepsilon^{+}$ cells on the $CD3^{-}$ population. For each sample, the percentage of $CD3^{-}CD61^{+}PKC\varepsilon^{+}$ was then normalized on the percentage of total $CD3^{-}CD61^{+}$ cell population.

4 Statistical analysis

For statistical analysis, categorical variables were reported as count and relative frequency (percentage), while numerical variables were represented by their median and range. Continuous variables were represented ad mean±SEM of independent experiments, and compared using t test, Mann–Whitney test, One-way Anova and Tuckey test or Kruskal–Wallis test when applicable. Categorical variable comparison was instead assessed by $\chi 2$/Fisher exact test. Moreover,

correlation between PKCε-expressing platelet percentage and serum cTnI levels was assessed using Spearman-rank correlation coefficient. Receiver-operating characteristic (ROC) curves, obtained with PKCε-expressing platelet values, cTnI levels and combination of these two values by logistic regression, were generated to assess specificity and sensitivity for the diagnosis of CP-AMI. The areas under the ROC curve (AUC) were compared as recommended by Hanley et al. (Hanley et al., 1982). All statistical analyses were performed using IBM SPSS statistics 25 and Prism 9 (GraphPad Prism software, San Diego, CA, USA), *P* values <0.05 were considered statistically significant.

Materials and Methods II: Platelet gene expression profile in AMI

1. Study population

This study was carried out in collaboration with the Cardiology Unit of Parma University Hospital and was performed according to the Declaration of Helsinki. The research protocol was approved by the Ethical Committee of Parma University Hospital and all the enrolled subjects were asked to sign a written informed consent. Exclusion criteria included age <18 years, inability to provide informed consent, ongoing treatment with fibrinolytic agents, IIb/IIIa glycoprotein inhibitors, unfractionated or low-molecular weight heparin, oral anticoagulants or anti-platelet drugs (except aspirin) before the arrival at the hospital; documented haematological disease, severe anaemia (Hb levels < 8 g/dL), or any condition that did not ensure optimal participation in the study or that was deemed dangerous for the patient by physicians. For the platelet transcriptome analysis, we enrolled:

- 20 patients with ST elevation myocardial infarction (STEMI): STEMI was defined as “chest pain with electrocardiogram documentation of new ST segment elevation at the J point in two contiguous leads, with the cut-points: ≥0.1 mV in all leads other than leads V2–V3, for which the cut points were: ≥0.2 mV for men ≥40 years; ≥0.25 mV for men <40 years, or ≥0.15 mV for women; or evidence of new left bundle branch block” (Ibanez et al., 2018).
- 20 patients with stable coronary artery disease (SCAD): sCAD was defined as “a documented coronary artery stenosis of >70% in at least one epicardial main artery and documented inducible ischemia and/or symptoms without any characteristic of unstable disease (i.e. troponin elevation, rest angina, new-onset angina, recent onset of moderate-to-severe angina, or crescendo angina)” (Montalescot et al., 2013).
- 20 healthy donors (HD) without a previous documented history of hematological disease, chronic inflammatory, and without cardiovascular disorders or any risk factors for ischemic heart diseases.

The three groups (STEMI, sCAD and HD) were homogenous for gender and age (± 3 years).

2. Sample collection

After inform consent, each patient was subjected to a peripheral venous blood sampling (50ml in vacutainers containing 3.8% sodium citrate). All STEMI samples were collected within one hour from the hospital admission, and within six hours onset of chest pain/symptoms. Whole blood sampling was performed before coronary angiography or any invasive procedure, and before the administration of any anticoagulant or antiplatelet drugs (except for acetylsalicylic acid taken before the arrival at the hospital). The collection of all sCAD and HD samples was planned within one-hour from routine medical examination. All patients were on aspirin therapy but none of them were taking antiplatelet agents, P2Y12 inhibitor or anticoagulants, while all HD were therapy free. All blood samples have been processed within one hour of collection.

3. Platelet purification

Samples were centrifuged at 160g for 20 minutes at RT in order to obtain platelet-rich plasma (PRP). Platelets were then isolated by immunomagnetic negative selection using magnetic microbeads coated with anti-human CD45 antibodies (Dynabeads™ CD45, Invitrogen, Carlsbad, CA, USA), to deplete leukocytes and obtain highly purified platelets, as described by Carubbi et al. (Carubbi et al., 2012). Briefly, PRP was labelled with Dynabeads™ and incubated for 20 minutes at RT on a rotator. PRP was placed in a magnetic field and the leukocyte-depleted platelets (LDPs) were collected as the negative fraction. The highly purified platelets were washed 3 times in PBS+ 0.01% BSA solution, counted, and mRNA cryopreserved adding an appropriate amount of TRIzol™ Reagent (Invitrogen, Waltham, MA, USA), following the manufacturer's protocol. For each sample, a small aliquot of highly purified platelets was used to check platelet purity by flow cytometry and hematoxylin-eosin staining (Figure 14). For flow cytometry assay, purified platelets were stained with anti-human CD41-PECy5 (widely used as a marker for platelets). Only samples with a percentage of $CD41^+$ cells >98% were used for further analysis.

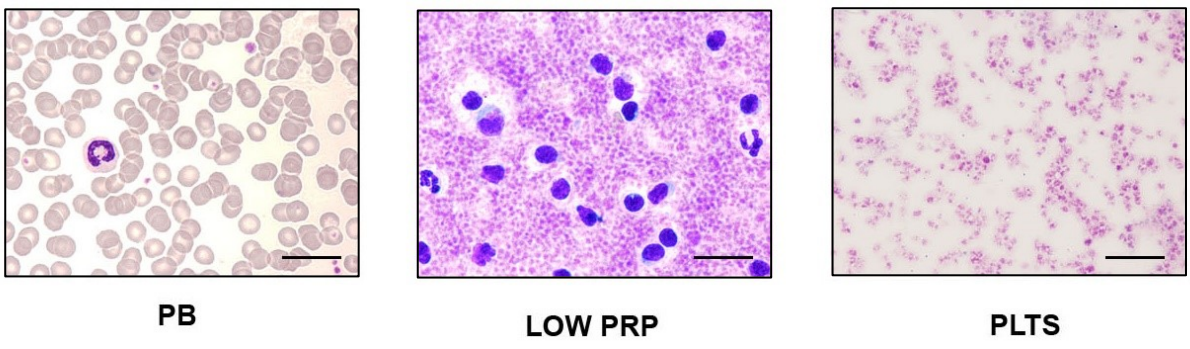

Figure 14. Evaluation of purified platelets by hematoxylin-eosin staining. Representative samples of peripheral blood (PB), low platelets enriched plasma (PRP) and purified platelets (PLTs) after $CD45^+$ cells depletion. Hematoxylin-eosin staining.

4. Microarray hybridisation

Platelet transcriptome profiling was evaluated by microarray assay, performed at the Sidney Kimmel Cancer Centre (Department of Cancer Biology, Thomas Jefferson University, Philadelphia, PA, USA). Platelet RNA was isolated from samples stored in TRIzol™ (Invitrogen, Waltham, MA, USA), according to the manufacturer's protocol. All isolated RNAs were quantified with a Nanodrop ND-100 spectrophotometer (Thermo Fisher Scientific, Waltham, MA, USA), and RNA quality was assessed by Agilent™ 2200 Bioanalyzer™ Instrument (Agilent Technologies, Palo Alto, CA). Amplified and biotinylated sense-strand DNA target from total platelet RNA was generated with the GeneChip WT Pico kit (Affymetrix, Santa Clara, CA, USA). In brief, with the first reverse transcription reaction, total RNA was turned into single-stranded cDNA with a T7-Oligo(dT) promoter sequences at the 5' ends (Figure 15, table 3).

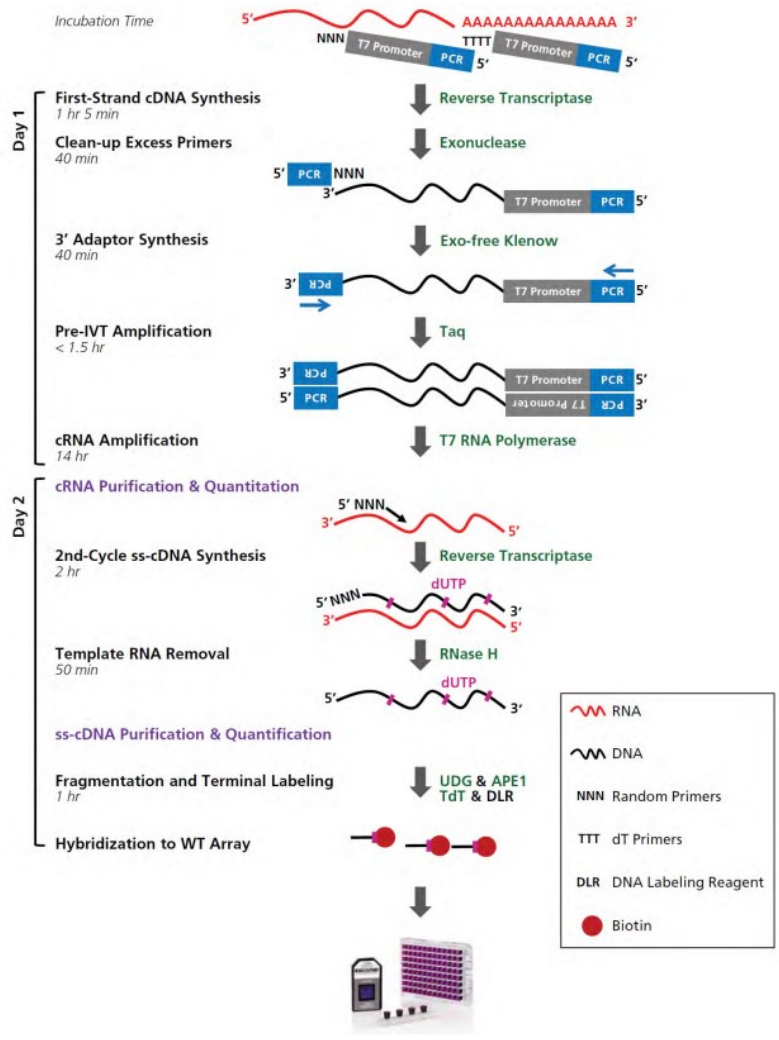

Figure 15. GeneChip™ WT Pico Reagent Kit Amplification and Labeling process workflow (from GeneChip™ WT Pico Reagent Kit user guide, Applied Biosystems).

Then 3' Adaptors were added to single-stranded cDNA, which serves an optimal template for the following synthesis of double stranded cDNA by a pre-T7 *in vitro* transcription (IVT) amplification

reaction. Subsequently, double-stranded cDNA was converted into antisense RNA or complimentary RNA (cRNA) and amplified by in vitro transcription (IVT) using a using T7 RNA polymerase (Van Gelder et al., 1990). cRNA was purified using purification beads and then quantified with a NanoDrop™ spectrophotometers. cRNA size distribution was instead checked with Agilent™ 2100 Bioanalyzer™. Twenty µg of cRNA were then reverse transcribed in a 2nd-Cycle ss-cDNA reaction to obtain sense-strand DNA (ssDNA), containing dUTPs instead of dTTPs. The ssDNA was purified to remove enzymes, salts, and unincorporated dNTPs, quantified, and prepared for the fragmentation and labelling step. The fragmentation reaction was performed treating ssDNA with uracil-DNA glycosylase (UDG) and apurinic/apyrimidinic endonuclease 1 (APE 1) which breaks DNA strand in correspondence to the dUTP incorporated in DNA sequences. Desoxynucleotidyl-transferase (TdT) was then used to label the ssDNA fragment 3' ends with biotin.

Protocol	Heated lid temperature	Step 1	Step 2	Step 3	Step 4	Volume
First-Strand cDNA Synthesis	42°C or 105°C	25°C for 5 minutes	42°C for 60 minutes	4°C for 2 minutes		10 µL
Cleanup	80°C or 105°C	37°C for 30 minutes	80°C for 10 minutes	4°C for 2 minutes		12 µL
3' Adaptor cDNA Synthesis	RT, disable, or left open	15°C for 15 minutes	35°C for 15 minutes	70°C for 10 minutes	4°C for 2 minutes	20 µL
Pre-IVT Amplification	105°C	95°C for 2 minutes	6, 9 or 12 cycles of 94°C for 30 seconds, 70°C for 5 minutes	4°C for 2 minutes		50 µL
In Vitro Transcription cRNA Synthesis	40°C or 105°C[1]	40°C for 14 hours	4°C, hold			80 µL
2nd-Cycle ss-cDNA Synthesis	70°C or 105°C	25°C for 10 minutes	42°C for 90 minutes	70°C for 10 minutes	4°C, hold	40 µL
RNA Hydrolysis	70°C or 105°C	37°C for 45 minutes	95°C for 5 minutes	4°C, hold		44 µL
Fragmentation and Labeling	93°C or 105°C	37°C for 60 minutes	93°C for 2 minutes	4°C hold		60 µL
Hybridization Control	65°C or 105°C	65°C for 5 minutes				variable
Hybridization Cocktail	99°C or 105°C	95°C or 99°C for 5 minutes	45°C for 5 minutes			variable

[1] Use 0.2 mL or larger volume tubes or plates when using heated-lid setting at 105°C.

Table 3. Thermal cycler protocols for GeneChip™ WT Pico Reagent Kit Amplification and Labeling process. (from GeneChip™ WT Pico Reagent Kit user guide, Applied Biosystems).

Five µg of fragmented and biotin-labelled cDNA were hybridised on the Affymetrix gene chips using a hybridisation cocktail (Human Transcriptome Array 2.0, Affymetrix, Santa Clara, CA, USA). Process cycle included: target denaturation for 5 minutes at 99°C, followed by 5 minutes at 45°C,

and hybridisation for 16 hours at 45°C with rotation at 60 rpm (Table 3). The hybridized probe array was then washed and stained with a streptavidin-phycoerythrin conjugate using the Affymetrix GeneChip hybridisation wash & stain kit (Applied Biosystems, Waltham, MA, USA) on a Gene Chip Fluidic Station 450 (Thermo Fisher Scientific, Waltham, MA, USA). Finally, microarrays were scanned by Affymetrix Gene Chip Scanner 3000 using the Command Console Software. The signal emitted at 570nm is proportional to the bound target at each location on the probe array. Experiment quality was checked using Expression Console Software v 1.4.1 (Affymetrix, Affymetrix, Santa Clara, CA, USA, www.affymetrix.com).

5. Microarray data processing

The data obtained from the Affymetrix gene level probe-sets (70.523) were processed using Expression Console software (Affymetrix, Santa Clara, CA, USA), with the default configuration. Samples with low-quality controls were excluded from the analysis. The remaining microarray data were processed applying Signal Space Transformation (SST), and then corrected by Robust Multiarray Average (RMA) algorithm, which includes a log2 data transformation and quantile normalization. After internal control probe-set check, only the 6,753 probe-sets that map biological features (genes, non-coding genes, etc.) were maintained for downstream analysis. The data are available at GEO, Accession No. GSE109048.

6. Real-Time Quantitative RT-PCR (qPCR)

Total RNA was extracted from highly purified platelets, stored in TRIzol™ (Invitrogen, Waltham, MA, USA), as previously described (Carubbi et al., 2012). Briefly, TRIzol™-treated platelets were added with chloroform and centrifuged at 12,000 g for 15 minutes at 4°C. The aqueous phase, containing RNA, was transferred in a new tube, and incubated with an equal volume of isopropanol. After incubation, the samples were centrifuged at 12,000 g for 15 minutes at 4°C, to obtain RNA pellets that were washed and resuspended in DEPC-treated water. TOTAL RNA yield and purity was check using a NanoDrop™ spectrophotometer. Samples were then reverse-transcribed using the Superscript-III Reverse Transcriptase (Thermo Fisher Scientific, Waltham, MA, USA) and random hexamers (Promega, Madison, WI, USA), according to manufacturer instructions. We used a semi-quantitative real-time PCR, qPCR, to evaluate the expression gene levels of *CLEC4E, FKBP5, SAMSN1, S100A12* and *S100P* using SYBR Premix Ex Taq II (Takara, Shiga, Japan) and a LightCycler 480 instrument (Roche, Basel, Switzerland). *ACTB* (Actin Beta) and *ITGA2B* (Integrin, Alpha 2b, Platelet Glycoprotein IIb of IIb/IIIa Complex, Antigen CD41) were used as loading control/housekeeping genes. All samples were run in triplicate, and data were analysed with GeNorm software (Vandesompele et al., 2002).

7. Reticulated platelet analysis

We investigated whether newly formed platelets, known to show a pro-thrombotic phenotype, could influence the platelet transcriptome (Bongiovanni et al., 2020). Platelet turnover was evaluated assessing the percentage of reticulated platelets, as previously described (Gonzalez-Porras et al., 2010; Cesari et al., 2013; Hoffmann, 2014). For each samples an aliquot (5µL) of whole blood, collected within six hours of the onset of symptoms, were diluted 1:20 in PBS (Euroclone, Milan, Italy) and incubated with 10µL of mouse anti-human CD41a-PECy5 monoclonal antibody (Beckton Dickinson, San Diego, CA, USA) for 15 minutes at RT in the dark. After the incubation, 400µL of thiazole orange (TO) (50 ng/mL) (Sigma- Aldrich, St. Louis, MO, USA) or PBS (for the negative control) were added and incubated for 45 minutes at RT in the dark. Samples were fixed in paraformaldehyde (2%) and analysed with Epics XL instrument and Expo ADC software (Beckman Coulter, Brea, CA, USA).

8. Statistical analysis

For the statistical analysis of microarray data, differentially gene expression between STEMI vs. HD was evaluated using Transcriptome Console Analysis (TAC) (Thermo Fisher Scientific, Waltham, MA, USA). Firstly, we performed a nonspecific-filtering of data to reduce the high-dimensional data sets, excluding genes that are either not expressed or do not vary among samples, and, at the same time, increase power to detect the differentially expressed genes (DEGs) (Bourgon et al., 2010). We performed a multiple unpaired t test and the DEGs with *P* value <0.05 were considered statistically significant. Heatmap of significantly differentially expressed platelet transcripts (adjusted p value < 0.05, |log2fc| > 1) from STEMI patients and HD, was generated with GENE-E (https://software.broadinstitute.org/GENE-E/). We subsequently restricted the analysis to only DEGs with P value<0.01. With the latter, a multiple was generated to calculate the log-odds ratio of the risk of STEMI. The model was validated applying a bootstrap analysis to discriminate between STEMI and sCAD. The receiver operating characteristics (ROC) curve of this logistic regression model and the related AUCs were generated for the STEMI *vs.* HD and STEMI *vs.* sCAD comparisons. Furthermore, continuous variables are represented as mean ± standard deviation (SD), while categorical variables are reported as frequencies and percentages. The differences between categorical variables were calculated using chi-square or Fisher's exact test, while we used Student's t test or the One-way ANOVA following by Tukey test for the analyses of continuous variables, as appropriate. Correlation analyses were performed by the Spearman rank correlation method. Data from qPCR were analysed using t-test comparing DEGs expression levels between STEMI vs. HD and STEMI vs. sCAD. The analyses were performed using R-scripts on R version 3.3.2 (http://www.r-project.org/).

Results

Results I: PKCε-expressing platelets in chest pain

*From: Carubbi C, Masselli E, **Pozzi G**, Mattioli M, Martini S, Goldoni M, Aloe R, Cervellin G, Vitale M, Gobbi G. Combination of Platelet expression of PKCepsilon and cardiac troponin-I for early diagnosis of chest pain patients in the emergency department. Sci Rep 9, 2125 (2019).*
https://doi.org/10.1038/s41598-019-38624-5

1. Clinical and biological characteristics of study population

For this study, 94 patients, complaining chest pain (CP), were enrolled by the Emergency Department of Parma University Hospital. Five patients were excluded since they voluntarily left the ED without completing their diagnostic process. Biological and clinical characteristics of the n.89 patients at the time of the enrolment are listed in table 4. Fifty-seven out of 89 patients (64.1%) were males, while 32 out of 89 patients (35.9%) were females. Considering the entire population, 12 out of 89 patients (13.5%) received a final diagnosis of AMI (CP-AMI); while in 77 (86.5%) cases, chest pain was due to other causes (CP-noAMI) (Figure 16, panel A; table 4). In the CP-AMI group, 8 patients (66.6%) were males, with a median age of 79 years (range, 53-88 years); whereas in the CP-noAMI group, 49 out of 77 patients were male (63.6%), with a median age of 72 years (range, 24-96 years). Therefore, the two groups were homogeneous for gender and age. Considering the laboratory features, no differences were found comparing red cell distribution width (RDW, 14± 1% *vs.* 14 ± 1%), mean platelet volume (MPV, 9 ± 1fL *vs.* 9 ± 1fL), glycemia (117 ± 34mg/dL *vs.* 146 ± 58mg/dL) or time of symptoms onset (32 ± 59h *vs.* 18 ± 28h). Moreover, the percentage of patients on therapy with anti-platelet drug(s) (such as clopidrogel, ASA or ticagrerol) was comparable in CP-AMI and CP-noAMI groups (Table 4).

	CP-noAMI	**CP-AMI**	**Statistical analysis**
N. of cases evaluated *n (%)*	77 (86.5)	12 (13.5)	
Demographics			
Males, *N (%)*	49 (63.6)	8 (66.6)	ns (Chi Square)
Females, *N (%)*	28 (36.4)	4 (33.4)	
Age yrs., *median (range)*	72 (24–96)	79 (53–88)	ns Mann-Whitney/Wilcoxon
Clinical and hematological characteristics			
RDW, *mean ± SD, %*	14 ± 1	14 ± 1	ns (Student t test)
MPV, *mean ± SD, fL*	9 ± 1	9 ± 1	ns (Student t test)
Glycemia, *mean ± SD, mg/dL*	117 ± 34	146 ± 58	ns (Mann-Whitney/Wilcoxon)
Time of symptom onset, *mean* ± SD, *h*	32 ± 59	18 ± 28	ns (Student t test)
Pharmacological treatment			
Pts on anti-PLT drugs, *n (%)*	27 (42.18)	7 (63.6)	ns (Chi Square)
Pts not on anti-PLT drugs, *n (%)*	37 (57.8)	4 (36.36)	

Table 4. Biological and clinical characteristics of the entire patient population. *H*, hours; *MPV: mean platelet volume; N: number; ns: no statistical significance; PLT: platelets; Pts: patients; RDW: Red Cell Distribution Width; SD: standard deviation; yrs: years*.

Focusing on CP-AMI group, ECG revealed a persistent elevation of ST segment in the 50% of cases (50% of STEMI vs. 50% of NSTEMI) (Figure 16, panel B). In CP-noAMI patients, chest pain was attributed to unstable angina in 6.5% (5/77) of cases, to cardiac causes different from coronary artery disease in 27% (21/77), to non-cardiac causes 36.8% (28/77), and to symptoms of unknown origin in 29.8% of patients (23/77) (Figure 16, panel C).

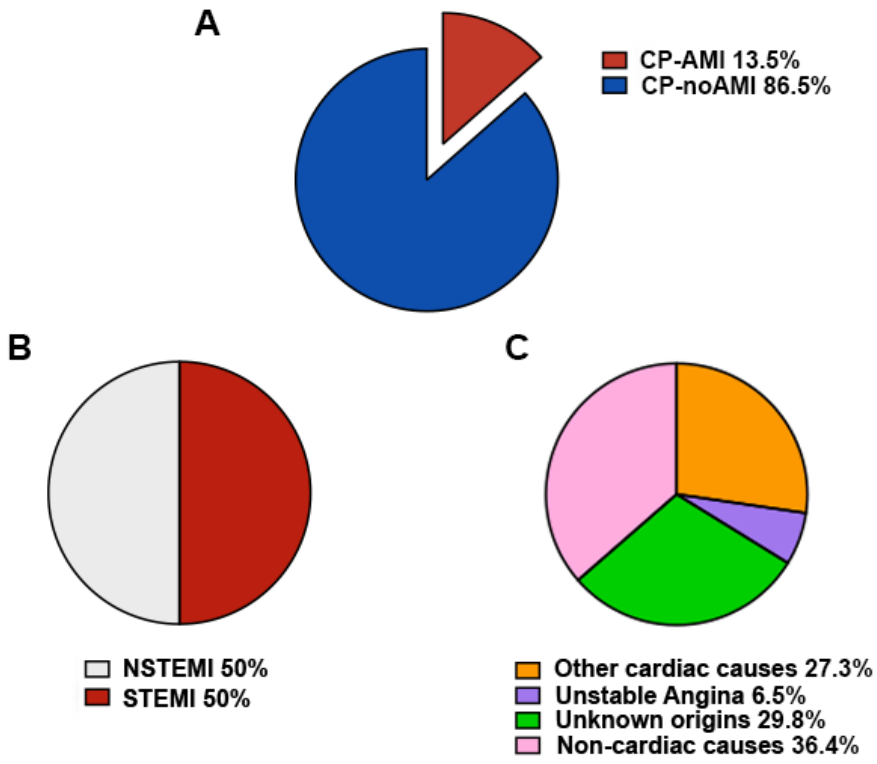

Figure 16. Differential diagnosis of the entire CP patient population. A) Percentage of chest pain patients with (CP-AMI) or without (CP-noAMI) final diagnosis of acute myocardial infarction in the entire study population (n.89); B) Percentage of CP-AMI patients with final diagnosis of ST-segment elevation myocardial infarction (STEMI) and non-ST-segment elevation myocardial infarction (NSTEMI) in CP-AMI patients of the entire study population; C) Percentage of CP-noAMI patients of the entire study population with final diagnosis of unstable angina, cardiac causes different from coronary artery disease, non-cardiac causes, and symptoms of unknown origin.

2. CP-AMI patients show an elevated percentage of CD61+PKCε+ platelets

Evidence from literature have highlighted that PKCε is not expressed in platelets of healthy subjects or in platelets of patients with stable coronary artery disease (Pears et al., 2008), while its expression has been reported in platelets of patients with acute myocardial infarction, suggesting the expression of PKCε in platelets as a predictive biomarker of AMI (Carubbi et al., 2012).

These data have been obtained by techniques that require a long period to complete such as western blot and RT-qPCR assay. These time-consuming techniques are often not suitable for emergency setting. Therefore, we sought to evaluate PKCε expression in platelets using FCM.

We performed a whole blood double staining (n.89 CP patients) with anti-human CD61-PE and anti-human PKCε-FITC mAb and percentage of $CD61^{+}PKC\varepsilon^{+}$ platelets was assessed by FCM (Figure 17). Figure 17 shows a representative gate analysis of a CP-noMI sample (panels A-C) and a CP-MI sample (panels D-F). Since the total number of platelets vary significantly among samples, we normalized the percentage of $CD61^{+}PKC\varepsilon^{+}$ cells on the percentage of total $CD61^{+}$ platelet population. CP-AMI patients expressed a significantly higher percentage of $CD61^{+}PKC\varepsilon^{+}/CD61^{+}$ as compared to CP-noAMI (Figure 17, panel G).

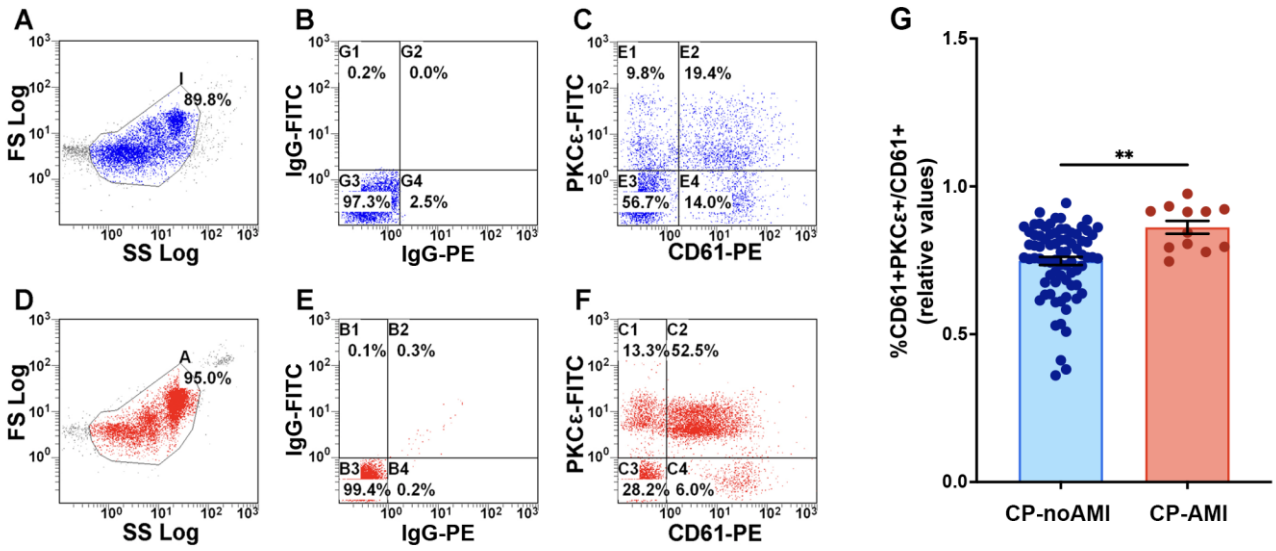

Figure 17. Flow cytometry analysis of PKCε-expressing platelet by double staining. A-F) FCM gating strategy used to detect PKCε-expressing platelets, identified as $CD61^{+}PKC\varepsilon^{+}$ cells, in representative CP-noAMI (panels A-C) and CP-AMI patients (panels D-F). A, D) Morphological gate of whole blood cells referred to the forward scatter (FS Log) *vs.* side scatter (SS Log) parameters. B, E) Isotype control, obtained labelling cells with IgG-PE and IgG-FITC mAb. C-F) CD61-PE and PKCε-FITC expression on whole blood cells. G) FCM analysis of PKCε-expressing platelets, identified as $CD61^{+}PKC\varepsilon^{+}/CD61^{+}$ cell population. Data are reported as mean ± SEM (**, $P<0.01$, Student's t-test).

3. Clinical and biological characteristics of subset population

Considering that i) platelet activation triggers the formation of aggregates between platelets and nucleated cells, such as monocytes or lymphocytes ii) elevated levels of circulating platelet–leukocytes aggregates (PLAs) have been observed in pathological conditions and cardiovascular diseases (Gremmel et al., 2016) and iii) leucocytes express PKCε in normal and pathological conditions, we excluded lymphocytes population using an immunological gate based on a triple staining in a subset of n.53 CP patients. Biological and clinical characteristics of n.53 patients at the time of the enrolment are listed in table 5. Twenty-three out of 53 patients (54,7%) were males, while 24 out of 53 patients (45.3%) were females. In this subset, 8 out of 53 patients (15.1%) received a final diagnosis of AMI (CP-AMI); while in 45 (84.9%) cases chest pain was due to other causes (CP-noAMI). In the CP-AMI group, 5 patients (62.5%) were males, with a median age of 74 years (range, 53-86); whereas in the CP-noAMI group, 24 out of 54 patients were male (53.3%), with a median age of 72 years (range, 29-83 years). Therefore, the two groups were homogeneous for gender and age. Considering the clinical parameters, no differences were found comparing RDW (14± 1% *vs.* 13 ± 1%), MPV (9 ± 2fL *vs*. 8 ± 2fL), glycemia (118 ± 37 mg/dL *vs.* 144 ± 62 mg/dL), or time of symptom onset (25 ± 41h *vs*. 23 ± 31h). Moreover, the percentage of patients on therapy with anti-aggregant or anticoagulant drugs was comparable in CP-AMI and CP-noAMI groups (Table 5).

	CP-noAMI	CP-AMI	Statistical analysis
N. of cases evaluated *n (%)*	45 (84.9)	8 (15.1)	
Demographics			
Males, *N (%)*	24 (53.3)	5 (62.5)	ns (Chi Square)
Females, *N (%)*	21 (46.7)	3 (37.5)	
Age yrs., *median (range)*	72 (29–83)	74 (53–86)	ns Mann-Whitney/Wilcoxon
Clinical and hematological characteristics			
RDW, *mean ± SD, %*	14 ± 1	13 ± 1	ns (Student t test)
MPV, *mean ± SD, fL*	9 ± 2	8 ± 2	ns (Student t test)
Glycemia, *mean ± SD, mg/dL*	118 ± 37	144 ± 62	ns (Mann-Whitney/Wilcoxon)
Time of symptom onset, *mean* ± SD, *h*	25 ± 41	23 ± 31	ns (Student t test)
Pharmacological treatment			
Pts on anti-PLT drugs, *n (%)*	12 (31.6)	3 (42.8)	ns (Chi Square)
Pts not on anti-PLT drugs, *n (%)*	26 (68.4)	4 (57.2)	

Table 5. Biological and clinical characteristics of subset patient population. *H*, hours; *MPV: mean platelet volume; N: number; ns: no statistical significance; PLT: platelets; Pts: patients; RDW: Red Cell Distribution Width; SD: standard deviation; yrs: years*.

In the subset population used for triple staining analysis, AMI was diagnosed in the 15.1% of cases; of which 75% showed a persistent elevation of ST segment with ECG revealed (75% STEMI and 25% NSTEMI). In 4.4% of CP-noAMI patients, chest pain was ascribed to unstable angina, in 31.1% to cardiac causes different from coronary artery disease, in 33.3% to non-cardiac causes and in 31.2% of cases to unknown origin (Figure 18).

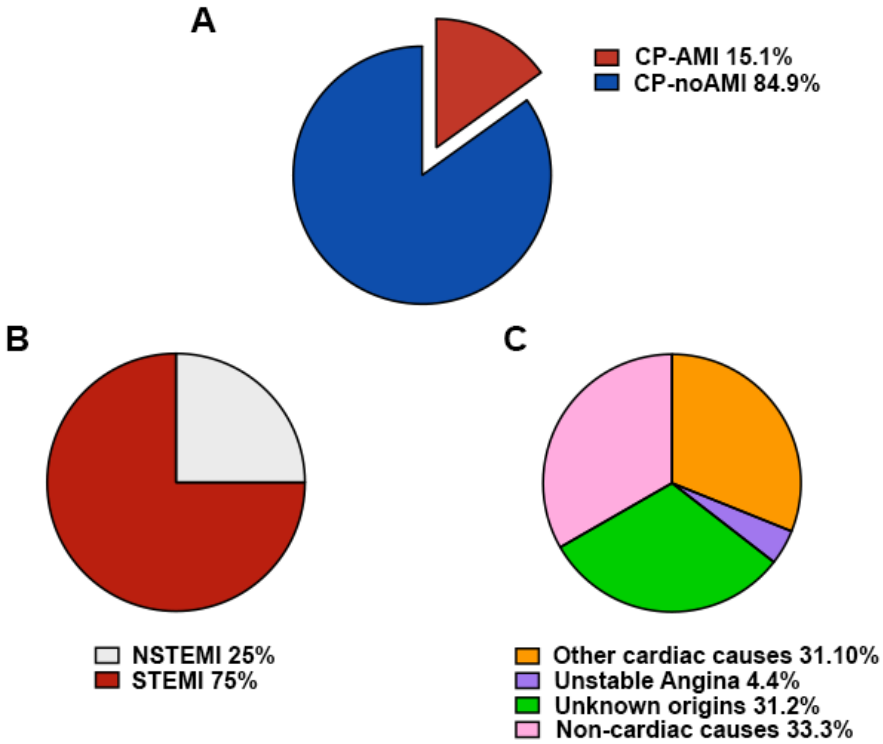

Figure 18. Differential diagnosis of the subset CP patient population. A) Percentage of chest pain patients with (CP-AMI) or without (CP-noAMI) final diagnosis of acute myocardial infarction in the subset study population (n.53); B) Percentage of CP-AMI patients with final diagnosis of ST-segment elevation myocardial infarction (STEMI) and non-ST-segment elevation myocardial infarction (NSTEMI) in CP-AMI patients of the subset study population; C) Percentage of CP-noAMI patients of the subset study population with final diagnosis of unstable angina, cardiac causes different from coronary artery disease, non-cardiac causes, and symptoms of unknown origin.

4. CP-AMI patients show an elevated percentage of CD3-CD61+PKCε+ platelets

In a subset of 53 patients, we performed a triple staining using anti-human CD3, anti-human CD61 and anti-human PKCε mAb, in order to exclude lymphocytes expressing PKCε from the analysis. Figure 19 shows the full gating strategy adopted to evaluate PKCε expression in $CD3^-CD61^+$ cells, in CP-noMI (panels A-C) and CP-MI patients (panels D-F), respectively. Percentage of $CD61^+PKC\varepsilon^+$ was determined on $CD3^-$ gated population, and then normalized to $CD3^-CD61^+$ platelets population. As previously found, the percentage of PKCε-expressing platelets (% of $CD3^-CD61^+PKC\varepsilon^+/CD3^-CD61^+$) was significantly higher in CP-AMI patients as compared to CP-noAMI patients (Figure 19, G).

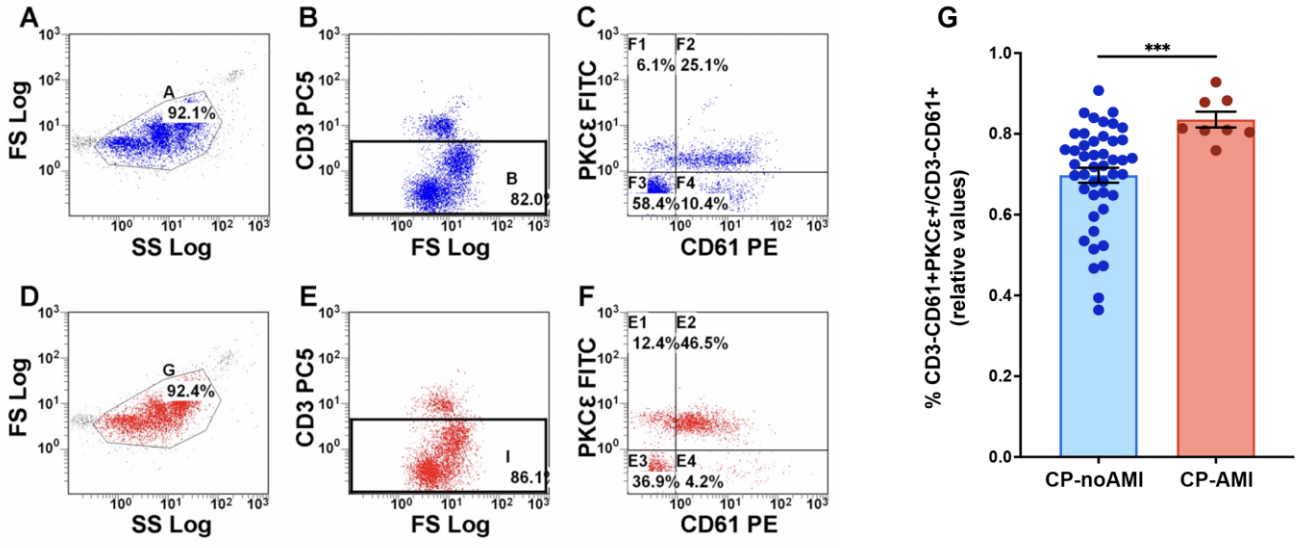

Figure 19. Flow cytometry analysis of PKCε-expressing platelet by triple staining. A-F) FCM gating strategy used to detect PKCε-expressing platelets, identified as $CD3^-CD61^+PKC\varepsilon^+$ cells, in representative CP-noAMI patient (panels A-C) and CP-AMI patients (panels D-F). A, B) Morphological gate of whole blood cells referred to the forward scatter (FS Log) *vs.* side scatter (SS Log) parameters**.** B, E) CD3-PC5 expression on whole blood cells. The gate in black identified $CD3^-$ cell population. C, F) CD61-PE and PKCε-FITC expression on $CD3^-$ gated cells. G) FCM analysis of PKCε-expressing platelets, identified as $CD3^-CD61^+PKC\varepsilon^+/CD3^-CD61^+$ cell population. Data are reported as mean ± SEM (***, $P<0.001$, Student's t-test).

Focusing on CP-AMI patients, we wondered whether there could be differences in PKCε-expressing platelets between STEMI and NSTEMI patients. Stratifying patients according to ECG results, we observed comparable percentage of PKCε-expressing platelets within the two groups in both double and triple staining (Figure 20, panels A, B). Considering CP-noAMI patients, no differences were found in the percentage of PKCε-expressing platelets among patients with chest pain due to causes other than AMI, in both double staining and triple staining (Figure 20, panles C, D).

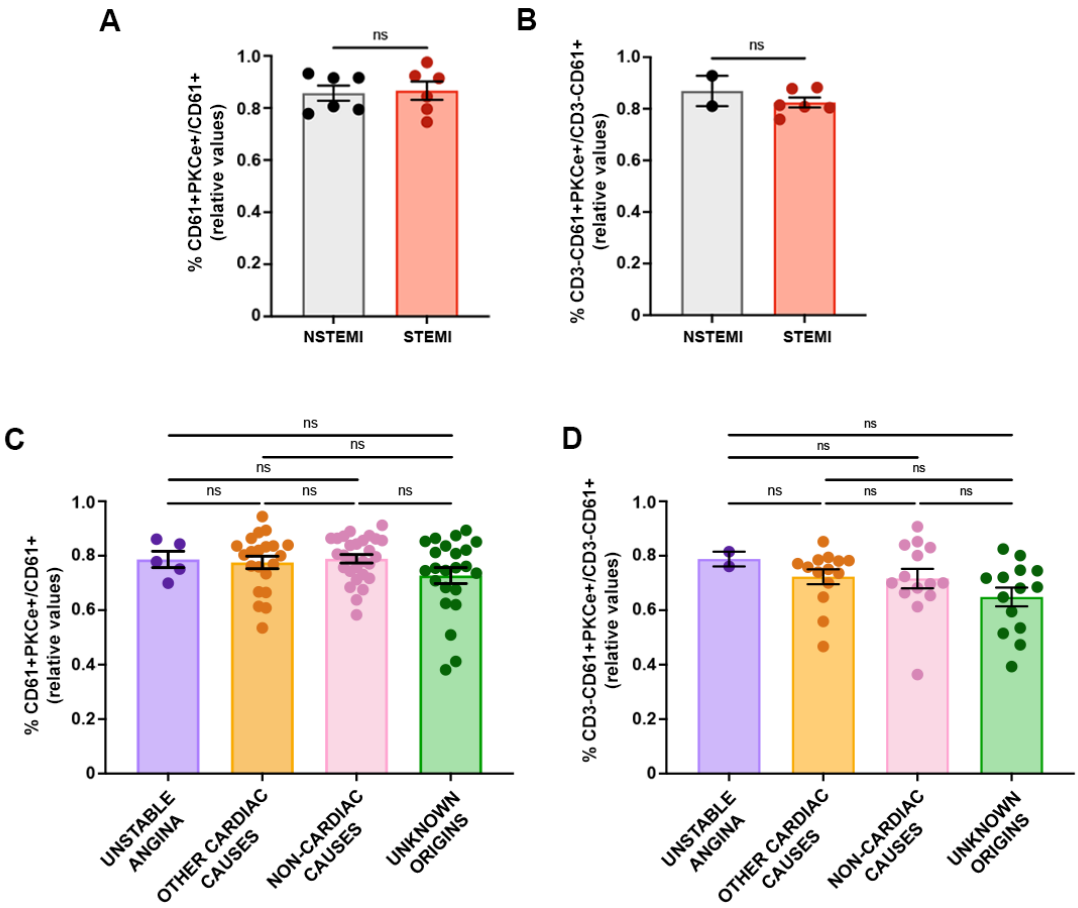

Figure 20. FCM analysis of PKCε-expressing platelets in STEMI *vs.* NSTEMI patients and among subtypes of CP-noAMI patients. A) Percentages of PKCε-expressing platelets assessed by double staining in STEMI (n.6 patients) and NSTEMI (n.6 patients) of the entire patient population. B) Percentages of PKCε-expressing platelets assessed by triple staining in STEMI (n.2 patients) and NSTEMI (n.6 patients) of the subset patient population. C) Percentages of PKCε-expressing platelets, assessed by double staining, in CP-noAMI patients stratified according to the final diagnosis (unstable angina, cardiac causes different from coronary artery disease, non-cardiac causes, and of unknown origin). D) Percentages of PKCε-expressing platelets, assessed by triple staining, in CP-noAMI patients stratified according to the final diagnosis (unstable angina, cardiac causes different from coronary artery disease, non-cardiac causes, and of unknown origin. In double staining, PKCε-expressing platelets are identified as $CD61^{+}PKC\varepsilon^{+}/CD61^{+}$ cells, while in triple staining as $CD3^{-}CD61^{+}PKC\varepsilon^{+}/CD3^{-}CD61^{+}$. Data are reported as mean±SEM (ns, Student's t test and One-way Anova followed by Tukey test).

Furthermore, we asked whether anti-coagulant or anti-platelet drugs could alter PKCε-expressing platelets levels in our cohort of patients. Clinical information were collected retrospectively from medical records. As mentioned above, the percentage of patients on therapy with anti-platelet drug(s) (such as clopidrogel, ASA or ticagrerol) was comparable in CP-AMI and CP-noAMI groups. Moreover, no differences were found in terms of PKCε-expressing platelets among patients on or off therapy with anti-platelet drugs in the entire population, CP-AMI and CP-noAMI groups (Figure 21).

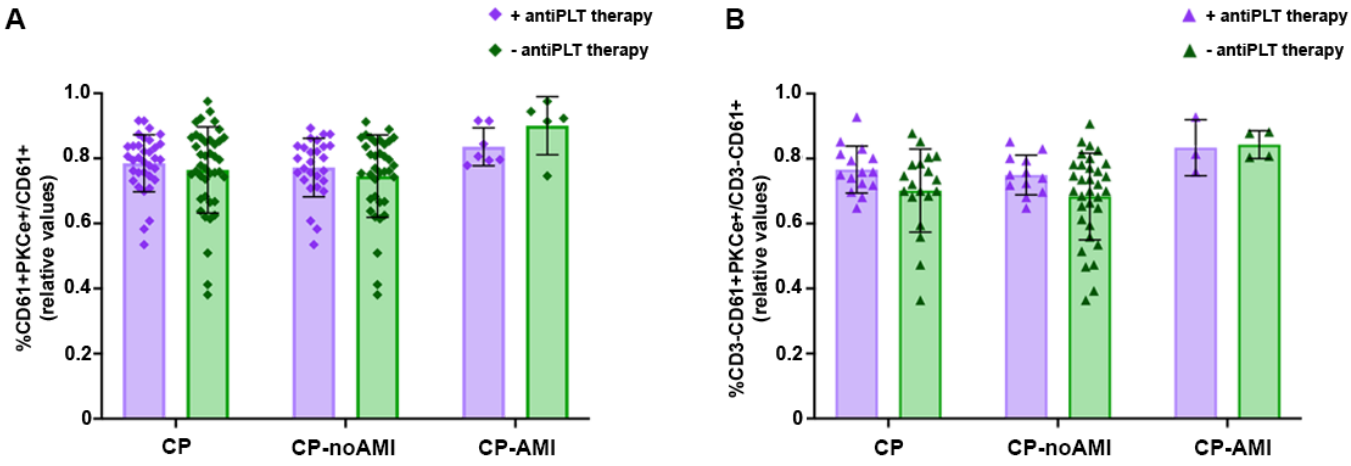

Figure 21. FCM analysis of PKCε-expressing platelets in patients on or off anti-platelet therapy. A) Percentages of $CD61^{+}PKC\varepsilon^{+}/CD61^{+}$ cells in CP, CP-noAMI and CP-AMI patients on anti-platelet therapy (light violet) and in patients not on anti-platelet therapy (light green). B) Percentages of $CD3^{-}CD61^{+}PKC\varepsilon^{+}/CD3^{-}CD61^{+}$ cells in CP, CP-noAMI and CP-AMI patients on anti-platelet therapy (light violet) and in patients not on anti-platelet therapy (light green). Data are reported as mean±SEM (ns, Student's t test).

5 Flow cytometry detection of PKCε-expressing platelets shows a good diagnostic accuracy

Since percentage of PKCε-expressing platelets was significantly higher in CP-AMI as compared to CP-noAMI, we asked whether this assay could be used in ED for a rapid and efficient diagnosis of CP-AMI. Therefore, we applied the receiver-operating characteristic (ROC) curve analysis of FCM detection of PKCε-expressing platelets to measure diagnostic accuracy of the test and calculate the optimal cut-off value, estimating double and triple staining analysis specificity and sensitivity.

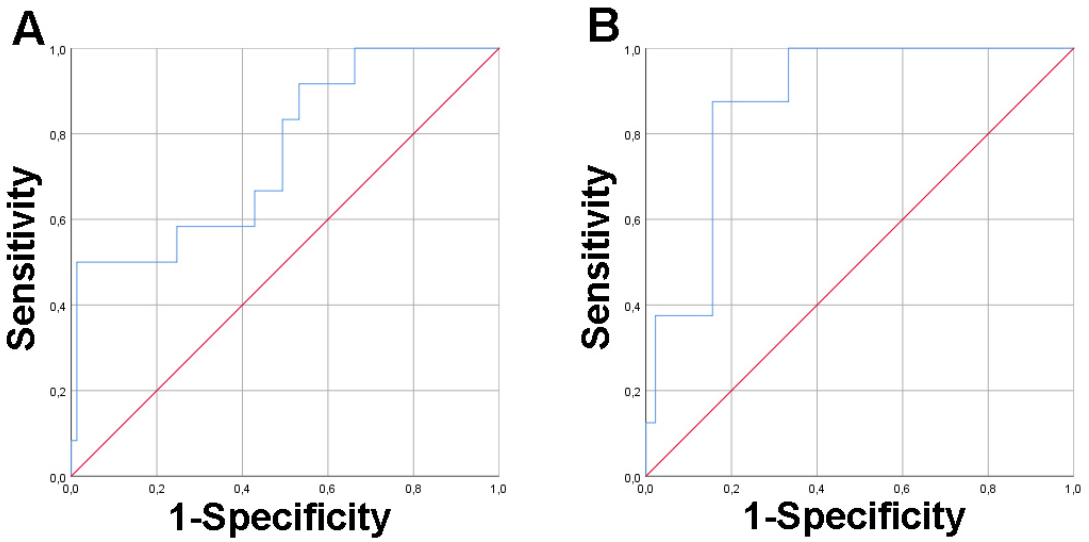

C

	AUC [CI 95%]	Cut-off	Sensitivity	Specificity	PPV	NPV
CD61+PKCε+/CD61+	0.756 [0.606–0.907]	0.913	50%	98.7%	85.7%	92.6%
CD3–CD61+PKCε+/CD3–CD61+	0.875 [0.774–0.976]	0.802	87.5%	84.4%	50%	97.7%

Figure 22. ROC curves FCM analysis of PKCε-expressing platelets with double and triple staining. A) ROC curve obtained from the FCM detection of PKCε-expressing platelets identified as $CD61^+PKC\varepsilon^+/CD61^+$ cells (double staining) in the entire study population. B) ROC curve obtained from the FCM detection of PKCε-expressing platelets identified as $CD3^-CD61^+PKC\varepsilon^+/CD3^-CD61^+$ cells (triple staining) in the subset population. C) Summary table showing area under the curves (AUC), confidential intervals (CI), cut-off values, sensitivity, specificity, positive predictive value (PPV) and negative predictive value (NPV) of FCM detection of PKCε-expressing platelets.

The ROC curve obtained from FCM analysis of PKCε-expressing platelets, using the double staining, shows an area under the curve (AUC) of 0.756 [CI of 95%: 0.606–0.907] (Figure 22, panels A, C). This assay shows an optimal cut-off value of 0.913 with a specificity of 98.7% and a sensitivity of 50%, with a positive predictive value (PPV) of 85.7% and a negative predictive value (NPV) of 92.6% (Figure 22, panel C).

Considering triple staining and excluding lymphocytes population from the analysis, the assay shows an AUC of 0.875 [CI of 95%: 0.774–0.976] (Figure 22, panels B, C), an optimal cut-off value of 0.802, with a specificity of 84.4% and a sensitivity of 87.5%. The PPV is 50% while the NPV reaches the 97.7% (Figure 22, panel C).

These data indicate that the FCM detection of $CD61^{+}PKC\varepsilon^{+}/CD61^{+}$ platelet population shows fair diagnostic accuracy, whereas the FCM detection of $CD3^{-}CD61^{+}PKC\varepsilon^{+}/CD3^{-}CD61^{+}$ platelet population demonstrates a good diagnostic accuracy. For this reason, the subsequent analyses were performed using percentage of $CD3^{-}CD61^{+}PKC\varepsilon^{+}/CD3^{-}CD61^{+}$ platelets obtained with the triple staining on the subset population.

6 Combination of PKCε-expressing platelets and cardiac troponin cut-off values results highly efficient in discriminating CP-AMI patients

At the ED admittance, levels of cTn were below the diagnostic cut-off value of 0.06µg/L in 46 out of 53 (86.8%) CP patients and 43 out of 46 of these patients received a final diagnosis of CP-noAMI. Despite levels of cTnI below the cut-off, three patients received a final diagnosis of CP-AMI, suggesting that cTnI levels at the ED arrival were not indicative for the final diagnosis and serial sampling was strongly required for a safe patient rule-out. Moreover, CP patients remained in the ED for further investigations, the 56.5% (26/46) was subjected to a second troponin assay and the 43.5% (20/46) to a third troponin assay. These data bring us to investigate whether FCM detection of PKCε-expressing platelets could be used in combination with the conventional cardiac troponin assay to an accurate and early diagnosis.

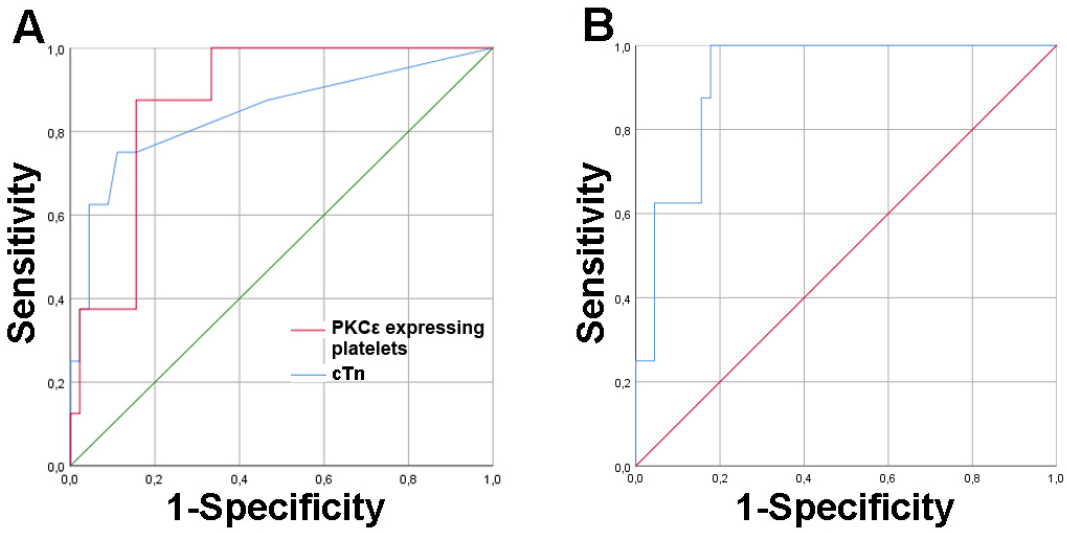

C

	AUC [CI 95%]	Cut-off	Sensitivity	Specificity	PPV	NPV
PKCε-expressing PLTs (CD3-CD61+PKCε+/CD3−CD61+)	0.875 [0.774–0.976]	0.802	87.5%	84.4%	50%	97.7%
cTnI (µg/L)	0.843 [0.666–1]	0.06	62.5%	86.6%	45.4%	92.8%
Logistic regression of PKCε-expressing PLTs and cTnI	0.922 [0.848–0.997]	0.139	100%	84.4%	53.3%	100%

Figure 23. ROC curves of FCM assay, cTnI assay and logistic regression model of the two parameters. A) ROC curves obtained from the FCM detection of PKCε-expressing platelets identified as $CD3^-CD61^+PKC\varepsilon^+/CD3^-CD61^+$ cells (triple staining) (red line) and cTnI assay (light blue line). B) ROC curve obtained from logistic regression of PKCε-expressing platelets, analysed as $CD3^-CD61^+PKC\varepsilon^+/CD3^-CD61^+$, and cTnI in the subset population. C) Summary table showing area under the curves (AUC), confidential intervals (CI), cut-off values, sensitivity, specificity, positive predictive value (PPV) and negative predictive value (NPV) of FCM detection of PKCε-expressing platelets, cTnI and logistic regression model combining these two parameters.

First, we compared diagnostic accuracy between cTnI assay and FCM detection of PKCε-expressing platelets in our subset population. Interestingly, ROC curve analysis reveals that the AUC value of our FCM assay is not statistically different from that of cTnI assay (AUC [95%CI]: 0.875 [0.777–0.976] *vs* 0.843 [0.666–1], respectively, Haley test) (Figure 23, panels A, C). Moreover, at the diagnostic cut-off value of 0.06µg/L, cTnI shows a sensitivity of 62.5% and a specificity of 86.6%, with a PPV of 45.4% and a NPV of 92.8% (Figure 23, panel C). These data suggests that the FCM detection of PKCε-expressing platelets has a better sensitivity with a slight reduction of specificity as compared to cTnI assay.

We performed the Spearmann's Correlation test to evaluate the association between percentage PKCε-expressing platelets and cardiac troponin levels. The analysis demonstrates that PKCε-expressing PLTs and cTnI levels are two independent factors ($P > 0.05$). Therefore, we applied a logistic regression combining these two parameters and even if the model achieves a very good diagnostic performance, it fails to significantly improve the diagnostic accuracy of PKCε-expressing PLTs or cTnI alone (AUC [95%CI]: 0.922 [0.848–0.997] *v s.* AUC [95%CI]: 0.843 [0.666–1] *or vs.* 0.875 [0.777–0.976], respectively) (Figure 23, panels B, C).

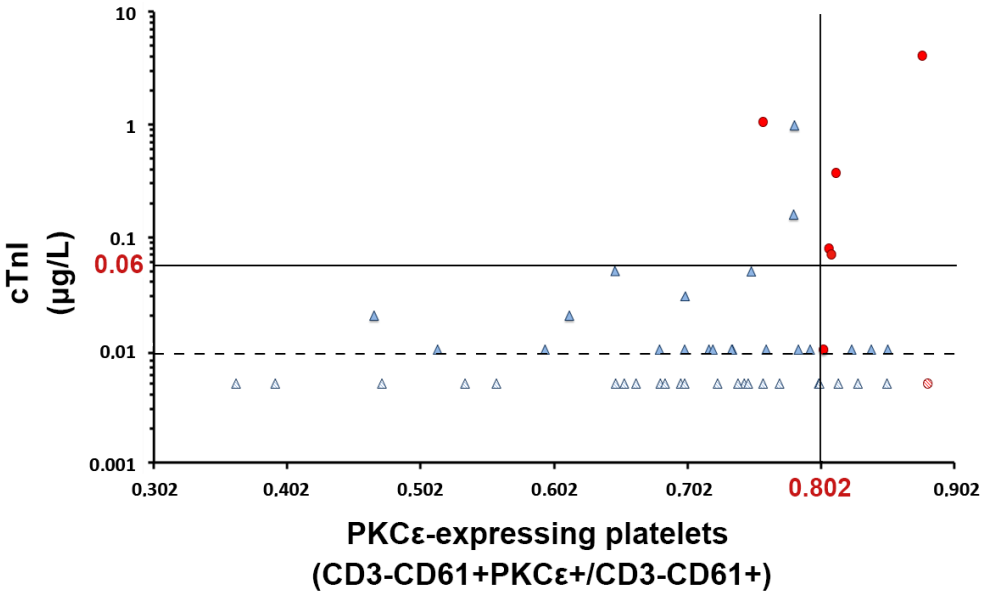

Figure 24. Combination of PKCε-expressing platelet and cTnI level cut-off values. CP patients of the subset population are stratified according to their cTnI (Y-axis) and PKCε-expressing platelet (defined as $CD3^{-}CD61^{+}PKC\varepsilon^{+}/CD3^{-}CD61^{+}$) percentage (X-axis) at the first ED admittance. The cut-off values are represented as black lines, while cTnI limit of detection is represented as dotted black line. CP-AMI patients are reported as red spots, CP-noAMI as light blue triangles and CP patients with undetectable values of cTnI as dotted spots or triangles.

Finally, we decided to stratify CP patients according to both cTnI and PKCε-expressing platelet parameters simultaneously, using the two cut-offs as discriminating factors (Figure 24). The results show that CP patients could be stratified in 3 risk categories:

- *Low-risk patients*: CP patients with both cTnI and PKCε-expressing platelets parameters below the cut-off values (0.06µg/L and 0.802, respectively), who can be safely discharged if there are no other suspicions of AMI.

- *Intermediate-risk patients*: CP patients with only one parameter (cTnI or PKCε-expressing platelets) above the cut off value, who require further monitoring.

- *High-risk patients*: CP patients, with both cTnI and PKCε-expressing platelet levels exceeding the cut-off values (0.06 µg/L and 0.802, respectively), who require immediate intervention.

Results II: Platelet gene expression profile

From: *Gobbi G, Carubbi C, Tagliazucchi GM, Masselli E, Mirandola P, Pigazzani F, Crocamo A, Notarangelo MF, Suma S, Paraboschi E, Maglietta G, Nagalla S,* ***Pozzi G****, Galli D, Vaccarezza M, Fortina P, Addya S, Ertel A, Bray P, Duga S, Berzuini C, Vitale M, Ardissino D. Sighting acute myocardial infarction through platelet gene expression. Sci Rep. 2019 Dec 20;9(1):19574.*

DOI: 10.1038/s41598-019-56047-0

1. Biological and clinical parameters of study and control populations

Platelet gene expression profile was investigated in 20 healthy donors (HD), 20 patients with ST elevation myocardial infarction (STEMI) and 20 patients with stable coronary artery disease (sCAD), using microarray technology. Demographical, biological and clinical parameters are listed in table 6.

The three groups were homogeneous for age (median age 50-82 years) and gender (15 males and 5 females in all groups). Data reported in clinical records showed that 7/20 (35%) of STEMI patients had history of major cardiovascular events (which included: peripheral artery thrombosis, deep venous thrombosis, acute myocardial infarction, and stroke/TIA), 10/20 (50%) were current smokers; 11/20 (55%) suffered from hypertension, 9/20 (45%) had dyslipidemia, 5/20 (25%) diabetes mellitus and 2/20 (10%) were obese (Table 6).

Regarding sCAD patients, only 3/20 (15%) of patients had a history of major cardiovascular even and were current smokers; 17/20 (85%) had hypertension, 11/20 (55%) dyslipidemia; 7/20 (35%) diabetes mellitus and 3/20 (15%) were obese. Furthermore, the 30% of STEMI patients (6/30) were on therapy with aspirin but none of them were taking antiplatelet agents, such as P2Y12 inhibitor or anticoagulant. All sCAD patients instead were on aspirin.

	STEMI	HD	sCAD
Number of cases, N.	20	20	20
Demographics			
Age, median yrs (range)	65.5 (51–82)	62.5 (49–81)	63.5 (51–80)
Male, n (%)	15 (75)	15 (75)	15 (75)
Female, n (%)	5 (25)	5 (25)	5 (25)
Clinical risk factors			
Family history of ischemic heart disease, N (%)	7 (35)	0 (0)	3 (15)
Hypertension, N (%)	11 (55)	0 (0)	17 (85)
Smoking, N (%)	10 (50)	0 (0)	3 (15)
Dyslipidemia, N (%)	9 (45)	0 (0)	11 (55)
Diabetes Mellitus, N (%)	5 (25)	0 (0)	7 (35)
Obesity, N (%)	2 (10)	0 (0)	3 (15)
ST elevation			
Inferior- lateral, N (%)	3 (15)	0 (0)	0 (0)
Anterior, N (%)	9 (45)	0 (0)	0 (0)
Inferior, N (%)	7 (35)	0 (0)	0 (0)
Lateral, N (%)	1 (5)	0 (0)	0 (0)
Angiography			
CX occlusion, N (%)	4 (20)	N/A	1 (5)
LAD occlusion, N (%)	9 (45)	N/A	10 (50)
RCA occlusion, N (%)	7 (35)	N/A	1 (5)
CX, LAD	0	N/A	2 (10)
CX, RCA	0	N/A	1 (5)
LAD, RCA	0	N/A	1 (5)
CX, LAD, RCA	0	N/A	4 (20)
Thrombosis			
Thrombotic events, N (%)	20 (100)	N/A	0 (0)
CK-MB, ng/mL, mean ± SD	172.39 ± 95.30	normal	normal
cTnI, ng/ml, mean ± SD	48.44 ± 28.32	normal	normal
Ongoing therapies			
Aspirin, N (%)	6 (30)	0 (0)	20 (100)
P2Y12 Inhibitors, N (%)	0 (0)	0 (0)	0 (0)
Anticoagulants, N (%)	0 (0)	0 (0)	0 (0)

Table 6. Biological and clinical characteristics of STEMI, sCAD patient and HD populations. *ST elevation: location of ST elevation; CX: circumflex coronary artery; LAD: left anterior descending coronary artery; RCA: right coronary artery; Thrombosis: coronary thrombosis at angiography; CK-MB: creatine kinase; cTnI: cardiac troponin I; N: number of patients. N/A: not applicable.*

2. Platelet gene expression profiling of STEMI patients

We investigated platelet gene expression profile to determine a specific set of differentially expressed genes (DEGs), that represents a gene expression "fingerprint" that could predict acute myocardial infarction. Gene expression data have been first analyzed to identify modulated genes between STEMI and HD. We applied a one-way Anova between subsets, considering a *P* value of 0.05 and a fold-change of 1.5. The heatmap showing differentially expressed platelet transcripts (up- and down-regulated) in STEMI as compared to HD is reported in figure 25.

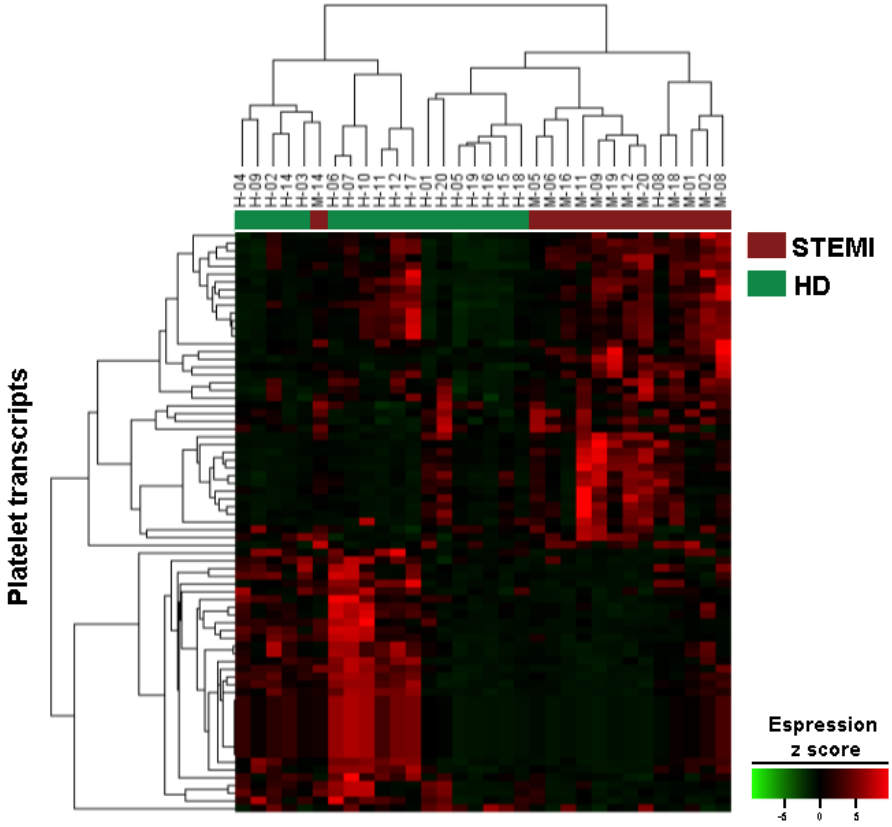

Figure 25. Platelet differentially expressed genes in STEMI and HD. Heatmap showing the differentially expressed platelet transcripts (adjusted *P* value < 0.05, |log2fc| > 1) from STEMI patients and HD. Up-regulated genes were represented in red and down-modulated genes were represented in green.

Transcript Cluster ID	Gene Symbol	Description	Fold Change STEMI *vs.* HD OR (95% CI)	*P* value
TC01003260.hg.1	S100A12	S100 Calcium Binding Protein A12	2.35 (1.51-4.52)	0.0017
TC06004150.hg.1	FKBP5	FKBP Prolyl Isomerase 5	204.06 (12.11-15705.95)	0.0026
TC21001069.hg.1	SAMSN1	SAM Domain, SH3 Domain And Nuclear Localization Signals 1	2.76 (1.42-6.53)	0.0075
TC12001178.hg.1	CLEC4E	C-Type Lectin Domain Family 4 Member E	1.97 (1.26-3.47)	0.0079
TC04000072.hg.1	S100P	S100 Calcium Binding Protein P	3.35 (1.48-9.25)	0.0082
TC01001254.hg.1	S100A9	S100 Calcium Binding Protein A9	2.31 (1.29-4.77)	0.0104
TC13000871.hg.1	IRS2	Insulin Receptor Substrate 2	5.56 (1.74-25.74)	0.0108
TC04000856.hg.1	SAP30	Histone Deacetylase Complex Subunit SAP30	32.29 (3.83-876.22)	0.0123
TC03000563.hg.1	-----		2.04 (1.24-3.98)	0.0138
TC01003261.hg.1	S100A8	S100 Calcium Binding Protein A8	3.08 (1.33-8.49)	0.0154
TC01002372.hg.1	-----		5.41 (1.59-25.27)	0.0155
TC01000510.hg.1	SMAP2	Stromal Membrane-Associated GTPase-Activating Protein 2	2.92 (1.39-8.11)	0.0157
TC12002425.hg.1	IRAK3	Interleukin-1 receptor-associated kinase 3	3.79 (1.48-14.27)	0.0178
TC16001896.hg.1	linc-TOX3-4	long non coding RNA, lincRNA, TOX high mobility group box family member 3	2.78 (1.26-7.06)	0.0178
TC19002254.hg.1	ZNF667-AS1	long non coding RNA, lncRNA	0.33 (0.12-0.77)	0.0197
TC01005397.hg.1	CR597056		2.79 (1.3-7.59)	0.0202
TC07002399.hg.1	NCF1B	Neutrophil Cytosolic Factor 1B Pseudogene	2.21 (1.17-4.75)	0.024
TC04000965.hg.1	MIR675	microRNA, miRNA	0.29 (0.09-0.78)	0.0248
TC13001572.hg.1	-----		4.12 (1.37-16.9)	0.0253
TC02002528.hg.1	ENST00000 417539	lincRNA	0.53 (0.28-0.89)	0.0296
TC02003777.hg.1	-----		1 0.71 (0.51-0.96)	0.0312
TC11000824.hg.1	ACER3	Alkaline Ceramidase 3	2.23 (1.15-5.26)	0.0318
TC15001008.hg.1	ENST00000 553658	lncRNA	0.31 (0.09-0.81)	0.0318
TC09001548.hg.1	GGTA1P	Glycoprotein Alpha-Galactosyltransferase 1	0.34 (0.11-0.81)	0.0325
TC13001686.hg.1	-----		0.32 (0.1-0.82)	0.0334
TC04002623.hg.1	SPARCL1	MAST9, High Endothelial Venule Protein	2.15 (1.15-4.83)	0.034
TC19000924.hg.1	ZNF667-AS1	lncRNA	0.37 (0.13-0.87)	0.0342
TC11002483.hg.1	IFITM2	Interferon Induced Transmembrane Protein 2	1.93 (1.11-3.89)	0.0346
TC07000438.hg.1	NCF1B	Neutrophil Cytosolic Factor 1B Pseudogene	2.04 (1.1-4.24)	0.0349
TC0X002155.hg.1	BTK	Bruton Tyrosine Kinase	0.48 (0.21-0.88)	0.0354
TC04002084.hg.1	TCONS_l2_ 0002059-XLOC_l2_01	lncRNA	0.43 (0.17-0.84)	0.0365

	0724			
TC19002252.hg.1	FUNDC2P2	FUN14 Domain Containing 2 Pseudogene 1	0.4 (0.15-0.88)	0.0374
TC09002775.hg.1	GGTA1P	Glycoprotein Alpha-Galactosyltransferase 1 (Inactive)	0.43 (0.17-0.86)	0.0377
TC06003570.hg.1	-----		5.45 (1.35-34.19)	0.0381
TC0X001218.hg.1	BTK	Bruton Tyrosine Kinase	0.37 (0.12-0.86)	0.039
TC06001488.hg.1	IFITM4P	Interferon Induced Transmembrane Protein 4 Pseudogene	4.55 (1.26-23.45)	0.0391
TC6_mcf_hap5000107.hg.1	IFITM4P	Interferon Induced Transmembrane Protein 4 Pseudogene	4.55 (1.26-23.45)	0.0391
TC07001516.hg.1	NCF1C	Neutrophil Cytosolic Factor 1C Pseudogene	2.22 (1.1-5.18)	0.0392
TC15000268.hg.1	C15orf54	Long Intergenic Non-Protein Coding RNA 2915	0.52 (0.24-0.88)	0.0395
TC09001985.hg.1	TCONS_l2_00028817	lncRNA	0.73 (0.52-0.96)	0.0406
TC07003026.hg.1	NCF1C	Neutrophil Cytosolic Factor 1C Pseudogene	2.08 (1.08-4.54)	0.0414
TC22000381.hg.1	DQ586951	Piwi-interacting (piRNA)	0.47 (0.21-0.9)	0.0419
TC06001350.hg.1	HIST1H2BG	Histone H2B type 1-C/E/F/G/I	0.69 (0.46-0.95)	0.0424
TC11001230.hg.1	IFITM3	Interferon Induced Transmembrane Protein 3	2.6 (1.14-7.65)	0.0433
TC09001372.hg.1	HSD17B3	Hydroxysteroid 17-Beta Dehydrogenase 3	0.36 (0.11-0.88)	0.0441
TC0X002204.hg.1	SLC25A5	Solute Carrier Family 25 Member 5	0.6 (0.34-0.96)	0.0463
TC19000134.hg.1	MCEMP1	Mast Cell Expressed Membrane Protein 1	2.4 (1.08-6.3)	0.0467
TC01000152.hg.1	----		1.56 (1.03-2.53)	0.0476
TC19000921.hg.1	ZNF542P	Zinc Finger Protein 542, Pseudogene	0.36 (0.11-0.9)	0.0494
TC08001365.hg.1	FABP4	Fatty Acid Binding Protein 4	3.08 (1.15-11.33)	0.0494

Table 7. List of 51 DEGs emerged from microarray analysis of platelet transcriptome of STEMI vs. HD (*P* value of <0.05).

We identified 51 DEGs with a *P* value <0.05, as reported in table 7. Therefore, we restricted the analysis on the first five platelet DEGs with a *P* value <0.01, which included S100 calcium binding protein A12 (*S100A12*, FI *vs.* HD = 2.35, 95% CI = 1.51-4.52, *P* =0.0017); FKBP prolyl isomerase 5 (*FKBP5*, FI *vs.* HD = 204.06, 95% CI = 12.11-15705.95, *P* =0.0026); SAM Domain, SH3 Domain And Nuclear Localization Signals 1 (*SAMSN1*, FI *vs.* HD=2.76, 95% CI=1.42-6.53, *P*=0.0075); C-Type Lectin Domain Family 4 Member E (*CLEC4E*, FI vs. HD=1.97, 95% CI=1.26-3.47, *P*=0.0079) and S100 Calcium Binding Protein P (*S100P*, FI vs. HD=3.35, 95% CI=1.48-9.25, *P*=0.0082) (Figure 26 and table 7,).

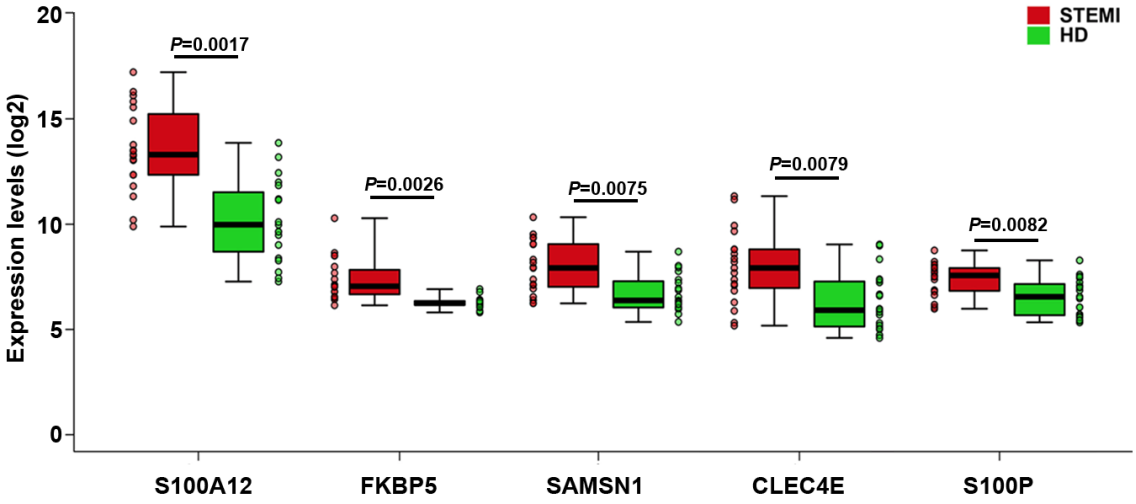

Figure 26. Gene expression values of the five identified DEGs in STEMI *vs*. HD. Box plots showing gene expression values of *S100A12, FKBP5, SAMSN1, CLEC4E* and *S100P* in STEMI patients (red), and healthy subjects, HD (green). Data are represented as median and interquartile ranges of the five identified genes. (*P* values, reported in the figure, are obtained by One-way Anova between subsets).

The expression of the five DEGs was also evaluated by qPCR. As shown in figure 27, mRNA levels of all DEGs, except for *S100P*, were significantly higher in platelets from STEMI patients as compared to HD (Figure 27).

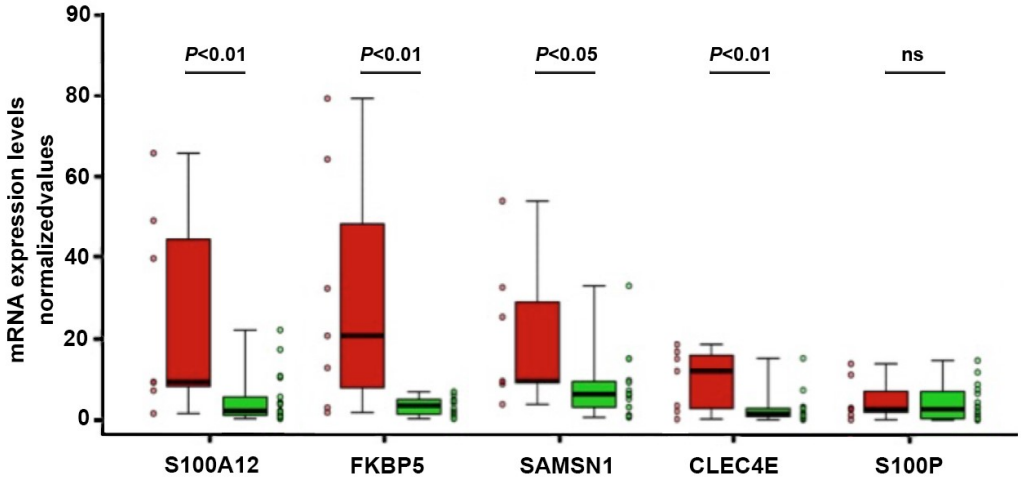

Figure 27. The mRNA expression levels of 5 DEGs in STEMI and HD platelets. *S100A12, FKBP5, SAMSN1, CLEC4E* and *S100P* mRNA expression levels assessed by qPCR in platelets from STEMI patients (red) and HD (green). Box plots show median and interquartile range each gene. Data are normalised to the expression levels of the *ACT*B and I*TGA2B* genes. For each sample, three technical replicates were performed. (*P* values, reported in the figure, are obtained by t test).

Furthermore, we asked whether the expression of these five DEGs could be affected by the time of sample collection in STEMI patients. Indeed, even if all STEMI samples were collected within one hour from patient admission at the hospital and within six hours from symptoms onset, there were a substantial difference in the time of sample collection among patients. To exclude this bias, we applied a Spearman correlation test, and we found no correlation between *S100A12, FKBP5, SAMSN1, CLEC4E* and *S100P gene* expression and time of blood withdrawal (Figure 28).

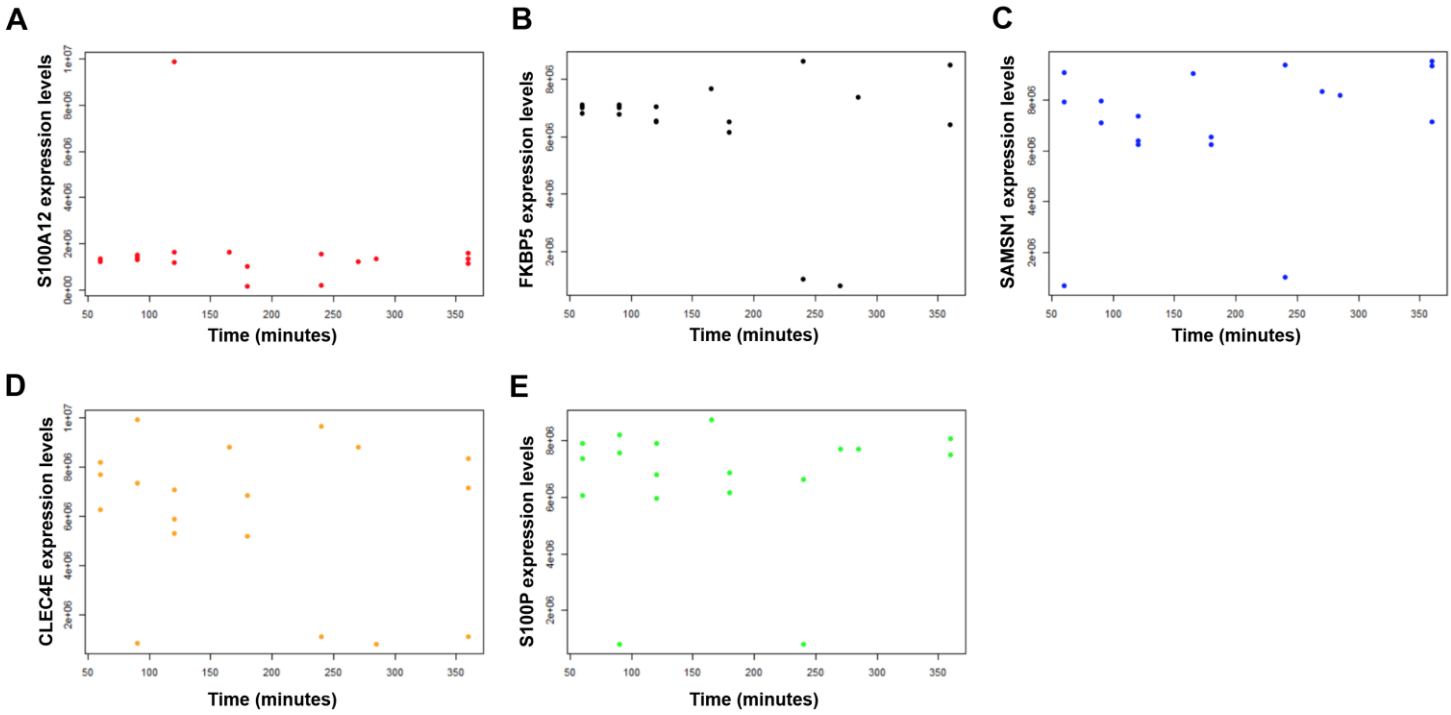

Figure 28. Correlation between the 5 DEGs and time from the onset of symptoms to blood sampling. Scatterplots of the correlation between time of blood withdrawal (X axis) and gene expression levels (Y axis) for each STEMI patient: *S100A12* (panel A), *FKBP5* (panel B), *SAMSN1* (panel C); *CLEC4E* (panel D) and *S100P* (panel E) (ns, Spearman correlation test).

Moreover, we evaluated the possible correlation between the expression of each DEG with serum creatine kinase (CK-MB) and cardiac troponin I levels (cTnI), that represent clinical biomarkers of myocardial injury released in the bloodstream after the acute event. We did not find any significant correlation, except for *S100P*. Indeed, as shown in figure 29, a moderate correlation was reported between *S100P* and CK-MB ($R = 0.56$, $P = 0.0120$) and between *S100P* and cTnI serum levels ($R = 0.57$, $P = 0.0110$) (Figure 29), as previously demonstrated by Cai and colleagues in rat model of myocardial infarction (Cai et al., 2011).

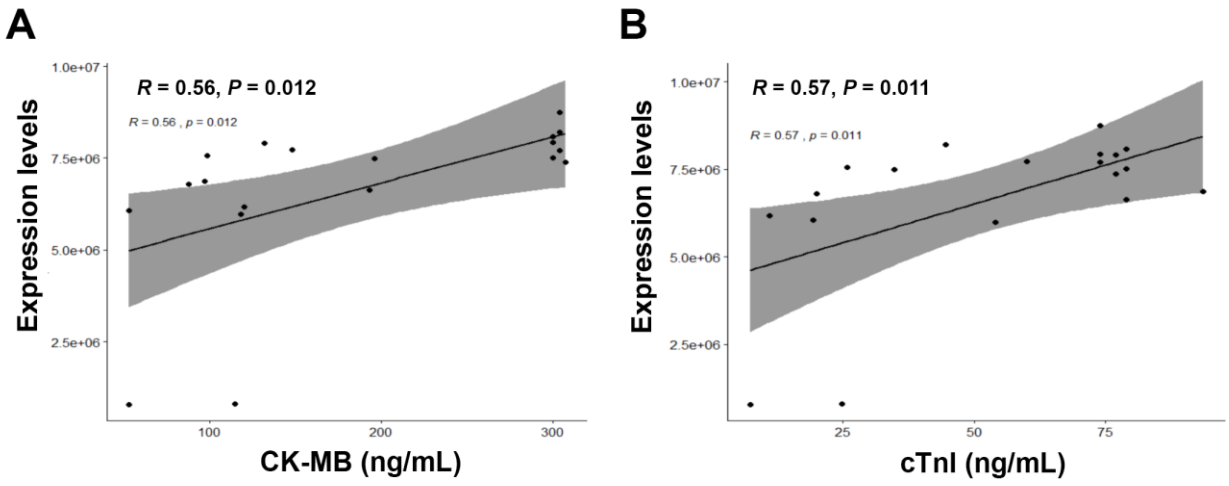

Figure 29. Correlation between *S100P* expression and creatine kinase and between *S100P* expression and cardiac troponin serum levels. Panel A) Scatterplot showing the correlation between creatine kinase serum levels (CK-MP, ng/mL) and S100P expression levels CK-MB (*R* = 0.56, *P* = 0.012; Spearman correlation test). Panel B) Scatterplot showing the correlation between cardiac Troponin-I levels and S100P expression levels (*R* = 0.57, *P* = 0.011; Spearman correlation test).

3. The expression of the five DEGs is independent of reticulated platelets

We then asked whether platelet gene expression profile could be due to the presence of reticulated platelets in STEMI patients. Indeed, reticulated platelets are considered newly produced, hyperactive platelets that are increased in peripheral blood of patients with acute myocardial infarction, who display an enhanced platelet turnover.

Therefore, we evaluated the percentage of reticulated platelets by flow cytometry in peripheral blood of 6 STEMI patients, 7 sCAD and 5 HD. As described in materials and methods, peripheral blood samples were stained with anti-human CD41a mAb conjugated with PeCy5 and thiazole orange (TO) and the reticulated platelets were identified as $CD41a^{+}TO^{+}$ cells.

As shown in figure 30, the percentage of $CD41a^{+}TO^{+}$ cells was comparable among STEMI, sCAD and HD.

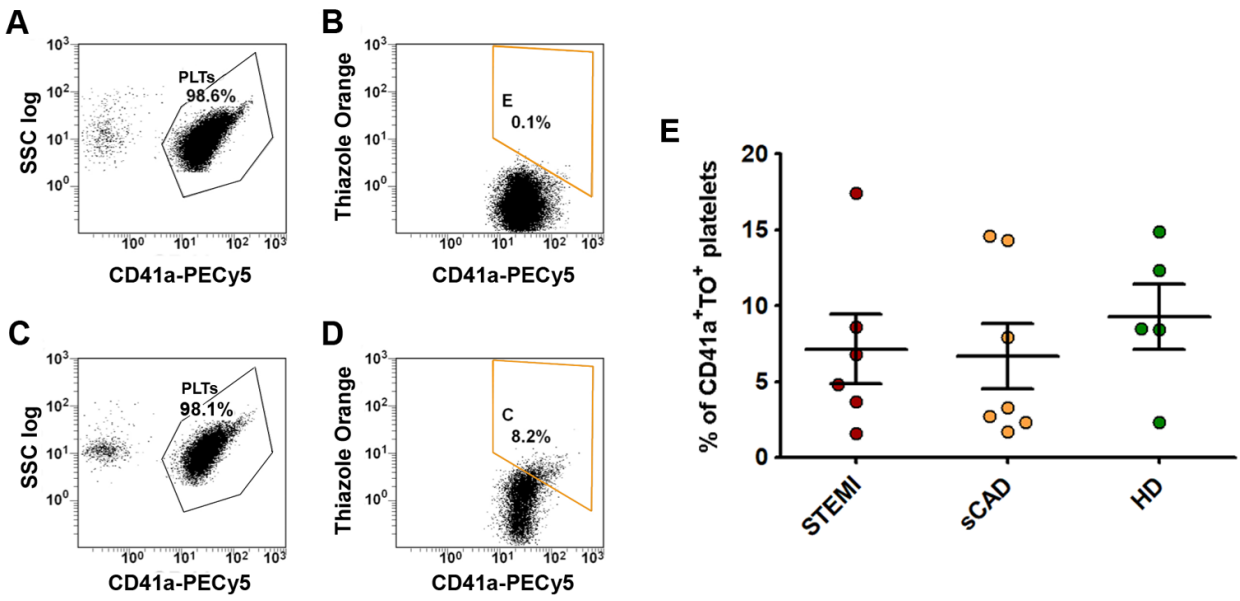

Figure 30. Flow cytometry analysis of reticulated platelets in STEMI, SCAD and HD patients. A-D) representative dot plots showing gating strategy adopted to identified reticulated platelet. Platelets are identified as CD41a positive cells and reticulated platelets are represented as $CD41a^{+}TO^{+}$ cells. B) Representative dot plot of a negative control without TO. D) Representative dot of a TO stained patient. E) Percentages of $CD41a^{+}TO^{+}$ platelets in STEMI (N.6), sCAD (N.7) and HD (N.5). Data are reported as mean ± SEM (ns in all comparison, One-way Anova and Tukey test).

4. The logistic model based on the five DEGs shows a good diagnostic performance in discriminating STEMI *vs*. HD and STEMI *vs*. sCAD

Since DEGs expression was significantly higher in STEMI patients as compared to HD, we asked whether DEGs could represent a platelet signature to predict STEMI. Therefore, we generated a logistic regression model that considers all five DEGs, and we calculated the receiver-operating characteristic (ROC) curve and relative area under the curve (AUC).

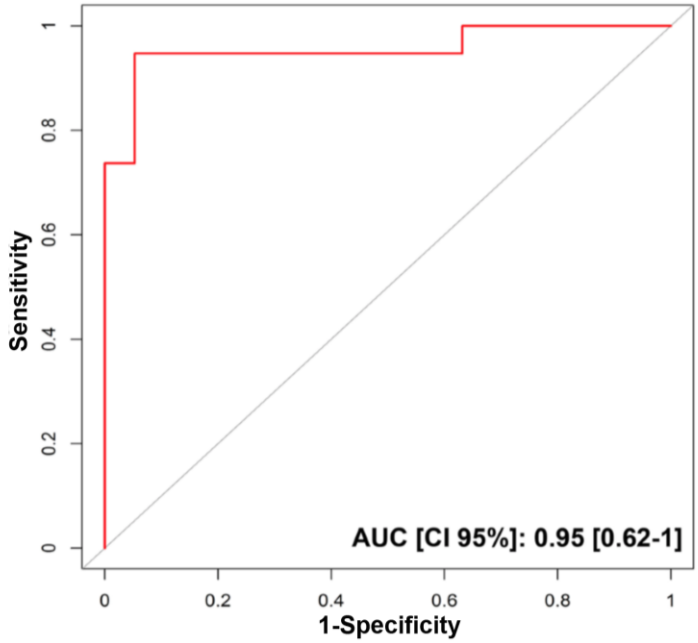

Figure 31. ROC curve of logistic regression model based on the five DEGs to discriminate STEMI *vs*. HD. ROC curve obtained from logistic regression model based on *S100A12, FKBP5, SAMSN1, CLEC4E* and *S100P* gene expression AUC of 0.95 (95% confidence interval 0.62–1.00).

The ROC curve obtained from the logistic regression model based on the five DEGs shows an AUC of 0.95 [CI of 95%: 0.62–1] (Figure 31). The result was validated by applying a bootstrap analysis and k-nearest neighbour models (kNN) to estimate the performance in discriminating STEMI vs. HD.

The accuracy of the five identified DEGs genes to discriminate subjects with high-risk of myocardial infarction was externally validated comparing platelet gene expression profile of STEMI patients to sCAD, a clinical condition phenotypically close to STEMI.

The expression levels of the five identified DEGs were significantly higher in platelets from STEMI patients as compared to sCAD (*S100A12*, *P*=0.0046; *FKBP5*, *P*=0.0071; *SAMSN1*, *P* = 0.0051; *CLEC4E*, *P* = 0.0053 and *S100P*, *P* =0.0008) (Figure 32).

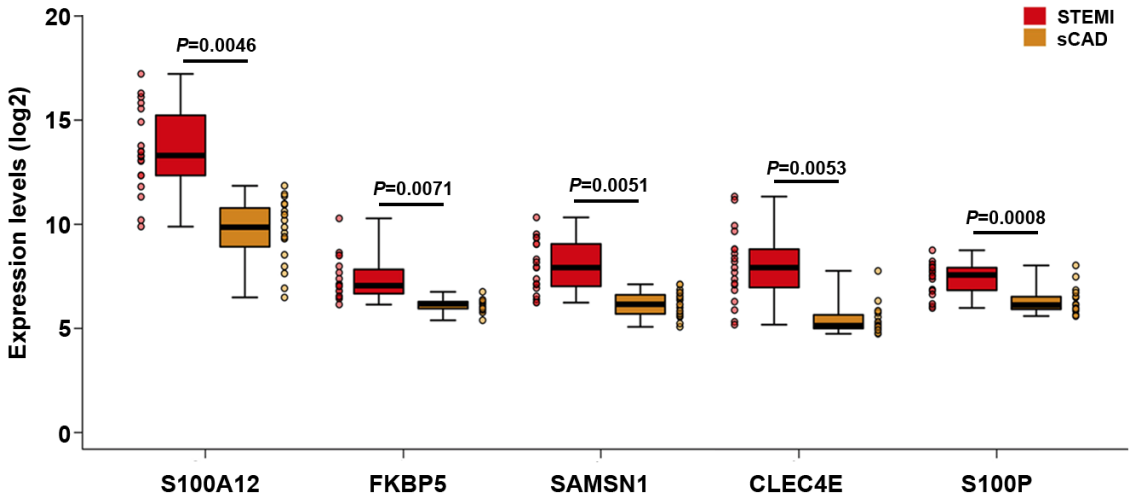

Figure 32. Gene expression values of the five identified DEGs in STEMI *vs*. sCAD. Box plots showing gene expression values of *S100A12, FKBP5, SAMSN1, CLEC4E* and *S100P* in STEMI patients (in red), and sCAD (in orange). Data are represented as median and interquartile ranges of the five identified genes. (*P* values, reported in the figure, are obtained by T test).

Finally, we used the logistic regression model combining the five identified DEGs to generate a ROC curve and calculated the diagnostic accuracy of this model to discriminate STEMI from sCAD. The ROC curve shows an AUC of 0.93 [CI of 95%: 0.6–1.00] (Figure 33).

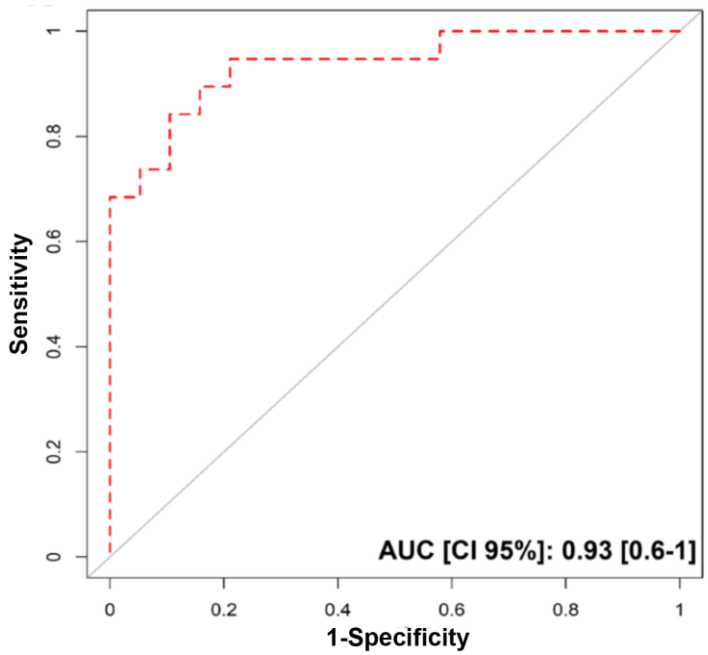

Figure 33. ROC curve of logistic regression model based on the five DEGs to discriminate STEMI *vs*. sCAD. ROC curve obtained from logistic regression model based on *S100A12, FKBP5, SAMSN1, CLEC4E* and *S100P* gene expression AUC of 0.93 (95% confidence interval 0.6 - 1.00)**.**

Discussion

Acute myocardial infarction is a multifactorial disease, and it represents one of the major causes of death and disability worldwide. Although considerable advances have been made in prevention and treatment, it remains a leading health problem in the world, given its unpredictability and confounding symptoms. The main AMI clinical manifestation is chest pain, but often this symptom can be associated to different underlying pathological conditions other than AMI, as musculoskeletal conditions, gastrointestinal diseases, stable coronary artery diseases (CAD), panic disorders, and pulmonary diseases (Gulati et al., 2021). Only the 15% of chest pain patients generally receives a final diagnosis of AMI, and erroneously discharged patients show a twofold-increased probability of morbidity and mortality in the following 30 days (Pope et al., 2000).
For these reasons, prolonged monitoring (12-24 hours) is required to avoid inadvertent early discharge. A timing and accurate differential diagnosis as well as risk stratification of AMI patients at the initial presentation represents an imperative in ED, but also in the outpatient setting. Diagnostic algorithms and risk scoring systems are constantly updated with the introduction of new biomarkers and the development of new diagnostic techniques. Nevertheless, the role and the contribution of these new biomarkers and predictive factors remains to be fully determined.

Here, we investigated and sought to validate two different diagnostic approaches for AMI: the detection of PKCε expressing platelets by flow cytometry, and the analysis of platelet gene expression profile by microarray assay.

Currently, the differential diagnosis of AMI is mainly based on a composite evaluation of patient medical history, physical examination, ECG and biomarkers of myocardium necrosis (Roffi et al., 2016; Thygesen et al., 2018; Ibanez et al., 2018). Cardiac troponin (cTnT) is considered the biomarker of choice for the assessment of myocardium necrosis as consequence of AMI, however cTnI levels can be measured only hours after AMI (Babui and Jaffe, 2005). Moreover, the introduction of high-sensitivity cTn (hs-cTn) assay, which requires only two serial cTnT evaluations, have reduced testing time to 3-6 hours after patients' admission to the ED (Twerenbold et al., 2017). However, it has been suggested that cTn release in bloodstream is not closely associated only to myocardium necrosis but also to normal turnover of myocardial cells, apoptosis, increased cellular wall permeability, the formation and release of membranous blebs (Garg et al., 2017). Moreover, it provides no information on the pathological mechanism, which underlies myocardium necrosis. Elevated cTn levels were, indeed, detected in plasma of many cardiovascular diseases, as acute or aortic dissection, atrial fibrillation, chronic heart failure, myocarditis, Takotsubo cardiomyopathy, and stroke (Eggers et al., 2017).

Both our potential diagnostic approaches are based on platelets. Platelets play a central role in the development of atherothrombosis, contributing directly and indirectly to plaque rupture and thrombus formation (Meadows and Bhatt, 2007; Koupenova et al., 2018). We used flow cytometry

to evaluate PKCε-expressing platelets in patients attending ED with a complaint of chest pain, and we tested the diagnostic accuracy of this assay in discriminating patients with or without AMI.
PKCε is a serine/threonine kinase, which is virtually absent in human platelets under physiological conditions. We previously demonstrated an ectopic expression of PKCε in pathological conditions. In patients with primary myelofibrosis (PMF), a myeloproliferative neoplasm closely associated to thrombotic risk, a significant elevated expression of PKCε was documented in mature MKs and platelets, in which it correlated with an increase of platelet reactivity (Masselli et al, 2015; Masselli et al., 2017). Moreover, an aberrant PKCε expression was also found in platelets from patients with AMI as compared to sCAD and healthy controls. Of note, PKCε expression affects platelet adhesion and activation capacity (Carubbi et al., 2012).
Here, we found that the percentage of PKCε-expressing platelets is significantly higher in patients with chest pain that received a final diagnosis of AMI (CP-AMI) as compared to those patients with chest pain due to other causes (CP-noAMI).
Furthermore, no differences were found in terms of PKCε-expressing platelets among patients on or off therapy with anti-platelet drugs in the entire population of chest pain patients, including CP-AMI and CP-noAMI groups. Moreover, no differences were also observed in STEMI and NSTEMI and among patients with chest pain due to other causes. Unstable angina patients showed a slight increase of percentage of PKCε-expressing platelets as compared to other CP-noAMI causes. However, this difference was not statistically significant due to the very small number of cases.
This result is consistent with data by Carubbi et al., confirming the ectopic expression of PKCε in human platelets during the acute thrombotic event.
Moreover, we demonstrated that FCM evaluation of PKCε-expressing platelets show a high sensitivity and specificity (87.5% and 84.4%, respectively) and a good diagnostic accuracy (AUC: 0.875) comparable to that of cardiac troponin (AUC: 0.843), in our study population.
These data indicate PKCε-expressing platelets as a potential biomarker of AMI.

As compared to other diagnostic tools, FCM shows some relevant advantages. Firstly, it is considered the most suitable tool for studying platelet functions. PKCε expression analysis by FCM requires almost 80 minutes, allowing a rapid and complete characterization in a single-shot analysis. Furthermore, FCM analysis requires only 5μL of peripheral venous blood *per* assay, and a minimal manipulation of samples to maintain platelets in their physiological environment and minimize the possibility of artefacts formation. Therefore, FCM assay is suitable for standardization and clinical application in ED setting.

On the other hand, the final target of our assay is focused on platelets, which are the main immune cells with leukocytes involved in the pathogenesis of AMI. Platelet abnormalities in number or functions are consequences but mainly causes of the acute events. Unlike the other markers,

whose levels are detectable only hours after AMI and are affected by several clinical factors (Panteghini, 2009; Eggers and Lindahl, 2017), PKCε expression in human platelets is closely related to the acute event. This kinase has been found overexpressed in both reticulated and mature platelets of AMI patients and it returns negative after 15 days after the acute event. Therefore, PKCε is exclusively expressed in platelets in the "peri-infarctual" period.

Then, we asked whether the evaluation of PKCε-expressing platelets might add diagnostic benefit to the conventionally used cTn assay. The logistic regression model, obtained by the combination of cTnI and PKCε-expressing platelets, achieved a very good diagnostic accuracy (AUC: 0.922), but it did not statistically improve that of single cTnI assay. Nevertheless, we used the two identified cut-offs simultaneously to discriminate chest pain patients. Of note, we found that patients showing both values exceeding the cut-offs were all CP-AMI; and patients with both values below the cut-offs were all CP-noAMI (36/53, 68% of our population). These data reveal that the 15% (8/53) of patients would correctly receive a diagnosis of AMI at ED admission only after the first troponin and FCM assays. Furthermore, with this approach, patients with chest pain who require further monitoring and serial troponin assay would have been reduced from 34 (34/53, 64.1%) to 13 (13/53, 24.5%) patients.
Accordingly, patients risk stratification, using cTn and PKCε-expressing platelets, could be performed already after the first blood sampling at ED admission.

This dual marker strategy allows to classify patients into three categories: 1) low-risk CP patients with both cTnI and PKCε-expressing platelets parameters below the cut-off values (0.06µg/L and 0.802, respectively), who can be safely discharged, if there are no other suspicions of AMI; 2) intermediate-risk CP patients with only one parameter (cTnI or PKCε-expressing platelets) above the cut off value, who require further monitoring; and 3) high-risk CP patients, with both cTnI and PKCε-expressing platelet levels exceeding the cut-off values (0.06 µg/L and 0.802, respectively), who require immediate intervention.

The second approach is focused on platelet gene expression profile by microarray assay.
Microarray assay represents a rapid and semi-quantitative technique for gene expression profiling by which the expression of thousands of genes from multiple samples could be evaluated simultaneously. Human platelets have a unique mRNA signature, mainly derived from their hematopoietic precursors. Here, we used the microarray technique to investigate platelet gene expression signature that typifies STEMI. Focusing on the up-regulated genes, we found 51 DEGs in platelets of STEMI *vs*. HD. Five genes with a *P* value <0.01 were identified: *S100A12*, *FKBP5, SAMSN1, CLEC4E,* and *S100P.* Microarray data were also confirmed by qPCR; indeed, except for

S100P, mRNA levels of DEGs were significantly higher in platelets from STEMI as compared to HD. Based on these 5 DEGs, we generated a logistic regression model that showed a very good diagnostic accuracy (AUC: 0.95) in discriminating STEMI patients and healthy subjects.

S100A12 and *S100P* are members of the S100 family of calcium-binding proteins, which are widely known to play a relevant role in thrombosis. Indeed, the heterodimer protein product of *S100A8* and *S100A9* genes, myeloid-related protein (MRP) 8/14, regulates via the interaction with CD36 the formation of thrombus (Wang et al., 2014) and induces inflammatory and thrombogenic response in human microvascular endothelial cells, increasing the transcription of adhesion molecules and proinflammatory chemokines (Vienman et al., 2005). In our study, we found that *S100A8* and *S100A9* were significantly overexpressed in platelets form STEMI (FI *vs.* HD = 3.08, 95% CI= 1.33-8.49, and FI *vs.* HD = 2.31, 95% CI= 1.29-4.77 respectively), although they showed a *P* value >0.01 (*P*=0.015 and *P*=0.010, respectively).

S100A12 is a pro-inflammatory protein predominantly secreted by granulocytes (Meijer et al., 2012). Elevated levels of S100A12 were found in plasma of patients with carotid atherosclerosis as compared to healthy control subjects, and the highest levels were observed in patients with recent symptoms (Abbas et al., 2012). Furthermore, S100A12 plasma levels were also elevated in patients with acute coronary artery disease and correlated with other inflammatory markers as C-reactive protein (Goyette et al., 2009). On the other hand, S100P plasma levels, together with S100B, S100A6, were associated to ACS, and with myocardial infarction size in rat model of cardiac ischemia-reperfusion (I/R) (Cai et al., 2011).

FKBP5 encodes for a cis-trans prolyl isomerase, also known as FK506 binding protein 51, which is involved in immunoregulation and basic cellular processes as protein folding and trafficking. It is implicated in stress physiology, acting as a co-chaperone to regulate glucocorticoid receptor (GR) sensitivity (Fries et al., 2017). Recently, higher *FKBP5* mRNA levels in immune cells were found associated to a higher inflammatory burden and to an altered NF-κB-related gene networks (Zannas et al., 2019). Of note, our result was consistent with data by Eicher et al. evaluating platelet transcriptome by RNA-seq. Indeed, *FKBP5* transcript was upregulated in platelets from STEMI as compared to NSTEMI patients (Eicher et al., 2016).

Moreover, *SAMSN1* gene, also known as *HACS1*, encodes for a ubiquitous adaptor or scaffolding protein that has been studied in vascular disease as peripheral arterial occlusive disease (Fu et al., 2008). *CLEC4E* transcript encodes for a C-type lectin pattern recognition receptor, which binds cellular debris or cholesterol crystals and triggers their degradation. *CLEC4E* was found expressed in atherosclerotic plaque, promoting macrophage activation and plaque development (Clement et al., 2016), and in megakaryocytes in mouse model of sepsis (Freishtat et al., 2009).

Several studies have used microarray technique or RNAseq to identify a gene signature specific for AMI, although most of these studies focused on whole blood (Kim et al., 2014; Muse et al., 2017; Chiesa et al., 2020), with the main limitation that changes in gene expression patterns could be due to all the cell types present in the sample. We focused on a single cell population, platelets. The circulating platelet pool contains a mixed population of different aged platelets; and the mRNA profile represents an average of this heterogeneous platelet population. We evaluated the percentage of reticulated platelets that could affect gene expression profile. Of note, no differences were observed in terms of percentage of $CD41^{+}TO^{+}$ platelets among STEMI, sCAD and HD. Since platelets inherit a specific set of mRNA from their hematopoietic precursors, platelet transcripts could mirror the alterations in megakaryocyte transcript expression due to environmental and /or extracellular stimuli that occurs before or in concomitance to the acute event.

The main limitations of our approach include the relatively small sample size and the lack of a validation cohort. However, we validated the accuracy of our set of DEGs by comparing *S100A12*, *FKBP5*, *SAMSN1*, *CLEC4E,* and *S100P* gene expression in STEMI vs. sCAD, a clinical condition phenotypically close to STEMI. We observed that *S100A12*, *FKBP5*, *SAMSN1*, *CLEC4E,* and *S100P* mRNA were significantly higher in STEMI not only *vs*. HD but also *vs*. sCAD. Moreover, the 5 DEGs also showed a very good accuracy in discriminating STEMI *vs*. sCAD, suggesting this set of DEGs as a predictive biomarker of AMI.

Furthermore, our approach suffers from the limitations associated with the microarray technique, including the high cost, limited access, and lack of standardization. We compared STEMI, sCAD patients and healthy subjects matched for age, gender, cardiac vascular related factors, and with no comorbidities, to reduce the effects of confounding factors. The fact that we have selected therapy free patients matched by gender and age with the control population probably increased the specificity and sensitivity of the differential gene expression profile, by contrast these constraints probably reduced the generalizability of our results.

Moreover, the amount and the quality and integrity of mRNA represent the major challenge in microarray assay (Russo et al., 2003; Macaulay et al., 2005). Only a few studies are available on platelet transcriptome, probably because of technical issues related to paucity of platelet cytoplasmic RNA and the risk of leukocyte contamination. In our study, blood was collected at patient admission, before any intervention, and samples were rapidly processed within two hours from the sampling. Platelet purity was check for each sample by flow cytometry and hematoxylin-eosin staining, and RNA quality was evaluated prior to microarray assay to increase the robustness and reliability of the DEGs and make more feasible a future clinical application.

Unfortunately, we did not find *PRKCE* mRNA among the up-regulated genes in platelets from STEMI patients, and this data seems to be in contrast with our previous results on the peculiar expression of PKCε in platelets from AMI patients. This result can be explained by the weak correlation between platelet transcriptome and proteome, due to post-translational modifications, rapid response to external stimuli, and protein secretion (Macaulay et al., 2005; McRedmond et al., 2014; Londin et al., 2014). In addition, to mRNAs, platelets also inherit a variable number of proteins from their progenitors. Therefore, we can speculate that the elevated protein levels of PKCε, observed in platelets of AMI patients, may reflect the elevated levels of this kinase in the megakaryocyte precursors.

Overall, we demonstrated the diagnostic accuracy of two different approaches both based on platelets that could be used in combination to the well-established ECG and cTn assay to identify patients with AMI. Collectively, our results configure the combination of PKCε-expressing platelets and cardiac troponin as a dual marker strategy potentially useful for a rapid rule-in or rule-out of myocardial infarction in chest pain patients at the ED admittance. Moreover, our data on platelet gene expression by microarray define a gene signature specific for AMI that could be used as a potential useful tool for the AMI diagnosis and patients risk stratification. Future studies will be focused on the validation of the diagnostic and prognostic value of both approaches on a larger cohort of patients and on the study of DEGs involvement in the pathogenesis of myocardial infarction.

Part II

The prognostic value of the rs1024611 SNP of CCL2 and the role of CCL2/CCR2 chemokine system in primary myelofibrosis

Introduction

1. Myeloproliferative Neoplasms

The Myeloproliferative Neoplasms (MPNs) are hereditary clonal stem cell disorders characterized by excessive proliferation and abnormal differentiation of myeloid cell lineages. MPNs can be classified in polycythemia vera (PV), essential thrombocythemia (ET), myelofibrosis (MF). All MPNs arise from a single hematopoietic stem cell (HSC), which harbors a somatic mutation and begins to expand. The abnormal expansion of this neoplastic clone is associated to single or multilineage hyperplasia. Indeed, PV is characterized not only by a predominant erythroid lineage involvement with an excess of erythrocytes, but it is also associated with a hyperplasia of the megakaryocytic and granulocytic lineages. ET is characterized by megakaryocytic hyperplasia and increased platelet count, whereas PMF, the most heterogeneous among MPNs for its clinical and biological characteristics, is characterized by megakaryocytic hyperplasia and the presence of bone marrow fibrosis (Vainchenker and Kralovics, 2017).

William Dameshek (1900–1969) was the first who described and suggested the concept of “myeloproliferative disorders” (MPDs) in 1951. According to Dameshek, MPDs included chronic myelogenous leukemia (CML), polycythemia vera (PV), essential thrombocythemia (ET), primary myelofibrosis (PMF) and erythroleukemia (Di Guglielmo’s syndrome) (Dameshek, 1951).

Later, in the 1960s, the association of CML with the Philadelphia chromosome (Ph), which arises from the reciprocal translocation of the long arm of chromosome 9 (9q) and the long arm of chromosome 22 (22q) (t(9; 22) (q34; q11)) (Nowell and Hungerford, 1960; Lugo et al., 1990), and the revision of erythroleukemia as a variant of acute myeloid leukemia (Acute Myeloid Leukemia, AML) led to the definition of PV, ET and PMF as three "classic" Philadelphia negative chronic myeloproliferative syndromes (Ph-MPN).

In 2001, the World Health Organization (WHO) committee for the classification of myeloid neoplasms grouped CML, ET, PV, and MF under the category of chronic myeloproliferative diseases (CMPDs), which also included the “non-classical” syndrome as chronic eosinophilic leukemia/hypereosinophilic syndrome (CEL/HES), chronic neutrophilic leukemia (CNL), and ‘CMPD, unclassifiable’ (Michiels et al., 2006).

Over the years, the WHO diagnostic criteria have been revised considering the new cytogenetic and molecular discoveries of somatic mutations that typify ET, PV, and MF. The current classification system, edited in 2016 by WHO committee, includes in the MPNs category: CML, chronic neutrophilic leukemia, PV, ET, primary myelofibrosis (PMF), chronic eosinophilic leukemia-not otherwise specified and MPN-unclassifiable (MPN-U) (Barbui et al., 2018). Given the close correlation and overlapping features of these diseases, PV, ET, and MF are grouped together and defined as “the *JAK2/CALR/MPL* mutation-related MPNs*”.* Indeed, MPNs are characterized by the uncontrolled activation and proliferation of hematopoietic stem cell (HSC) due to mutations that

boost JAK-STAT pathway with different mechanisms including the gain of function mutations in the Janus kinase 2 (*JAK2*) gene, present in all cases of PV, or mutually exclusive mutations in *JAK2*, calreticulin (*CALR*) or thrombopoietin receptor (*MPL*) genes in ET and PMF (Vainchenker and Kralovics, 2017).

Of note, this new definition of "neoplasms" instead of "disorders" highlights the clonal and neoplastic nature of these diseases. Furthermore, in this new classification system a greater relevance is given to mutational screening and bone marrow examination, both crucial for an accurate diagnosis of MPNs.

The guidelines for the diagnosis of these Ph-MPNs, defined in the 2016 WHO revision, include the evaluation of laboratory parameters as hemoglobin, platelet and white blood cell count karyotype, morphological abnormalities in bone marrow biopsy, biochemical and clinical features, and molecular genetic markers, such as somatic mutations in *JAK2, MPL* and *CALR*, namely "driver mutations" (see the dedicated paragraph) (Rumi and Cazzola, 2017).

In most cases, diagnostic strategy implies a differential diagnosis based on a composite evaluation these parameters. Indeed, the diagnosis of PV from secondary erythrocytosis is related to the concomitant evaluation of *JAK2*V617F mutation, present in the 97% of PV patients, and the evaluation of erythropoietin serum levels (Epo). The approximately 3% of PV patients, who are negative for *JAK2*V617F, frequently display increased Epo levels and most of them harbors *JAK2* exon 12 mutations (Tefferi, 2017).

MPNs can also show overlapping features that make an accurate and early diagnosis often challenging but indispensable to optimize the patient management. Indeed, MF may arise *de novo* as primary myelofibrosis (PMF), or evolve from a previous PV or ET, namely secondary myelofibrosis (sMF). In most cases ET can be confounded with PMF, and the specific diagnosis requires both mutational profile evaluation and bone marrow biopsy, since BM hyper-cellularity with an increased number of neutrophils and atypical megakaryocytes (with "cloud-like" and "balloon shaped" nuclei) represent the most important criteria for distinguishing between these two MPNs. Additionally, the clinical observation that early or "pre-fibrotic" PMF (prePMF, displaying low grade bone marrow fibrosis) shows a distinct pathological phenotype and prognosis, led the 2016 WHO committee to recognize prePMF from overt fibrotic PMF, typified by higher grade of bone marrow fibrosis (≥ II) (Arber et al., 2016).

Even if MPNs share clinical and biological features, MPNs vary significantly in terms of disease severity, progression to the burn out phase (for ET and PV), risk of blast transformation and survival. ET and PV are considered the early-stage disease with a milder phenotype as compared to MF. PMF and especially sMF represent the advanced, fibrotic (also called spent) phase with the highest rates of mortality and risk of transformation in AML (Vainchenker et al, 2017).

2. Primary myelofibrosis

2.1 Definition and epidemiology

Primary myelofibrosis (PMF) is the rarest and the most complex of the classic Ph-MPNs with an annual incidence range from 0.22 to 0.99 per 100,000 person-years and a pooled annual rate of 0.47 per 100,000 (Titmarsh et al., 2014). In a recent analysis of the Surveillance, Epidemiology, and End Results (SEER) and North American Association of Central Cancer Registries databases, PMF have an incidence of 0.3 per 100,000 in USA and it varies according to geographical regions (Duggan et al., 2016).

Regarding the age of disease onset, PMF patients tend to be slightly older than ET and PV patients, indeed the PMF median age at first diagnosis ranges between 65–67 years, with differences depending on patient's ethnicity. SEER data, collected from 2001 to 2016, suggest a median age at PMF diagnosis of 69 years (Shallis et al., 2020). Besides older age, also male gender represents an independent risk factor for the onset and outcome in PMF and generally in MPNs. Although women have a higher risk to develop MPN and outnumber men in ET and PV, there is a male predominance in PMF (PMF vs ET relative risk is about 3.2; $P< .001$; and PMF vs PV relative risk is about 2.1; $P< .001$) (Karantanos et al., 2020; Geyer et al., 2017).

Furthermore, gender appears to affect symptom burden, disease natural history and clinical outcome in MPNs, including PMF. In a recent study by Karantanos and colleagues, male gender was described as an independent predictive factor of poorer outcomes and reduced survival. Independently of age, phenotype, or MPN-specific driver mutation, male gender was also associated to higher risk of progression to sMF, transformation to AML and higher mortality due to second cancers. Finally, men had a higher $CD34^+$ cell mutational burden and a higher risk of non–MPN-specific somatic mutations, including high-risk mutations (Karantanos et al., 2020).

Clinical manifestations in PMF affect 85% of patients and include abdominal pain/discomfort, microvascular symptoms as fatigue, headache, insomnia, concentration difficulties, dizziness, severe anemia, bone pain, splenic infarct, pruritus, and cachexia (Tefferi, 2000; Mesa et al., 2009). In addition, thrombotic and haemorrhagic events, second cancers and, rarely, leukemic transformation represent common complications related to PMF which significantly contribute to morbidity and mortality (Tefferi, 2018). Indeed, reported median survival is variable and ranges from 4 to 7 years from disease onset (Cervantes et al., 1997; Cervantes et al., 2009).

2.2 Megakaryocyte and bone marrow morphological alterations in PMF

Among Ph-MPNs, PMF is the most heterogeneous. It is characterized by clonal myeloproliferation due to the hypersensitivity of hematopoietic progenitors to growth factors, bone marrow hypercellularity and peripheral blood cytopenia or cytosis (Barosi, 1999). Inefficient hematopoiesis leads to a lower production of red blood cells (anemia), an impaired megakaryocytopoiesis (thrombocytopenia or thrombocytosis) and platelet activation, and an increase of immature myeloid cells in the peripheral blood. Profound alterations in the architecture of bone marrow stroma are also observed, including bone marrow fibrosis, osteosclerosis and neo-angiogenesis (Zahr et al., 2016). Insufficient haematopoiesis and bone marrow fibrosis are closely associated, and they result by the interaction between the neoplastic clone and stromal cells of the surrounding microenvironment. Bone marrow biopsy typically reveals clusters of abnormal megakaryocytes, elevated number of hematopoietic progenitor cells and an increased microvessel density. Abnormalities in the process of megakaryocyte (MK) differentiation are peculiar in PMF. In PMF, MKs are markedly hyperplastic and display peculiar morphological abnormalities such as tight clustering, cellular pleomorphism (presence of the so called “micromegakariocytes” or “dwarf megakaryocytes”), smaller size and hypolobulated nuclei (Thiele, 2009) (Figure 35).

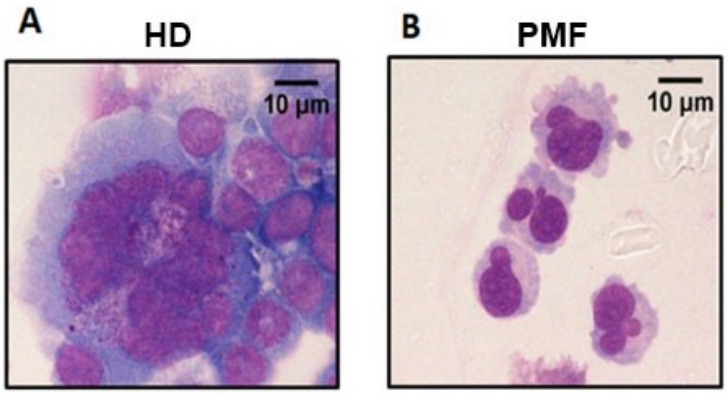

Figure 35. Morphological alterations of megakaryocytes in PMF. Representative megakaryocytes (MKs) from a healthy donor (panel A, HD) and a PMF patient (panel B, PMF), obtained *in vitro* from TPO-treated $CD34^+$ cells after 14 days. A) MKs from HD are usually larger and display multilobulated nuclei. B) MKs from PMF show smaller size and nuclear hypolobulation (May–Grünwald Giemsa staining, scale bar: 10 µm) (adapted from Masselli et al., 2015).

Balduini and colleagues have also demonstrated that PMF MKs impaired capacity of differentiation is associated to a decrease in *in vitro* proplatelet formation as compared to MKs from PV, ET, or healthy subjects (Balduini et al., 2011). Furthermore, MKs are considered the main sources of the “cytokine storm” that lead to BM fibrotic changes and neoplastic clone selection; and promote genomic instability (Papadantonakis et al., 2012).

Considering bone marrow alterations, the hematopoietic tissue is progressively replaced by the reticulin and collagen fibres deposition, while bone trabeculae thicken and undergo distortion. These structural changes are associated to bone marrow exhaustion and extramedullary haematopoiesis, which consists in the mobilization and migration of the hematopoietic precursors towards extramedullary niches in the spleen and the liver, resulting in spleno- and hepatomegaly. The molecular mechanism underling the homing of hematopoietic precursors is still under investigation; however pro-inflammatory cytokines, as TGF1β, seems to be involved in this process (Zingariello et al., 2013).

2.3 Classification and diagnostic criteria in MF

As mentioned above, myelofibrosis can be distinguished into two disease subtypes. MF can occur de novo, and it is considered as primary myelofibrosis (PMF) or results from the progression of a previous ET or PV (almost in 15% of ET and PV patients), which develop a “PMF-like phenotype” (post-ET/PV MF or sMF) during the clinical course. PMF and sMF are phenotypically identical and currently no biomarkers can predict the evolution of ET and PV toward sMF.
Bone marrow histology is crucial in the diagnosis and classification of MPN (true-ET *vs.* prePMF) and MF subtypes (prePMF *vs*. overtPMF). Nowadays, the differential diagnosis of “true” essential thrombocythemia (true-ET) from pre-fibrotic/early primary myelofibrosis (prePMF) is based on the histological evaluation of bone marrow biopsy, including cell morphology and lack of reticulin fibres at the disease onset. During the past two decades, different grading systems have been described to evaluate bone marrow fibrosis in pathological conditions, most of them deriving from the Bauermeister scale (Bauermeister et al., 1971).

In 2005, a panel of expert pathologists published the European Consensus on grading of bone marrow fibrosis, in which they outlined the guidelines for bone marrow histological analysis (Thiele et al., 2005). Based on the qualitative (reticulin or collagen) and quantitative evaluation of bone marrow fibrosis, four categories have been defined, ranging from MF-0 (Table 8), which represents normal bone marrow, to MF-3, in which coarse bundles of collagen fibrosis can be observed accompanied by significant osteosclerosis (Thiele et al., 2005) (Figure 36).

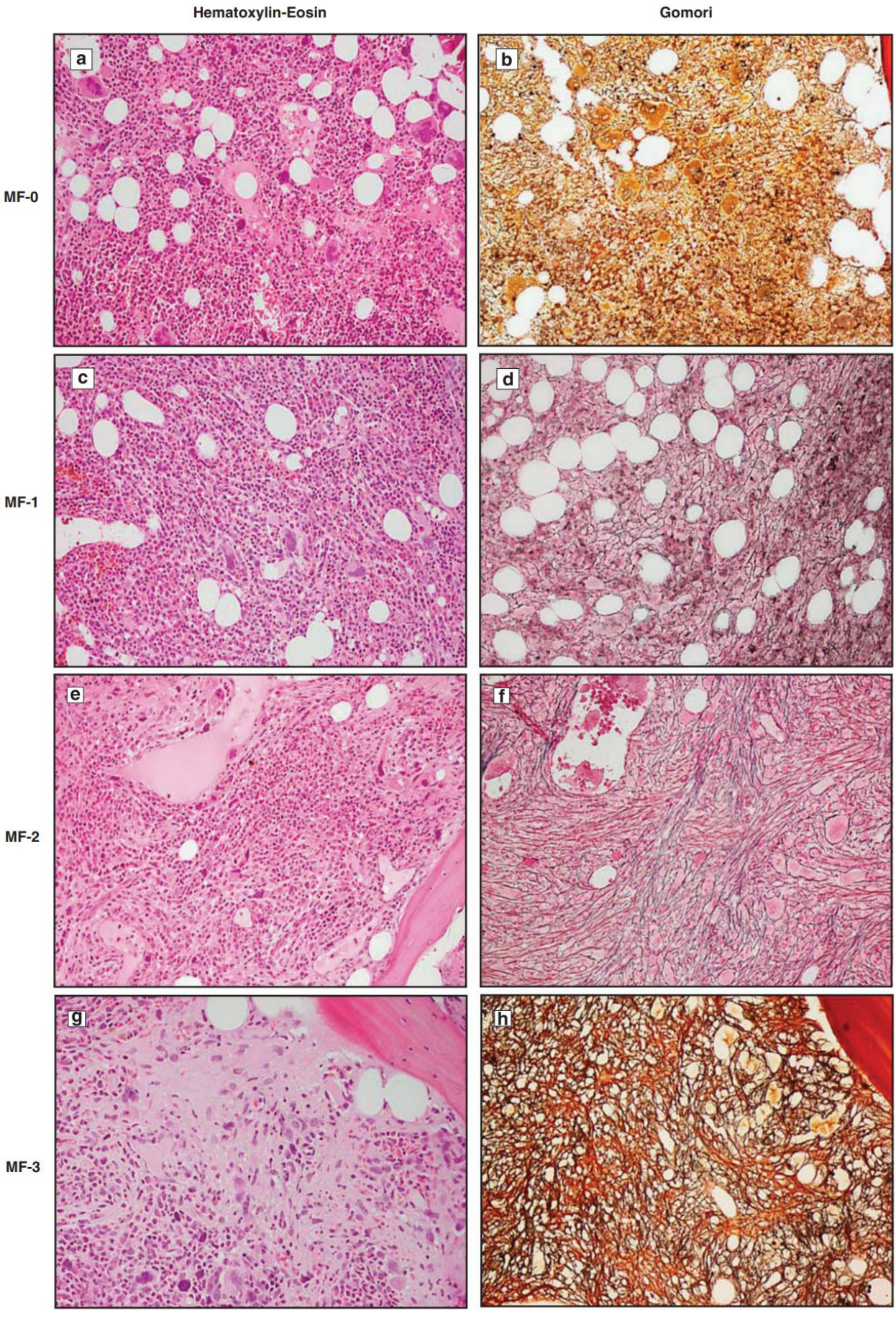
Hematoxylin-Eosin
Gomori
MF-0
MF-1
MF-2
MF-3
a
b
c
d
e
f
g
h

Figure 36. Morphologiacal features of bone marrow in PMF. Representative images of formalin-fixed, paraffin-embedded bone marrow biopsies, stained with haematoxylin–eosin and Gomori's silver impregnation to evaluate bone maroow alterationds and grading of fibrosis. A, B) Pre-fibrotic primary myelofibrosis (MF-0): scattered linear reticulin fibres with no intersections. C, D) Early-stage primary myelofibrosis (MF-1): loose network of reticulin fibres with many intersections, especially in perivascular areas. E, F) Fibrotic stage primary myelofibrosis (MF-2): diffuse and dense increase in reticulin fibres, with extensive intersections and occasionally with focal bundles of collagen. G, H) Overt fibrotic stage primary myelofibrosis (MF-3): diffuse and dense increase in reticulin fibres, with extensive intersections and coarse bundles of collagen (Gianelli et al., 2012).

Myelofibrosis grading	
MF-0	Scattered linear reticulin with no intersections (crossovers) corresponding to normal BM
MF-1	Loose network of reticulin with many intersections, especially in perivascular areas
MF-2	Diffuse and dense increase in reticulin with extensive intersections, occasionally with focal bundles of thick fibers mostly consistent with collagen, and/or focal osteosclerosis*
MF-3	Diffuse and dense increase in reticulin with extensive intersections and coarse bundles of thick fibers consistent with collagen, usually associated with osteosclerosis*

Table 8. Grading of bone marrow fibrosis. Semiquantitative grading of BM fibrosis (MF) with minor modifications concerning collagen and osteosclerosis. Fiber density should be assessed only in hematopoietic areas. *In grades MF-2 or MF-3 an additional trichrome stain is recommended (from Arber et al., 2016).

Futhermore, in the 2016 WHO diagnostic system PMF is sub-classified according to the grading of bone marrow fibrosis in prePMF (<II) and overtPMF (≥II) (Arber et al., 2016). The main diagnostic criteria for prePMF and overtPMF are listed in the tables below (Tables 9 and 10).

WHO prePMF criteria
Major criteria
1. Megakaryocytic proliferation and atypia, without reticulin fibrosis >grade 1*, accompanied by increased age-adjusted BM cellularity, granulocytic proliferation, and often decreased erythropoiesis
2. Not meeting the WHO criteria for *BCR-ABL1*⁺ CML, PV, ET, myelodysplastic syndromes, or other myeloid neoplasms
3. Presence of *JAK2*, *CALR*, or *MPL* mutation or in the absence of these mutations, presence of another clonal marker, † or absence of minor reactive BM reticulin fibrosis ‡
Minor criteria
Presence of at least 1 of the following, confirmed in 2 consecutive determinations:
a. Anemia not attributed to a comorbid condition
b. Leukocytosis ≥11 × 10^9/L
c. Palpable splenomegaly
d. LDH increased to above upper normal limit of institutional reference range
Diagnosis of prePMF requires meeting all 3 major criteria, and at least 1 minor criterion

Table 9. WHO criteria for the diagnosis of prePMF. "† In the absence of any of the 3 major clonal mutations, the search for the most frequent accompanying mutations (ASXL1, EZH2, TET2, IDH1/IDH2, SRSF2, SF3B1) are of help in determining the clonal nature of the disease. ‡ Minor (grade 1) reticulin fibrosis secondary to infection, autoimmune disorder or other chronic inflammatory conditions, hairy cell leukemia or other lymphoid neoplasm, metastatic malignancy, or toxic (chronic) myelopathies" (from Arber et al., 2016).

WHO overt PMF criteria
Major criteria
1. Presence of megakaryocytic proliferation and atypia, accompanied by either reticulin and/or collagen fibrosis grades 2 or 3*
2. Not meeting WHO criteria for ET, PV, BCR-ABL1+ CML, myelodysplastic syndromes, or other myeloid neoplasms
3. Presence of JAK2, CALR, or MPL mutation or in the absence of these mutations, presence of another clonal marker, † or absence of reactive myelofibrosis ‡
Minor criteria
Presence of at least 1 of the following, confirmed in 2 consecutive determinations:
a. Anemia not attributed to a comorbid condition
b. Leukocytosis ≥11 × 109/L
c. Palpable splenomegaly
d. LDH increased to above upper normal limit of institutional reference range
e. Leukoerythroblastosis
Diagnosis of overt PMF requires meeting all 3 major criteria, and at least 1 minor criterion

Table 10. WHO criteria for the diagnosis of overtPMF. "† In the absence of any of the 3 major clonal mutations, the search for the most frequent accompanying mutations (ASXL1, EZH2, TET2, IDH1/IDH2, SRSF2, SF3B1) are of help in determining the clonal nature of the disease. ‡ BM fibrosis secondary to infection, autoimmune disorder, or other chronic inflammatory conditions, hairy cell leukemia or other lymphoid neoplasm, metastatic malignancy, or toxic (chronic) myelopathies" (from Arber et al., 2016).

Several studies have evaluated the prognostic relevance of bone marrow fibrosis in MF with controversial results (Gianelli et al., 2012; Nazha et al., 2013). The study by Nazha et al. demonstrated that bone marrow fibrosis was associated with adverse clinical features of PMF such as lower hemoglobin level, larger spleen, and higher percentage of peripheral blood blasts, but rates of overall survival, event-free survival, and frequency in blast transformation were similar in preMF vs. overtPMF (Nazha et al., 2013). By contrast, in a retrospective analysis on 131 patients with PMF, Lekovic and colleagues found that BM fibrosis grade >1 was associated with shorter overall survival (median: 51 months) as compared to grade ≤1 (median: 147 months), suggesting high grade of BM fibrosis as an independent prognostic factor to predict patient outcome (Lekovic et al., 2014).

2.4 Risk stratification and therapeutic options

Prognostic stratification of MF patients is pivotal to make appropriate therapeutic decisions. Previous studies have identified several adverse prognostic factors for survival and various prognostic scoring systems have been proposed during the years.

The International Prognostic Scoring System (IPSS) risk score, proposed in 2009 by the International Working Group on Myeloproliferative Neoplasms Research and Treatment, is the

routinely used prognostic score for patient risk stratification at the time of first diagnosis. Although these scores have been validated only on PMF patients, they are applied in clinical practice also to sMF. The IPSS is based on five independent adverse factors: age (above 65 years); presence of constitutional symptoms; hemoglobin levels (lower than 10 g/dL); leukocyte count (higher than 25×10^9/L) and percentage of circulating blasts (≥ 1%). According to this scoring systems, patients are stratified into four prognostic categories: low risk (0 predictive factor, median survival of 135 months); intermediate risk 1 (1 predictive factor, median survival of 95 months); intermediate risk 2 (2 predictive factors, median survival of 48 months) and high risk (3 or more predictive factor, median survival of 27 months) (Cervantes et al.,2009). In 2010, the IWG-MRT proposed a dynamic prognostic system, namely DIPSS, based on the same prognostic factors used in IPSS but applicable at any time during disease course (Passamonti et al., 2010). The DIPSS gives a higher prognostic power to anaemia, two adverse points instead of one, and it is routinely used to predict the risk of blast transformation of patients during the follow-up. The DIPSS scoring system has subsequently been converted into the DIPSS plus by incorporating three additional independent predictive factors: platelet count (<100x109/L) (Patnaik et al., 2010), transfusion dependency (Tefferi et al., 2009; Elena et al., 2011) and unfavourable karyotype ("complex karyotype or sole or two abnormalities that include 18, 27/ 7q-, i(17q), inv(3), 25/5q-, 12p- or 11q23 rearrangement") (Hussein et al., 2010; Caramazza et al., 2011). Risk categories has been modified as well, and according to these new eight parameters PMF patients are stratified into: low (no risk factors), intermediate-1 (one risk factor), intermediate -2 (2/3 risk factors) and high (4 or more risk factors) with median survivals of 15.4, 6.5, 2.9 and 1.3 years, respectively. (Gangat et al., 2011).

Two novel prognostic scoring systems have been recently developed: the MIPSS 70 scoring system (mutation and karyotype enhanced international prognostic scoring system) (Guglielmelli et al., 2018)) and the GIPSS scoring system (genetically inspired prognostic scoring system) (Tefferi et al., 2018).

The GIPSS scoring system is exclusively based on genetic risk factors (karyotype and mutations). Indeed, international collaborative studies from the Mayo Clinic (USA) and the University of Florence (Italy) have highlighted the prognostic independent relevance of the absence of type 1 or type 1-like CALR mutations, and the presence of one or more high molecular-risk (HMR) mutations of myeloid genes including *ASXL1, DNMT3A, EZH2, IDH1/IDH2, SRSF2, TET2* and *U2AF1*. Among these, *ASXL1* mutation appears to have the greatest impact. Indeed, in the study by Tefferi and co-workers $CALR^-ASXL1^+$ patients have showed a significantly reduced OS (median 2.3 years) as compared to $CALR^+ASXL1^-$ patients (median 10.4 years) (Tefferi et al., 2014).

The MIPSS 70 system and the last version, the MIPSS70 plus system, take into consideration the integration of clinical data with genetic profiling obtained with next generation sequencing (NGS) and genome-wide association study (GWAS). Indeed, it has been demonstrated that driver

mutations and HMR mutations represent useful prognostic tools not only for the prediction of overall survival and leukemic transformation, but also for risk stratification of PMF patients undergoing allogenic hematopoietic stem cell transplant (alloSCT) (Guglielmelli et al., 2018).
The new prognostic parameters are indispensable in planning early patient management and choosing the best therapeutic option for each individual patient.

MF could be considered as a “treatment-orphan disease”. The current “conventional” therapeutic strategies for leukocytosis or thrombocytosis, splenomegaly, and constitutional symptoms in PMF and sMF patients, include corticosteroids, androgens (such as danazol), erythropoiesis stimulating agents (ESA), immunomodulatory drugs (ruxolitinib, IMIDs, thalidomide/lenalidomide), interferon (INF), and cytoreductive therapy (hydroxiurea, melphalan and busulfan). Splenectomy or splenic irradiations are procedures reserved for those patients with marked, symptomatic splenomegaly. All these therapeutic options are only palliative and aimed to relieve symptoms and preserve the quality of patient life. Indeed, none of them have ever been shown to have a consistent, reliable, and lasting impact on the clinical manifestations of PMF in the context of large randomized controlled clinical trials. The promising ruxolitinib (or INCB018424) is a JAK1/2 inhibitor approved by the EMA in 2012 for patients with intermediate (1-2) or high-risk MF who are not eligible for hematopoietic stem cell transplantation. Although it has demonstrated efficacy in spleen size, symptom burden and circulating cytokines reduction, it failed to reverse bone marrow fibrosis or induce complete cancer remission (Cervantes et al., 2013; Harrison et al., 2016).
Therefore, alloSCT currently remains the only potentially curative option for transplant-eligible patients. Successful alloSCT has been associated to long-term remissions, eradication of the neoplastic clone, and increased survival. Unfortunately, not all patients are eligible for allo-SCT. Data from the European Society for Blood and Marrow Transplantation (EBMT) show that only MF patients with age <70 years, intermediate-2- or high-risk disease according to the IPSS, DIPSS or DIPSS-plus and whose median survival is expected to be less than 5 years, should be considered as potential candidates for allo-SCT (Kröger et al., 2015; Kroger et al., 2009).

However, alloSCT is associated to a significant risk of mortality and morbidity, associated to both graft versus Host Disease (GVHD) and non-GVHD. The estimated relapse rate is up to 25% within 5 years and the estimated 1-year post transplant mortality rate is around 30%. Therefore, clinical prognostic scoring systems play a pivotal role in decisions regarding allo-SCT and then in patient outcome.

2.5 Molecular pathogenesis

The genetic landscape of PMF was emerged with the discovery of the first driver mutation in *JAK2* gene, in 2005. Since then, increasing evidence have highlighted the key role of somatic mutations in the disease pathogenesis and evolution. Somatic mutations are functionally grouped as 'driver' and 'other/nondriver' mutations. Driver mutations are responsible for the clonal nature of MPNs. Although they are not disease specific, they all affect the JAK/STAT pathway, leading to the constitutive activation of downstream gene transduction, independently of the ligand binding (Szuber and Tefferi, 2018).

Driver mutations are mutually exclusive; however, they have rarely been detected in the same patient but usually in different neoplastic clones or in different subclone populations. Driver mutations include *JAK2* (located on chromosome 9p24) (James et al., 2005), *MPL* (myeloproliferative leukemia virus oncogene; located on chromosome 1p34) (Pikman et al., 2006) and *CALR* (calreticulin; located on chromosome 19p13.2) (Nangalia et al., 2013).

The *JAK2* mutation is the most frequent, with frequencies that range from 50% to 60% in ET, and from 55% to 65% in PMF, reaching approximately 95-98% in PV (Tefferi and Pardanani, 2015). The remaining 5-2% of PV patients usually carries a somatic mutation of *JAK2* exon 12 (Scott et al., 2007). *CALR* and *MPL* mutations are virtually absent in PV, with rare exceptions, and frequencies are approximately 20-25% in both ET and PMF for *CALR*; and 3-4% in ET and 6-7% in PMF for *MPL* (Tefferi and Pardanani, 2015) (Figure 37).

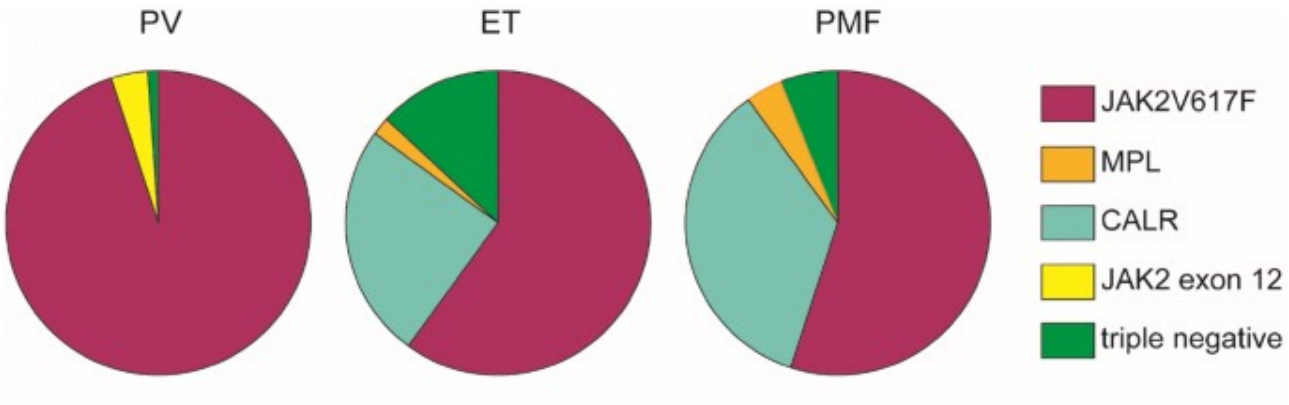

Figure 37. Distribution of driver mutations in MPNs. JAK2, MPL and CALR mutations account for the vast majority of the classical MPN cases (Jia and Kralovics, 2020).

However, there is a small group of patients (around 5-10%) in which none of the driver mutations has been observed; these patients are called “triple-negative”. There are significant differences in terms of disease phenotype and clinical outcome among patients with different driver mutations. Indeed, PMF patients carrying *CALR* mutations generally have a lower risk of anemia, leukocytosis, and thrombocytopenia as compared to the other subtypes. On the other hand, PMF patients with *JAK2* mutations have a higher incidence of thrombosis and leukemic transformation as compared to patients with *CALR* mutations. However, triple-negative patients are those who display the worst clinical features and the most aggressive phenotype. Indeed, triple-negative patients were usually older, had lower platelet count, lower hemoglobin level, and higher IPSS risk (Rumi et al., 2014).

In a recent study on 617 PMF patients, Rumi and co-workers demonstrated that triple negative PMF patients had a very poor prognosis with an extremely high risk of leukemic transformation. The triple negative patients had the lowest overall survival (OS) with an average of 3.2 years from the date of the diagnosis, while the *CALR* mutated patients had the highest (with an average of 17.7 years). Mutations in *JAK2* and *MPL* genes respectively conferred a median life expectancy of 9.2 years and 9.1 years (Rumi et al., 2014) (Figure 38). Similar results were obtained by Teffery and collegues in a study on PMF cohort patients from the Mayo Clinic. (Tefferi et al., 2014).

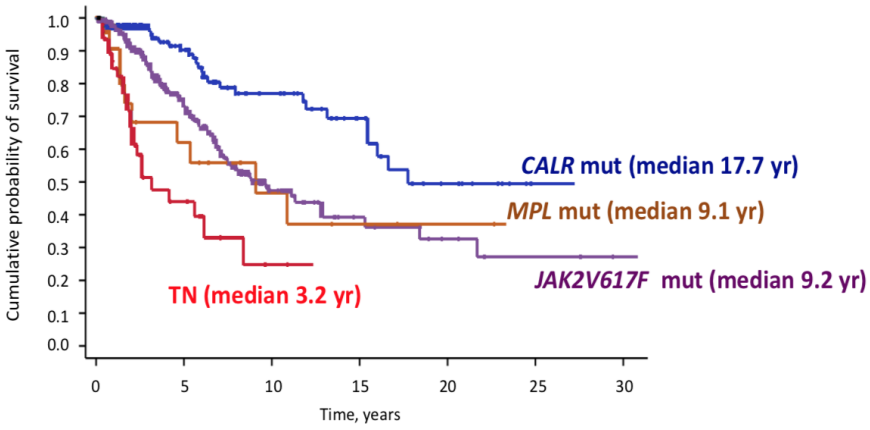

Figure 38. Overall survival of PMF patients stratified according to their driver mutations. Kaplan-Meier analysis of survival, vertical tick marks indicate right-censored patients. The univariate analysis demonstrated thet CALR-mutant patients (in blue) had a better OS as compared to JAK2-mutant (in violet) (HR 2.3, P < .001), MPL-mutant (in orange) (HR 2.6, P = .009), and triple-negative patients (in red) (HR 6.2, P < .001) (Rumi et al., 2014).

- ***Janus kinase 2: V617F and exon 12 mutations***

The Janus kinases (JAKs) are a family of highly conserved non-receptor tyrosine kinases (NRTKs), which include four members: JAK1, JAK2, JAK3 and Tyrosine kinase 2 (Tyk2). JAK1

and 2 were initially known as “Just Another Kinase” but were renamed Janus kinase to reflect the highly homologous kinase domains, one of which was later shown to be a pseudokinase. JAKs are critically involved in cell growth, survival, development, and differentiation of hematopoietic and immune cells (Ghoreschi et al., 2009).

The genes coding for *Jak1* and *Jak2* are located at chromosome 1p31.3 and 9p24, respectively. Tyk2, is located on chromosome 19p13.2 and clustered together with *Jak3* gene, located at 19p13.1 (Pritchard et al., 1992).

Jak proteins contain more than 1,000 amino acids with seven distinct Jak homology regions (JH1 to JH7). JH1 domain, at the carboxyl-terminus, represents the catalytically active kinase domain, which phosphorylates the downstream substrates allowing signal transduction, while the adjacent JH2 domain is a pseudokinase domain, enzymatically inactive but able to regulate JH1. As demonstrated by several studies, in absence of cytokine binding, the JH2 pseudo-kinase domain can inhibit trans-phosphorylation of two residues (Ser523 and Tyr570) in JH1 domain, inducing conformational changes that make the kinase inactive (Silvennoinen et al., 2013) (Figure 39).

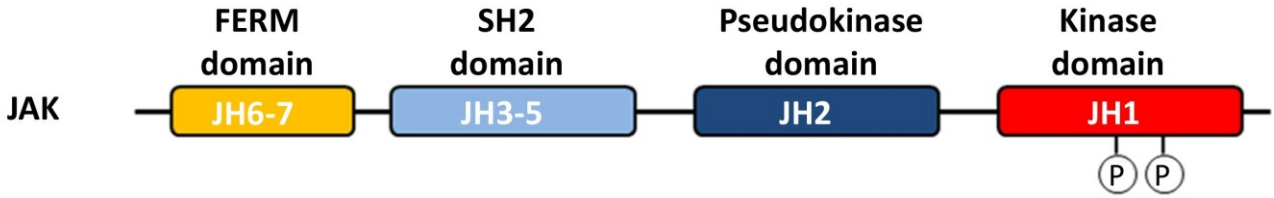

Figure 39. Schematic structure of Jaks. The Jak family comprises four structurally related kinases: Jak1, Jak2, Jak3, and Tyk2. Seven Jak homology regions (JH) contain: the catalytically active kinase domain (JH1), the pseudokinase domain (JH2), the SH2 domain (JH3, JH4), and a FERM domain (JH6, JH7). The FERM domain mediates Jak binding to the transmembrane cytokine receptor and regulates kinase activity. (Durham et al., 2019).

Furthermore, Jak contains a SH2-like domain (JH3-JH4) and a 4.1, ezrin, radixin, moesin (FERM) homology domain (JH6 and JH7) at the amino-terminus. Mutations in the FERM domain seem to affect Jak binding to its cognate transmembrane cytokine receptor, as demonstrated in mutated-FERM domain of Jak3 and Jak1 (Zhou et al., 2001; Haan et al., 2008), or regulate catalytic activity as in Jak2 (Funakoshi-Tago et al., 2008). The role of the SH2 domain is not completely known, it is thought that it may be involved in protein folding rather than signaling, as a mutation of the SH2 domain in JAK1 do not affect its catalytic activity or receptor binding.

In physiological conditions, JAK plays a key role in myelopoiesis, mediating signal transduction activated by the interaction of cytokines such as the erythropoietin and thrombopoietin, or growth factors with their receptor. Ligand binding to its membrane receptor induces a conformational change in the receptor cytoplasmic tail allowing formation of a multimeric complex and the further

induction of signal transduction. Upon activation, Jaks phosphorylate cytoplasmic transcription factors that belong to the STAT (signal transducer and activator of transcription) protein family. After phosphorylation, STATs dimerize and subsequently translocate to the nucleus to regulate gene transcription (Shuai and Liu, 2003) (Figure 40). Indeed, STAT proteins bind specific regulatory sequences in target gene promoter regions to activate or repress transcription of target genes. Besides STATs, JAK proteins also trigger the activation of alternative downstream pathways such as Ras-MAPK, phosphoinositide 3-kinase and AKT/mammalian target of rapamycin (mTOR) pathways, involved into proliferation, survival, and inhibition of apoptosis (Silvennoinen

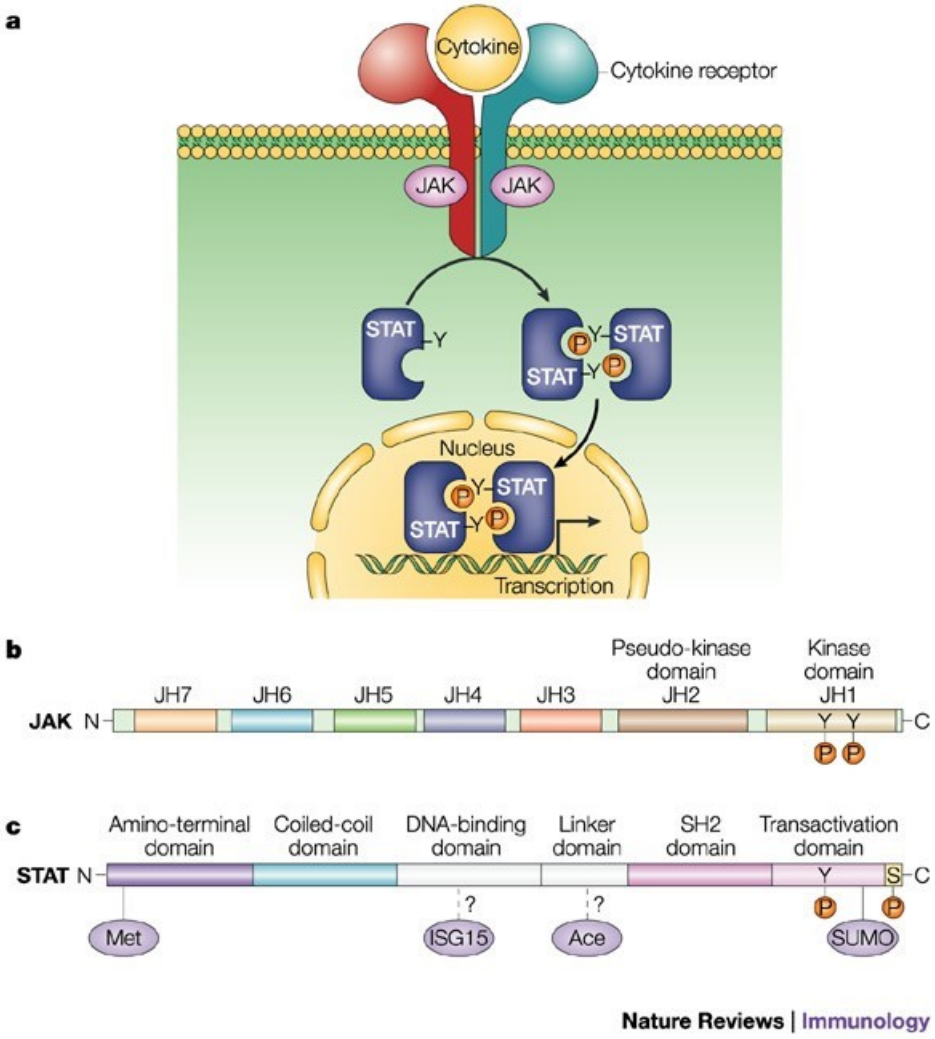

and Hubbard, 2015).

Figure 40. Jak/STAT signaling pathway. A) Schematic representation of the JAK–signal transducer and activator of transcription (STAT) pathway. After cytokine binding, the activation of JAKs results in the phosphorylation of STATs, which dimerize and then translocate to the nucleus to activate gene transcription. B) The protein structure of JAKs. C) The protein structure of STATs. The STATs activity is regulated by protein modification, including tyrosine and serine phosphorylation, methylation (Met), sumoylation (SUMO), ISGylation (ISG15) and acetylation (Ace) (Shuai and Liu, 2003).

Several somatic mutations of *Jak*s have been described in different types of hematopoietic neoplasms and solid tumors. The central role of JAK in oncogenesis has been emphasized in 2005 when different research teams described a Janus kinase 2 mutation (*JAK2*V617F), a clonal recurrent point mutation in the pseudokinase domain of *JAK2*, in patients with MPNs. The *JAK2*V617F mutation consists of a guanine to thymidine somatic point mutation at nucleotide 1849, in exon 14, that results in a valine (Val; V) to phenylalanine (Phe; F) substitution at codon 617 within the JH2 autoinhibitory domain (James et al., 2005). The *JAK2*V617F mutation determines the constitutive hyperactivation of the kinase and allows the hematopoietic mutated clone to be independent of cytokine stimulation for proliferation (Vainchenker et al., 2013). In absence of cytokine binding, the JH2 pseudo-kinase domain negatively regulates the catalytic activity of the JH1 domain, inhibiting its trans-phosphorylation and stabilizing its inactive conformation.

The *JAK2*V617F mutation may arise in multi-potent hematopoietic progenitors, it has been detected in all myeloid lineages, and in B-lymphoid cells, natural killer cells (NK) and more rarely in T cells. Although it has been found in endothelial cells of the spleen of patients with MF, it is virtually absent in non-hematopoietic cells (Vainchenker and Kralovics, 2017).

The gene dosage analysis revealed that the *JAK2*V617F mutation often undergoes a transition from heterozygosis to homozygosis due to of mitotic recombination between chromatids of homologous chromosomes 9p. The stochastic loss of heterozygosity (LOH) on the short arm of chromosome 9 (9pLOH) affects *JAK2*V617F mutant allele burden. The variant allele frequency (VAF) is usually low in ET (around 25%), higher in PV (over 50%), variable but frequently high in PMF reaching 100% in sMF (Rumi et al., 2014).

As mentioned above, the *JAK2*V617F is present in almost all cases with PV, however *JAK2* exon 12 mutations have been also documented in *JAK2V617F*-negative PV patients and generally in MPNs (Scott et al., 2007). Most of these mutations are in-frame small deletions and insertions that fall in the linker between the Src homology 2 (SH2) and in the pseudokinase domain between amino acids 536 and 547, around Lys 539. Among the exon 12 mutations, the most frequent ones are represented by the N542-E543del (23%), E543-D544del (11%), and F537-K539delinsL and K539L (10%). As demonstrated by Passamonti and colleagues, PV patients with exon 12 mutations have significantly higher hemoglobin levels, lower platelet and leukocyte counts at the time of the diagnosis as compared to JAK2V617F-positive PV, however they show a comparable outcome (Passamonti et al., 2011).

- **MPL Virus Oncogene Mutations**

Sequencing analysis of the *MPL* virus oncogene, encoding TPO receptor, led to the discovery of another molecular abnormality in *JAK2*-negative MPN patients (Pikman et al, 2006; Pardanani et al, 2006).

The *MPL* gene, placed in 1p34.2 position of the human genome, encodes the thrombopoietin receptor, the most important regulatory factor of megakaryocytopoiesis and platelet formation. The most frequent *MPL* mutations occur in exon 10, on the tryptophan W515 between the transmembrane and the cytosolic domains of MPL. This domain plays an important role in preserving the cytosolic conformation of MPL and preventing spontaneous activation of the receptor. The main *MPL* mutations consist in the substitution of a tryptophan in position 515 with another amino acid such as leucine, lysine, or arginine (W515L/K/A) leading to the constitutive activation of the MPL receptor and the downstream JAK/STAT pathway. However, several other substitutions have been described such as W515R and W515G (Skoda et al, 2015) (Figure 41).

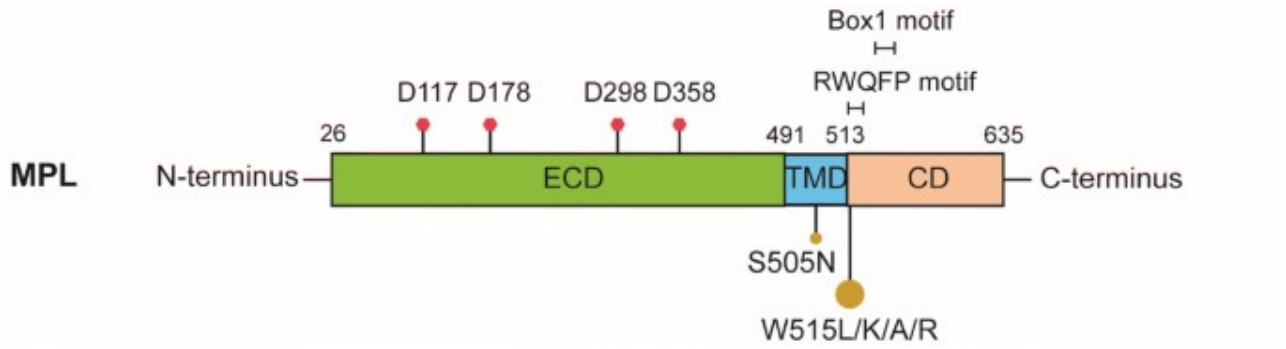

Figure 41. Schematic representation of thrombopoietin receptor MPL protein. The MPL protein (635 amino acids) consists of an extracellular domain (ECD), a transmembrane domain (TMD) and a cytosolic domain (CD). The ECD domain presents a signal peptide of 25 amino acids at N-terminus and four N-linked glycosylation sites, which mediate the trafficking of the receptor. TMD and the adjacent amphipathic helical RWQFP motif block the activation of the receptor in absence of the cytokine. Box1 motif at the CD is required for the binding and the consequent activation of JAK2 (Jia and Kralovics, 2020).

As for *JAK2*, *MPL* mutations are usually in a heterozygous status, but they can become homozygous during disease course. Furthermore, patients with high *MPL*-mutant allele burden (greater than 50%) usually display a marked grading of marrow fibrosis, suggesting the acquired copy-neutral loss of heterozygosity of chromosome 1p as a molecular mechanism of fibrotic progression in *MPL*-mutated MPNs (Rumi et al., 2013). Recurrent *MPL* mutations, including *MPL*W515L and *MPL*W515K mutations, occur in approximately 15% of *JAK2*V617F-negative MPN cases, in approximately 5% of ET and 10% of PMF (Alshemmari et al, 2016).

- **Calreticulin mutations**

Calreticulin (CALR) is a Ca^{2+}-binding protein in the endoplasmic reticulum of different type of human cells. The gene is located on chromosome 19p13.13, and it seems to regulate intracellular calcium homeostasis (transport of calcium from the endoplasmic reticulum) and protein synthesis and folding, acting as a molecular chaperone (Alshemmari et al, 2016). The CALR protein exerts its functions also outside of the endoplasmic reticulum, where it plays a role in a variety of cellular processes, as cell adhesion, cell migration and apoptotic cell clearance (Gardai et al., 2010). Furthermore, calreticulin has been found also in the nucleus, acting as gene transcription modulator (Burns et al., 1994).

In 2013, Klampfl's and Nangalia's, research team, simultaneously, identified somatic mutations in *CALR* gene in patients with PMF and ET, negative for *JAK2* and *MPL* mutations. *CALR* mutations were detected in about 67% of ET patients and 88% of PMF patients, and it was absent in PV patients (Klampfl et al., 2013; Nangalia et al., 2013). A total of 36 types of mutations were identified, and all *CALR* mutations are insertion or deletion mutations in the last exon, which corresponds to the C-terminal amino acids of the protein. Most of these mutations are in a heterozygous state and determine the frameshift of the reading frame resulting in the rearrangement of the C-terminal sequence (Figure 42).

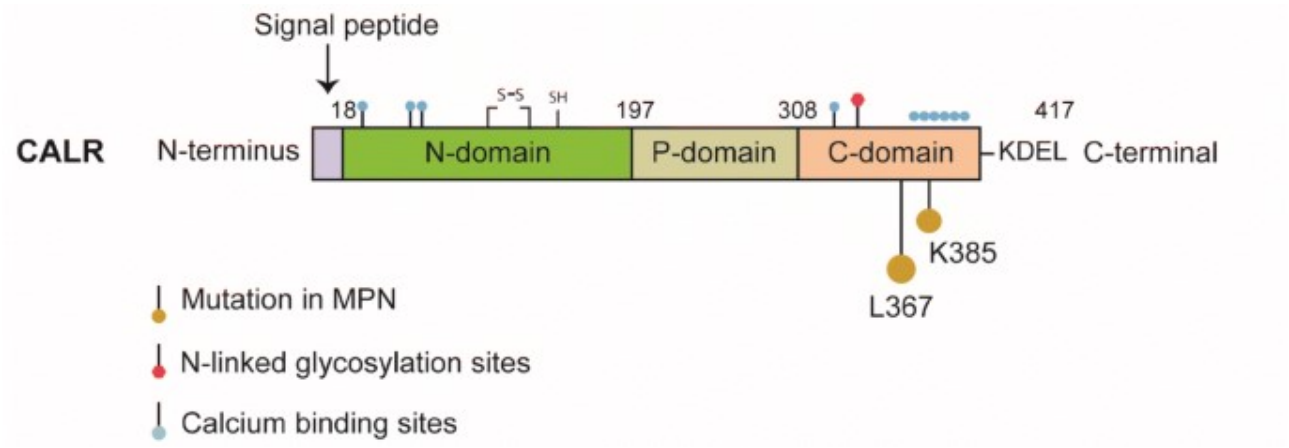

Figure 42. Schematic representation of calreticulin human protein. Human CALR protein (417 amino acids) consists of an N-terminal ER signal peptide, an N-domain, a P-domain, a C-domain, and an ER-retention signal (KDEL) at C-terminus. The N domain contains four amino acids accounting for the interaction with Ca^{2+} ions, which is important for maintaining the secondary structure of the protein. The P-domain is enriched in proline residues and has an extended arm-like structure, crucial for the molecular chaperone function. The C-terminus of calreticulin contains several negative charged amino acids that bind to Ca^{2+} with high affinity. The last four amino acids KDEL represent an ER retention signal which is responsible for the ER localization of the protein (Jia and Kralovics, 2020).

The C-terminus of calreticulin contains four amino acids (KDEL), which are essential for the retention of calreticulin within the endoplasmic reticulum. In mutated *CALR*, this sequence is completely absent, and the novel C-terminal sequence is enriched in arginine and methionine and

bears positively charged. These alterations affect protein localization in the cytoplasm and its Ca^{2+} binding capacity (Klampfl et al., 2013).

The two main *CALR* mutations are type 1, a 52-bp deletion (L367fs*46), and type 2, a 5-bp TTGTC insertion (K385fs*47) (Nangalia et al., 2013). Other mutations have been identified in *CALR* gene and they have been classified in “type 1–like” and “type 2–like”, according to the structural changes. *CALR* mutations are usually heterozygous, although type 2 mutations have been identified in homozygous state in a few cases. There are great differences in terms of frequency and outcome between type 1 and type 2 mutations in ET and PMF. Indeed, type 1 and type 2 mutations are homogeneous in ET (55% vs. 35%), whereas type 1 variant is predominant (75% vs. 15%) in PMF (Cabagnols et al., 2015). Furthermore, patients with type 2 or 'type-2-like' variants of CALR display a poorer prognosis and a reduced OS (median OS of 3.1 years) as compared to patients with type 1 or 'type-1-like' variants (median OS of 10.3years), but similar to that of *JAK2*V617F-positive patients with PMF (Alshemmari et al, 2016).

Mutant *CALR* exerts its oncogenic function via MPL interaction. Cell line models (Ba/F3 cells) overexpressing the type 1 mutant *CALR* were able to proliferate even in the absence of mitogen signals, and were sensitive to the JAK family kinase inhibitor, suggesting therefore the involvement of JAK/STAT signalling pathway. Moreover, the mutated *CALR* seemed to be associated to *MPL*. The mutant-specific carboxyl terminal portion of CALR can bind the P-domain of CALR and allow the N-domain to interact with MPL and to induce the constitutive activation of JAK2/STAT/PI3K downstream pathways (Araki et al., 2016; Elf et al., 2016).

- **Non-driver mutations in PMF**

MPN patients are characterized by a gene expression signature associated with activated JAK2 signaling pathway, indeed driver mutations lead to activation of JAK-STAT transcriptional cascade or of an alternative pathway downstream of JAK-STAT signaling (Kleppe et al., 2015) (Figure 43).

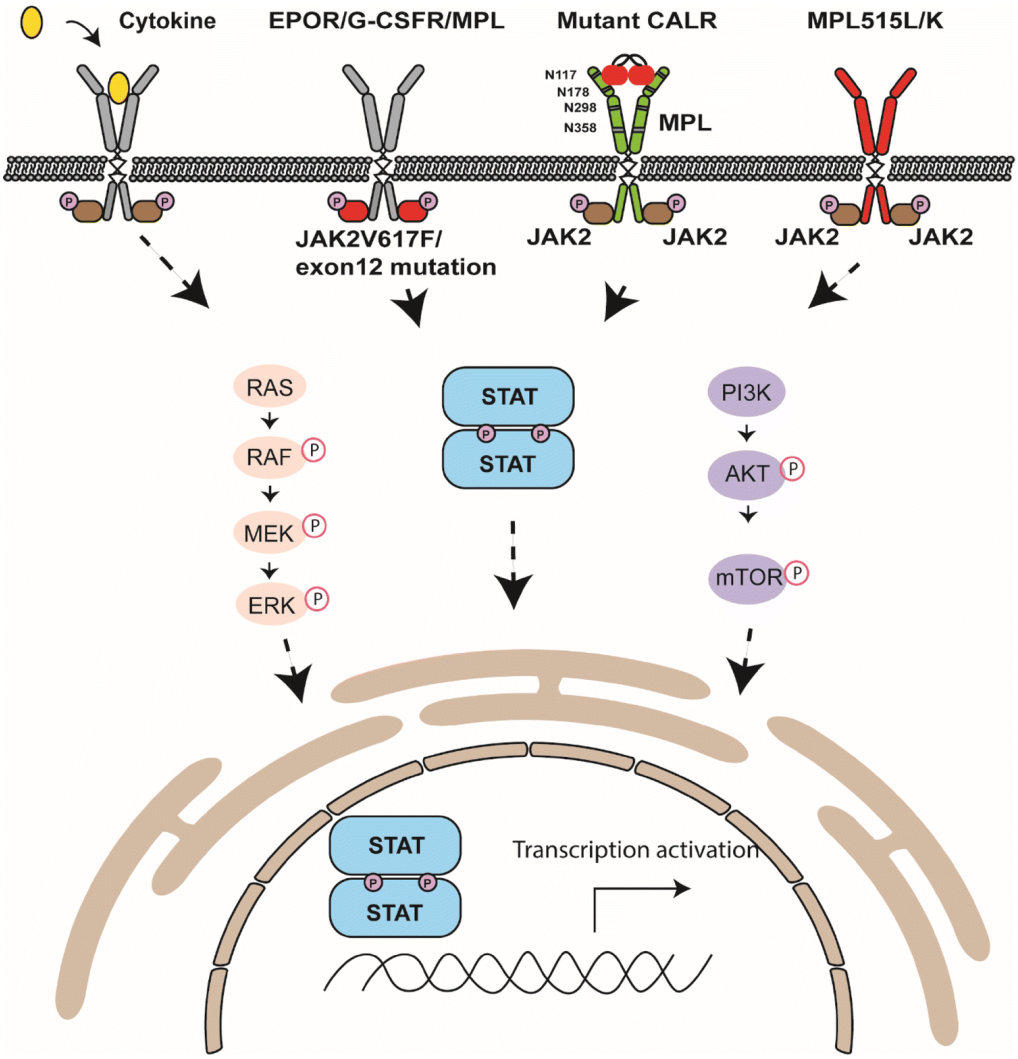

Figure 43. The central role of JAK/STAT pathway in MPN pathogenesis. In the normal physiological conditions, cytokines such as EPO, TPO and GM-SCF, bind their cytokine receptors, which dimerize and activate JAK2. The activated JAK2 phosphorylates and activates STAT1/3/5 as well as (PI3K)/AKT/mTOR and MAPK pathways. STAT molecules translocate into the nucleus, it acts as transcription factors and activate the corresponding genes. In the MPN disease model, JAK2, CALR and MPL mutations constitutively activate these pathways regardless of the cytokine activation (Jia and Kralovics, 2020).

Nevertheless, a great heterogeneity was observed in MPN patients sharing the same driver mutation, in terms of disease phenotype and outcome. Currently, “targeted therapy” with JAK inhibitors has only proved to be useful in ameliorating PMF-associated symptoms and splenomegaly but has failed to induce selective suppression of the neoplastic clone and resolve bone marrow fibrosis (Tefferi, 2012). Apart from driver mutations, many other mutations contribute to MPN phenotype and the disease heterogeneity. Several somatic mutations have been identified

using high-resolution genome analysis using next-generation sequencing (NGS) in MPNs. These mutations are also found in other myeloid malignancies, as MDS and AML, suggesting a common pathogenesis. These co-operating oncogenic mutations include genes involved in cell signalling pathways (*LNK, CBL, FLT3, NRAS* and *NF1*), epigenetic regulation (DNA methylation: *TET2*, *DNMT3A*, *IDH1* and *IDH2*) (Tefferi et al., 2009; Pardanani et al., 2010; Stegelmann F et al, 2011); and histone modifications: *EZH2* and *ASXL1*) (Guglielmelli P et al., 2011; Vannucchi AM et al., 2013), transcriptional regulation (*TP53, RUNX1*) and mRNA processing (*SF3B1, SRSF2, U2AF1*, *ZRSR2*) (Vainchenker e Kralovics, 2017). Nowadays, the exact role of each mutation and their impact on MPN initiation and phenotype is not completely clear. These mutations are thought not to directly act on proliferation, but they can modify and boost the phenotypic effects of driver mutations. It is not clear the sequential order of mutation acquisition and whether these mutations occur before or after driver mutations. According to Vainchenker et al., driver mutations and especially *JAK2*V617F mutation may not be the initial event and other genetic events are required for disease development (Vainchenker et al., 2011). These hypothesis led to the concept of a "pre-*JAK2* event". Indeed, three different genes involved in epigenetic regulation, *TET2, ASXL1*, and *EZH2* are thought to promote second genetic events and, therefore they may precede *JAK2* mutation in MPNs (Swierczek et al., 2011; Saint-Martin et al., 2009). According to this hypothesis, MPNs are not consequence of a single genetic event, but the results of a complex combination of mutations that does not follow a linear dynamic, or a precise timing and that may give rise to different subclones. The accumulation of mutations in the neoplastic clone can influence hematopoietic progenitor biology as well as disease phenotype and outcome but also sensitivity to specific therapy (Ortmann et al., 2015).

The frequency of these "non-driver" mutations varies according to the disease subtypes and it is higher in PMF as compared to ET and PV. In PMF, mutations with frequencies of 10% or more include *ASXL1* (additional sex comb like 1), *SRSF2* (serine/arginine rich splicing factor 2), *TET2* (ten eleven translocation oncogene family member 2) and *U2AF1* (U2 small nuclear RNA auxiliary factor 1) (Vannucchi et al., 2013). The non-driver mutations occur in fewer than 30% of patients during the chronic phase, but usually increase during the blast phase. The most frequent mutations in the blast phase include *IDH1* and *IDH2* (isocitrate dehydrogenase 1 and 2), *DNMT3A* (DNA cytosine methyltransferase 3A), *TP53* (tumor protein P53), *IKZF1* (IKAROS family zinc finger) and *LNK* mutation (an adaptor protein which regulates JAK2 activation) (Tefferi 2010; Rampal et al., 2014).

Some of these mutations have been demonstrated to affect the transcriptional output in MPNs independently from driver mutations (Rampal et al., 2014). Furthermore, it has been suggested that they could play a role in disease progression or transformation into AML, given their higher

prevalence in blast-phase MPNs. Recently, this hypothesis was confirmed in murine model in which co-expression of *JAK2*V617F and *TET2* loss induced disease progression, while *JAK2*V617F and *TP53* mutations led to overt AML (Tsuruta-Kishino et al., 2017; Zhao et al., 2012; Chen et al., 2014).

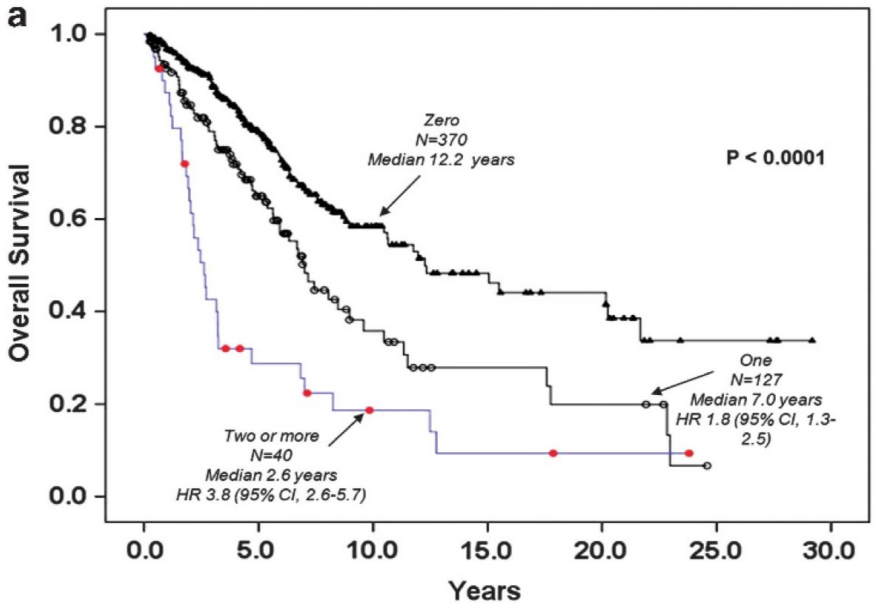

Figure 44. Survival data of 537 patients with primary myelofibrosis from the European cohort stratified by the number (zero, one, two or more) of prognostically detrimental mutations (ASXL1, EZH2, SRSF2 or IDH1/2 (Guglielmelli et al., 2014).

Some of these mutations were also associated to poor diagnosis and reduced overall survival. Guglielmelli and colleagues recently defined a gene panel composed of five mutated genes associated to detrimental prognosis. PMF patients harboring one or more of these mutated genes, including *ASXL1*, *EZH2*, *SRSF2* and *IDH1*/*IDH2*, are considered to belong to the “high-molecular risk” (HMR) category. The presence of one or more of these HMR mutations could discriminate PMF patients with significantly reduced OS (median OS of 2.6 years for PMF patients with two or more HMR mutations *vs*. 7.0 years for PMF patients carrying only one HMR mutation *vs*. 12.3 years for non-mutated ones) and increased risk of blast transformation, independently from IPSS- and DIPSS-plus risk categories (Guglielmelli et al., 2014) (Figure 44).

3. The role of host genetic variant in defining disease risk, phenotype, and outcome

*From: Masselli E, **Pozzi G**, Carubbi C, Vitale M. The Genetic Makeup of Myeloproliferative Neoplasms: Role of Germline Variants in Defining Disease Risk, Phenotypic Diversity and Outcome. Cells. 2021 Sep 29;10(10):2597. doi: 10.3390/cells10102597.*

The high phenotypic variability observed in MPNs cannot be exclusively due to driver mutations and high-risk mutations, but it is reasonable to think that it mirrors the heterogeneity of MPN mutational landscape.

In this context, evidence from epidemiological and familial studies (Rumi E et al., 2007) strongly suggest that host genetic variants, such as single nucleotide polymorphisms (SNPs), may influence disease onset and evolution, as well as explain the phenotypic pleiotropy and different clinical outcomes observed in patients with the same somatic mutations (McMullin and Anderson, 2020).

The genetic predisposition to MPNs includes incomplete penetrance, germline host genetic variants detected in the healthy population, whose presence promote the acquisition of somatic driver mutation in a pluripotent hematopoietic stem cell (Tashi et al., 2017).

We recently reviewed the current literature on the role of host genetic variants in determining individual predisposition to develop an MPN, disease phenotype, course, therapy response and outcome.

According to their biological functions, these SNPs could also be grouped into five functional categories: i) SNPs involved in hematopoiesis, ii) SNPs involved in epigenetic regulation; iii) SNPs involved in cellular aging; iv) SNPs involved in DNA repair and tumor suppression; v) SNPs involved in inflammatory processes (Figure 45). Regarding the biological implications MPN-related SNPs, we can observe that some of these genes exert multiple functions, and consequently belong to different overlapping categories.

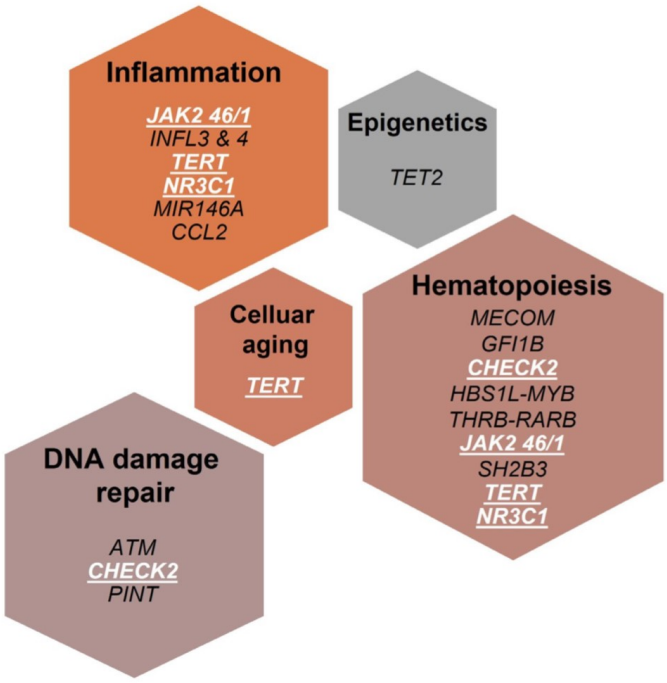

Figure 45. Germline SNPs associated with MPN risk, phenotype, outcome, and therapy response classified according to their biological function (hematopoiesis, DNA damage repair, epigenetics, cellular aging, and inflammation). Genes exerting multiple functions are highlighted in white (Masselli E et al., 2021).

Concerning the host genetic variants that affect individual predisposition to develop an MPN, genome-wide association studies (GWAS) have identified several germline genetic patterns (Table 11).

SNPs	Gene Function (Relative to Hematopoiesis)	Associated Driver Mutations	Associated MPN Phenotype	Ref.
***JAK2* 46/1** haplotype	Hematopoiesis, cytokine receptor signaling	All (>*JAK2*V617F)	All (>PV and PMF)	(Kilpivaara et al., 2009; Oddsson et al., 2014; Tapper et al., 2015; Hinds et al., 2016; Bao et al., 2020)
TERT rs2736100 rs7705526 rs2853677	Telomere length	All	All	(Oddsson et al., 2014; Tapper et al., 2015) (Hinds et al., 2016; Bao et al., 2020) (Hinds et al., 2016; Bao et al., 2020)
MECOM rs2201862 rs3851397 rs9847631	HSC maintenance, differentiation	*JAK2*V617F and *CALR* type 1/type 1-like	PV MF and ET (only in presence of *CALR)*	(Tapper et al., 2015) (Hinds et al., 2016) (Bao et al., 2020)
HBS1L-MYB rs9376092	Peripheral blood cell counts, fetal hemoglobin levels	none	ET (only in presence of *JAK2*V617F)	(Tapper et al., 2015; Hinds et al., 2016)

GFI1B rs621940 rs1633768 rs524137	HSC quiescence, erythroid and megakaryocytic differentiation	n/a	n/a	(Hinds et al., 2016) (Bao et al., 2020) (Bao et al., 2020)
CHEK2 rs555607708 rs17879961	DNA damage response	n/a	n/a	(Hinds et al., 2016) (Bao et al., 2020)
SH2B3 rs7310615	Negative regulation of normal hematopoiesis	n/a	n/a	(Hinds et al., 2016; Bao et al., 2020)
ATM rs1800057	DNA damage response	n/a	n/a	(Hinds et al., 2016; Bao et al., 2020)
TET2 rs1548483 rs62329718	HSC self-renewal, commitment, terminal differentiation of monocytes	n/a	n/a	(Hinds et al., 2016) (Bao et al., 2020)
PINT rs58270997	DNA damage response, hematopoietic stem cell maintenance, and differentiation (via PRC2)	n/a	n/a	(Hinds et al., 2016; Bao et al., 2020)
THRB-RARB rs4858647	unknown	none	PMF	(Tapper et al., 2015)
GATA2 rs9864772	HSC activity and self-renewal, myeloid and myelo-erythroid differentiation, erythroid precursors maintenance	n/a	n/a	(Bao et al., 2020)
SCHIP1 rs77249081	unknown	n/a	n/a	(Bao et al., 2020)
KPNA4 rs74676712	unknown	n/a	n/a	(Bao et al., 2020)
NUDT3 rs116466979	unknown	n/a	n/a	(Bao et al., 2020)
MKLN1 rs61471615	unknown	n/a	n/a	(Bao et al., 2020)
MRPS31 rs8002412	unknown	n/a	n/a	(Bao et al., 2020)
ZNF521 rs9946154	HSC differentiation and B-lymphoid cell development	n/a	n/a	(Bao et al., 2020)
RUNX1 rs55857134	Differentiation of megakaryocytes and lymphocytes	n/a	n/a	(Bao et al., 2020)

Table 11. Genome-wide significant host genetic variants defining the MPN risk. Abbreviations: HSC: Hematopoietic Stem Cell; n/a: not assessed; PRC2: polycomb repressive complex 2; > indicates a stronger association.

Among the germline variants which reach the conventional threshold (P<5x10^{-8}), *JAK2* "46/1", *TERT*, *MECOM*, *GFI1B* and *CHEK2* have been widely investigated.

The ***JAK2* "46/1"** or "GGCC" haplotype has been the first host genetic variant described in MPNs in 2009. It is located in a region of about 250-280kb, on the short arm of chromosome 9 including, in addition to *JAK2*, also Insulin-like 6 (*INSL6*) and *INSL4* genes. The haplotype is made up of a

combination of four SNPs - rs3780367, rs10974944, rs12343867, and rs1159782 - mapping on JAK2 introns 10, 12, 14 and 15, producing the so called “GGCC” sequence. These SNPs are in complete linkage disequilibrium and therefore inherited *en block*. The haplotype frequency is around 45% in the healthy population and its presence has been associated to an increased risk of developing MPNs, especially *JAK2*V617F mutated MPNs. Hermouet and colleagues have hypothesized that the 46/1 haplotype may promote *JAK2* overexpression by recombination or methylation of the gene promoter. *JAK2* activation boosts myeloid cells proliferation, which in turn elicit genomic instability and increases risk of DNA replication errors and mutations. Moreover, the overexpression of *INSL4* and *INSL6* (also part of the haplotype) in bone marrow stromal cells may lead to increased production of pro-inflammatory cytokines, generating a permissive microenvironment for the mutated clone expansion (Hermouet and Vilaine, 2011).
Telomere reverse transcriptase gene (***TERT***) encodes for the catalytic component of telomerase, a ribonucleoprotein enzyme, which regulates telomere length, preventing the activation of the cellular senescence program (Savage, 2009). The rs2736100 SNP, located in the second intron of *TERT* gene at 5p15, has been associated to increased risk of cancer (Thompson et al., 2020), including *JAK2*V617F-positive MPNs. Although the biological relevance of this gene is evident in cancer onset, the underlying functional mechanism is still debated. *TERT* gene is highly polymorphic, and different SNPs have been found enriched in MPN patients, including rs2736100, rs7705526 and the rs2853677 (Hinds et al., 2016; Bao et al., 2020). Telomere length is genetically determined by, at least, other 10 SNPs (*ZNF676* rs412658, *CTC1* rs3027234, *DHX35* rs6028466, *NAF1* rs7675998, *PXK* rs6772228, *ZNF208* rs8105767, *OBFC1* rs9420907, *ACYP2* rs11125529, *TERC* rs10936599 and *ZBTB46* rs755017) (Codds et al., 2013; Giaccherini et al., 2020). A polygenic risk score, called "teloscore", is based on these 11 SNPs. Interestingly, Giaccherini et al. have recently tested the teloscore to predict MPN onset and they have found that genetically determined longer telomeres are associated to higher MPN risk (Giaccherini et al., 2020).

Furthermore, *TERT* is not only involved in telomere length regulation, but it is also involved in cell cycle regulation, promotion of cell growth and proliferation, and control of mitochondrial integrity following oxidative stress (Thompson et al., 2020). In addition, Wang and co-workers observed a “dose-dependent effect” of *TERT* rs2736100 polymorphic allele on IL-6 production in non-small cell lung cancer, suggesting a role for this SNP in *IL6* gene expression modulation and cytokine production (Thompson et al., 2020; Wang et al., 2014).

Another widely investigated polymorphisms are that localized at ***MECOM*** gene (3q26.2 and 3q26.3) and at the intergenic region between *HBS1L* and *MYB* (the so called HMIP region), which have been considered a predisposing factor for MPN onset. *MECOM* (*MDS1* And *EVI1* Complex Locus) gene encodes for a transcription factor involved in hematopoietic stem cell maintenance,

differentiation and leukemogenesis (Yamazaki et al., 2014). The role of *MECOM* in hematologic neoplasms has been widely investigated. Somatic mutations provoke of a rare inherited bone marrow failure syndrome characterised by megakaryocytic thrombocytopenia and multi-organ malformations (Yamazaki et al., 2014). In addition, chromosomal rearrangements between 3q21 and 3q26 increases the risk of severe acute myeloid leukemia, because of the GATA2 enhancer reposition near the *MECOM* locus, which results in both *EVI1* overexpression and GATA2 haploinsufficiency (Yamaoka et al., 2020).

Three different *MECOM* SNPs have been identified as susceptibility alleles in MPNs: the rs22018862 (Tapper et al., 2014), the rs3851397 (Hinds et al., 2016) and the rs9847631 (Bao et al., 2020). The rs22018862 SNP, located in a non-coding region downstream *MECOM*, correlates with PV and *CALR*-mutated ET and PMF; and it is the only germline variant that, with the *JAK2* 46/1 haplotype, maintained genome-wide significance when the analysis was restricted to *JAK2*V617F-negative MPNs (Tapper et al., 2014).

HMIP SNPs, mapped in the intergenic region between *HBS1L* and *MYB* genes, are responsible for inter-individual variability of hematologic parameters in healthy subjects, since it affects platelet, erythrocyte and monocyte counts (Soranzo et al., 2009; Ferreira et al., 2009), and they have relevant functional and clinical implications in β hemoglobinopathies (Sankaran et al., 2011; Stadhouders et al., 2014). The rs9376092 SNP was identified as a predictive host genetic variant for increased MPN risk (Tapper et al., 2014; Hinds et al., 2016). The rs9376092 is in strong linkage disequilibrium with the other SNPs of the HMIP region. This SNP modulates the flanking genes expression, especially of *MYB* gene, which is significantly down-modulated. Interestingly, *MYB* down-regulation accounts for enhanced normal and clonal megakaryopoiesis, since *MYB* knockdown in normal human hematopoietic progenitors promotes megakaryocyte differentiation, and in murine model induces a myeloproliferative phenotype that mimics ET (Beauchemin et al., 2020). Consistently, Trifa and colleagues demonstrated that the rs9376092 SNP is preferentially associated to *JAK2*V617F-positive ET (Trifa et al., 2018). Finally, SNPs targeting ***GFI1B*** and ***CHEK2*** genes, firstly identified by Hinds et al., represent genome-wide significant loci for increased risk of MPN risk (Hinds et al., 2016). Recently, Bao and co-workers highlighted the functional mechanism by which *GFI1B* and *CHEK2* SNPs impact on the MPN risk regulating hematopoietic stem cell fate (Bao et al., 2020).

GFI1B mutations have been reported to promote a rare congenital platelet disorder namely *GFI1B*-related thrombocytopenia (*GFI1B*-RT), caused by the presence of truncated GFI1B proteins with dominant-negative properties on megakaryocytopoiesis and thrombopoiesis (Beauchemin et al., 2020).

The SNPs associated to high MPN risk are the rs621940 (Hinds et al., 2016), the rs1633768, and rs524137 (Bao et al., 2020), of which the last two are located in a region of hematopoietic-accessible chromatin 12 kb downstream of *GFI1B* gene.

On the other hand, *CHEK2* gene encodes for a checkpoint kinase critical for the DNA damage response pathway. Host genetic variants that predispose to MPNs include the rs555607708 (Hinds et al., 2016) and the I157T missense variant (rs17879961) (Bao et al., 2020), which have been previously linked to an increased risk for several types of cancer, including hematologic neoplasms as chronic lymphocytic leukemia (Rudd et al., 2006).

Recently, Bao and colleagues provided the first experimental evidence that the rs524137 SNP of *GFI1B* and the rs17879961 SNP of *CHEK2* are functionally relevant in MPN context, since they reduce, respectively, *GFI1B* expression and *CHEK2* function in hematopoietic stem cell and therefore these SNPs boots HSC self-renewal (Bao et al., 2020).

Although they do not represent predisposing factors for MPNs, several SNPs have been described to affect disease phenotype, hematologic parameters, disease course, and outcome (Table 12).

SNPs	Gene Function (Relative to Hematopoiesis)	Detection Methods	Allele Variant	MPN Cohort	Disease Subtype Associations	Disease Phenotype Associations	Ref.
***JAK2* 46/1 haplotype** rs12343867 (T/C)	Hematopoiesis, cytokine receptor signaling	RT-PCR	T allele (wild type)	130 PMF	n/e	↓ OS	(Tefferi et al., 2010)
		RT-PCR	T allele (wild type)	414 PMF	n/e	↓ OS	(Tefferi et al., 2019)
NR3C1 rs6198 (A/G)	Immune response regulation, erythrocytosis	PCR-SSCP + sequencing	G-allele	57 MPNs 22 CTRLs	PV	n/e	(Varricchio et al., 2011)
		HRM analysis + sequencing	G-allele (homozygous)	499 PMF 2948 CTRLs	PMF	↑ CD34+ cells, splenomegaly, ↑WBC, ↓ LFS*	(Poletto et al., 2012)
CCL2 rs1024611 (A/G)	Chemokine production	RT-PCR	G-allele	177 MPNs 149 CTRLs	sMF	↓ Hb, ↑ IPSS, ↑ blasts, ↑ fibrosis	(Masselli et al., 2018)
MIR146A rs2431697 (C/T)	NF-κB signaling modulation	RT-PCR	T-allele (homozygous)	967 MPNs 600 CTRLs	sMF	↓ MF-free survival in PV and ET	(Ferrer-Marin et al., 2020)

Table 12. Host genetic variants affecting MPN phenotype and/or outcome. Abbreviations: RT-PCR: real-time Polymerase Chain Reaction; OS: Overall Survival; PCR-SSCP: Polymerase chain reaction-single-stranded conformation polymorphism; HRM: High-Resolution Melting; n/e: not evaluated; WBC: White Blood Cells; LFS: Leukemia-free survival; Hb: hemoglobin; IPSS: International Prognostic Scoring System. *only for *JAK2*V617Fpos PMF.

The early identification of these SNPs represents an informative tool for personalized patient follow-up and management. For instance, the *JAK2* haplotype has been identified as a biomarker of disease outcome in PMF by Tefferi's group. Firstly, nullizygosity for the *JAK2* haplotype was

associated to shortened survival in a cohort of 130 PMF patients (Tefferi et al., 2010). Subsequently, in a follow-up study carried out on a cohort of 414 molecularly annotated PMF, the authors confirmed that wild-type patients showed a reduced overall survival as compared to the other genotypes, independently from well-established genetic and cytogenetic markers of poor outcome (karyotype, driver mutational status and presence of high-molecular-risk mutations) (Tefferi et al., 2019).

Among the host genetic variants reported in table 12, the rs6198 SNP of human glucocorticoid receptor gene, *NR3C1*, has been recently studied in PV and PMF patients. *NR3C1* gene, mapped on the 5q31-32 cyto-band of chromosome 5, is composed of nine exons with five splicing variants: GRα, GRβ, GRγ, GR-A, and GR-P. The alternative splicing of exons 9α and 9β accounts to produce GRα and GRβ, respectively. While GRα, in the absence of ligand, resides primarily in the cytoplasm in its inactive conformation and can interact with endogenous or synthetic agonists; GRβ constitutively resides in the nucleus, where it controls transcription primarily by a dominant-negative effect on GRα-induced gene expression (Zhou et al., 2005).

The rs6198 SNP of *NR3C1* consists of A to G substitution within the 3' untranslated region of the gene and it increases the stability of GRβ mRNA, reaching a half-life up to ≥ 6 hours, enhancing, therefore, GRβ expression (Derijk et al., 2001). In healthy subjects, this SNP is present with an allele frequency between 4% (sub-Saharan Africans) and 20% (Europeans), but its frequency increases in patients with autoimmune disorders, where it also regulates glucocorticoid resistance (Varricchio and Migliaccio, 2014).

The biological role of rs6198 SNP was first investigated in MPNs by Varricchio and co-workers (Varricchio et al., 2011). The authors found that polymorphic allele variant was significantly more frequent in PV patients as compared to healthy control subjects (allelic frequency: 55% *vs.* 9%). Furthermore, the GRβ isoform is selectively expressed in erythroid cells in PV patients, and it is reported to induce proliferative and pro-survival signaling leading to erythrocytosis. The same research group evaluated frequency of the rs6198 SNP of GR and its impact on disease phenotype and outcome in a cohort of 499 PMF. Although the polymorphic allele showed a higher frequency in PMF patients as compared to two different control populations the rs6198 SNP of GR represent only a minor MPN risk factor. However, homozygosity for this SNP correlates with higher white blood cell count, splenomegaly, and higher number of circulating blasts at the time of diagnosis. Finally, *JAK2*V617F-positive PMF carrying two copies of the G alleles display shorter overall and leukemia-free survival as compared to the wild type and heterozygous patients (Poletto et al., 2012). Therefore, the rs6198 SNP should be considered a host genetic factor for aggressive disease and adverse outcome (when associated to the *JAK2*V617F mutation) in PMF.

In addition, several host genetic variants have been found to affect cytokines production and

cytokine-signaling activation, predisposing to chronic inflammatory state.

We have recently investigated the rs1024611 SNP in *CCL2* gene, which encodes for the chemokine CCL2, also known as Monocyte Chemoattractant Protein-1 (MCP-1). *CCL2* gene is located in the q11.2-12 cytoband of chromosome 17 and it is highly polymorphic. The rs1024611 SNP consists in an A to G substitution in the distal regulatory region of the gene, and it modulates the transcriptional activity of *CCL2*. Indeed, the G/G individuals are reported to be the highest chemokine producers in response to pro-inflammatory noxa. Recently, our research group have studied the rs1024611 SNP of CCL2 in MPNs, demonstrated a significant association with sMF and with more aggressive disease phenotype at the time of diagnosis in MF patients (Masselli et al., 2018) (see the dedicated chapter).

As mentioned above, Hermouet et al. (Hermouet et al., 2011) suggested the *JAK2* 46/1 haplotype as a marker of abnormal myeloid response to cytokines, leading to an enhanced inflammatory state, myeloid neoplasm development, and impaired defence against infection. Additionally, the 46/1 haplotype may potentially induce the expression of other genes within the haplotype such as *INSL6* and *INSL4*, which in turn may exacerbate pro-inflammatory cytokines production. Similarly, the rs2736100 SNP of *TERT* has been found to modulate the expression of IL-6 in solid cancer (Wang et al., 2014), and it may be envisioned as a putative link between genetic predisposition to cytokine overproduction and MPN onset (Oddsson et al., 2014).

Furthermore, Ferrer-Marin et al. investigated two functional SNPs that regulate miR-146a levels, rs2910164 and rs2431697, in MPNs. The rs2431697 T/T genotype is enriched in post ET/PV MF; and independently predicts a shorter time to MF progression in PV and ET. This SNP has also been associated to increased pro-inflammatory cytokine levels in MPN patients. Indeed, the wild type miR-146a counteracts the NF-κB-dependent proinflammatory signal via inhibition of TNF Receptor-Associated Factor 6 (TRAF6) and Interleukin 1 Receptor-Associated Kinase 1 (IRAK1) (Ferrer-Marin et al., 2020). NF-κB downstream signaling has been found hyperactivated in mouse models of MPN as well as in MF and MPN blast phase (Fisher et al., 2021). In addition, NF-κB itself mediates the signal transduction downstream of several cytokine and chemokine receptors, including CCR2 (Melgarejo et al., 2009) and it has been suggested to cooperate with JAK2 signaling pathway in supporting cytokine overproduction (Fisher et al., 2021). Therefore, miR-146a deficiency is responsible for a chronic inflammatory phenotype promoting myeloproliferation.

The emerging evidence of host genetic variants modulating cytokine production and affecting inflammatory burden suggest a specific “cytokine gene expression profile” for MPNs.

Finally, some host genetic variants are responsible for the interindividual variability observed in therapy response. SNPs located near the *IL28B* gene, encoding for interferon-λ 3 (IFNL3), and in the *IFNL4* gene encoding for interferon-λ 4, were recently associated to an INF-α-based regimen

response in PV patients. In particular, the homozygosity (C/C genotype) for the rs12979860 located in between *IFNL3* and *IFNL4* was significantly associated with complete hematologic response (HR) in PV patients (Lindgren et al., 2018). Furthermore, the rs8099917 T/T, rs12979860 C/C, and rs368234815 TT/TT genotypes individually correlated with higher molecular response MR rates (Jäger et al., 2021).

4. Chronic inflammation and cytokine profile in PMF

From Masselli E, **Pozzi G***, Gobbi G, Merighi S, Gessi S, Vitale M, Carubbi C. Cytokine Profiling in Myeloproliferative Neoplasms: Overview on Phenotype Correlation, Outcome Prediction, and Role of Genetic Variants. Cells. 2020 Sep 21;9(9):2136*
*These authors contributed equally to this work.

Chronic inflammation plays a pivotal role in the pathogenesis of MPNs. It is characterized by the persistent activation of immune cells, continuous release of pro-inflammatory mediators, which lead to DNA damage, tissue destruction, remodelling and progressive fibrotic process. Typically, cytokines/chemokines are released in response to harmful stimuli, pathogen invasion, infected cells, toxic substances, or tissue injury, and act on several cell types to orchestrate the immune response.

Pro-inflammatory cytokines, promoting the recruitment and activation of immune cells, are normally counterbalanced by anti-inflammatory cytokines, which regulate cellular stress and minimize tissue damage, in a self-limiting manner to promote healing. When this balance is lost, the acute inflammatory response turns into a chronic inflammatory condition, which underlies several diseases such as autoimmune and neurodegenerative disorders, atherosclerosis, and cancer (Chen et al., 2017).

Several authors have described the deep interaction between chronic inflammation and cancers, especially in solid cancers, as well as the concept of “tumor-associated immune dysregulation”. In this scenario, neoplastic clones take control of the physiological wound healing program and generate - through pro-angiogenic (i.e., Vascular Endothelial Growth Factor (VEGF), Fibroblast Growth Factor (FGF), and IL-8) and immunosuppressive (primarily IL-10 and TGF-β) cytokines - a permissive milieu that promotes immunosurveillance escape and uncontrolled tumor cell proliferation. The neoplastic clone itself represents a relevant source of inflammatory mediators that stimulate non-malignant and stromal cells to promote clone expansion.

Besides the role in clonal expansion, chronic inflammation could also predispose to cancer onset, providing sustained levels of pro-inflammatory cytokines such as TNF-α, IL-6, and IL-8, which enhance cell proliferation, inhibit apoptosis, elicit genomic instability, and promote cell migration. This auto-fuelling mechanism generates a vicious cycle that leads to cancer initiation and progression (Landskron et al., 2014; Hua and Bergers, 2019).

Although the contribution of both inflammation and stromal microenvironment is well established in solid tumors, it is still under investigation in hematological malignancies (Hasselbalch, 2013).

In the context of hematologic malignancies, MPNs are considered a “Human Inflammation Model for Cancer Development” (Hasselbalch, 2013), and represent the paradigm of “onco-inflammation” (Bottazzi et al., 2018; Hasselbalch 2012). In this complex crosstalk between cancer cells and the surrounding microenvironment, chronic inflammation plays a pivotal role in disease pathogenesis and progression, acting as a trigger for and a driver of clonal evolution and fibrotic changes (Figure 46).

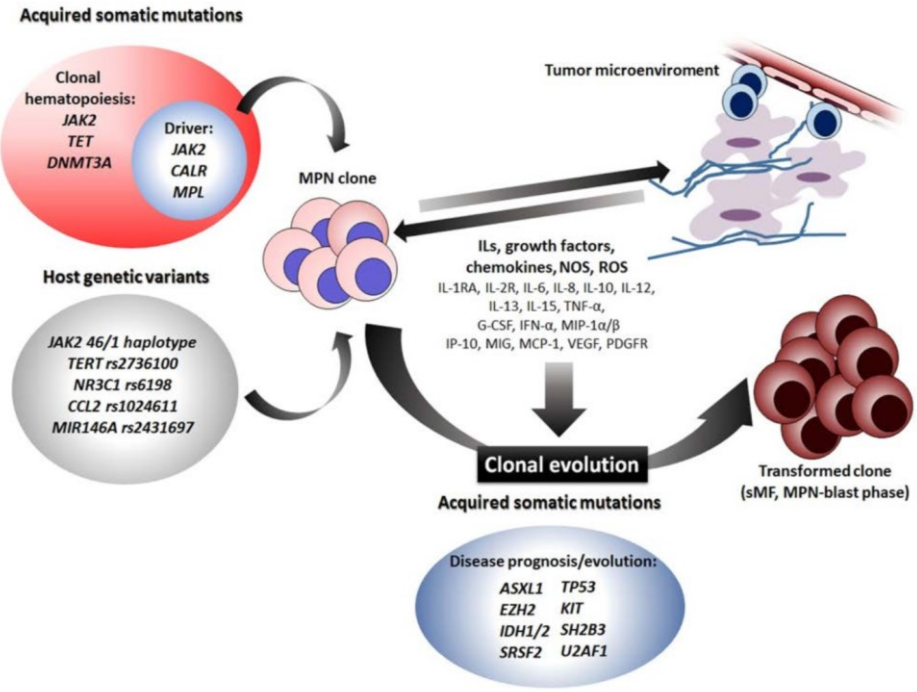

Figure 46. The model of onco-inflammation in MPNs. Acquired somatic mutations and inherited genetic variants contribute to determine malignant clone expansion and pro inflammatory state. The neoplastic clone itself is source of ILs, growth factors, chemokines, NOS, and ROS which are released both at a local and a systemic level. The interplay between the neoplastic clone and the tumoral surrounding microenvironment (bone marrow immune, stromal, and endothelial cells) affect in turn the disease phenotype and the MPN clone evolution into a more aggressive disease (sMF or/and blast phase). ILs: interleukins; NOS: Nitric Oxide Species; ROS: Reactive Oxygen Species; sMF: secondary Myelofibrosis (Masselli et al., 2021).

Chronic inflammation is considered directly responsible for some pathological manifestations of MPNs, such as bone marrow fibrosis and anemia. Abnormal secretion and activity of pro-inflammatory cytokines and chemokines have been found in MPNs, especially in MF, the most severe and advanced disease entities in which bone marrow fibrosis represents the consequence of “the inflamed bone marrow”, “the wound that won’t heal” (Dvorak, 1986).

Moreover, several studies demonstrated a positive correlation between elevated inflammatory mediators and systemic symptoms in MPNs such as fatigue, weight loss, pruritus, and fever that are typically exacerbated during the advanced myelofibrosis stage. Elevated levels of IL-6 have

been correlated to fatigue and depression in a cohort of 1788 MPNs (Scherber et al., 2014) and increased levels of IL-8 to constitutional symptoms in PMF patients (Tefferi et al., 2011). IL-4 levels, instead, were associated to microvascular symptoms in PV patients (Vaidya et al., 2012).

The contribution of chronic inflammation in MPN pathogenesis has been proved by several evidence (recently reviewed by Fisher et al., 2021): of note, the inhibition of specific pro-inflammatory cytokines, such as IL-1β, can decrease the expansion of MPN hematopoietic colonies *in vitro* (Estrov et al., 1991); a significant reduction of pro-inflammatory cytokines was documented in patients on therapy with immunomodulatory and anti-inflammatory drugs as interferons (IFNs) and the JAK1/2 inhibitor ruxolitinib, and cytokines reduction was associated to symptoms improvement (Verstovsek et al., 2010). Indeed, ruxolitinib has shown clinical efficacy against constitutional symptoms and symptomatic splenomegaly in PMF patients, and IFNα has been demonstrated to induce regression of bone marrow fibrosis and to affect angiogenesis in MF (Deininger et al., 2015; Pizzi et al., 2015).

Chronic inflammation is also involved in the development of MPN-related comorbidities including pro-thrombotic state, premature atherosclerosis, and higher risk of second cancer (Hasselbalch, 2013; Fleischman, 2015). Although only few and often contradictory data are available on correlation between a history of thrombotic events and the cytokine profile, inflammatory microenvironment is considered a potential trigger for these complications (Hasselbach, 2013), which represent the main cause of morbidity and mortality in MPNs (Falanga et al., 2014). In this context, several potential pro-thrombotic biomarkers have been identified such as pentraxin-3 in PV and ET (Lussana et al., 2017; Barbui et al., 2011; Barbui et al., 2013), high-sensitivity C-reactive protein in PV, ET, PMF, and post-ET/PV MF, as well as protein kinase C epsilon in PMF and post-ET/PV MF (Masselli et al., 2017).

As previously mentioned, the JAK/STAT pathway plays a key role in cytokine signaling and inflammation by regulating proliferation, survival, but also differentiation of immune and hematopoietic cells (Mui, 1999; Coffer et al., 2000). Indeed, JAK/STAT represents the target of all driver mutations, and it leads to cytokine hypersensitivity, cytokine-independent growth, and decreased apoptosis in hematopoietic stem cells. Moreover, STATs proteins, which are downstream NF-κB and JAK pathways, activate the transcription of genes involved in cancer-promoting inflammation including matrix metalloproteinases, classic immunomodulatory cytokines including IL-6, IL-10, IL-17, and IL-23, and growth factors (e.g., VEGF and FGF). These pro-inflammatory mediators create an autocrine positive feedback loop that reinforces chronic inflammation.

Some authors investigated whether the elevated levels pro-inflammatory cytokine(s) could be associated with the mutational profile of MPNs patients and the presence of phenotypic driver mutation(s), primarily *JAK2*V617F, or other somatic high-risk mutation(s).

Pourcelot and co-workers reported that the *JAK2*V617F status of PV and ET patients significantly impacted TNF-α and PDGF levels (Pourcelot et al., 2014); while Cacemiro et al. reported a significant association between the presence of *JAK2*V617F mutation and elevated levels of IP-10 in PMF (Cacemiro et al., 2018). Øbro and co-workers have recently confirmed these data showing a positive correlation between IP-10 and *JAK2*V617F allele burden in ET, PV, and MF patients (Øbro et al., 2020). Furthermore, Wong and colleagues observed that TGFβ-2 was significantly upregulated (3.1-fold) in *MPL*-mutated patients (Wong et al., 2019), while Barosi et al. demonstrated the elevated levels of sIL2RA had a prognostic impact only in *JAK2*V617F and not in *CALR*-mutated PMF patients (Barosi et al., 2020).

In addition to the aberrant cytokine production by the MPN clones, several evidence suggests that other components of the hematopoietic niche could also take part in MPN pathogenesis. Recently, the concept of the “bad seeds in bad soil” has been proposed (Le Bousse-Kerdilès, 2012). Within the bone marrow niches, hematopoietic stem cells are in constant crosstalk with different stromal cell populations as mesenchymal stromal cells (MSC), endothelial cells, macrophages, osteoclasts, fibrocytes and megakaryocytes.

The niche could regulate HSCs behaviour through both direct adhesive interactions (cell-cell interaction or cell-extracellular interaction) and the secretion of soluble mediators with paracrine effects. Bone marrow fibrosis, osteosclerosis and $CD34^+$ cell mobilization and homing towards the spleen and liver, that characterize PMF and couple with clonal myeloproliferation, are mainly associated to the microenvironment alterations. Indeed, abnormal $CD34^+$ cell trafficking could be due to the alterations in CXCL12/SDF-1α/CXCR4 axis, but also to the extensive extracellular matrix proteolytic activity, accounting for loss of adherence molecules (Bogani et al., 2008; Xu et al., 2005). Bone marrow remodelling is primarily due to an increased deposition of total collagen, including types I, III, IV, and V collagens (Hasselbalch, 1993), laminin and adhesive glycoproteins (vitronectin, fibronectin and tenascin) accompanied by a decrease in matrix degradation. In this context, transforming growth factor 1 β (TGFβ1) seems to be the main actor, exerting fibrogenic effects. The expression of several TGF-β1 signaling genes was altered in marrow and spleen of MF patients, respectively. TGF-β1 signaling promotes the synthesis of extracellular matrix components and tissue inhibitors of metalloproteinase (TIMP) as TIMP-1 (Le Bousse-Kerdilès and Martyré, 1999), and decreases the secretion of matrix metalloproteinases (MMP) as MMP3 (Agarwal et al., 2016). In GATA-1^{low} mice, a murine model of myelofibrosis, the inhibition of TGF-β1 led to rescue of megakaryocyte differentiation, with reduced fibrosis, neovascularization, and osteogenesis in the bone marrow, and consecutively reduced splenomegaly (Zingariello et al., 2013).

Pro-inflammatory mediators include transcription factors (i.e., NF-κB and STAT-3), cytokines (i.e., IL-1; TNF; IL-6), and chemokines (i.e., IL-8, Monocyte chemoattractant protein-1 (MCP-1))

(Bottazzi et al., 2018). However, not only cytokines/chemokines fuel inflammation and promote the malignant clone, but also Reactive Oxygen Species also (ROS) and Nitric Oxygen Species (NOS) could trigger epigenetic changes, genomic instability, and additional DNA mutations, which favor the evolution of the original neoplastic clone towards the burn out stage and predispose to both hematological and non-hematological secondary malignancies (Hasselbach, 2012; Hasselbach 2013). ROS levels were found to be elevated in both *JAK2*V617F-positive and *CALR*-mutated MPN (Bjørn and Hasselbalch, 2015). Moreover, Marty and colleagues demonstrated that murine *JAK2*V617F knock-in model display significantly elevated ROS levels, which correlate with increased risk of double-strand breaks (DSBs) and damage in DNA repair process (Marty et al., 2013). Of note, splenomegaly, neoplastic cell infiltration, and DNA damage were reduced when *JAK2*V617F-KI mice were treated with the antioxidant N-acetylcysteine (NAC), which acts on ROS production. Recently, NAC and antioxidant compounds have proved their potential to reduce the thrombotic risk in murine model of MPNs, suggesting their applications in clinical trial (Craver et al., 2020).

4.1 The role of the megakaryocytic clone in chronic inflammation in MPNs

As mentioned above, the neoplastic clone itself represents a relevant source of inflammatory mediators within the niche. In MPNs, especially in MF, megakaryocytic clone plays a pivotal role in cytokine production (Ciurea et al., 2007).

Aberrant megakaryocytopoiesis and megakaryocyte (MKs) hyperplasia are distinctive hallmark of MPNs and represent a clinically relevant feature for differential diagnosis of prePMF vs. ET. Among the three MPNs, MF is predominantly characterized by profound alterations of megakaryocytopoiesis, including MK hyper-proliferation and impaired differentiation (Ciurea et al., 2007; Masselli et al., 2015; Balduini et al., 2011). MKs hyperplasia, observed in MF, has been associated to the increased capacity of hematopoietic stem cell to proliferate and differentiate towards the megakaryocyte lineage or to the inhibition of the apoptotic process. As described by several research groups, MKs obtained *in vitro* from PMF $CD34^+$ cells, show similar abnormalities of PMF MKs *in vivo*, including smaller dimensions and reduced ploidy, but also impaired capacity to generate proplatelet (Ciurea et al., 2007; Masselli et al., 2015; Balduini et al., 2011). Consistently, MF patients display alterations in platelet number (increased or decreased), morphology (presence of giant platelets), and functions (Falanga and Marchetti, 2014; Parashar et al., 2016).

Furthermore, MKs and monocyte-derived fibrocytes are supposed to be the main sources of pro-inflammatory cytokines involved in bone marrow fibrotic changes, osteosclerosis and neo-angiogenesis observed in MF. The pro-fibrotic cytokines produced by neoplastic MKs include TGF-β, Platelet Derived Growth Factor (PDGF), FGF, VEGF, thrombospondin, CXCL4, Macrophage

Inflammatory Protein (MIP)-1α, MIP-1β, IL-8, and lipocalin-2 (Malara et al., 2018).
TGFβ1 is a pleiotropic cytokine, secreted as inactive protein and stored in the extracellular matrix. ROS, extracellular proteases, integrins and thrombospondin-1 (TSP-1), convert the inactive latent TGFβ1 to the biologically active form. Besides pro-fibrotic properties, TGFβ1 has direct effects on hematopoietic cells and promotes cancer invasion and endothelial–mesenchymal transition during the development of fibrosis (Blank and Karlsson, 2011; Erba et al., 2017). MKs from PMF patients expressed high levels of TGF-β1 receptor type I but normal levels of TGF-β1 and its type II receptor (Chou et al., 2003). Furthermore, data from sera, $CD34^+$ cells, and MKs indicated that PMF patients showed significantly higher levels of total and bioactive TGF-β1 as compared to healthy subjects (Campanelli et al., 2011). In $Gata1^{low}$-murine model of MF, it has been demonstrated that extramedullary hematopoiesis is supported by P-selectin and TGF-β pathways, triggered by the abnormal expression of P-selectin on MKs, that leads to neutrophil-megakaryocyte emperipolesis, increases TGF-β content in the surrounding microenvironment and activates fibrocyte (Zingariello et al., 2015; Zingariello et al., 2020; Spangrude et al 2016). These results provide a rationale of TGF-β inhibition as a therapeutic strategy in MF (Ceglia et al., 2016). In the same $Gata1^{low}$ mice, very recently Kramer et al. investigated the role of PDGFRα and PDGFRβ signaling regulation in BM fibrotic evolution. Increased mRNA expression levels of PDGFRα and β as well as the ligand PDGFβ was detected in fibrotic $Gata1l^{ow}$ mice. Moreover, an increased protein expression of PDGFRβ and its ligand PDGF-B was observed in overt fibrotic mice. The proximity ligation assay revealed a strong interaction between PDGFRβ and PDGF-B, which are in closed proximity in overtly fibrotic bone marrow. The results obtained by Kramer and colleagues highlight the crosstalk between neoplastic clone and the microenvironment in which MKs pronominally express PDGFRα and secrete PDGFβ, and stromal cells express PDGFRβ (Kramer et al., 2020).

4.2 Cytokine profile in MPN patients

Given the relevance of chronic inflammation in the context of MPNs, extensive efforts have been made to identify a specific “cytokine signature” that might provide novel pathogenetic insights and could be useful for stratifying patients, predicting and monitoring disease progression and therapy response. We recently reviewed the main studies on cytokine profiling in MPNs, with particular attention to the phenotype correlation and outcome prediction (Masselli et al., 2020). Cytokine expression levels for each MPN, determined by ELISA, cytokine array or by gene expression analysis, were summarized in Table 14. A number of studies have investigated bone marrow and circulating cytokines levels, as well as cytokine gene expression profile in MPNs, with some inconsistencies and contradictory findings. This can be due to different factors including: (i)

different methods used for cytokine measurement, (ii) the choice of cellular sources and RNA collection/processing methods, (iii) heterogeneous patient populations in terms of disease stage and treatment, (iv) the fact that early studies also included CML, and (v) evolution of MPN diagnostic criteria according to the WHO classification. The discrepancy between cytokine mRNA levels and data from circulating/bone marrow measurements could be probably due to the fact that mRNA levels not always correlate with protein levels, and mRNA transcript analysis does not evaluate post-translational modification and sub-cellular/extra-cellular protein localization, affecting protein function. Moreover, the age of patients could represent a bias for cytokine studies in MPNs. Indeed, MPNs prevalence increases with age, which is *per se* a condition associated with a chronic, low-grade, subclinical inflammatory state (the so-called "inflammageing") (Ferrucci and Fabbri, 2018).

Although specific cytokine profile cannot be defined yet, a differential expression of determined cytokines/chemokines has been found among PV, ET, and MF, depicting MPN patients as "dysfunctional cytokine producers" (Table 14).

		ET	PV	PMF	References
Pro-Inflammatory Cytokines	IL-1α	=	=	=	(Boutantas et al., 1999; Panteli et al., 2005)
	IL-1β	↑/=	↑	↑/=	(Boutantas et al., 1999; Panteli et al., 2005; Tefferi et al., 2011; Cacemiro et al., 2018; Wong et al., 2019)
	IL-2	↑	↑	↑/=	(Boutantas et al., 1999; Panteli et al., 2005; Tefferi et al., 2011)
	IL-2R	↑	↑	↑	(Boutantas et al., 1999; Panteli et al., 2005; Tefferi et al., 2011; Mambet et al., 2018; Barosi at al., 2020)
	IL-5	↑/=	↑	=	(Tefferi et al., 2011; Vaidya et al., 2012; Cacemiro et al., 2018)
	IL-6	↑/=	↑	↑	(Hsu et al., 1999; Bourantas et al., 1999; Panteli et al., 2005; Tefferi et al., 2011; Vaidya et al., 2012; Cacemiro et al., 2018)
	sIL-6	↑	nd	nd	(Hsu et al., 1999)
	IL-7	nd	↑	=	(Tefferi et al., 2011; Vaidya et al., 2012)
	IL-12	↑	↑	↑	(Tefferi et al., 2011; Vaidya et al., 2012; Cacemiro et al., 2018)

	IL-13	nd	↑	↑	(Tefferi et al., 2011; Vaidya et al., 2012)
	IL-15	nd	nd	↑	(Tefferi et al., 2011)
	IL-17	=	=	↑ /=	(Tefferi et al., 2011; Cacemiro et al., 2018)
	IL-23	=	↑	nd	(Gangemi et al., 2012)
	TNF-α	↑ /=	↑	nd	(Tefferi et al., 2011; Cacemiro et al., 2018; Wong et al., 2019; Øbro et al., 2020)
	INF-α	↑	↑	↑	(Tefferi et al., 2011; Cacemiro et al., 2018)
	INF-γ	=	↑	↓/↑	(Tefferi et al., 2011; Vaidya et al., 2012; Cacemiro et al., 2018)
Anti-Inflammatory Cytokines	IL-1RA	nd	↑	↑	(Tefferi et al., 2011; Vaidya et al., 2012)
	IL-4	↑	↑	↑/=	(Tefferi et al., 2011; Skov et al., 2012; Cacemiro et al., 2018)
	IL-6	↑/=	↑	↑	(Hsu et al., 1999; Tefferi et al., 2011; Vaidya et al., 2012; Cacemiro et al., 2018)
	IL-10	↑/=	↑/=	↑	(Bourantas et al., 1999; Tefferi et al., 2011; Gangemi et al., 2012; Skov et al., 2012; Cacemiro et al., 2018)
	IL-11	nd	↑	nd	(Hermouet et al., 2002; Boissinot et al., 2010)
	IL-13	nd	↑	↑	(Tefferi et al., 2011; Vaidya et al., 2012; Cacemiro et al., 2018)
Chemokines	MCP-1	↑/=	↑/=	↑/=	(Hermouet et al., 2002; Boissinot et al., 2010; Tefferi et al., 2011; Vaidya et al., 2012; Cacemiro et al., 2018; Wong et al., 2019)
	MIP-1α	↑	↑	↑	(Ho et al., 2007; Tefferi et al., 2011; Vaidya et al., 2012; Cacemiro et al., 2018)
	MIP-1β	↑	↑	↑/=	(Tefferi et al., 2011; Vaidya et al., 2012; Cacemiro et al., 2018)
	IL-8	↑	↑	↑	(Hsu et al., 1999; Hermouet et al., 2002; Boissinot et al., 2010; Tefferi et al., 2011; Vaidya et al., 2012; Øbro et al., 2020)
	RANTES	↑	=/↓	↑/=	(Tefferi et al., 2011; Vaidya et al., 2012; Cacemiro et al., 2018)
	IP-9	↑	↑	↑	(Mambet et al., 2018)
	IP-10	=	↑	↑	(Tefferi et al., 2011; Vaidya et al., 2012; Cacemiro et al., 2018; Wong et al., 2019; Øbro et al., 2020)

	MIG	nd	↑	↑	(Tefferi et al., 2011; Vaidya et al., 2012; Skov et al., 2012)
	GRO-α	↑	=	=	(Øbro et al., 2020)
	CCL11	↑	↑	=	(Tefferi et al., 2011, Øbro et al., 2020)
Growth Factors	GM-CSF	↑	↑	↑/=	(Vaidya et al., 2012; Cacemiro et al., 2018)
	G-CSF	nd	nd	↑	(Tefferi et al., 2011; Skov et al., 2012)
	HGF	nd	↑	↑	(Hermouet et al., 2002; Boissinot et al., 2010; Tefferi et al., 2011; Skov et al., 2012; Vaidya et al., 2012)
	PDGF	↑	↑	↑	(Mambet et al., 2018; Wong et al., 2019)
	VEGF	=	↑/=	↑	(Tefferi et al., 2011; Vaidya et al., 2012; Skov et al., 2012)
	EGF	↑	↓/↑	↑	(Skov et al., 2012; Vaidya et al., 2012; Mambet et al., 2018; Øbro et al., 2020)
	FGF	nd	nd	=	(Tefferi et al., 2011)
	TPO	=	=	↑	(Hsu et al., 1999; Panteli et al., 2005)
	SCF	↑	nd	nd	(Hsu et al., 1999)
	TGFβ	=	=	↑	(Wong et al., 2019)
Pro-Fibrotic Cytokines	MCP-1	↑/=	↑/=	↑/=	(Hermouet et al., 2002; Boissinot et al., 2010; Tefferi et al., 2011; Vaidya et al., 2012; Cacemiro et al., 2018; Wong et al., 2019)
	IL-8	↑	↑	↑	(Hsu et al., 1999; Hermouet et al., 2002; Boissinot et al., 2010; Tefferi et al., 2011; Vaidya et al., 2012; Øbro et al., 2020)
	PDGF	↑	↑	↑	(Mambet et al., 2018; Wong et al., 2019)
	EGF	↑	↓/↑	↑	(Vaidya et al., 2012; Skov et al., 2012; Mambet et al., 2018; Øbro et al., 2020)
	FGF	nd	nd	=	(Tefferi et al., 2011)
	TGFβ	=	=	↑	(Wong et al., 2019)

Table 14. Cytokine expression profile in myeloproliferative neoplasm (MPN) subtypes vs. healthy controls. Summary of cytokine levels in peripheral blood and bone marrow of essential thrombocythemia (ET), polycythemia vera (PV), and primary myelofibrosis (PMF) patients (determined by ELISA, cytokine array or by gene expression analysis) as compared to control healthy subjects (HD). Cytokines are grouped according to their function and cytokines with multiple functions are listed in each category. ↑ increased vs. HD; = similar to Hd; ↓ reduced vs. HD; nd: not determined.

Considering gene expression, all three MPNs displayed an increased expression of pro- and anti-inflammatory cytokines, chemokines, growth factors, and fibrogenic mediators as compared to

healthy subjects (Table 14). Only *INF*-γ (Tefferi et al., 2011), and *RANTES* and EGF gene expression was found decreased in PMF and in PV, respectively (Vaidya et al., 2012). However, this latter result was not confirmed by other works.

Several studies have focused on MF, which among MPNs, is characterized by the highest inflammatory burden. Of note, of the 29 cytokines whose levels and/or expression have been investigated in PMF as compared to ET and PV, 15 are found significantly increased (IL-2, sIL-2R, IL-6, IL-12, IL-17, TNF-α, INF-α, IL1RA, IL-4, IL-10, MIP-1β, RANTES, FGF, TPO, TGF-β) (Panteli et al., 2005; Vaidya et al., 2012; Cacemiro et al., 2018; Wong et al., 2018), MCP-1 similar or increased, according to different studies (Cacemiro et al., 2018; Wong et al., 2018), and IL1-α levels are similar (Panteli et al., 2005). Furthermore, IL-7, VEGF, MIG, GRO-α, and CCL11 levels are instead decreased (Vaidya et al., 2012; Øbro et al., 2020; Skov et al., 2012), and INF-γ, MIP-1α, IP-10, GM-CSF, EGF show contradictory findings (both increased and decreased according to different reports) (Vaidya et al., 2012; Cacemiro et al., 2018; Øbro et al., 2020; Skov et al., 2012) (Table 15). Of note, pro-fibrotic cytokines, such as TGF-β, MCP-1, and FGF (Table 15) are found elevated in PMF by different research groups, suggesting that while inflammation is a common feature of all MPNs, PMF is characterized by a peculiar "fibrogenic cytokine signature" (Hsu et al., 1999; Hermouet et al., 2002; Boissinot et al., 2010; Tefferi et al., 2011; Vaidya et al., 2012; Øbro et al., 2020)

		PMF	References
Pro-Inflammatory Cytokines	IL-1α	=	(Boutantas et al., 1999; Panteli et al., 2005)
	IL-1β	↑/=	(Boutantas et al., 1999; Panteli et al., 2005; Tefferi et al., 2011; Cacemiro et al., 2018; Wong et al., 2019)
	IL-2	↑	(Boutantas et al., 1999; Panteli et al., 2005; Tefferi et al., 2011)
	IL-2R	↑	(Boutantas et al., 1999; Panteli et al., 2005; Tefferi et al., 2011; Mambet et al., 2018; Barosi at al., 2020)
	IL-5	nd	
	IL-6	↑	(Hsu et al., 1999; Bourantas et al., 1999; Panteli et al., 2005; Tefferi et al., 2011; Vaidya et al., 2012; Cacemiro et al., 2018)
	sIL-6	nd	
	IL-7	↓	(Tefferi et al., 2011; Vaidya et al., 2012)

	IL-12	↑	(Tefferi et al., 2011; Vaidya et al., 2012; Cacemiro et al., 2018)
	IL-13	nd	
	IL-15	nd	
	IL-17	↑	(Tefferi et al., 2011; Cacemiro et al., 2018)
	IL-23	nd	
	TNF-α	↑	(Tefferi et al., 2011; Cacemiro et al., 2018; Wong et al., 2019; Øbro et al., 2020)
	INF-α	↑	(Tefferi et al., 2011; Cacemiro et al., 2018)
	INF-γ	↓/↑	(Tefferi et al., 2011; Vaidya et al., 2012; Cacemiro et al., 2018)
Anti-Inflammatory Cytokines	IL-1RA	↑	(Tefferi et al., 2011; Vaidya et al., 2012)
	IL-4	↑	(Tefferi et al., 2011; Skov et al., 2012; Cacemiro et al., 2018)
	IL-6	nd	
	IL-10	↑	(Bourantas et al., 1999; Tefferi et al., 2011; Gangemi et al., 2012; Skov et al., 2012; Cacemiro et al., 2018)
	IL-11	nd	
	IL-13	nd	
Chemokines	MCP-1	↑/=	(Hermouet et al., 2002; Boissinot et al., 2010; Tefferi et al., 2011; Vaidya et al., 2012; Cacemiro et al., 2018; Wong et al., 2019)
	MIP-1α	↑	(Ho et al., 2007; Tefferi et al., 2011; Vaidya et al., 2012; Cacemiro et al., 2018)
	MIP-1β	↑/=	(Tefferi et al., 2011; Vaidya et al., 2012; Cacemiro et al., 2018)
	IL-8	↑	(Hsu et al., 1999; Hermouet et al., 2002; Boissinot et al., 2010; Tefferi et al., 2011; Vaidya et al., 2012; Øbro et al., 2020)
	RANTES	↑/=	(Tefferi et al., 2011; Vaidya et al., 2012; Cacemiro et al., 2018)
	IP-9	↑	(Mambet et al., 2018)
	IP-10	↑	(Tefferi et al., 2011; Vaidya et al., 2012; Cacemiro et al., 2018; Wong et al., 2019; Øbro et al., 2020)

	MIG	↑	(Tefferi et al., 2011; Vaidya et al., 2012; Skov et al., 2012)
	GRO-α	=	(Øbro et al., 2020)
	CCL11	=	(Tefferi et al., 2011, Øbro et al., 2020)
Growth Factors	GM-CSF	↑/=	(Vaidya et al., 2012; Cacemiro et al., 2018)
	G-CSF	↑	(Tefferi et al., 2011; Skov et al., 2012)
	HGF	↑	(Hermouet et al., 2002; Boissinot et al., 2010; Tefferi et al., 2011; Skov et al., 2012; Vaidya et al., 2012)
	PDGF	↑	(Mambet et al., 2018; Wong et al., 2019)
	VEGF	↑	(Tefferi et al., 2011; Vaidya et al., 2012; Skov et al., 2012)
	EGF	↑	(Skov et al., 2012; Vaidya et al., 2012; Mambet et al., 2018; Øbro et al., 2020)
	FGF	=	(Tefferi et al., 2011)
	TPO	↑	(Hsu et al., 1999; Panteli et al., 2005)
	SCF	nd	(Hsu et al., 1999)
	TGFβ	↑	(Wong et al., 2019)
Pro-Fibrotic Cytokines	MCP-1	↑/=	(Hermouet et al., 2002; Boissinot et al., 2010; Tefferi et al., 2011; Vaidya et al., 2012; Cacemiro et al., 2018; Wong et al., 2019)
	IL-8	↑	(Hsu et al., 1999; Hermouet et al., 2002; Boissinot et al., 2010; Tefferi et al., 2011; Vaidya et al., 2012; Øbro et al., 2020)
	PDGF	↑	(Mambet et al., 2018; Wong et al., 2019)
	EGF	↑	(Vaidya et al., 2012; Skov et al., 2012; Mambet et al., 2018; Øbro et al., 2020)
	FGF	=	(Tefferi et al., 2011)
	TGFβ	↑	(Wong et al., 2019)

Table 15. Cytokine expression profile in PMF vs. ET and PV. Summary of cytokine levels in peripheral blood and bone marrow of PMF patients (determined by ELISA, cytokine array or by gene expression analysis) as compared to ET or PV. Cytokines are grouped according to their function and cytokines with multiple functions are listed in each category; ↑ increased vs. PV/ET; = similar to PV/ET; ↓ reduced vs. PV/ET; nd: not determined.

In addition, Skov et al. performed a whole blood transcriptional analysis describing a significant over expression (top 10 up-regulated genes) of *CSF3* (encoding for G-CSF), *EGF*, *HGF*, *VEGFA*, and *CXCL9* (encoding for MIG) in PMF as compared to other MPNs. The *HGF* gene was

significantly up-regulated across all MPN patients (including N=9 PMF, N=16 ET and N=36 PV), but PMF showed the highest level; on the contrary *VEGFA* was up-regulated in patients with PMF but not in ET and PV (Skov et al., 2012).

In 2019, Wong and colleagues (Wong et al., 2019) analyzed the expression of inflammatory genes in 108 MPNs (including N=13 prePMF, N=23 overtPMF, N=31 ET, N=25 PV, and N=16 MPN-unclassifiable) by measuring RNA transcript abundance in bone marrow biopsies using Nanostring technology. The authors demonstrated that the inflammatory gene expression profile correlates with bone marrow fibrosis. Indeed, MPN patients with fibrosis grade 0–1 (pre-fibrotic) display a "low" cytokine gene expression profile, whereas MPNs with grade 2–3 (overtly fibrotic) are typified by a marked over-expression of inflammatory genes. Indeed, genes encoding for pro-fibrogenic growth factors (*TGFB1*, *TGFB3*, and *PDGFA*) were 2.6- and 1.3-fold upregulated in overtly fibrotic as compared to pre-fibrotic MPNs; and pro-inflammatory cytokine genes as *TNF* and *IL1B* were increased by 1.9- and 1.5-fold, respectively. Interestingly, chemokine genes such as *CCL2* (encoding for MCP-1) and *CXCL10* (encoding for IP-10) expression was > 3- fold higher in overtly fibrotic patients. Therefore, the up-regulation of fibrogenic genes seems to be not strictly related to overt-PMF *per se*, but in general to MPNs at overtly fibrotic stage (i.e., MPN-unclassifiable with ≥2 degree of bone marrow fibrosis) (Wong et al., 2019), highlighting how different inflammatory signaling pathways could lead to a common phenotype of clonal-derived bone marrow fibrosis. At the same time, bone marrow remodelling due to the fibrotic process may affect cytokine/chemokine gene expression profile, in particular by boosting the expression of genes involved in osteoclast differentiation, fibrocyte proliferation, and neo-angiogenesis (Wong et al., 2019).

Regarding the circulating and bone marrow cytokines levels, the preliminary study by Hsu and co-workers was carried out on a cohort of patients with clonal thrombocytosis (N=70) caused by myeloproliferative disorders (N=31 ET, N=22 PV, and N=17 chronic myeloid leukemia, CML), and patients with reactive thrombocytosis (N=28), as compared to control subjects (N=35) (Hsu et al., 1999). The authors observed that Stem Cell Factor (SCF), IL-6, soluble (s) IL-6 receptor (R), IL-8, and Thrombopoietin (TPO) were significantly increased in both serum and bone marrow of MPN patients or patients with reactive thrombocytosis as compared to healthy controls, with IL-6 significantly increased in clonal vs. reactive disorders, and SCF and IL-8 selectively elevated in clonal thrombopoiesis (Hsu et al., 1999). Furthermore, Bourantas and colleagues measured cytokines serum levels including TNF-α, IL-1α, IL-1β, IL-2, sIL-2R, IL-6, and IL-10 in MPNs patients (N=55 MPNs of which N=10 PV, N=15 CML, N=10 PMF, and N=20 ET) at the time of the first diagnosis, during follow-up and at the time of blast-phase evolution (which occurred for N = 3 PV and N = 5 PMF), and in control subjects (N=100). Surprisingly, only IL-2 and sIL-2R levels were significantly increased in MPN patients, whereas IL-lα, IL-1β serum concentrations were either not

detectable in MPN patients at diagnosis and during the stable phase and IL-6, IL-10 levels were comparable to those of normal subjects. IL-2 and sIL-2R levels progressively and significantly increased with leukemic evolution (Bourantas et al., 1999). These results are consistent with the findings by Panteli et al., who demonstrated that IL-2 and sIL-2RA serum levels were significantly higher in patients with PMF, PV, ET, and CML (N=25, N=8, N=40, and N=10 patients, respectively) as compared to healthy subjects (HD), while IL-1α and IL-1β levels were comparable in patients and HD. Cytokine levels varied among diseases, indeed, TPO and IL-6 levels were selectively elevated only in PMF patients who showed increased levels of IL-2, sIL-2RA, IL-6 *vs*. PV and ET.

Analysing phenotype associations, a negative correlation in all patients has found between IL-2, sIL-2RA, IL-6 serum levels and hemoglobin and platelet count, and a positive correlation with liver and spleen size. Focusing on each single disease, only an association between anemia and IL-2 in PMF, and sIL-2RA in ET were observed. In line with the previous study, IL-2, sIL-2RA, and IL-6 levels significantly increased according to disease progression, during the transformation phase of CML, the progression of PMF to blast phase, and ET or PV to secondary myelofibrosis (Panteli et al., 2005).

Furthermore, Tefferi's group extensively investigated cytokine levels in MF comparing to other MPNs. In their first report in 2007, the authors detected multiple cytokines in the plasma of 20 therapy-naïve MPN patients (N = 10 PMF, N = 5 PV, and N = 5 ET) and controls (N = 4) using human cytokine array method (combining the individual assets of ELISA, enhanced chemiluminescence, and the high-throughput of microspot). They observed higher levels of Tissue Inhibitor of Metalloproteinase (TIMP-1), MIP-1, and Insulin-like Growth Factor Binding Factor-2 (IGFBP-2) in PMF patients as compared to ET, PV, and controls (Ho et al., 2007). In 2011, the same research group performed a comprehensive analysis of plasma levels of 127 PMF patients with complete hematological, histopathological, and cytogenetic information, using ELISA. PMF patients displayed increased interleukin-1beta (IL-1beta), IL-1RA, IL-2R, IL-6, IL-8, IL-10, IL-12, IL-13, IL-15, TNF-α granulocyte colony-stimulating factor (G-CSF), IFN-α, MIP-1α, MIP-1β, HGF, IFN-γ–inducible protein 10 (IP-10), monokine induced by IFN-gamma (MIG), MCP-1, and VEGF levels as well as decreased IFN-γ levels as compared to healthy controls (N=35). In general, males exhibited significantly higher cytokine levels (especially IL-2R, IL-8, and IL-15) (Tefferi et al., 2011). Furthermore, cytokine levels have been demonstrated to have prognostic relevance. In therapy-näive PMF patients (N=90), increased levels of IL-8, IL-2R, IL-12, IL-15, and IP-10 were independently predictive of inferior survival (Figure 47).

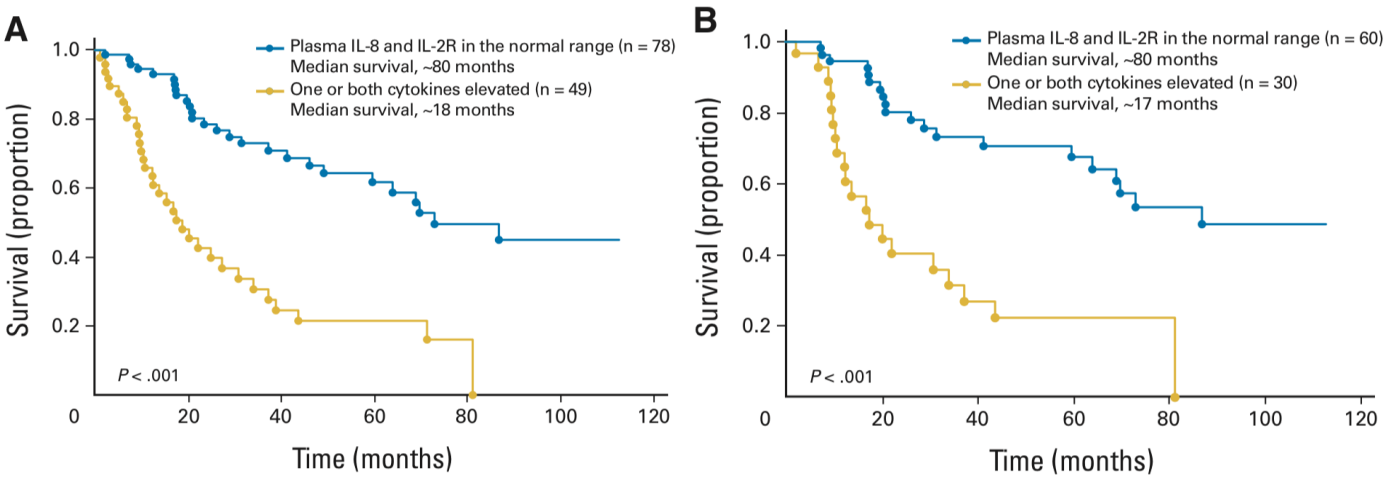

Figure 47. Overall survival of PMF patients with normal and elevated IL8 and IL-2R levels. Survival data of (A) 127 PMF patients and (B) 90 therapy-naive PMF patients stratified according to the presence (in yellow) and absence (in blue) of interleukin 8 (IL-8) and IL-2R levels that exceed three standard deviations above the normal mean (from Tefferi et al., 2011).

The multivariate analysis encompassing the entire study cohort revealed that IL-8, IL-2R, IL-12, and IL-15 prognostic value remained significant after risk stratification, according to the DIPSS-plus model. The authors also described a positive association of (i) IL-8 with constitutional symptoms, increased leukocytes and peripheral blasts, and leukemic evolution; (ii) IL-2R, IL-12, and transfusion need; (iii) IP-10 and thrombocytopenia; (iv) HGF, MIG, IL-1RA, and marked splenomegaly (Tefferi et al., 2011). Moreover, Pardanani and colleagues assessed the potential role of increased cytokines in modulating the anemia response to pomalidomide in myelofibrosis (both PMF and post PV/ET MF). Elevated circulating levels of MCP-1, IL-2R, IL-15, and IL-8 predicted poor anemia response and increased levels of sIL-2R, IL-15, and MCP-1 were associated to splenomegaly (Pardanani et al., 2011).

In 2018, Cacemiro and co-workers tried to identify a disease specific cytokine profile for each MPN subsets (N=16 PMF, N=11 ET, and N=20 PV). They found elevated plasma levels of GM-CSF, IFNα, IFNγ, IP-10, MCP-1, MIP-1α, MIP-1β, RANTES, IL-1, IL-4, IL-5, IL-6, IL-10, IL-12, and IL-17 in all MPNs as compared to healthy controls (N=34). The analysis of each disease subtype showed that PMF had higher IL-12, IL-4, and GM-CSF compared to PV and increased IFN-γ, IL-12, IL-17, and IP-10 compared to ET. Cytokine levels were similar in ET and PV, except for RANTES, which was significantly overexpressed in ET (Cacemiro et al., 2018). Radar chart representation summarizing the percentage of high producers of each cytokine/chemokine in the three patient cohorts demonstrates that, consistently with Hasselbalch's model (Hasselbach, 2013), PMF is the MPN subtype characterized by the highest inflammatory burden. In addition, Barosi et al. studied sIL2RA in PMF, confirming that PMF patients showed elevated cytokine levels as compared to healthy controls, and demonstrating that sIL2RA levels correlated with an increased risk of disease progression (indicated by hematological parameters including decreased

hemoglobin and platelet concentrations, increased percentage of blood blasts, increased spleen size, and increased concentration of circulating CD34+ cells) in *JAK2*V617F-positive but not in *CALR*-mutated patients (Barosi et al., 2020).

In the last years, a large-scale multicentre study analysed the serum cytokine profiles of a considerable cohort of more than 400 MPNs, to identify specific inflammatory cytokine signatures according to disease subtypes and evolution (Øbro et al., 2020). Ten cytokines, namely, INF-γ, IL-1RA, IL-6, IL-8, IP-10, EGF, eotaxin (CCL11), TNF-α, TGF-α, and Growth-Regulated Oncogene (GRO-α) correlated at least one MPN subtype, disease severity, and overall survival. Specifically, PMF confirmed its association with increased levels of TNF-α, IP-10, and IL-8; ET and PV displayed higher eotaxin and EGF, while ET showed a novel, unique, and specific inflammatory cytokine signature consisting of elevated GRO-α. Surprisingly, hydroxyurea treatment did not affect individual cytokine levels.

In ET, elevated GRO-α levels at the time of diagnosis correlated also with an increased risk of progression into secondary MF (but not with blast-phase evolution) and the predictive value of GRO-α remained significant after inclusion of fibrosis grade as a covariate. Of note, $CD56^{+}$/CD14+ monocytes were identified as the main cellular source of GRO-α in ET.

Given the prognostic value of cytokine profile, the authors introduced a novel prognostic model that includes cytokine profiling to the other well-established risk factors as age, gender, and high-risk mutations (Øbro et al., 2020). As previously described by Hasselbalch, this study highlights the key role of chronic inflammation not only in modulating MPN phenotype but also in predicting disease outcome and shows how the cytokines profile may be an informative tool for patient risk stratification and monitoring.

5. The CCL2/CCR2 chemokine system

5.1 Chemokines

Chemokines (chemoattractant cytokines), first identified in 1977, constitute a large family of secreted proteins (60–100 amino acids) structurally related to cytokines, whose main function is to regulate cell migration and trafficking (Wu et al., 1977). Chemokines are mainly secreted in response proinflammatory stimuli, and they exert their function selectively attracting monocytes, neutrophils, and lymphocytes. The migration of cells expressing chemokine receptor occurs along a chemical ligand gradient (namely chemokine gradient), towards sites with high local concentration of the chemokine.

Besides regulating chemiotaxis, chemokines play a central role in immune cell differentiation, homeostasis of the immune system and in both immune and inflammatory responses. The chemokine superfamily is composed by more than 50 human chemokines and 20 chemokine receptors (O'Hayre et al., 2008). Chemokines can be classified into four subfamilies based on the number and well-conserved position of cysteine residues at the N-terminus. Conventionally, they are subdivided into CXC, CC, CX3C, and C, according to cysteine motif (Rollins, 1997). The human genes encoding for CXC chemokines are mapped mainly on chromosome 4q12–21, whereas genes for CC chemokines are located mainly on chromosome 17q11.2 (Nomiyama et al., 2001). The protein structure includes three distinct domains: (1) a highly flexible N-terminal domain, which contains disulfide bonds between the cysteine residue to maintain the folding of the chemokine monomer; (2) a central loop with three antiparallel β-sheets; and (3) a C-terminal α-helix that overlies the sheets (Deshmane et al, 2009).

Chemokines can also be classified according to their function into three main categories: inflammatory, homeostatic and dual-type (homeostatic/inflammatory) chemokines. Homeostatic chemokines (as e.g. CXCL1) are constitutively expressed and secreted to regulate leucocyte trafficking to and within secondary lymphoid organs as the bone marrow and the thymus during hematopoiesis and immune surveillance. Homeostatic functions include cell survival, proliferation, endocytosis, all steps of leukocyte migration (which include actin polymerization, cytoskeletal remodelling, integrin activation and cell adhesion) and chemotaxis (López-Cotarelo et al., 2017).

Inflammatory chemokines (e.g. CXCL8), instead, are induced in response to noxa and orchestrate cell recruitment to sites of inflammation or infection (Deshmane et al, 2009), acting as "alarm signals" to restore homeostasis (Moser et al., 2004). The inflammatory functions include respiratory burst, neutrophil extracellular trap (NET) formation, phagocytosis (of pathogens), degranulation, and exocytosis (López-Cotarelo et al., 2017). Dual-type (homeostatic/inflammatory) chemokines (e.g., CXCL1, CCL21), instead, can be homeostatic or inflammatory in specific pathological condition and according to the type of organ and tissue.

Upon secretion, some chemokines are active as monomer, while others form homodimers or heterodimers, which localize mainly to extracellular matrix (ECM) and regulate processes other than cell migration (Proudfoot, et al., 2003).

Chemokines exert their function through the activation of seven-transmembrane G-protein-coupled receptors (GPCRs), which also involves adhesion molecules and ECM protein as glycosaminoglycans (GAGs) (O'Hayre et al., 2008). Chemokine receptors could be classified according to the type of chemokine to which they bind in XC, CC, CXC, or CX3C categories. In addition, inflammatory chemokine receptors display promiscuous ligand binding, and the chemokines are in turn redundant in their action on target cells, binding to multiple different chemokine receptors (Mantovani, 1999). The chemokine/receptor interaction induces a conformational change in the receptor intracellular tail leading to the activation of complex downstream signalling pathways (Figure 48).

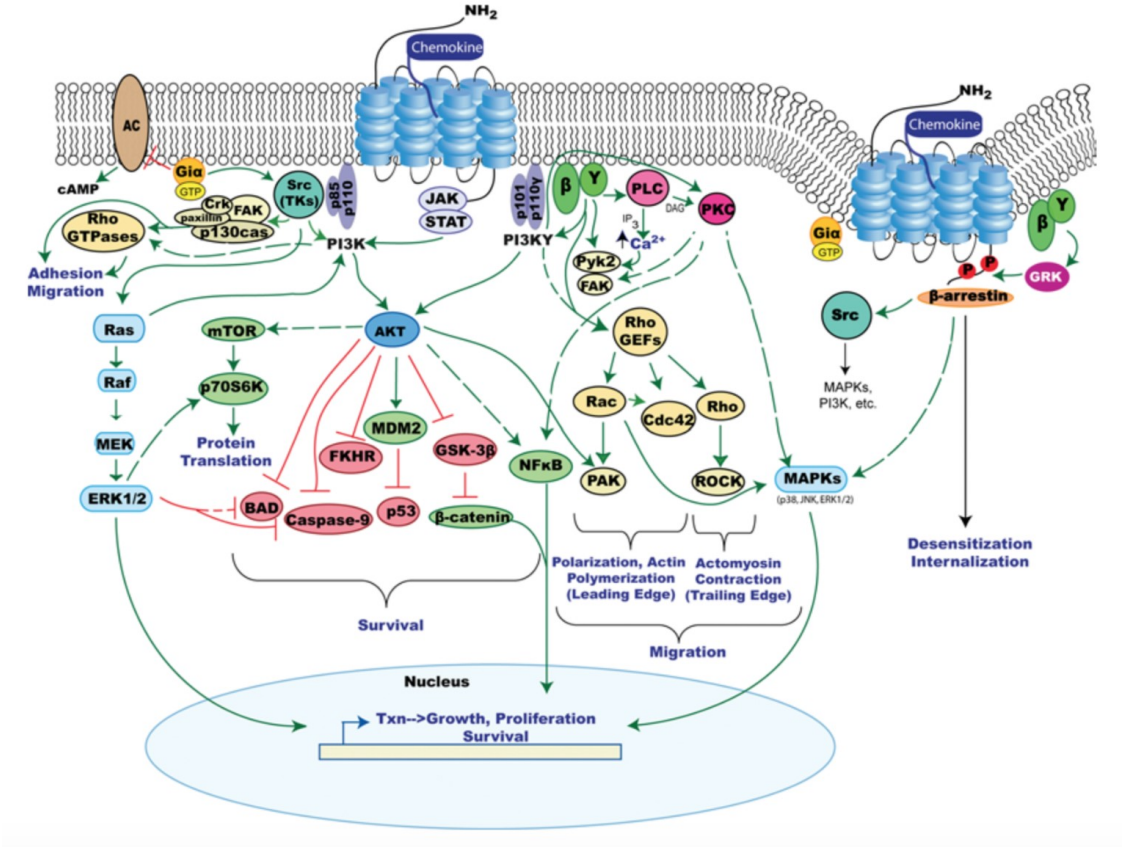

Figure 48. Signaling pathways downstream of chemokine receptor activation. The main signalling cascades activated by chemokine/receptor axis are involved in cell migration, survival, and proliferation. They include: $G_{\beta\gamma}$-dependent signalling through PI3Kγ (phosphoinositide 3-kinase γ) which activates Rac and subsequently PAK (p21-activated kinase); PLC (phospholipase C) pathway; Gi-dependent signalling through PI3K and various protein tyrosine kinases which induce the activation of Akt, Rac and Cdc42; JAK/STAT signaling, which activates Pi3K and subsequently Ras and Akt; β-arrestin activation which leads to the activation of several proteins including Src, MAPK (ERK, p38, JNK) and PI3K (from O'Hayre et al., 2008).

Accumulating evidence show that rapid functional responses, as chemiotaxis, are regulated by the family of G proteins G_i and $G_{\beta\gamma}$. Downstream of G proteins, serine/threonine kinases including MAPKs, Akt, and tyrosine kinases such as JAK, PKC, Src, and Pyk2 have been implicated in regulating chemotaxis, migration, and adhesion (Tripathi et al., 2020) On the other hand, long-term functional effect are mediated by multiple transcriptional factors, including STATs, NF-κB, AP-1 (activation protein-1), CREB (cAMP response element-binding) protein, NFAT (nuclear factor of activated T cells), and FOXO1/3 (forkhead box O transcription factors 1/3) (O'Hayre et al., 2008).

5.5 The monocyte chemoattractant protein-1 (MCP-1 or CCL2)

The monocyte chemoattractant protein-1 (MCP-1), also known as CCL2 (C-C Motif Chemokine Ligand 2) is the first discovered and most widely studied human C-C chemokine. CCL2 is one of the most potent chemotactic factors for monocytes. In humans, *CCL2* gene is located on chromosome 17q11.2, and encoded for a protein composed of 76 amino acids. Currently, four human CCL isoforms (CCL2/MCP-1, CCL7/MCP-3, CCL8/MCP-2 and CCL13/MCP-4) have been identified and characterized.

Human CCL2 was supposed to be the homologue of the murine fibroblast protein encoded by the *JE* gene, one of the first platelet-derived growth factor (PDGF)-inducible gene to be described (Rollins et al., 1989; Cochran et al., 1983). Human MCPs are produced as precursor molecules, which contain a hydrophobic N- terminal signal sequence of 23 amino acids. This sequence is cleaved to produce and secrete a mature protein of 74±76 amino acids. CCL2 could be secreted in two different molecular forms (of 9 kDa and 13 kDa, respectively), according to the post-translational modification and O-glycosylation of specific residues. Glycosylation has been shown to slightly reduce the chemotactic efficacy of CCL2 (Jiang et al., 1990; Van Coillie et al., 1999). The monomers of CCL2, as many other CC chemokines, is composed of four β-sheet regions residue 9–11 (β0), 27–31 (β1), 40–45 (β2), and 51–54 (β3)) and two overlying carboxy-terminal α-helixs (Deshmane et al. 2009). Two regions critical for biological activity have been identified: the sequence from Thr-10 to Tyr-13, and from residues Ser-34 and Lys-35. Mutations of within these sequences induce a decrease of CCL activity (Deshmane et al. 2009).

CCL2 is produced by a variety of cell types, including endothelial and epithelial cells, fibroblasts, smooth muscle cells, mesangial, astrocytic, microglial cells, and monocytes. However, mononuclear cells as monocyte/macrophages are found to be the main source of CCL2 (Yoshimura et al., 1989). CCL2 can be produced constitutively or in response to growth factors, cytokines, and oxidative stress (Deshmane et al. 2009). Indeed, CCL2 and other chemokines are typically overexpressed in tissue during inflammation and can be regulated in different cell types *in vitro* by pro-inflammatory mediators as TNF-α, IL-1β, IFN-γ and PDGF (Melgarejo et al., 2009).

NF-κB seems to be the main transcription factor, with AP-1, involved in *CCL2* induction. Molecular studies had identified two NF-κB binding sites within the *CCL2* promoter, approximately 2.6 kb from the transcription initiation site, which appear to activate *CCL2* transcription in response to IL-1β and TNF-α (Ping et al., 1996; Ueda et al., 1997). Furthermore, a 7-bp response element in the 3′ UTR region and elements closed to NB-κB binding site of *CCL2* have also been shown to regulate the chemokine transcription in response to PDGF (platelet-derived growth factor), in 3T3 cells (Freter et al., 1996). In addition to NF-κB, other two consensus elements for the AP-1 trans-acting factors have been identified in the human *CCL2* promoter. One of these consensus elements overlaps a consensus site for the Sp1 transcription factor that appears to be important for

the basal transcription activity of the gene (Timmers et al., 1990). The other one appears to mediate *CCL2* induction upon phorbol ester 12-O-tetradecanoylphorbol 13-acetate (TPA) stimulation (Li and Kolattukudy, 1994).

Recently, Najatsumi and co-workers described a NF-κB-independent alternative pathway, which is involved in the modulation of *CCL2* gene transcription. Indeed, *CCL2* expression is regulated by mTORC1, which induces the dephosphorylation of the transcription factor forkhead box K1 (FOXK1) via protein phosphatase 2A (PP2A). This pathway contributes to tumor progression *in vivo* by promoting macrophage (tumor-associated macrophage, TAM) infiltration at tumor sites (Nakatsumi et al., 2017).

5.3 CCL2 transmembrane receptor, CCR2

CCL2 exerts its biological functions by preferentially engaging its cognate receptor CCR2. CCR2 is a G-protein-coupled seven-transmembrane receptor, composed of a C-terminal intracellular region, seven hydrophobic transmembrane domains each connected by three extracellular and three intracellular loops, and a short extracellular N-terminus.

There are two alternatively forms of CCR2 according to their splicing, namely CCR2A and CCR2B, which differ only in their C-terminal tails (Charo et al, 1994). Between these two isoforms, CCR2A isoform is expressed mainly by mononuclear cells and vascular smooth muscle cells, whereas monocytes and activated NK cells express mainly the CCR2B isoform (Bartoli et al., 2001). In addition to CCL2/MCP-1, CCR2 is able to bind also CCL7/MCP-3, CCL8/MCP-2 as well as CCL13/MCP-4, with different levels of binding affinity.

CCR2 receptor is expressed in various tissues including blood, heart, brain, kidney, lung, liver, ovary, pancreas, spinal cord, spleen, and thymus (Lim et al., 2016).

CCL2/CCR2 binding induces the activation of a complex chemokine signaling networks (Figure 49). Huang and colleagues recently investigated the phosphoproteome resulting from CCL2/CCR2 axis activation in a CCR2-expressing cell line (FlpIn-HEK293T-CCR2). Differential expression analysis identified 699 significantly regulated phosphorylation sites on 441 proteins. Many of these proteins are known to participate in chemotaxis process, regulating actin cytoskeleton dynamics, cytoskeletal organization, cell adhesion and endocytosis. Several guanine nucleotide exchange factors and GTPase-activating proteins were also identified (Huang et al., 2020). Of note, most of the upregulated phosphoproteins were part of well-known molecular pathways, which include G-proteins, MAPK/ERK, PI3K/Akt and JAK/STAT pathway (Biswas and Sodhi, 2002; Werle et al., 2002; Ko et al., 2007). In addition, the authors also observed the phosphorylation of many proteins that exert theirs functions in the nucleus, and involved in DNA replication and repair, transcriptional regulation, RNA processing, cell cycle regulation and nuclear pore complex formation (Huang et al., 2020) (Figure 49).

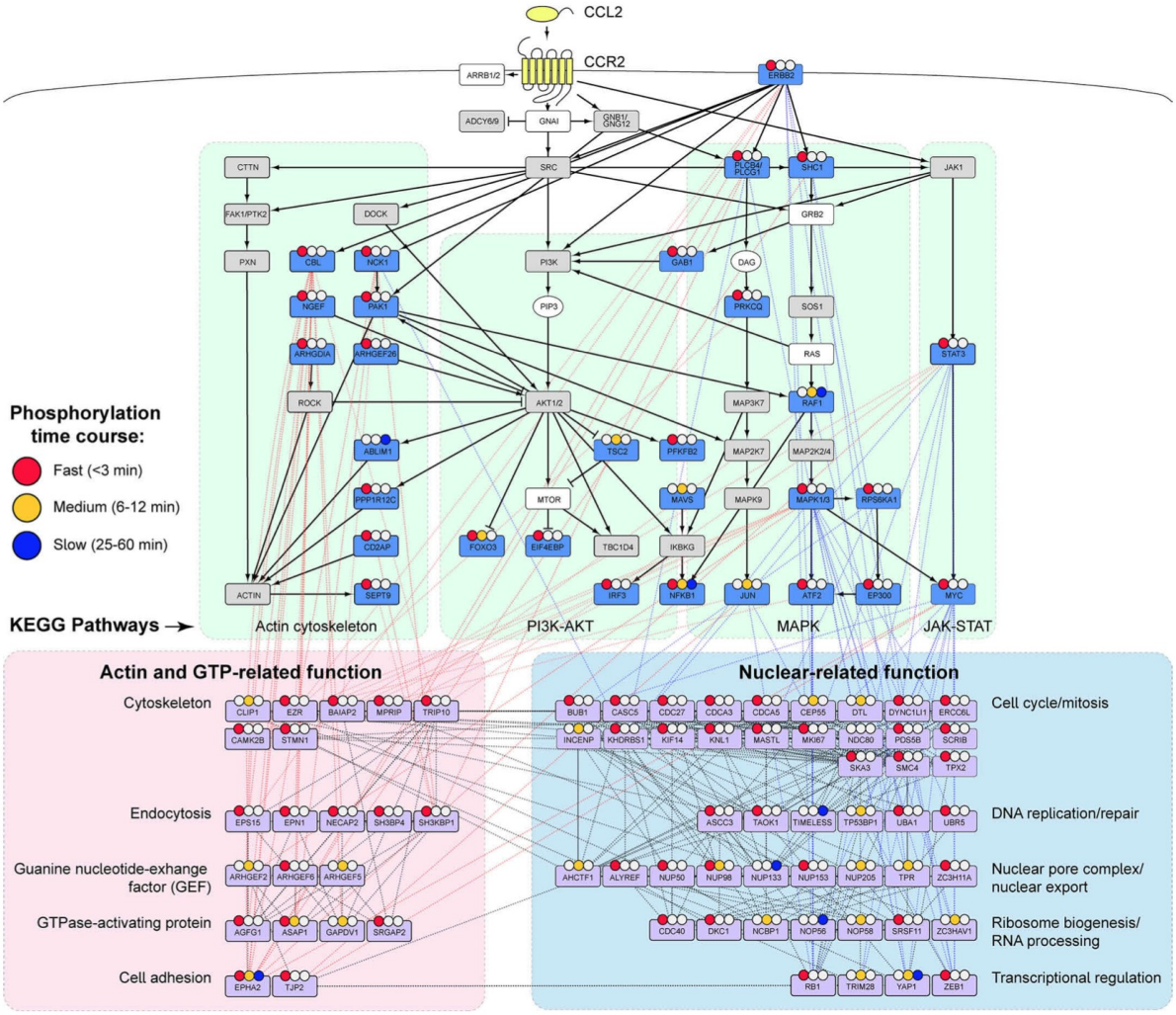

Figure 49. CCL2-CCR2 phosphoproteomic signaling network. Analysis of Kyoto Encyclopedia of Genes and Genomes (KEGG) pathways, using the Database for Annotation, Visualization, and Integrated Discovery (DAVID). Proteins with significantly regulated phosphorylation upon CCL2 stimulation were reported into a signaling network. KEGG pathways, in the green shaded areas, include proteins with significantly regulated phospho-sites (blue boxes), proteins with phosphor-sites that were observed but not regulated (gray boxes), proteins with no observed phospho-sites (white boxes), and non-protein components (white ovals). The black solid lines represent activating (arrow- head) or inhibitory (blunt head) interactions. Many additional proteins (light purple boxes) that have not been associated with chemokine receptor signaling but have known interactions with at least three other proteins in the network are broadly grouped into actin-related (pink shaded areas) and nuclear-related biological processes (blue shaded areas, respectively). Red and blue dashed lines indicate interactions between such proteins and KEGG pathway proteins, while black dashed lines indicate inter- and intra-molecular interactions between nuclear-related and actin/GTP-related proteins Phosphorylation events were reported as fast (red circles), medium (yellow circles), or slow (blue circles), according to the timing of the maximal phosphorylation response vs. the baseline (from Haung et al., 2020).

Through these pathways, the CCL2/CCR2 chemokine system exerts its homeostatic functions, regulating lymphocyte trafficking from blood to lymph nodes, cell extravasation, but also cell response to pro-inflammatory stimulation to enhance physiological tissue defence and repair. The role of CCL2/CCR2 signaling in leukocyte recruitment has been demonstrated using several animal models. Indeed, transgenic mice overexpressing CCL2 in alveolar epithelial cells and

pancreatic islets, showed a marked accumulation of mononuclear cells in the bronchoalveolar space (Gunn et al., 1997) and pancreas, respectively (Grewal et al., 1997). By contrast, $CCL2^{-/-}$ mice were unable to recruit monocytes in inflammation models. Mice lacking CCR2 developed normally without hematopoietic abnormalities, although they failed to recruit macrophages in experimental model of peritoneal induced inflammation and to counteract infection of intracellular pathogens (Kurihara et al., 1997).

Besides chemiotaxis, CCL2/CCR2 axis has been demonstrated to activate monocytes production of inflammatory cytokines (IL-1 and IL-6) and to drive monocyte polarization into M1 phenotype (Gschwandtner et al., 2019). Indeed, downregulation of CCL2 expression led to decreased M1 and enhanced M2 polarization evidenced by elevated expression of Arg1, Ym1, and TGFβ, both *in vitro* and *in vivo* murine models (Nio et al., 2012; Gu et al., 2017).

5.4 The role of CCL2/CCR2 inflammatory disorders and cancers

Deregulation of the CCL2/CCR2 signaling has been observed in various pathological conditions, especially those characterized by a chronic inflammatory state as atherosclerosis, allergic asthma, idiopathic pulmonary fibrosis, non-alcoholic fatty liver disease, inflammatory bowel disease and rheumatoid arthritis (O'Connor et al., 2015). Indeed, elevated levels of CCL2 have been detected in the synovial fluid of rheumatoid arthritis patients, suggesting an important role in the recruitment of mononuclear phagocytes (Stankovic et al., 2009). Moreover, elevated CCL2 levels have been found in the serum and bronchoalveolar lavage of patients with idiopathic pulmonary fibrosis (Suga et al., 1999), in which this chemokine it is thought to contribute to fibrosis by supporting monocyte/macrophage inflammatory response, angiogenesis, fibroblast collagen synthesis and myofibroblast. The CCL2/CCR2 axis has been proposed as biological target for the therapy of idiopathic pulmonary fibrosis, and a CCL2 monoclonal antibody, Carlumab, is in phase 2 of clinical trial (Raghu et al., 2015).

The CCL2/CCR2 axis has been implicated also in the pathogenesis of atherosclerosis, in which it regulates the inflammatory recruitment of classical monocytes towards the arterial lesion in atherosclerosis as well as in myocardial infarction. Indeed, CCL2 is elevated in human atherosclerotic plaques, and in vascular endothelial and smooth muscle cells exposed to modified lipids (Nelken et al., 1991). Boring and colleagues crossed $CCR2^{-/-}$ mice crossed with apolipoprotein (apo) E-null mice, which are known to develop severe atherosclerosis, and observed that the selective absence of CCL2 receptor accounted for a significant decrease in the lesion formation (Boring et al., 1998). More recently, CCL2 plasma levels have been associated with others risk factors for atherosclerosis and with an increased risk for death or myocardial infarction (de Lemos et al., 2003).

Given its pro-fibrotic functions, the CCL2/CCR2 axis has been widely described in fibrotic disorders including lung, liver and colon fibrosis, and others multi-organ fibrotic disease (Seki et al., 2009; Moore et al., 2001; Kuroda et al., 2019). In this context, CCL2 not only modulates monocyte migration to the inflamed site and fibroblast release of pro-fibrotic cytokines, but also the recruitment, proliferation and differentiation of fibrocytes in both humans and murine models (Ekert et al., 2011). Circulating fibrocytes are considered an intermediate stage between monocytes and fibroblasts or myofibroblasts and they are identified as $CD14^{+}/CD16^{-}$ population, which carry CCR2 on their surface (Pilling et al., 2009). Since $CCR2^{+}$ cells could represent a rational biomarker of inflammation in fibrotic disease, Brody's research team recently proposed a radiotracer, namely ^{64}Cu-DOTA-ECL1i, a peptide-based radiotracer, which recognizes the extracellular loop (ECL1) of CCR2. The ^{64}Cu-DOTA-ECL1i could be used to noninvasively track and monitor CCR2+ monocytes, fibrocytes and macrophages with positron emission tomography (PET). This radiotracer was tested in two different murine models of lung fibrosis: mice in which lung fibrosis was induced by intranasal administration of the bleomycin and mice in which inflammation and fibrosis were induced with radiation and compared to control animals and $CCR2^{gfp-/gfp-}$knockout mice. Interestingly, the ^{64}Cu-DOTA-ECL1i uptake was relevant in regions of lung inflammation and fibrosis only in fibrotic mice and significantly decreased after anti–IL-1β antibody treatment (Brody et al., 2021), suggesting the use of this non-invasive radiotracer in clinical trial to monitoring fibrotic patients.

The CCL2/CCR2 axis is also widely studied in cancer since chemokines and cytokines are relevant in modulating tumor microenvironment. CCL2/CCR2 signaling is involved in cancer cell proliferation and survival, cancer cell migration and invasion, and inducing inflammation and angiogenesis (Hao et al., 2020). CCL2 was initially described as a "tumor-derived chemotactic factor", and aberrant activation of the CCL2/CCR2 axis has been observed in different type of neoplastic cells as breast (Qian et al., 2011), prostate (Roca et al., 2008), colorectal (Chun et al., 2015), liver (Li et al., 2017), pancreatic (Sanford et al., 2013) cancers.

CCL2 could be produced by both neoplastic and surrounding stromal cells in the tumor microenvironment, exerting its pro-tumorigenic effects. It promotes cancer cells to evade the immune system and regulates the initial stage of metastatic process, driving cancer cells migration to secondary sites and boosting cell invasion and neo-angiogenesis (Lim et al., 2016).

Concerning hematologic neoplasms, the CCL2/CCR2 system has been studied in AML (Legdeur et al., 1997), multiple myeloma (Vande Broek et al., 2003), systemic mastocytosis (Greiner et al., 2017). AML blasts have been demonstrated to produce significant amounts of CCL2 to boost monocyte chemiotaxis, and CD14 committed AML blasts (monocytoid AML) showed an unusual expression of CCR2, which makes them responsive to recombinant CCL2 and to their own conditioned medium (Cignetti et al., 2003). Recently, Macanas-Pirard and co-workers have

described the biological function of CCL2/CCR2 axis in AML. AML patients (N=35) showed higher expression of CCR2 on $CD14^{+}CD34^{+}$ blasts as compared to HD (N=6), and CCR2 expressing AML blasts showed a marked tendency to migrate when exposed to elevated doses of CCL2. *In vitro* blasts migration was significantly abrogated in presence of both neutralizing CCL2 monoclonal antibody and blocking CCR2 monoclonal antibody (Macanas-Pirard et al., 2017). CCL2/CCR2 seemed to also affect cell proliferation, acting on cell cycle and significantly increasing the number of cells in S phase (Macanas-Pirard et al., 2017).

Moreover, primary multiple myeloma cells were found to express the chemokine receptor CCR2 and to migrate in response to high concentration of CCL2 produced by bone marrow stromal cells. These findings suggest an active role of CCL2/CCR2 axis in the bone marrow homing of multiple mieloma cells (Vande Broek et al., 2003). Recently, Greiner and colleagues investigated the CCL2/CCR2 system in systemic mastocytosis (SM). SM is a clonal disorder of hematopoietic stem cells characterized by mast cell infiltration in the bone marrow and an increased production of pro-fibrogenic and pro-angiogenic cytokines. The somatic mutation D816V of *KIT* gene is considered the main driver mutation accounting for BM microenvironment alterations, including increased angiogenesis, thickened bone trabeculae, and fibrosis. Interestingly, Greiner et al. demonstrated that *KIT*D816V promoted the expression of CCL2 in neoplastic mast cells via NF-κB. Indeed, CCL2 plasma levels were higher in SM patients as compared to HD and they were associated to disease severity and reduced overall survival. Furthermore, CCL2 knock-down in a xenotransplantation model using NSG mice, significantly reduced necrotic areas, leukocyte infiltration in the bone marrow, as well as a different deposition on collagen fibres and reduced microvessel density, suggesting the involvement of CCL2/CCR2 in angiogenesis fibrotic changes in SM. (Greiner et al., 2017).

The biological role of CCL2/CCR2 chemokine system in the pathogenesis of MPNs is still largely unknown. As mentioned in the dedicated chapter, MPN patients showed significantly higher circulating levels of pro-inflammatory and pro-fibrotic cytokines as CCL2 (Tefferi et al., 2011; Pardanani et al., 2011). Among MPNs, PMF patients seemed to be the higher producers of the chemokine. These data were confirmed by Kleppe and colleagues, who demonstrated that CCL2 was also aberrantly secreted by neoplastic cells obtained from PMF patients and myelofibrotic murine model harboring the MPLW515 mutation (Kleppe et al., 2015). Recently, Cominal's research group suggested tat CCL2 and other chemokine (CXCL8, CXCL10, and IL-18) had a direct role in promoting hematopoietic niche modifications, activation of angiogenesis, and deregulation of hematopoiesis. Indeed, investigating bone marrow levels of inflammatory soluble mediators in cohort of MPN patients (N=16 PMF, N=28 ET, N=19 PV) and healthy subjects (N=17 HD), bone marrow CCL2 levels were found significantly elevated in MPNs as compared to HD.

Furthermore, the aberrant secretion of CCL2 was associated to bone marrow fibrosis in PMF (Cominal et al., 2021), suggesting the role of this pro-inflammatory and pro-fibrotic chemokine in the bone marrow niche deregulation.

Concerning CCL2 receptor, the expression of CCR2 was recently investigated in monocytes obtained from MF patients. CCR2 is primarily expressed by classical monocytes (identified as $CD14^{++}/CD16^{+}$) and is progressively downregulated in the intermediate ($CD14^{+}/CD16^{+}$) and non-classical monocytes ($CD14^{+}/CD16^{++}$). The percentage of $CCR2^{+}$ total monocytes was significantly increased in MF as compared to healthy subjects and, surprisingly, intermediate, and non-classical monocytes expressing CCR2 were significantly increased in MF. Therefore, monocytes showed an atypical chemokine receptors profile in MF (Barone et al., 2020).

6. The rs1024611 single nucleotide polymorphism of CCL2 and MPNs

CCL2 expression levels are highly variable among individuals and this variability may contribute to different susceptibility to several inflammatory conditions (McDermott et al., 2005). The inter-individual variability in CCL2 expression levels have been associated to genetic variants as single nucleotide polymorphisms in the cis-regulatory regions of *CCL* gene. In 1999, Rovin and colleagues reported a novel single nucleotide polymorphism in the regulatory region the *CCL2* namely rs1024611. This SNP is located within the enhancer sequence, at position –2518 (or –2578) relative to the transcriptional starting site of the gene and it consists in an A to G substitution. The rs1024611 accounts for an increased CCL2 expression by mononuclear cells upon inflammatory noxa (Rovin et al., 1999). Indeed, peripheral blood mononuclear cells obtained from healthy individuals, heterozygous or homozygous for the -2518A/G SNP of CCL2 (A/G and G/G individuals) produced significantly higher CCL2 after IL1-β stimulation as compared to wild type healthy subjects (A/A). The chemokine production seemed to be “allelic dependent”, since G/G subjects produced more CCL2 than A/G, and A/G more than A/A. As for many SNPs, also the rs1024611 SNP of CCL2 varies according to ethnic groups. Specifically, the G allele frequency is increased in Asian and Mexican populations (47%), as compared to Caucasian (29%) and African American (22%) populations (Rovin et al., 1999).

This SNP has been investigated in several chronic inflammatory conditions, autoimmune disease as well as fibrotic disorders (Colobran et al., 2007) and G/G genotype has been frequently associated to disease severity and poor outcome.
Recently, our research group investigated the rs1024611 SNP of CCL2 in MPNs. As described before, MPNs are a well-established paradigm of onco-inflammatory disorders (Hasselbach, 2012), and the genetically determined host’s inflammatory background is thought to exert a relevant role in defining disease phenotype and outcome. In our study, *CCL2* genotype was evaluated in a cohort of 177 Caucasian MPN patients, of which 44 PV, 65 ET, 68 MF (N=45 PMF and N=23 sMF) and 149 healthy subjects (HD). No statistical differences were observed by comparing genotypic and allelic frequencies of overall MPNs, PV, ET, and MF patients *vs*. HD, as well as between single disease entities. Indeed, genotypic frequencies were in Hardy–Weinberg equilibrium both in the MPN patients and (HD). Focusing on MF, subjects heterozygous and homozygous for the rs1024611 SNP (A/G + G/G) were significantly more frequent in sMF *vs.* PMF (17/23, 73.9% vs. 14/45, 31.1%, respectively, $P = 0.0008$). Moreover, the percentage of polymorphic subjects was significantly more frequent in sMF patients as compared to pre-PMF (1/12, 8.3%, $P = 0.0002$) or overt-PMF (13/33, 39.4%, $P = 0.011$). Of note, the percentage of polymorphic subjects was also significantly higher in sMF as compared to HD ($P = 0.022$).

Furthermore, in MF population the rs1024611 SNP of CCL2 correlated with adverse clinical features as (i) intermediate-2/high IPSS, (ii) lower (Hb < 100 g/L) hemoglobin levels, (iii) presence of circulating blasts (≥ 1%), (iv) and higher (≥II) grading of bone marrow fibrosis. This latter association is consistent with the well-defined pro-fibrotic role of this chemokine in pathological conditions. On the other hand, no associations were found with age, gender, white blood cell and platelet count, LDH levels, presence of constitutional symptoms, spleen size, *JAK2*V617F mutation, and history of major thrombotic events.

Our data suggest that the rs1024611 SNP of CCL2 could represent a host genetic predisposition factor for sMF, and it could be use in clinical practice to identify and therefore monitor ET and PV patients who more likely will progress toward a spent phase, characterized by higher inflammation burden. Finally, the SNP represent a biomarker of disease severity in MF, which could help the physician in therapeutic decisions and in the careful monitoring of patients (Masselli et al., 2018).

Aim

Primary myelofibrosis is characterized by a local (bone marrow) and systemic cytokine-mediated pro-inflammatory state that is triggered by the interaction between clonal myeloid cells and surrounding bone marrow stromal cells.

Cell-intrinsic events such as the acquisition of somatic mutations in specific myeloid genes (driver mutations and high-risk mutations) have been extensively investigated, resulting critical for disease onset and progression. However, several evidence indicate that driver mutations and host genetic variants are not sufficient to fully explain the heterogeneity observed in MPN disorders, since patients with comparable mutational profile, in several cases, showed different phenotype and outcome. In this context, the role of host genetic variants that affect inflammatory background has recently emerged.
Among MPNs, myelofibrosis (MF) is the most aggressive subtype, representing the paradigm of onco-inflammation with a specific cytokine profile.
Among various pro-inflammatory cytokines/chemokines that have been found elevated in MF patient plasma by Tefferi's group studies, we focused on the monocyte chemotactic protein-1 (CCL2 or MCP-1), whose higher levels has been associated with transfusion dependent anemia, splenomegaly, and poor response to immunomodulating agents such as pomalidomide.

CCL2 is one the most potent CC-chemokine that induces the recruitment and activation of monocytes, T cells and NK cells toward inflamed sites and plays a pivotal role in organ fibrotic changes by preferentially binding its cognate receptor CCR2. Besides modulating leukocyte trafficking, the activation of CCL2/CCR2 chemokine system exerts pro-fibrogenic but also pro-tumorigenic effects, boosting cancer cell proliferation, survival, and metastasis.
CCL2 gene is highly polymorphic; especially, the rs1024611 SNP, identified in the 5′ distal regulatory region of its promoter (-2518A/G), accounts for an increased CCL2 production (at both mRNA and protein levels) upon inflammatory noxa. This SNP of CCL2 has been associated with a large variety of chronic inflammatory diseases, and has been recently studied, by our research group, in MPNs, in which it represents a host genetic predisposing factor for sMF and a marker of disease severity and aggressiveness.

Given this background, my PhD research project was focused on two main aims:

- AIM 1: the role of rs1024611 SNP of CCL2 in PMF. We sought to investigate the rs1024611 SNP of CCL2 in a large cohort of PMF patients with a long duration of follow-ups, assessing (i) genotype and allele frequency, (ii) genotype/phenotype correlation, (iii) the impact on disease outcome and patients' survival, (iv) the effects of rs1024611 polymorphism on CCL2 production

in PMF.

- AIM 2: the role of CCL2/CCR2 axis in PMF. We sought to study the biological role of the CCL2/CCR2 chemokine system in PMF, assessing (i) whether neoplastic hematologic stem cells could represent CCL2 target, (ii) which signalling pathways are activated downstream CCL2/CCR2 axis and (iii) the effects of therapy with JAK2 inhibitor on CCL2/CCR2 chemokine system, (iv) whether CCR2 expression on MPN CD34+ cells may have a diagnostic value to discriminate true ET from prePMF and prePMF from overtPMF.

Materials and Methods

Materials and Methods I: The role of the rs1024611 SNP of *CCL2* in PMF

1. Study population

This study was carried out in collaboration with the Centre for the Study of Myelofibrosis, IRCCS Policlinico S. Matteo (Pavia, Italy), the Hematology and BMT Unit of Parma University Hospital and the Medical Genetics Unit of Parma University Hospital (Parma, Italy). The research project was approved by the ethical committees of the Institutions (IRCCS Policlinico S. Matteo and Parma University Hospital, Parma, Italy, Prot. 11537-14/03/2019 and 18698-03/05/2019).

The study population was composed of 773 Caucasian PMF patients, consecutively recruited at the Centre for the Study of Myelofibrosis, IRCCS Policlinico S. Matteo, from 1990 to December 2019. The Unit of Medical Genetics (University Hospital of Parma) provided DNA from 323 Caucasian control subjects (CTRL).

For functional *in vitro* experiments, 32 PMF, 6 ET, 6 PV were enrolled by the Hematology and BMT Unit of Parma University Hospital (from September 2016 to January 2021) and 17 granulocyte colony stimulating factor (GCSF)-mobilized donors were used as healthy donors (HD). The diagnosis of ET, PV, pre- and overtPMF was formulated or revised according to the 2016 WHO classification. Biological characteristics at the time of the diagnosis and clinical and histopathological information were collected from patients' clinical records. Patients mutational profile was established by PCR analysis and Next Generation Sequencing detecting "driver mutations" in *JAK2, MPL, CALR* and "high molecular risk (HMR) mutations" in *EZH2, IDH1/IDH2, ASXL1*, and *SRSF2*, known to be relevant for the prognosis of PMF patients (Vannucchi et al., 2013).

2. Genotyping

After DNA extraction by PureLink® Genomic DNA Kit (Invitrogen, Waltham, MA, USA, cat. N. K182002) from 200 µL of whole blood, CCL2 rs1024611 SNP genotyping was performed by real-time PCR method based on a validated TaqMan® assay (TaqMan® Predesigned SNP Genotyping Assays, ID C___2590362_10 (rs 1024611), (Applied Biosystems Foster City, CA, USA)), as previously performed (Masselli et al, 2018). In brief, this method is based on pre-optimized PCR primer pairs, specific for CCL2, and two probes for allelic discrimination. The probes, with a FAM™ or VIC™ dye label on the 5´ end, are specific for the A allele or the G allele.

3. Next generation sequencing (NGS) analysis

Next generation sequencing (NGS) was performed using a Myeloid Solutions (MYS) Panel (SOPHiA Genetics, Saint Sulpice, Switzerland, Arrow Diagnostics). The MYS panel includes splicing junctions (± 25bp), coding regions and Internal Tandem Duplications (ITDs) of 30 genes, known to be associated with Myelodysplasic Syndromes (MDS), Myeloproliferative Neoplasms (MPN) and Leukemia (Table 16).

DISEASE	GENES
AML	*ASXL1, BRAF, CEBPA, DNMT3A, ETV6, EZH2, FLT3, IDH1, IDH2, KIT, KRAS, NPM1, NRAS, RUNX1, SRSF2, TET2, TP53, U2AF1, WT1, ZRSR2*
MDS	*ASXL1, BRAF, CBL, CEBPA, CSF3R, DNMT3A, EZH2, FLT3, HRAS, IDH1, IDH2, KRAS, MPL, NPM1, NRAS, RUNX1, SF3B1, SRSF2, TET2, TP53, U2AF1, WT1, ZRSR2*
MPN	***ASXL1, CALR, EZH2, IDH1, IDH2, JAK2, MPL**, SETBP1, **SRSF2***
JMML	*CBL, KRAS, NRAS, PTPN11, RUNX1, SETBP1, ZRSR2*
ALL	*ABL1, BRAF, FLT3, HRAS, JAK2, KRAS, NRAS, PTPN11*

Table 16. Gene included in the Myeloid Solutions (MYS) Panel (SOPHiA Genetics) and their association to disease subtypes. The genes taken in consideration for the analysis of mutational profiling of PMF patients were represented in bold.

After extraction, 200 ng of DNA were subjected to libraries preparation and pair-end sequencing on a MiSeq instrument (Illumina, San Diego, CA, USA), using the Reagent Kit V2 500 cycles cartridge, according to manufacturers. Alignment, base calling, and variant annotation were performed with SOPHiA DDM software, investigating the available databases (as NCBI, COSMIC, GNOMAD, CLINVAR, ExAC).

4. Cell Cultures

Mononuclear cells (MNCs) were obtained by a Ficoll–Hypaque gradient from peripheral blood of n. 24 therapy naïve PMF stratified according to the rs1024611 SNP of CCL2, from n.6 PMF before (T0) and after 1, 3 and 9 months of ruxolitinib therapy (T1, T2 and T3), and from 17 Healthy subjects (HD). PBMNCs were in part pelleted to evaluate CCL2 basal expression, and in part cultured 1 × 10^6 cells/mL in RMPI medium completed with 10% FBS, 1% L-glutamine, 1% penicillin/streptomycin, in presence or absence of 1.1 ng/mL of IL1-β for 20 h, as previously described (Rovin et al., 1999). CCL2 mRNA and protein expression were evaluated by real-time quantitative RTPCR (qRT-PCR) and western blotting at basal level and after IL1-β stimulation.

5. Real-Time Quantitative RT-PCR (qPCR)

CCL2 gene expression was evaluated in PBMNCs at basal level and after 20h of incubation with IL1-β, using real-time quantitative RT-PCR (qRT-PCR). Total mRNA was extracted using the RNeasy Mini Kit (Qiagen, Hilden, Germany, cat. N. 74106) and 1µg of total mRNA was reverse-transcribed using the High-Capacity RNA-to-cDNA kit (Applied Biosystems, Foster City, CA, USA, cat. N. 4387406). Twenty ng of cDNA were subjected to qRT-PCR using PowerUp™ SYBR™ Green Master Mix (Applied Biosystems, cat. N. A25742), The cDNAs were amplified in a StepOne™ Real-Time PCR System (Applied Biosystems, Foster City, CA, USA), using predesigned specific primers for *CCL2* (FW, 5′-CATAGCAGCCACCTTCATTCC-3′, and RV 5′-TCTCCTTGGCCACAATGGTC-3′); and for *GAPDH* (glyceraldehyde 3-phosphate dehydrogenase) (FW, 5′-TTGAGGTCAATGAAGGGGTC-3′, and RV 5′- GAAGGTGAAGGTCGGAGTCA-3′), using as housekeeping gene control. All samples were run in triplicate, including no-template and no-reverse-transcriptase controls for each experiment. For the results analysis, *CCL2* mRNA expression was normalized to *GAPDH* and fold-change of *CCL2* expression was calculated using ΔΔCT method [(2-[(CT *CCL2* - CT *GAPDH*)IL1-β − (CT *CCL2* - CT *GAPDH*)untr, relative $2^{-\Delta\Delta CT}$ values].

6. Immunoblotting

For protein expression analysis, cells were resuspended in RIPA lysis buffer (150 mM NaCl, 1% Nonidet P-40, 0.5% sodium deoxycholate, 0.1% SDS, 50 mM Tris (pH 7.4), 1 mM PMSF; 1 mM Na3VO4), freshly supplemented with 1% Protease Inhibitor Cocktail (Sigma Aldrich). Protein concentration was determined by bicinchoninic acid BCA protein assay kit (Pierce BCA Protein Assay Kit, Thermo Scientific, Rockford, IL) using the Victor 3V Spectrophotometer (Perkin Elmer, Waltham; MA, USA). Fifty µg of total proteins from each sample were then separated on SDS-polyacrylamide gel electrophoresis (14% of polyacrylamide), blotted onto a nitrocellulose membrane, and incubated with the following primary antibodies:

- Rabbit anti-human CCL2 (Thermo Fisher Scientific, Waltham, MA, USA, cat. N. MA5-17040), diluted 1:1000,
- Mouse anti-human GAPDH (Merck Millipore, Burlington, MA, USA, cat. N. MAB374), diluted 1:5000.

After primary antibody incubation, nitrocellulose membranes were washed and further incubated for 1.5 h at RT with 1:5000 peroxidase-conjugated anti-rabbit IgG antibody (Thermo Scientific) or with 1:2000 peroxidase-conjugated anti-mouse IgG (Sigma Aldrich). Proteins were revealed by ECL SuperSignal West Pico Chemiluminescent Substrate Detection System (Thermo Scientific) and densitometric analysis was performed using the ImageJ software system.

7. Statistical Analysis

For statistical analysis, we adopted a recessive genetic model to compare PMF patients carrying two copies of the G allele (G/G), defined as the CCL2 high-risk group, vs. A/A+A/G PMF, defined as the CCL2 low-risk group. Genotype-phenotype correlation, considering demographic and biological characteristics and disease parameters at the time of diagnosis, was performed using χ2/Fisher exact or Kruskal–Wallis tests, as applicable. To test the effect of homozygosity for the SNP on disease outcome, we assessed whether G/G PMF have a higher risk to incur into: (i) severe anemia, (ii) massive splenomegaly or leukocytosis; (iii) blast transformation; (iv) death for any causes (overall survival). The association between the homozygosity for the SNP and patient hematological outcomes (massive splenomegaly (>10 cm below left costal margin), severe anemia (<100 g/L), leukocytosis (>12x109/L) and blats transformation) was assessed by Cox proportional-hazards models, while overall survival was determined using a Kaplan-Meier product limit estimator.

Univariate and multivariate analysis were also performed including well-established clinical prognostic factors for PMF (IPSS score parameters). Differences between the actuarial estimates were tested using the log-rank test. All the analysis was performed with STATISTICA© software (DELL, Round Rock, TX, USA, release 13.1).

For *in vitro* functional experiments, data were shown as mean±SEM of independent experiments. Statistical analyses were performed using t-test, Mann-Whitney or One-way ANOVA followed by Tukey test, when applicable (GraphPad Prism software, San Diego, CA, USA). Differences with a *P* values < 0.05 were considered statistically significant.

Materials and Methods II: The role of CCL2/CCR2 chemokine system in PMF

1. Study population

The protocol was approved by the local ethical committee (Comitato Etico Area Vasta Emilia-Romagna, Prot. 11537-14/03/2019). From October 2019 till August 2021, 26 PMF, 6 PMF before and after ruxolitinib start, 22 ET, 16 PV were enrolled by the Hematology and BMT Unit of Parma University Hospital. After signing the written informed consent, ~30mL and 15mL of peripheral or bone marrow blood were collected in EDTA tubes. Among PMF, 13 were subclassified as prePMF, 9 as overtPMF. The diagnosis of ET, PV, pre- and overtPMF was based on the 2016 WHO classification. Leukapheresis bags from 10 granulocyte colony stimulating factor-mobilized donors were used as controls (HD). Biological characteristics at the time of the sampling as well as clinical and histopathological information were collected from patients' clinical records.

2. Primary hematopoietic stem cell isolation

Primary hematopoietic stem cells, identified as $CD34^+$ cells, were isolated by immunomagnetic positive selection (CD34 MicroBead Kit, Miltenyi Biotec, Bergisch Gladbach, Germany), as previously described (Masselli et al., 2018). A gradient separation with Lympholite-H (Cedarlane, Burlington, Ontario, Canada) was performed to isolate peripheral blood mononuclear cells (MNCs). Lympholite-H (1,077g/cm^3) is a density gradient separation medium specifically designed to purify MNCs from human peripheral blood or bone marrow aspirates, in removing granulocytes, erythrocytes and dead cells. $CD34^+$ cells fall into MNC layer. In brief, peripheral blood or bone marrow samples were diluted with PBS+EDTA 2mM (1:2 or 1:3) (Euroclone, Milan, Italy) and they were gently settled over the Lympholite-H in centrifuge tubes. Tubes were then centrifuged at 400g for 30 minutes at room temperature in a swinging-bucket rotor without brakes. Carefully, obtained MNC layers were aspirated, washed, counted, and subsequently processed for $CD34^+$ cells extraction. $CD34^+$ cell immunomagnetic selection was performed using the $CD34^+$ cell isolation Kit (human CD34 MicroBead Kit, Milteny Biotech, Bergisch Gladbach, Germany) in the magnetic field of autoMACS® Separator (Milteny Biotech, Bergisch Gladbach, Germany), according to manufacturer's protocol. Briefly, cells were labelled with anti-CD34-antibody conjugated with superparamagnetic beads (CD34 MicroBead) onto a MACS® Column which is placed in the magnetic field of the autoMACS® Separator. The magnetically labelled $CD34^+$ cells were retained within the column while the unlabelled cells eluted to deplete $CD34^-$ cells. After removing the column from the magnetic field, the magnetically retained $CD34^+$ cells could be eluted as the positively selected cell fraction. Cell purity was assessed by flow cytometry using an antibody anti-

human CD34-FITC (Beckman Coulter, Brea, CA, USA) and only samples with purity > 95% were used for subsequent experiments.

3. Flow cytometry

The expression of CCR2 on CD34+ cell surface was assessed by FCM immediately after cell isolation in MPNs (N=22 PMF of which N=13 prePMF and N=9 overtPMF; N=20 ET and N=16 PV) HD (N=10), and HEL 92.1.7 cell line. Samples were stained with anti-human CCR2-PE mAb (R&D Systems, Minneapolis, MN, USA, cat. N. FAB151P) and anti-human CD34-FITC mAb (Beckman Coulter, Brea, CA, USA). As isotype controls, cells were stained with IgG-FITC and IgG-PE (Beckman Coulter, Brea, CA, USA). After 30 minutes of incubation in the dark, samples were centrifuged at 1300rpm for 8 minutes and resuspended in PBS1x for the analysis. Samples were acquired on a CytoFlex (Beckman Coulter, Brea, CA, USA) and FCM data analysis was performed using the Kaluza Analysis Flow Cytometry Software (Beckman Coulter, Brea, CA, USA). The gating strategy used for the analysis was the same for all samples: cell population was identified based on its SSC/FSC properties (in FSC-(A)/SSC-(A) dot plot); then $CD34^+$ cells were gated and $CD34^+$ cells with an equal area and height were selected to accurately remove clumps (greater FSC(A) relative to FSC(H)) and debris (very low FSC). Then, a standard gate for $CD34^+CCR2^+$ cells was created and the percentage of $CD34^+CCR2^+$ cells was normalized to the total percentage of $CD34^+$ cell population for each sample. CCR2 expression was also evaluated on HEL 92.1.7 cell line, widely used as PMF cell model.

4. Primary hematopoietic stem cell culture

Primary CD34+ obtained from n.3 representative ET/PV cases (one ET carrying CALR type II mutation, one ET carrying JAK2V617F mutation and one PV carrying JAK2V617F) were cultured for 48h in serum-free X-vivo medium supplemented with 3 ng/mL IL-3, 50 ng/mL SCF and 200 ng/mL TPO (PeproTech, Rocky Hill, NJ, USA, cat. N. 200-03, 300-07 and 300-18) or in combination with: (1) rhCCL2 100 ng/mL; (2) IL-1β 1.1 ng/mL and TNFα 10 ng/mL (PeproTech, cat. N. 200-01B and N. 300-01A); (3) rhCCL2, IL-1β and TNFα. After incubation, CCR2 expression on CD34+ cell surface was evaluated by FCM. Similarly, CCR2 expression was also assessed in HEL cells cultured up to 48h in 10% FBS-enriched RPMI medium in absence or presence of: 1) rhCCL2 100 ng/mL; (2) IL-1β 1.1 ng/mL and TNFα 10 ng/mL; (3) rhCCL2, IL-1β and TNFα. To investigate downstream signaling pathways that could be activated by CCL2/CCR2 binding, CD34+ cells were isolated from n.7 PMF and n.3 HD and seeded in serum-free X-vivo medium with and without 100 ng/mL of rhCCL2 (R&D Systems, Minneapolis, MN, USA, cat. N. 279-MC). After 24h of incubation, cells were harvested to protein expression analysis.

5. Immunoblotting

To investigate CCL2/CCR2 downstream signaling pathway, cells were resuspended in RIPA lysis buffer (150 mM NaCl, 1% Nonidet P-40, 0.5% sodium deoxycholate, 0.1% SDS, 50 mM Tris (pH 7.4), 1 mM PMSF; 1 mM Na3VO4), freshly supplemented with 1% Protease Inhibitor Cocktail (Sigma Aldrich, St. Louis, MO, USA). Protein concentration was determined by bicinchoninic acid BCA protein assay kit (Pierce BCA Protein Assay Kit, Thermo Scientific, Waltham; MA, USA) using the Victor 3V Spectrophotometer (Perkin Elmer, Waltham, MA, USA). Fifty µg of total proteins from each sample were then separated on SDS-polyacrylamide gel electrophoresis (10% of polyacrylamide) blotted onto a nitrocellulose membrane and incubated with the following primary antibodies:

- Rabbit anti-human JAK2 (Cell Signaling Technology, Danvers, MA, USA, cat. N. 3230), diluted 1:1000,
- Rabbit anti-human phospho-JAK2 (Tyr 1007/1008) (Cell Signaling Technology, cat. N. 3771), diluted 1:1000,
- Rabbit anti-human STAT5 (Cell Signaling Technology, cat. N. 9358), diluted 1:700,
- Rabbit anti-human phosphor-STAT5 (Tyr 694) (Cell Signaling Technology, cat. N. 9314), diluted 1:700,
- Rabbit anti-human Akt (Cell Signaling Technology, cat. N. 9272), diluted 1:1000,
- Rabbit anti-human phopsho-Akt (Ser 473) (Cell Signaling Technology, cat. N. 9271), diluted 1:1000,
- Rabbit anti-human p44/42 ERK1/2 (Cell Signaling Technology, cat. N. 4695), diluted 1:1000,
- Rabbit anti-human phospho-p44/42 ERK1/2 (Thr202/Tyr 204) (Cell Signaling Technology, cat. N. 9101), diluted 1:1000,
- Mouse anti-human GAPDH (Merck Millipore, Burlington, MA, USA, cat. N. MAB374), diluted 1:5000.

After primary antibody incubation, nitrocellulose membranes were washed and further incubated for 1.5 h at RT with 1:5000 peroxidase-conjugated anti-rabbit IgG antibody (Thermo Fisher Scientific, Waltham; MA, USA) or with 1:2000 peroxidase-conjugated anti-mouse IgG (Sigma Aldrich, St. Louis, MO, USA). Proteins were revealed by ECL SuperSignal West Pico Chemiluminescent Substrate Detection System (Thermo Fisher Scientific, Waltham; MA, USA) and densitometric analysis was performed using the ImageJ software system.

6. Statistical analysis

Statistical analyses were performed using Mann-Whitney, Paired T test, or Kruskal Wallis followed by Dunns's test, when applicable. Receiver-operating characteristic (ROC) curves of flow cytometry evaluation of the percentage of $CD34^{+}CCR2^{+}$ cells, were generated to assess diagnostic accuracy in terms of specificity and sensitivity to discriminate between prePMF vs. true ET and prePMF vs. overtPMF. The areas under the ROC curve (AUC) values were evaluated as recommended by Hanley et al. (Hanley et al., 1982). All statistical analyses were performed using Prism 9 (GraphPad software San Diego, CA, USA), and only differences with a *P* values < 0.05 were considered statistically significant.

Results

Results I: The role of the rs1024611 SNP of *CCL2* in PMF

From:

- *Masselli E, Carubbi C, **Pozzi G**, Percesepe A, Campanelli R, Villani L, Gobbi G, Bonomini S, Roti G, Rosti V, Massa M, Barosi G, Vitale M. Impact of the rs1024611 Polymorphism of CCL2 on the Pathophysiology and Outcome of Primary Myelofibrosis. Cancers (Basel). 2021 May 22;13(11):2552.*
  DOI: 10.3390/cancers13112552

- ***Pozzi G**, Masselli E, Carubbi C, Gobbi G, Galli D, Mirandola P, Micheloni C, Arcari ML, Aversa F, Vitale M. The -2518 A/G single nucleotide polymorphism of MCP-1 in myelofibrosis: functional characterization on ex-vivo patient cells. Italian Journal of Anatomy and Embryology. 2018; 123(1): 175.*

- *Masselli E, Carubbi C, **Pozzi G**, Percesepe A, Campanelli R, Villani L, Gobbi G, Rosti G, Massa M, Barosi G, Vitale M. Homozygosity for -2518 G Allele Variant of MCP-1 Predisposes to Adverse Presentation and Outcome in Primary Myelofibrosis. Blood 2019; 134 (Supplement_1): 1689.*
  DOI: https://doi.org/10.1182/blood-2019-122750

- *Masselli E, **Pozzi G**, Gobbi G, Bonomini S, Mirandola P, Vitale M, Carubbi C. Ruxolitinib down-regulates selectively-activated CCL2/CCR2 signaling axis in Primary Myelofibrosis cells. EHA Library. Masselli E. 06/09/21; 324784; EP1061*

1. Biological and clinical parameters of study and control populations

For this project, 773 PMF patients and 323 control subjects were recruited. Biological and clinical characteristics of PMF and control populations are reported in table 17.

	PMF **N. 773**	**CTRL** **N. 323**
Age (diagnosis) Median (range), y	52 (6-83)	63 (28-86)
Male pts N (%)	464 (60)	180 (55.7)
Pre-fibrotic MF (pre-PMF) N (%)	428/768 (55.7)	*N/A*
IPSS Low Intermediate-1 Intermediate-2 High	416/684 (60.8) 112/684 (16.4) 92/684 (13.4) 64/684 (9.3)	
***JAK2*V617F** Mutated, N (%) Homozygous, N (%)	500/757 (66) 194 (38.8)	
MPLW515 Mutated, N (%)	42 (5.5)	
CALR (type 1&2) Mutated, N (%)	165 (20.3)	
Triple-negative Mutated, N (%)	61 (8.1)	
HMR mutation Mutated, N (%)	50/225 (22.2)	
Follow-up Median, months	77	
Death (for any causes) N (%)	191 (24.7)	
Blast transfomation (BT) N (%)	138 (17.8)	
Allogenic stem cell transplant (ASCT) N (%)	86 (11.1)	

Table 17. Biological and clinical characteristics of PMF and control populations. Abbreviations: N: number, pts: patients, y: years.

Considering the PMF cohort, 464 out of 773 PMF patients (60%) were males, with a median age of 52 years (range, 6-83 years). Bone marrow biopsy at the time of the diagnosis was available in 768 cases: PMF patients were classified in pre-fibrotic myelofibrosis (prePMF) (n.428/768, 55.7%) and overt–fibrotic myelofibrosis (overtPMF) (n.340/768, 44.3%), according to the WHO classification. Stratifying patients according to the International Prognostic Scoring System (IPSS), n. 416/684 (60.8%) had a low-risk score, n. 112/684 (16.4%) had an intermediate-1 risk score, n. 92/684 (13.4%) has an intermediate-2 risk score, and n. 64/684 (9.3%) a high-risk score. Driver mutations were evaluated in 757 (98%) patients and occurred as follows: 500 (66%) harbored *JAK2*V617F mutation (of which n.194, 38.8% at the homozygous state), 145 (20.3%) harbored *CALR* mutations (type 1 and 2), 42 (5.5%) had *MPL*W515 mutation, and 61 (8.1%) were triple negative. Moreover, mutation profile was analysed in 225 PMF patients and 50 (22.2%) fell into “High Molecular Risk” (HMR) category (Table 17).

Median follow-up was about 77 months of 773 PMF patients: 86 (11.1%) received ASCT, 138 patients had documented blast transformation (BT) (17.8%), while 191 (24.7%) died. Other main causes of death were due to PMF-related complications (37% of cases, including cachexia, bone marrow failure, infections, and multi-organ-failure); ASCT-related complications (15%) and thrombosis/haemorrhage (18%) (Table 17).

Concerning control population, 108 out of 323 CTRL were males (55.7%) with a median age of 63 years (range 28-86 years) (Table 17).

2. Male subjects homozygous for the rs1024611 SNP of *CCL2* have an elevated risk of developing PMF

Genotype frequencies of the rs1024611 SNP of *CCL2* in our PMF population and in normal control group are listed in table 18. PMF and control populations were homogenous for age and gender distribution. Consistently with our previous data, genotype frequencies were in Hardy–Weinberg equilibrium both in PMF and CTRL cohorts ($P > 0.05$) (Masselli et al., 2018). Therefore, when we analyse the entire PMF population, we could assert that the rs1024611 SNP of *CCL2* does not represent a major host predisposing factor for PMF. Moreover, no statistical differences in term of allelic frequencies were observed comparing the *CCL2* rs1024611 high-risk variant (G/G genotype) in PMF (400/1546 alleles; 25.9%) and in CTRL (152/646 alleles, 23.5%; OR, 1.13; *P*= 0.09). Genotype frequencies in PMF and CTRL were similar as well (PMF: A/A: 55.6%, A/G: 37.0%, G/G 7.4%; CTRL: A/A 57.6%, A/G 37.8%, G/G 4.6%, Table 18).

		Genotypic frequencies			***P* value O.R., [95% CI]**
	N. of cases evaluated	**A/A**	**A/G**	**G/G**	**(G/G *vs.* A/A+A/G)**
PMF demographics					
PMF, tot N, %	773	430 (55.6%)	286 (37.0%)	57 (7.4%)	*P*= 0.09 vs. CTRL tot.
PMF, males N, %	464	247 (53.2%)	174 (37.5%)	43 (9.3%)	**P=0.014 vs. PMF females OR, 2.15 [1.15-4.00] P=0.015 vs. CTRL tot. OR, 2.10 [1.14-3.84] P=0.022 vs. CTRL males OR, 2.52 [1.11-5.72]**
PMF, females N, %	309	183 (59.2%)	112 (36.2)	14 (4.5%)	
PMF, tot Age yrs., median (range)	773	50 (6-80)	51 (16-81)	54 (18-83)	*P*=0.048
CTRL demographics					
CTRL, tot N, %	323	186 (57.6%)	122 (37.8%)	15 (4.6%)	
CTRL, males N, %	180	101 (56.1%)	72 (40.0%)	7 (3.9%)	*P*=0.5 vs. CTRL females
CTRL, females N, %	143	85 (59.4%)	50 (35.0%)	8 (5.6%)	
CTRL, tot Age, yrs. median (range)	323	63 (31-86)	61 (28-85)	64 (52-75)	*P*=0.9

Table 18. Demographic features of PMF (at the time of diagnosis) and CTRL, stratified according to the rs1024611 SNP of *CCL2*. (A/A= wild type; A/G= heterozygous; G/G homozygous). Statistically significant correlations are highlighted in **bold**.

Then we analysed PMF and CTRL population according to gender and age (Table 18). When both overall PMF and CTRL population were stratified by gender, genotype frequencies in PMF males (n. 247) were as follows: 247/464 (53.2%) were A/A, 174/464 (37.5%) were A/G and 43/464 (9.3%) were G/G. Genotype frequencies in PMF females were as follows: 183/309 (59.2%) were A/A, 112/309 (36.2%) were A/G and 14/309 (4.5%) were G/G. Control males were 101/180 (56.2%) A/A, 72/180 (40%) A/G and 7/180 (3.9%) G/G. Control females were 85/143 (59.4%) A/A, 50/143 (35%) A/G and 8/143 (5.6%) G/G. Interestingly, the number of subjects carrying a homozygous genotype was significantly higher in PMF males *vs*. CTRL males (OR, 2.52, 95% CI, 1.11-5.72, *P*=0.022), suggesting that G/G male subjects have a higher risk of developing PMF as compare to A/A+A/G.

Moreover, G/G genotype was associated with the male gender in PMF. Indeed, G/G subjects were significantly higher in the PMF male cohort (43/464, 9.3%) as compared to the PMF female cohort (14/309, 4.5%, OR = 2.15, 95% CI, 1.15–4.00, *P* =0.014); G-allele frequency was significantly higher as well (28% vs. 22.7%, OR = 1.33, 95% CI, 1.05–1.68, *P* =0.02).

On the contrary, we did not observe any differences in the distribution of genotype and allelic frequencies among the PMF- and CTRL- female cohorts (Table 18). These data suggest a potential association between male gender and the rs1024611 G-allele variant, which could impact the risk of developing a PMF.

The analysis of genotypic and allelic frequencies of both PMF and CTRL cohorts, stratified by age at the time of diagnosis, revealed that PMF patients were relatively younger than CTRL (median age 50.7 years, range 6-83). Nevertheless, PMF patients carrying two copies of the G-allele were slightly older (median 54.4 years, range 18-83) as compared to A/A and A/G PMF patients (median 50.4 years, range 6-81, *P* =0.048, Table 16). This result is in line with previous findings by Barosi and co-workers, who demonstrated that older age (≥52 years) correlates with a higher inflammatory burden and a phenotype of severe disease (Barosi et al., 2017).

3. Homozygosity for the rs1024611 SNP of *CCL2* represents an independent prognostic factor for survival PMF

			Genotypic frequencies			***P* value**
	N. of cases evaluated	**All patients**	**A/A**	**A/G**	**G/G**	**G/G *vs.* A/A+A/G**
Clinical and haematological characteristics						
Hb mean (range), g/dL	768	12.7 (3.0-22.0)	12.9 (4.0-22.0)	12.6 (3.0-22.0)	12.6 (5.0-20.0)	0.71
Pts. with Hb <10 g/dL N. (%)	768	142 (18.5)	78 (54.9)	50 (35.2)	14 (9.9)	0.22
WBC* mean (range), $x10^9$/L	761	10.0 (1.8-64.3)	9.9 (1.9-64.3)	10.2 (1.8-45.4)	10.2 (2.6-50.9)	0.81
Pts. with WBC >12$x10^9$/L N. (%)	761	172 (22.6)	91 (52.9)	69 (40.1)	12 (7)	0.77
PLT mean (range), $x10^9$/L	764	509 (21-2926)	523 (22-2926)	488 (21-2000)	508 (37-1783)	0.98
Pts. with PLT <150 $x10^9$/L, N. (%)ù	764	113 (14.8)	56 (49.6)	46 (40.7)	11 (9.7)	0.29
Spleen index** mean (range), cm^2	761	151.0 (70-1200)	150 (70-850)	154 (89-1200)	143 (90-486)	0.57
Pts. with spleen index** >150 cm^2 N. (%)	761	213 (28.0)	110 (51.6)	86 (40.4)	17 (8)	0.75
LDH mean (range), mU/mL, x ULN	429	1.66 (0.19-8.48)	1.58 (0.41-8.48)	1.70 (0.19-7.60)	2.02 (0.67-7.38)	0.07
PB $CD34^+$ cells mean (range), $x10^6$/L	355	64.0 (0.4-1601)	53.9 (0.4-1152)	83.1 (0.9-1601)	64.8 (0.4-1601)	0.71
Inflammatory biomarkers						
hs-CRP mean (range), ng/mL	222	0.70 (0.01-12.6)	0.68 (0.01-12.6)	0.74 (0.02-7.9)	0.75 (0.02-4.38)	0.90
Pts. with hs-CRP >0.3 ng/mL N. (%)	222	88 (39.6)	52 (59.1)	27 (30.7)	9 (10.2)	0.05

Table 19. Clinical and laboratory parameters of PMF patients at the time of diagnosis stratified according to the rs1024611 SNP of *CCL2*. (A/A=wild type; A/G=heterozygous; G/G=homozygous). a) White-blood cell count (WBC) was normalized to the total number of circulating erythroblasts, b) Spleen index is the product of the longitudinal by the transverse spleen axis, the latter defined as the maximal width of the organ. Abbreviations: Hb: hemoglobin, hs-CRP: high-sensitivity C reactive protein, LDH: Lactate dehydrogenase, PB: peripheral blood; PLT: Platelet count, Pts: patients, WBC: white blood cell count.

Focusing of PMF patients, we evaluated whether G-allele variant of *CCL2* could impact disease phenotype at the time of diagnosis. We adopted a recessive model to compare G/G PMF to the other genotypes, A/A+G/G. We performed a genotype-phenotype correlation study, considering clinical and hematological parameters such as hemoglobin levels (Hb), white blood cell count (WBC), platelet count (PLT), spleen index, lactate dehydrogenase levels (LDH) and percentage of circulating blasts ($CD34^+$ cells). The baseline characteristics of the 773 patients, who were included in the current study, were listed in Table 19.

The results showed no genotype-phenotype association comparing baseline clinical and hematological characteristic of G/G PMF vs. A/A+A/G PMF patients (Table 19). Moreover, no significant association were found between homozygousity for the SNP and bone marrow fibrosis, but we found that the frequency of the G allele was significantly higher in patients with fibrosis grading ≥ 2 (196/680 alleles, 28.8%) *vs*. < 2 (203/856 alleles, 23.7%, P=0.023), suggesting a correlation between the G allele and the overt-PMF subtype. Overall, these data suggest that PMF patients homozygous for the rs1024611 SNP of *CCL2* display clinical parameters comparable to those of heterozygous and wild type PMF patients at the time of diagnosis.

We then investigated whether the homozygosity for the SNP might affect the disease outcome, evaluating whether G/G PMF have a significant higher risk to incur into: (i) massive splenomegaly (≥10 cm below costal margin), severe anemia (Hb < 100 g/L) or leukocytosis (WBC ≥ 12 × 10^9/L); (ii) blast transformation (defined as “bone marrow blast count of ≥20% or peripheral blood blast content of ≥20% associated with an absolute blast count of ≥1 × 10^9/L that lasts for at least 2 weeks” according to the International Working Group-Myeloproliferative Neoplasms Research and Treatment (IWG-MRT) criteria (Mesa et al., 2007); (iii) death for any causes (defined as overall survival). According to the recessive genetic model, the hazard ratio (HR) to develop massive splenomegaly, anemia, or leukocytosis or to incur into blast transformation in the homozygous PMF *vs*. heterozygous and wild type PMF was not significantly different (HR, 1.31, *P* =0.183; HR, 1.03, P =0.927; HR, 1.19, *P* =0.438 and HR, 1.07, *P* =0.849, respectively).

Moreover, in order to test whether the *CCL2* variant might affect the disease progression, we analysed the risk of incurring into death for any causes, and the composite endpoint which included time to death for any causes, progression to blast transformation or allotransplant, whatever occurred first (PMF fatality endpoints).

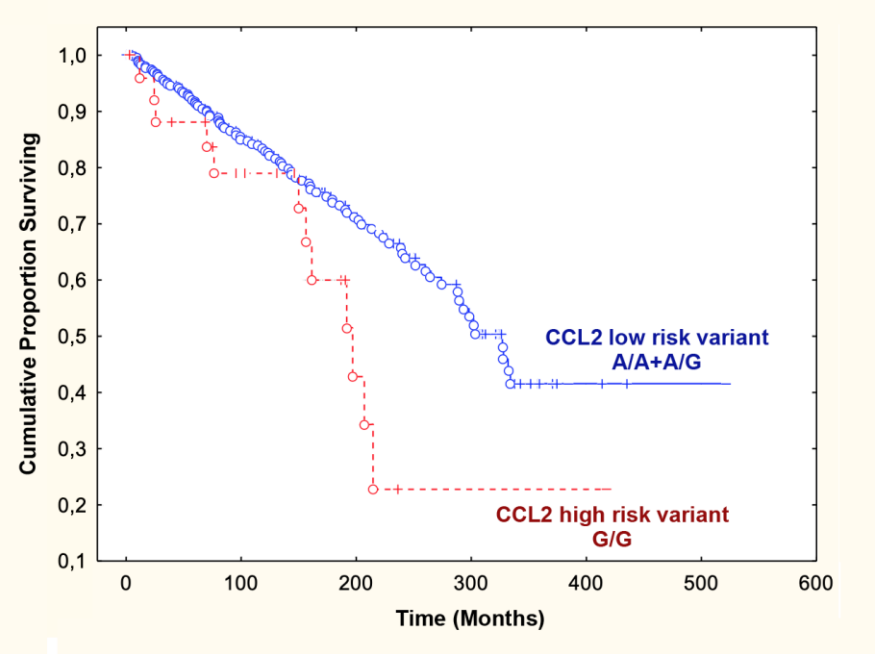

Figure 50. Overall survival of PMF patients stratified according to the rs1024611 SNP of *CCL2*. Cumulative survival (Kaplan Meier) estimates during follow-up of 773 genotyped PMF, stratified into *CCL2* high-risk variant group (G/G) and CCL2 low-risk variant group (A/A+A/G). G/G PMF patients were represented in red, while A/A+A/G PMF patients were represented in blue (*, *P*= 0.032).

Of note, G/G PMF showed a significantly reduced overall survival (in terms of time to death and time to fatality endpoint) as compared to the other genotypes (HR, 1.69, 95% CI, 1.05–2.70; *P* =0.032, Figure 50).

Furthermore, we tested the prognostic accuracy of the G/G high risk variant in predicting patient survival, comparing it with other well-established clinical prognostic biomarkers included in the IPSS scoring system, such as: age >65 years, constitutional symptoms Hb <100g/L, WBC >25x10^9/L and peripheral blasts ≥1) (Table 20).

We found the GG genotype for the rs1024611 SNP of *CCL2* showed a significant correlation in both univariate and multivariate analysis (Table 20), suggesting that homozygosity for the rs1024611 SNP could represent an independent prognostic factor to predict survival in PMF.

		Univariate analysis		Multivariate analysis	
Variable	**N. at risk**	**HR (95% CI)**	**P**	**HR (95% CI)**	**P**
Age (diagnosis) > 65 yrs	122	6.66 (4.76-10)	<0.001	4.11 (3.03-8.25)	<0.001
Constitutional symptoms	154	5.88 (4.16-8.33)	<0.001	2.60 (1.75-3.85)	<0.001
Hb < 100 g/L	142	4.54 (3.83-6.25)	<0.001	2.19 1.85-4.00)	<0.001
WBC > 25 x10^9/L	28	5.00 (2.70-9.09)	<0.001	3.88 (1.82-5.66)	<0.001
Peripheral blasts ≥1	68	5.55 (3.45-9.09)	<0.001	3.17 (1.76-5.69)	<0.001
***CCL2 rs1024611* G/G genotype**	57	1.69 (1.05-2.70)	0.032	1.65 (1.01-2.70)	0.039

Table 20. Univariate and multivariate analysis of prognostic factors for overall survival in PMF. Analysis was performed in 773 PMF and it included IPSS parameters and homozygosis for the rs1024611 SNP of *CCL2*. Abbreviations: Hb: hemoglobin, WBC: white blood cell count.

Finally, to exclude the correlation of the G/G genotype with the presence of prognostically detrimental mutated genes, which could impact on overall survival; we evaluated the mutational profile of PMF patients by PCR and NGS.

Mutational profile included driver mutations in *JAK2*, *MPL* and *CALR*, which are involved in the neoplastic clone expansion and contribute to adverse disease phenotype; and the so called "high risk mutations" (*ASXL1, EZH2, SRSF2* and *IDH1*/2), known to have a detrimental impact on disease progression and outcome (Table 21).

Of note, the cohort of G/G patients was not significantly enriched in adverse molecular features, such as driver mutations, triple-negativity or HMR mutations (Table 21), suggesting that the effect of the homozygosity for the *CCL2* SNP on patient survival is not correlated with patient mutational profile.

	N. of cases evaluated	All patients	Genotypic frequency			*P* value
			A/A	A/G	G/G	G/G *vs.* A/A+A/G
Mutations						
*JAK2*V617F positive N. (%)	757	500 (66.0)	277 (55.4)	185 (37.0)	38 (7.6)	0.77
*JAK2*V617F negative N. (%)		257 (34.0)	142 (55.3)	97 (37.7)	18 (7.0)	0.77
*JAK2*V617F positive, heterozygous N. (%)	500	306 (61.2)	174 (56.9)	109 (35.6)	23 (7.5)	1
*JAK2*V617F positive, homozygous N. (%)		194 (38.8)	103 (54.1)	76 (39.2)	15 (7.7)	1
CALR positive (type 1 or 2) N. (%)	762	157 (20.6)	85 (54.1)	60 (38.2)	12 (7.7)	0.87
CALR negative N. (%)		605 (79.4)	337 (55.7)	224 (37.0)	44 (7.3)	0.87
*MPL*W515 positive N. (%)	761	42 (5.5)	25 (59.5)	16 (38.1)	1 (2.4)	0.20
*MPL*W515 negative N. (%)		719 (94.5)	396 (55.1)	268 (37.3)	55 (7.6)	0.20
Triple-negative N. (%)	757	61 (8.1)	34 (55.7)	22 (36.1)	5 (8.2)	0.80
Non triple-negative N. (%)		696 (91.9)	385 (51.0)	260 (34.3)	51 (6.7)	0.80
≥ HMR category* N. (%)	225	50 (22.2)	26 (52.0)	17 (34.0)	7 (14.0)	0.39
Non-HMR category* N. (%)		175 (77.8)	107 (61.1)	51 (29.1)	17 (9.8)	0.39

Table 21. Mutational profile of PMF patients at the time of diagnosis according to the rs1024611 SNP genotype. (A/A=wild type; A/G=heterozygous; G/G=homozygous), * Defined as presence of at least one mutated gene among *ASXL1, EZH2, SRSF2, IDH1/2.*

4. Homozygosity for the rs1024611 SNP of *CCL2* impact on CCL2 production in PMF.

Given the clinical impact of the G/G genotype on PMF patient survival, we sought to investigate the functional role of the rs1024611 SNP of *CCL2* in PMF cells. Peripheral blood MNCs were purified from n.27 PMF patients and n.17 HD used as controls, to assess basal CCL2 expression at both mRNA and protein levels.

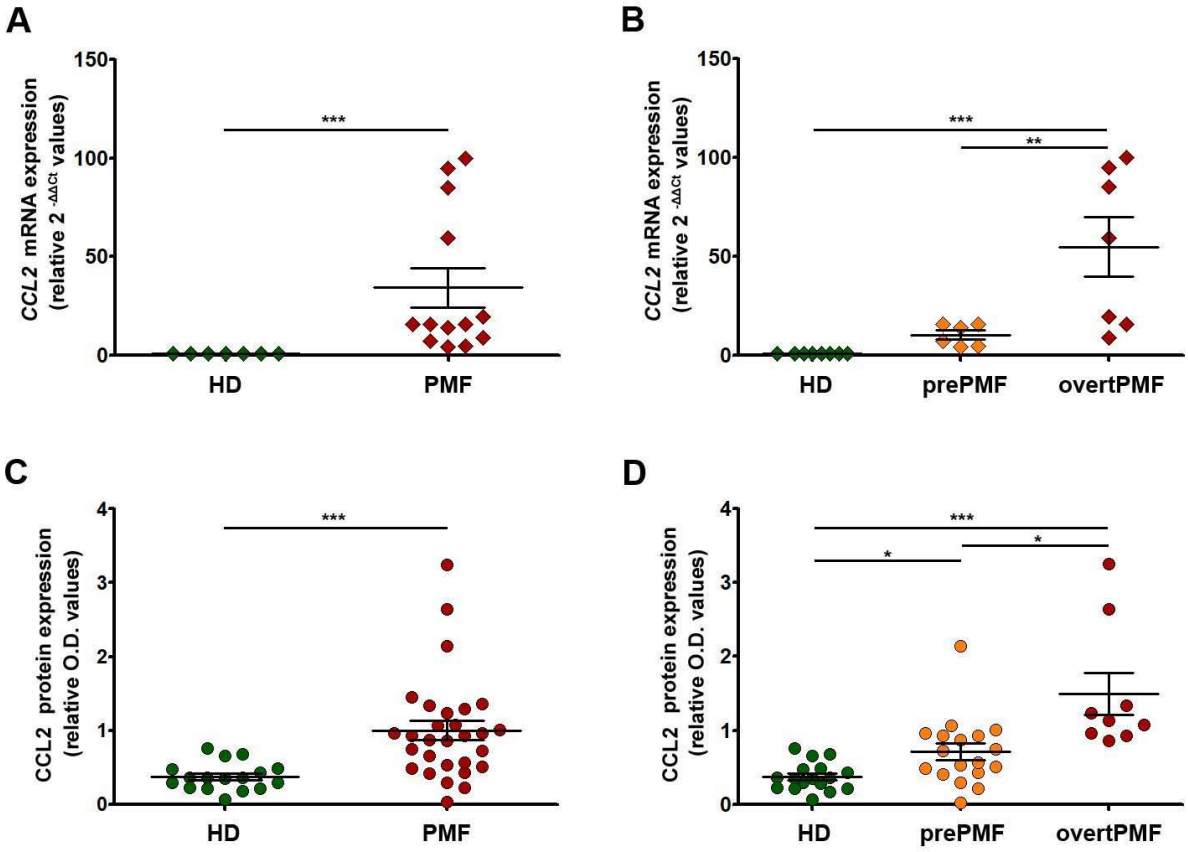

Figure 51. Basal CCL2 expression (mRNA and protein) in MNCs from HD and PMF patients. A) *CCL2* mRNA expression in MNCs obtained from HD (n.8) and PMF patients (n.13). B) *CCL2* mRNA expression in MNCs obtained from HD (n.8) and PMF patients, stratified in prePMF (n.6) and overtPMF (n.7). *CCL2* mRNA levels are normalized to *GAPDH* mRNA levels and showed as fold change vs. HD. Data are expressed as mean ± SEM. (** $P < 0.01$, *** $P < 0.001$ by Mann-Whitney test (A), and Kruskal-Wallis followed by Dunn's test (B)). C) CCL2 protein expression in MNCs obtained from HD (n.17) and PMF patients (n.29). D) CCL2 protein expression in MNCs obtained from HD (n.17) and PMF patients, stratified in prePMF (n.18) and overtPMF (n.9). CCL2 protein levels are normalized to GAPDH protein levels (the loading control). Data are expressed as mean ± SEM. (** $P < 0.01$, *** $P < 0.001$ by Mann-Whitney test (C), and Kruskal-Wallis followed by Dunn's test (D)).

As shown in figure 51, basal mRNA (panel A) and protein levels of CCL2 (panel C) are significantly higher in MNCs from PMF patients as compared to HD (P=0.0003 and P <0.0001 by Mann-Whitney test, respectively, Figure 51, panels A, C). These results are in line with data by Tefferi et al. on CCL2 serum levels (Tefferi et al., 2011). Moreover, if we focused on PMF and we stratified

patients according to grading of bone marrow fibrosis, overtPMF patients show the highest levels of CCL2 (both mRNA and protein), significantly overexpressing the chemokine as compared to HD (*P*<0.001, Figure 51, panel B) and prePMF (*P*<0.01, Figure 51, panel D).

We then stratified PMF according their genotype in A/A (wild type), A/G (heterozygous for the SNP) and G/G (homozygous for the SNP) patients. MNCs were seeded and stimulated *ex vivo* with 1.1 ng/mL of IL-1β (*Rovin et al., 1999*), and CCL2 expression (mRNA and protein) was assessed after 20h of incubation (Figure 52).

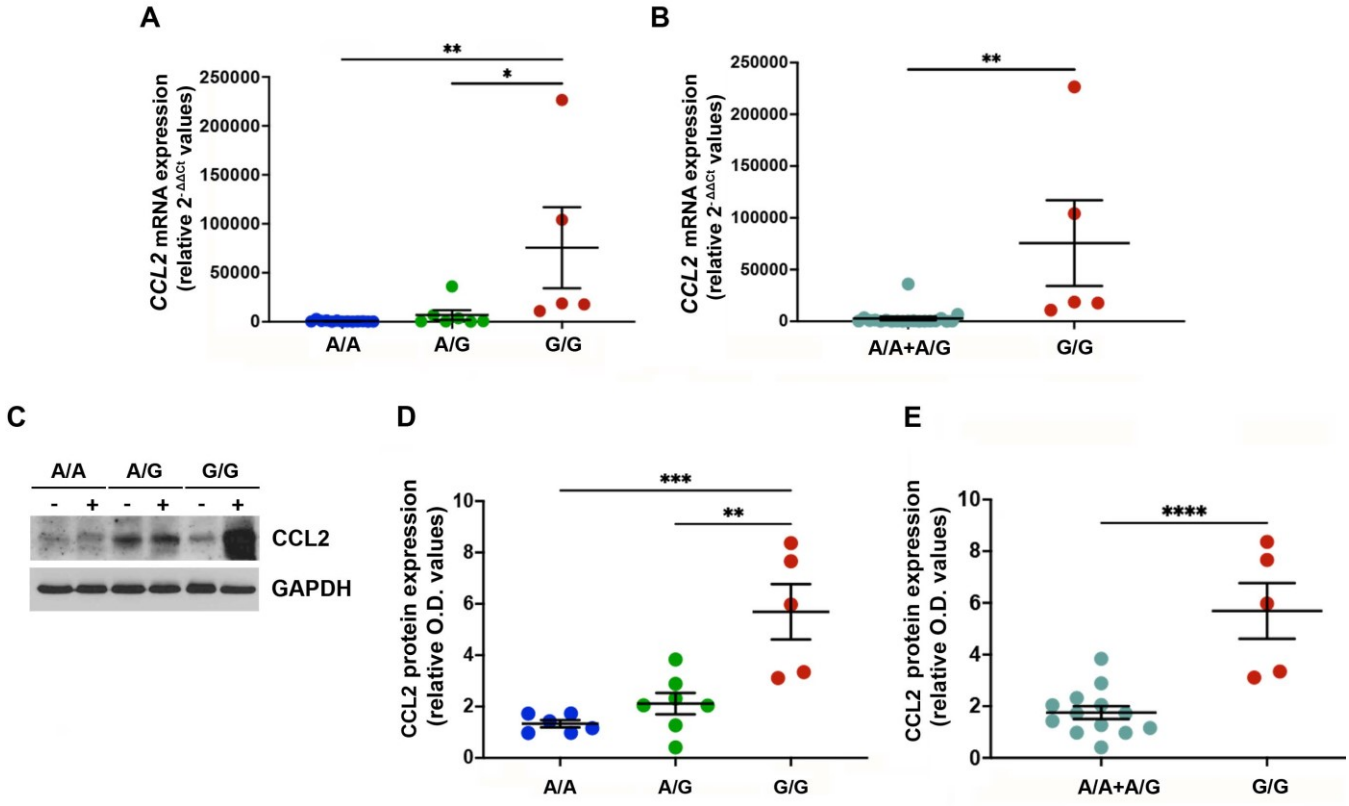

Figure 52. CCL2 expression (mRNA and protein) by MNCs from PMF patients according to the rs1024611 SNP. A-B) *CCL2* mRNA expression upon *ex vivo* IL1-β stimulation of MNCs from PMF patients, stratified according to the rs1024611 genotype: A/A (n. 13) vs. A/G (n. 7) vs. G/G (n.5) (A); and A/A + A/G (n. 20) vs. G/G (n. 5) (B). *CCL2* mRNA levels, normalized to *GAPDH*, are showed as fold change of samples upon IL1-β stimulation (+) vs. basal state (-). Data are expressed as mean ± SEM (* *P* < 0.05, ** *P* < 0.01 by one-way ANOVA, followed by Tukey test (A) or Mann-Whitney test (B)). C) Representative blot showing CCL2 protein expression in MNCs from A/A, A/G and G/G PMF, at basal state (−) and upon IL1-β stimulation (+). D, E) CCL2 protein expression upon *ex vivo* IL1-β stimulation of MNCs from PMF patients stratified according to the rs1024611 genotype: A/A, n. 6 vs. A/G, n. 7 vs. G/G, n.5 (D) and A/A + A/G, n. 13 vs. G/G n. 5 (E). CCL2 protein expression is normalized to GAPDH and showed as fold change of the expression upon IL1-β stimulation (+) vs. basal state (-). Data are expressed as mean ± SEM (** *P*< 0.01, *** *P* < 0.001 by ANOVA followed by Tukey test (D) or Mann-Whitney (E)).

Interestingly, we observe a "dose-dependent effect" of the rs1024611 SNP on CCL2 expression. Indeed, patients carrying two copies of the G allele are the highest producers of the chemokine: G/G PMF patients significantly overexpress *CCL2* mRNA (relative $2^{-\Delta\Delta CT}$ values: 75,564.1 ±

41,453.6) (Figure 52, panel A) and protein (relative O.D. values: 5.69 ± 1.08) (Figure 52, panels C, D) as compared to A/A (relative 2−ΔΔCT values: 571.1 ± 213.6, P< 0.01; relative O.D. values: 1.33 ± 0.14, *P*< 0.001) and A/G (relative 2−ΔΔCT values: 6,770.2 ± 4,964.9, *P*< 0.05; relative O.D. values: 2.11 ± 0.41, *P*< 0.01) genotypes (Figure 52, panels A, C, D). Furthermore, analysing data with the same recessive genetic model used for genotype-phenotype correlation, we observe that PMF belonging to the high-risk group (G/G patients) significantly overexpress *CCL2* mRNA and protein as compared to the low-risk group (A/A+A/G patients) (Figure 52, panels B, E). These results suggest G/G PMF as “the highest chemokine-producer” in PMF.

5. CCL2 expression is downmodulated by ruxolitinib

We then evaluated the effects of ruxolitinib, an anti-inflammatory and immunomodulatory drug widely used for PMF therapy, on CCL2 expression. As mentioned above, MNCs were isolated from n.6 PMF before (T0) and after 1, 3 and 9 months of ruxolitinib therapy (T1, T2 and T3). MNCs were seeded and *ex vivo* stimulated with 1,1ng/ml of IL1-β for 20 h and CCL2 expression was assessed at both mRNA and protein levels.

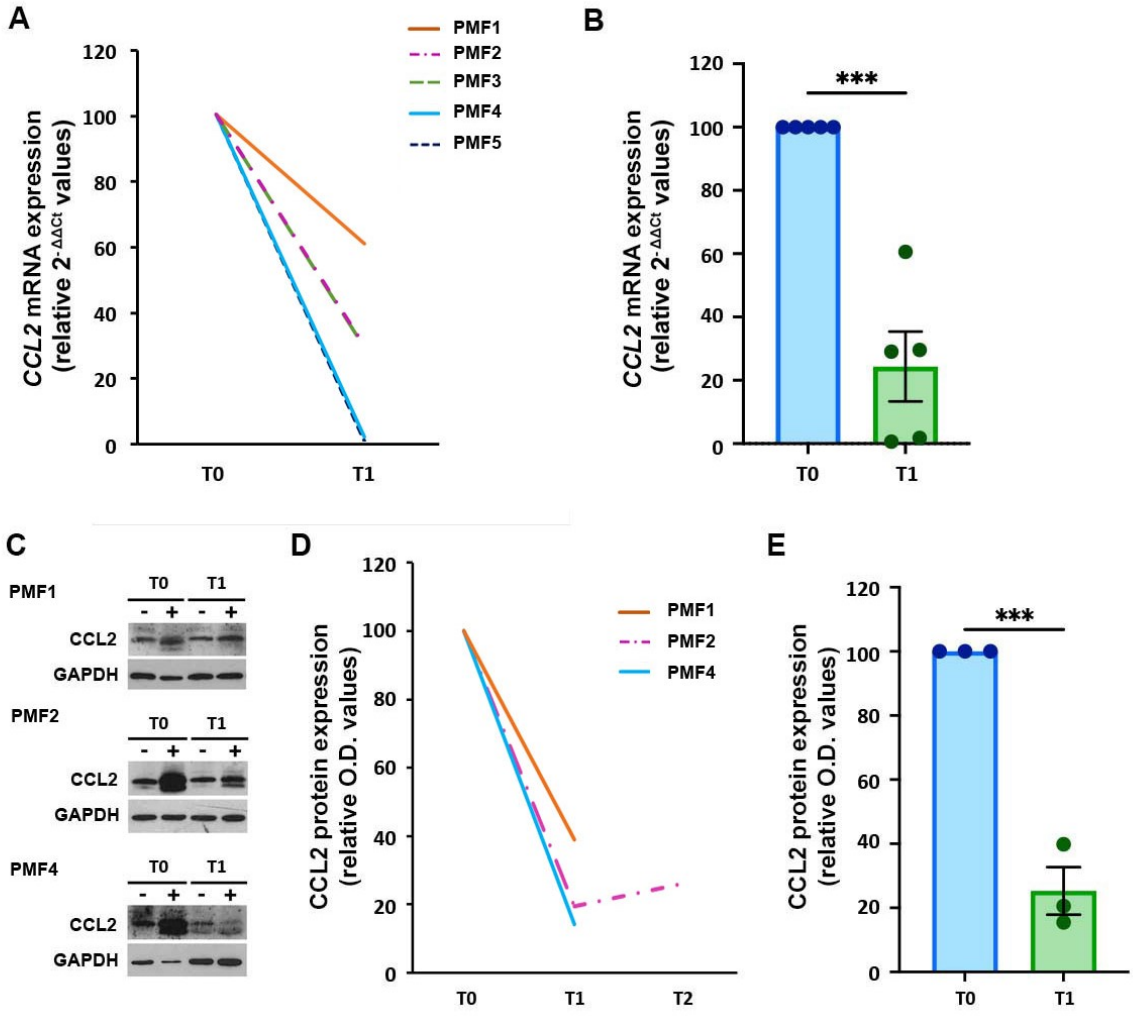

Figure 53. Effects of ruxolitinib on CCL2 expression. A) Fold-decrease curves of *CCL2* mRNA levels after *ex vivo* IL1-β stimulation of MNCs obtained from PMF (n.4) patients before (T0) and after 1 month (T1) of ruxolitinib therapy. T0 values are set as reference. B) *CCL2* mRNA levels analysis. Data are normalized to T0 and expressed as mean ± SEM (*** *P*< 0.001, by t-test). C) Representative blots obtained from patients PMF16.43, PMF20.6, and PMF20.0, showing CCL2 protein expression in MNCs at basal state (−) and upon IL1-β stimulation (+), before (T0) and after 1 month of ruxolitinib (T1). D) Fold-decrease curves of CCL2 protein expression after *ex vivo* IL1-β stimulation of MNCs obtained from PMF (n.3) patients before (T0) and after 1 (T1) and 3 months (T2) of ruxolitinib therapy. T0 values are set as reference E) CCL2 protein expression analysis. Data are normalized to T0 and expressed ad mean ± SEM (*** *P*< 0.001, by t-test).

Interestingly, ruxolitinib drastically reduced MNCs capacity to express CCL2 after pro-inflammatory stimulation (Figure 53). Indeed, MNCs of patients on therapy with ruxolitinib showed a significantly reduced expression of CCL2 at both mRNA and protein levels as compared to T0 upon IL1-β stimulation (Figure 53, panels A, C). The statistical analysis revealed that, after only one month of therapy, MNCs capacity to produce CCL2 is significantly reduced by approximately 80% (P<0.001 Figure 53, panels B, E).

Moreover, stratifying patients according to the rs1024611 genotype, ruxolitinib effects are more evident in homozygous patients; indeed G/G PMF patients are the ones who show the most marked reduction in CCL2 expression (both mRNA and protein levels) on ruxolitinib therapy (Figure 54, panels A, B). Although it was not possible to perform a statistical analysis due to the very small sample size, it appears that homozygous group are the most sensitive patients to immunomodulatory drugs.

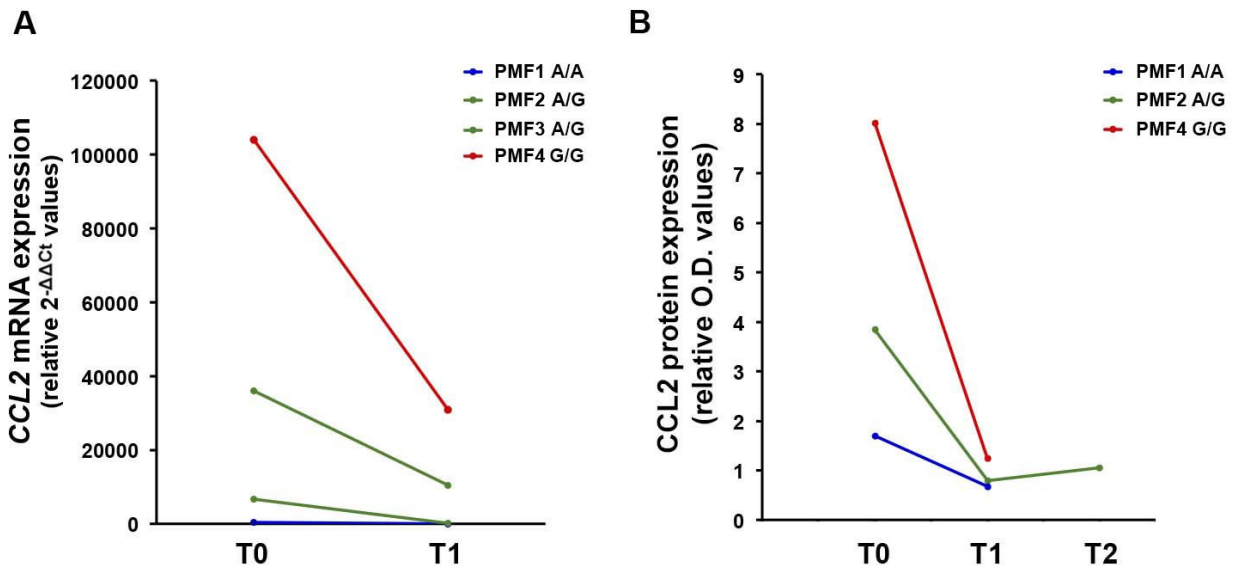

Figure 54. Ruxolitinib effects on CCL2 expression in PMF cells according to the rs1024611 genotype. A) Fold-decrease curves (2-[(CT CCL2-CT GAPDH)IL1-β − (CT CCL2-CT GAPDH)untr, relative $2^{-\Delta\Delta CT}$ values) of *CCL2* mRNA expression upon *ex-vivo* IL1-β stimulation of MNCs from 4 PMF patients before (T0) and after 1 month (T1) of ruxolitinib therapy, stratified according to the rs1024611 genotype. B) Fold-decrease curves [(O.D.CCL2/O.D.GAPDH)IL-1β/[(O.D.CCL2/O.D.GAPDH)UNTR, relative western blot optical density (O.D.) values] of CCL2 protein expression upon *ex-vivo* IL1-β stimulation of MNCs from 3 PMF patients before (T0) and after 1 (T1) and 3 month (T2) of ruxolitinib therapy, stratified according to the rs1024611 genotype.

Results 2: The role of CCL2/CCR2 chemokine system in PMF

*From Masselli E, Carubbi C, **Pozzi G**, Percesepe A, Campanelli R, Villani L, Gobbi G, Bonomini S, Roti G, Rosti V, Massa M, Barosi G, Vitale M. Impact of the rs1024611 Polymorphism of CCL2 on the Pathophysiology and Outcome of Primary Myelofibrosis. Cancers (Basel). 2021 May 22;13(11):2552.*
DOI: 10.3390/cancers13112552

1. Biological and clinical parameters of MPN and control populations

For this project, CCR2 expression was evaluated in 10 HD, 20 ET, 16 PV, 22 PMF of which 13 prePMF and 9 overtPMF. Biological, clinical, and histopathological characteristics of patients and control subjects at the time of sample collection are summarized in table 22.

Considering the PMF cohort, 11 out of 22 PMF patients (50%) were males, with a median age of 72 years (range, 37-84 years). Bone marrow biopsy at the time of the sampling was availablefor all patients: PMF patients were classified in pre-fibrotic myelofibrosis (prePMF) (n. 13, 59.1%) and overt-fibrotic myelofibrosis (overtPMF) (n.9, 40.9%), according to the WHO classification. Stratifying patients according to the DIPSS, n. 6 (27%) had a low-risk score, n. 9 (41%) had an intermediate-1 risk score, n. 5 (23%) had an intermediate-2 risk score, and n.2 (9%) had a high-risk score. Driver mutations were evaluated in 19 (86.4%) patients and occurred as follows: 12 (63%) harbored *JAK2*V617F mutation, 6 (31%) harbored *CALR* mutations (type 1 and 2), no patients had *MPL*W515 mutation, and 1 (6%) was triple negative. HMR mutations were evaluated by next-generation sequencing (NGS) in 4 out of 22 PMF patients (n.2 prePMF, n. 2 overtPMF). *ASXL1* mutation was identified in n. 3 patients (2 prePMF and 1 overtPMF) (Table 22).

Concerning ET population, 7 out of 20 ET were males (35 %) with a median age of 54 years (range 18-83 years). Driver mutations were evaluated in all patients and occurred as follows: 11 (55%) harbored *JAK2*V617F mutation, 3 (15%) harbored *CALR* mutations (type 1 and 2), 1 (5%) had *MPL*W515 mutation, and 5 (25%) were triple negative. Data on HMR mutations are available only in 2 patients and no HMR mutations were found.

In PV population, 9 out of 16 CTRL were males (56,2 %) with a median age of 64 years (range 36-85 years). All PV patients (100 %) harbored *JAK2*V617F mutation.

As we expected, median Hb values were significantly lower in overtPMF patients (Hb:11g/dL, range 7-13) as compared to other MPN categories, as expected (PV Hb:14g/dl, range 12-16; ET 13.2g/dl, range 10.8-15; prePMF Hb:12g/dl, range 8-15). Leucocytosis was observed only in overtPMF (median WBC:11x10^9/L, range 3.6-35); all MPN categories displayed higher platelet count (PV PLTs:564x10^9/L, range 178-1460; ET PLTs:728x109/L, range 416-1386; prePMF PLTs:522x10^9/L, range 97-961; overtPMF PLTs:421x10^9/L, range 117-663). The majority of the patients did not show constitutional symptoms (only in 4 PV, 2 ET and 6 PMF) and major thrombotic events were rare, occurring in approximately one-third of PV (as expected) and overtPMF.

	HD	PV	ET	MF	prePMF	overtPMF
Number of cases	10	16	20	22	13	9
Age, y median range	 39 (22-60)	 64 (36-85)	 54 (18-83)	 66 (37-84)	 65 (41-83)	 68 (37-84)
Gender Male, N (%) Female, N (%)	 9 (90) 1 (10)	 9 (56.2) 7 (43.8)	 7 (35) 13 (65)	 11 (50) 11 (50)	 6 (46) 7 (54)	 5 (56) 4 (44)
Hb, g/dl median range	/	 14 (12-16)	 13.2 (10.8-15)	 11.5 (7.1-15.2)	 12 (8-15.2)	 11 (7.1-13)
WBC, x 10^9/L median range	/	 9.2 (2.9-35.9)	 7.7 (5.15-10.8)	 9.5 (3.6-35)	 8.5 (3.7-19.8)	 11 (3.6-35)
PLT, x 10^9/L median range	/	 564 (178-1460)	 728 (416-1386)	 496 (97-961)	 522 (97-961)	 421 (117-663)
Constitutional symptoms Yes, N (%) No, N (%)	/	 4 (25) 12 (75)	 2 (10) 18 (90)	 6 (27) 16 (73)	 4 (31) 9 (69)	 2 (22) 7 (78)
Major thrombotic events Yes, N (%) No, N (%)	/	 5 (31) 11 (69)	 2 (10) 18 (90)	 5 (23) 17 (77)	 2 (15) 11 (85)	 3 (33) 6 (67)
DIPSS score Low, n (%) Intermediate-1, n (%) Intemediate-2, n (%) High, n (%)	/	/ / / /	/ / / /	6 (27) 9 (41) 5 (23) 2 (9)	 4 (31) 5 (38) 3 (23) 1 (8)	 2 (22) 4 (44) 2 (22) 1 (11)
Spleen (cm long. Ø) median range	/	 10 (9-14)	 11 (9-15.4)	 15.1 (9-30)	 14.8 (9-30)	 15.4 (10-25)
***JAK2*V617F^{pos}, N (%)**	/	16 (100)	11 (55)	12 (63)	7 (64)	5 (56)
***CALR*^{pos}, N (%)**	/	/	3 (15)	6 (31)	4 (36)	2 (22)
***MPL*^{pos}, N (%)**	/	/	1 (5)	0 (0)	0 (0)	0 (0)
Triple negative, N (%)	/	/	5 (25)	1 (6)	0 (0)	1 (11)
Therapy **Hydroxyurea,** N (%) **Ruxolitinib,** N (%) **Other,** N (%)	 / / /	 7 (47) 3 (20) 5 (33)	 8 (40) / 12 (60)	 10 (46) 6 (27) 6 (27)	 4 (31) 4 (31) 5 (38)	 6 (67) 2 (22) 1 (11)

Table 22. Biological and clinical characteristics of PV, ET, PMF and control populations. Spleen index is the product of the longitudinal by the transverse spleen axis, the latter defined as the maximal width of the organ. Abbreviations: Hb: hemoglobin, N: number; PLT: Platelet count, yrs: years; WBC: white blood cell count.

Concerning cytoreductive therapy, n. 7 PV (47%), n. 8 ET (40%), n. 4 prePMF (31%), n. 6 overtPMF (67%) were under hydroxyurea, Ruxolitinib was considered a second line treatment for n. 3 PV patients (20%) and a first-choice treatment for n. 6 PMF, of which n. 4 prePMF (31%) and n. 2 overtPMF (22%).

Moreover, 9 out of 10 (90%) healthy subjects (leukoapheresis donors) were male, with a median age of 39 years (range 22-60 years). HDs were significantly younger as compared to MPN patients (HD: 39 years, range 22-60 years, *vs.* MPN: 63 years, range 18-90 years) (Table 22).

2. CCR2 is exclusively expressed by PMF hematopoietic stem cells

Given the results on CCL2 expression in MNCs of PMF, we investigated whether hematopoietic stem cells, identified as CD34 positive cells ($CD34^+$ cells), could represent cell target of CCL2, evaluating expression of CCR2, the main CCL2 receptor, on $CD34^+$ cell membrane. We compared CCR2 expression on PMF $CD34^+$ cells to CCR2 expression on $CD34^+$ cells from other MPNs (PV/ET), healthy donors (HD) and *JAK2*V617F-positive HEL cells (Figure 55).

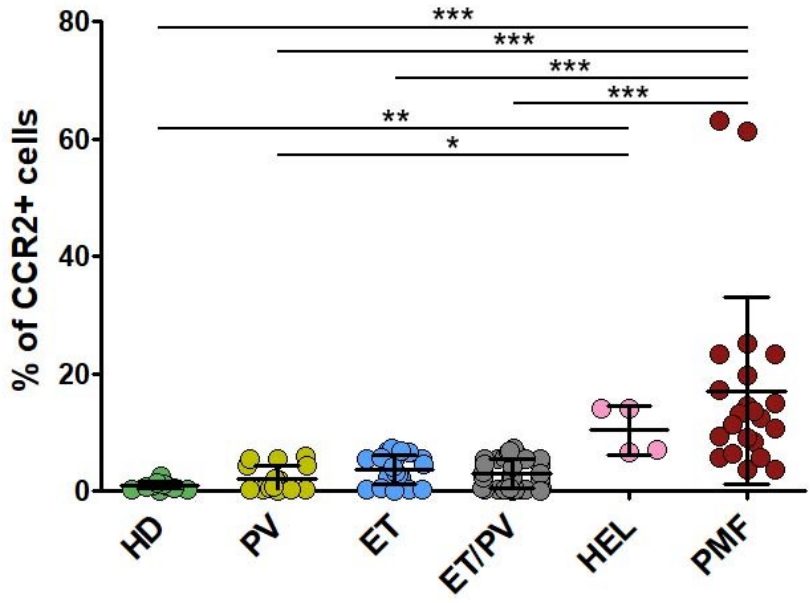

Figure 55. CCR2 expression on normal and MPN CD34+ cells. CCR2 expression in CD34+ cells isolated from cells from HD (n.10), PMF (n.22), ET (n.20), PV (n.16), and on *JAK2*V617Fpos HEL cells (n.4 experiments). In HD, PMF, ET and PV the percentage of $CD34^+CCR2^+$ cells was normalized to the percentage of total $CD34^+$ cells. Data are showed as mean ± SD (* $P < 0.05$, ** $P < 0.01$, *** $P < 0.001$ by Kruskal Wallis followed by Dunn's test).

As showed in figure 55, the percentage of $CD34^+CCR2^+$ cells is >20 fold-higher in PMF as compared to HD, in which, by contrast, it is virtually absent (% of $CD34^+CCR2^+$ cells: 0.82±0.70 in HD *vs.* 17.03±15.88 in PMF, *** $P < 0.001$; Figure 55). Furthermore, $CD34^+$ cells from ET and PV show a poor expression of CCR2, which is comparable to HD, and significantly lower than PMF, suggesting that CCR2 expression is an exclusive feature of PMF $CD34^+$ cells (% of $CD34^+CCR2^+$ cells: 0.82±0.70 in HD *vs*. 3.61±2.46 in ET *vs*. 2.00±2.23 in PV *vs*. 17.03±15.88 in PMF, *** $P < 0.001$ only *vs.* PMF). When grouping PV and ET together, the difference in CCR2 expression on $CD34^+$ cells remains statistically significant *vs.* PMF (2.89±2.43 in ET/PV *vs*. 17.03±15.88 in PMF, *** $P < 0.001$). HEL cells, which mimic PMF blasts, show an intermediate CCR2 expression between PMF and ET/PV.

We then stratified PMF patients according to the degree of bone marrow fibrosis in prePMF (with

fibrosis grading 0-1) *vs.* overtPMF (with fibrosis grading ≥ 2). $CD34^+$ cells from overtPMF significantly overexpress (2-times higher) CCR2 as compared to prePMF (% of CD34+/CCR2+ cells: 25.9±24.2 *vs*. 11.2 ± 7.1, respectively, *P*=0.02, Figure 56).

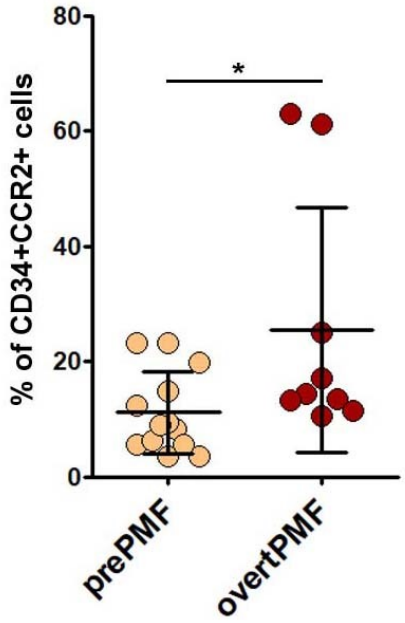

Figure 56. Percentage of CD34+CCR2+ cells in PMF according to grading of bone marrow fibrosis. CCR2 expression evaluated by flow cytometry: percentage of CCR2 positive cells on immunomagnetically isolated $CD34^+$ cells from prePMF patients with fibrosis grading 0-1 (n. 13) and overtPMF patients with fibrosis grading ≥2 (n. 9). The percentages of CD34+CCR2+ cells were normalized to the percentages of total CD34+ cells. Data are showed as mean ± SD (*, *P*<0.05 by Mann Whitney test).

We subsequently wondered whether a pro-inflammatory environment could induce CCR2 expression in a MPN neoplastic clone and in *JAK2*V617Fpos HEL and/or whether CCR2 expression was regulated by an autocrine loop.

Therefore, we evaluated CCR2 expression by flow cytometry in n.3 representative ET/PV cases (one ET carrying *CALR* type II mutation, one ET carrying *JAK2*V617F mutation and one PV carrying *JAK2*V617F) after 48 hours of culture in serum-free X-vivo medium supplemented with IL-3, SCF and TPO alone or in combination with: (1) rhCCL2 100 ng/mL; (2) IL-1β 1.1 ng/mL and TNFα 10 ng/mL; (3) rhCCL2, IL-1β and TNFα. CCR2 expression was also evaluated by flow cytometry in HEL cells cultured up to 48 hours in RPMI medium in the same experimental conditions.

As shown in figure 57, CCR2 is not induced by with IL-1β and TNFα, in presence and absence of rhCCL2, in both MPN $CD34^+$ and HEL cells.

Overall, these data indicate that CCR2 overexpression (and therefore chemokine susceptibility), is a unique characteristic of MF hematopoietic progenitors, and its expression is not triggered by proinflammatory milieu. Moreover, CCR2 expression correlates with the degree of bone marrow fibrosis.

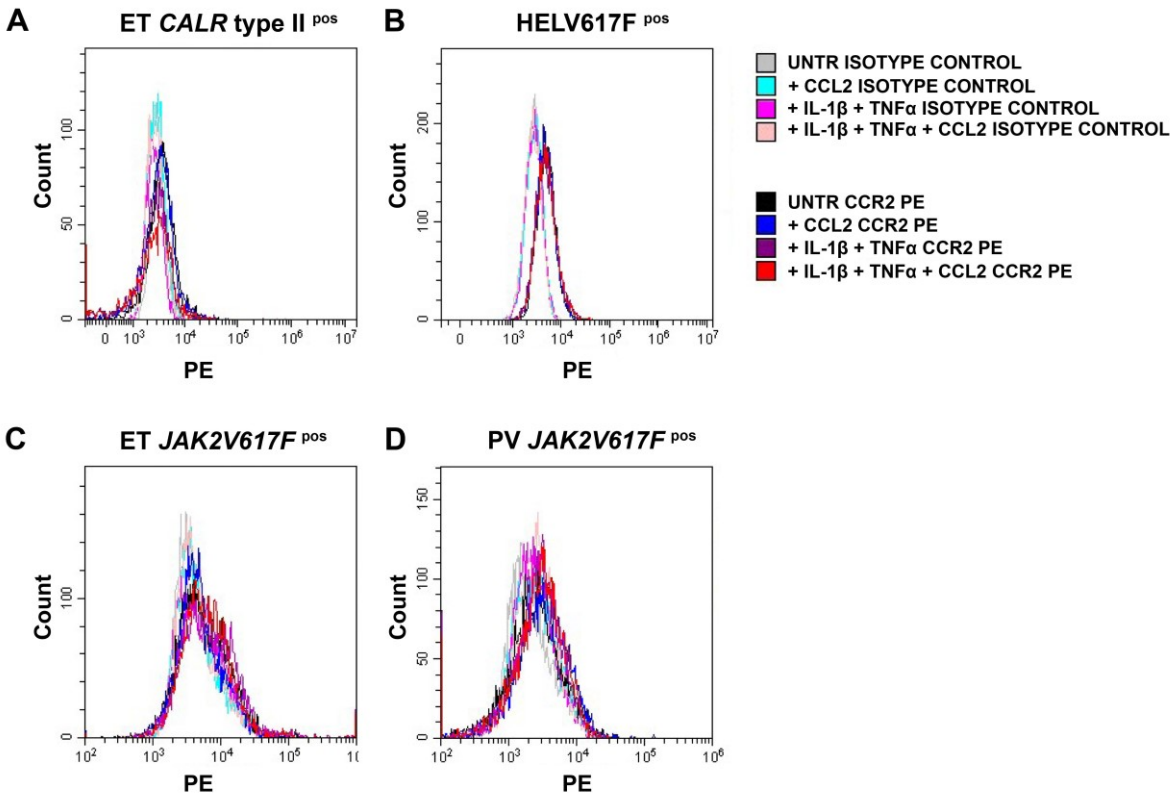

Figure 57. FCM analysis of CCR2 expression in CD34+ cells and HEL cell line stimulated with IL-1β, TNFα and rhCCL2. A) CCR2 expression in CD34+ cells from one *CALR* typeII^{pos} ET patient, B) *JAK2V617F*^{pos} HEL cells, C) one *JAK2V617F*^{pos} ET patient, D) one *JAK2V617F*^{pos} PV patient before (UNTR) and after stimulation with: (i) rhCCL2 100 ng/mL; (ii) IL-1β 1.1 ng/mL and TNFα 10 ng/mL; (iii) rhCCL2, IL-1β and TNFα rhCCL2. Histograms of CCL2-PE and IgG-PE (isotype-control) specific fluorescence are reported.

3. CCL2/CCR2 binding induces the activation of Akt signaling pathway in CD34⁺ cells of PMF

Given the peculiar expression of CCR2 on PMF CD34⁺ cells, we investigated which signal pathway could be activated by CCL2/CCR2 binding. Primary CD34⁺ cells were isolated from PMF (n. 7) and HD (n.3) and seeded in serum-free X-vivo medium with and without 100 ng/mL of rhCCL2. After 24h of incubation, we analysed JAK/STAT, Akt and MAP-kinase pathways, which are known to regulate cell proliferation and differentiation, and to play a key role in MPNs pathophysiology. Primary CD34⁺ cells from HD, who do not express CCR2, were exposed to the same experimental conditions and used as control.

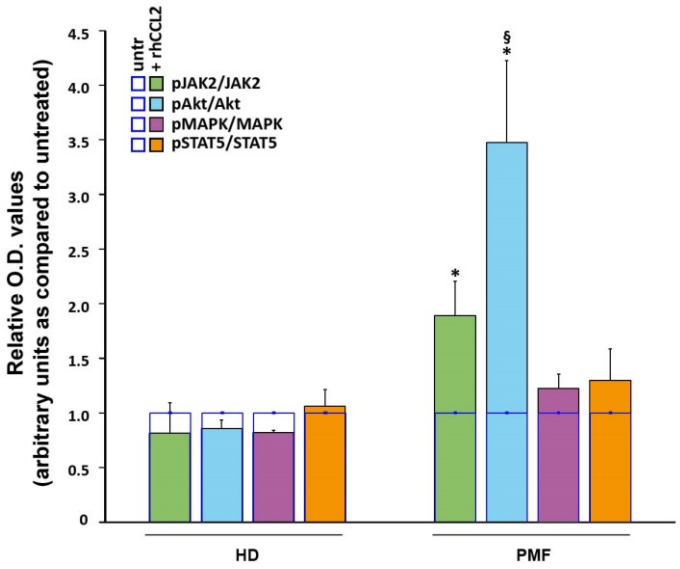

Figure 58. Analysis of signal transduction pathways activated by CCL2/CCR2 axis in CD34+ cells of PMF and HD. CD34+ cells from HD (n. 3) and PMF (n. 7) were incubated with 100ng/mL of rhccl2 for 24h and then analysed for protein expression. Relative JAK2/GAPDH, pJAK2/GAPDH, Akt/GAPDH, pAkt/GAPDH, MAPK/GAPDH, pMAPK/GAPDH, STAT5/GAPDH and pSTAT5/GAPDH O.D. values were first determined, and then phosphorylated/total protein ratio was calculated. Untreated samples were represented as blue histograms. Data are showed for both HD and PMF as arbitrary units of untreated samples (mean ± SEM, * vs. PMF untr, § vs. HD pAkt/Akt, $P < 0.05$ by t-test).

As we expected, CCR2-negative CD34⁺ cells from HD do not display CCL2-mediated activation of JAK/STAT, Akt or MAP-kinase pathways, since phosphorylated/total protein ratios are comparable in presence and absence of rhCCL2. Of note, when PMF CD34⁺ cells were stimulated with rhCCL2 *ex vivo*, a significant phosphorylation of JAK2 and Akt was detected. Indeed, pAkt/Akt and pJAK2/JAK2 protein ratio are significantly higher in PMF CD34⁺ cells treated with rhCCL2 as compared to PMF CD34⁺ untreated cells (* vs. PMF untr, $P < 0.05$ by t-test, Figure 58). Moreover, pAkt/Akt protein ratio is significantly higher in stimulated CD34⁺ cells from PMF as compared to stimulated CD34⁺ cells from HD (§ vs. HD pAkt/Akt, $P < 0.05$ by t-test) (Figure 58).

4. Ruxolitinib significantly reduces CCR2 expression on CD34⁺ cells in PMF

Finally, we evaluated the effects of ruxolitinib on CCR2 expression on PMF CD34⁺ cells. Primary CD34⁺ cells were isolated from n.6 PMF before (T0) and after one, three and nine months of ruxolitinib therapy (T1=1 month, T2=3 months and T3=9 months) and CCR2 expression was assessed immediately after cell purification.

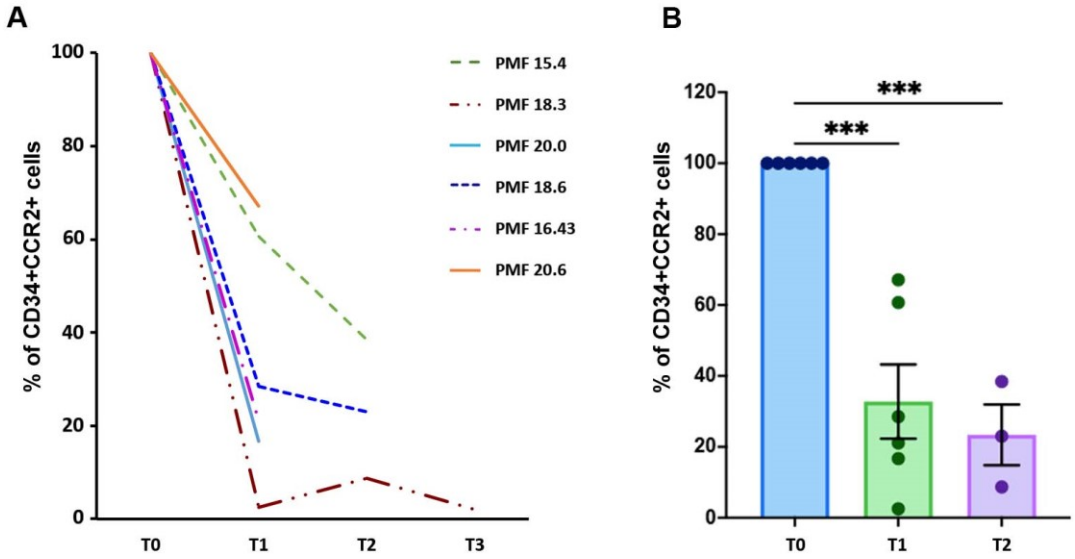

Figure 59. Effects of ruxolitinib therapy on CCR2 expression in CD34⁺ cells from PMF. A) Fold-decrease curves of CCR2 expression assessed by flow cytometry (% of positive cells) on immunomagnetically isolated CD34⁺ cells from PMF (n.6) before (T0) and after 1 (T1), 3 (T2) and 9 (T3) months of ruxolitinib. T0 values are set as reference. B) Percentage of CD34⁺CCR2⁺ (normalized on the percentage of total CD34⁺ cells) cells after 1 (T1) and 3 months (T2) of ruxolitinib therapy in 6 PMF. Data are expressed as mean ± SEM as compared to T0 (*** $P < 0.001$ by one-way ANOVA followed by Tukey test).

Flow cytometry analysis revealed that ruxolitinib induces a significant reduction of the surface expression of CCR2; indeed, the inhibition of CCL2 receptor is stable and persist until 3 months (>60% of reduction at T1 and >70% of reduction at T2, $P < 0.001$ vs. T0 in both cases) (Figure 59, panels A, B). Together with data on CCL2 expression, these results indicate that ruxolitinib therapy can stably inhibit the CCL2/CCR2 chemokine system in PMF.

5. Diagnostic accuracy of CCR2-expressing hematopoietic progenitors in discriminating trueET *vs.* prePMF and prePMF *vs.* overtPMF

Diagnosis of PMF is based on the 2016 WHO-criteria and the composite assessment of clinical, histopathological, genetic and laboratory parameters. Bone marrow biopsy currently represents the key diagnostic procedure to discriminate among MPN entities. However, the traditional grading systems are semi-quantitative, and suffer from some limitations related to subjectivity and heterogeneity of samples. Moreover, in some cases morphological differential diagnosis is problematic and ambiguous also for expert pathologists. For instance, the diagnosis between prePMF and true-ET is often critical, as the two diseases frequently share the same clinical presentation and mutational profile. Although similar at the disease onset, ET patients usually show a milder phenotype, while prePMF patients have a higher risk of blast transformation and a reduced survival (Vainchenker et al, 2017). Moreover, prePMF an overtPMF represent two different pathological entities, indeed overtPMF is typified by adverse clinical and molecular features and thus considered a more aggressive disease subtype (Nazha et al., 2013; Lekovic et al., 2014).

Given the peculiar expression of CCR2 in PMF, and the correlation with bone marrow fibrosis, we asked whether flow cytometry evaluation of percentage of $CD34^{+}CCR2^{+}$ cells could be used as diagnostic tool in support of bone marrow biopsy histopathological analysis for the differential diagnosis of MPN subtypes.

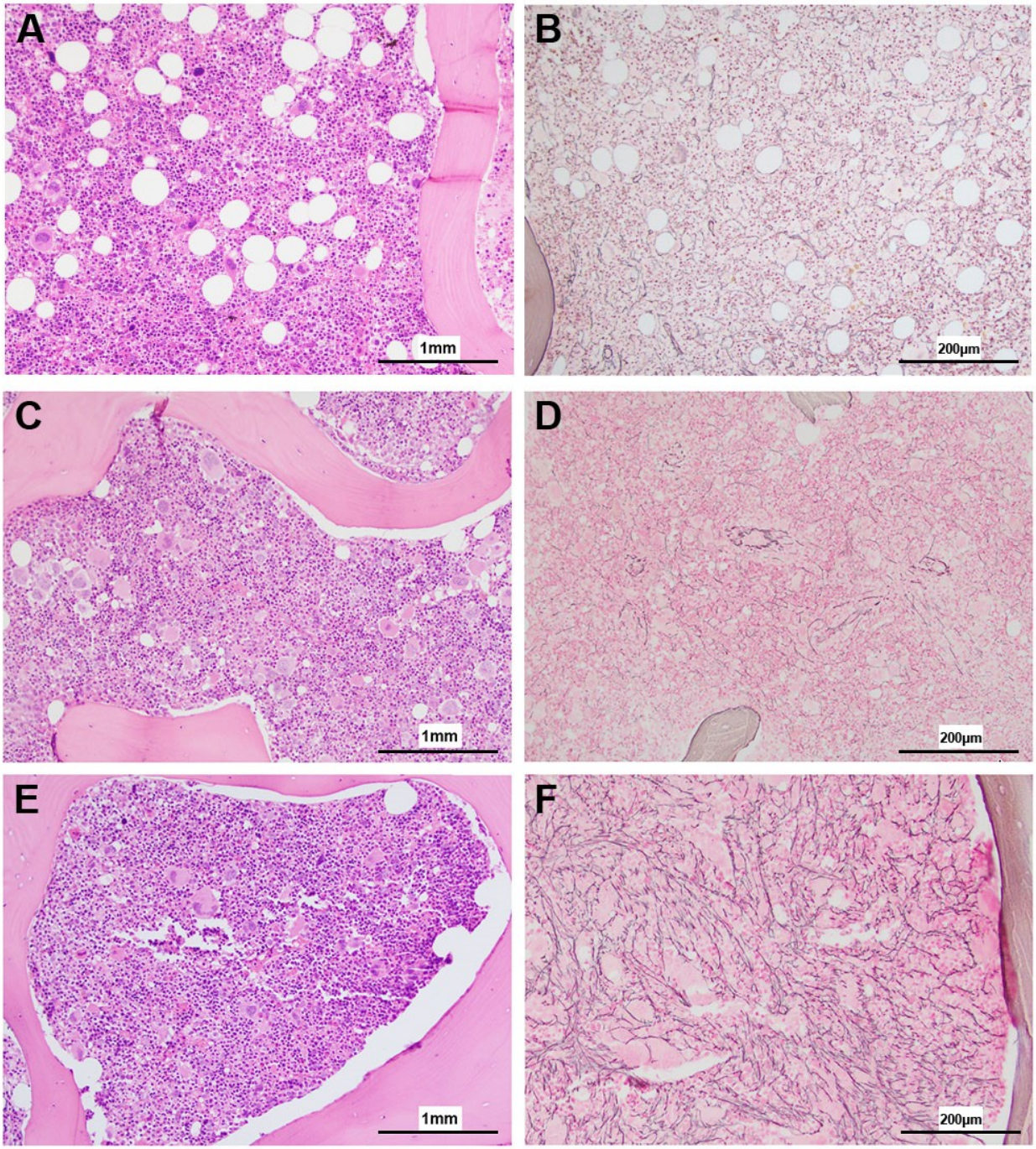

Figure 60. Bone marrow histopathological analysis of trueET, prePMF and overtPMF. A-F) BM histopathology in representative trueET (A, B), prePMF (C, D) and overtPMF patients (E, F). Scale bar = 1 mm (A, C, E) and scale bar = 200µm (B, D, F). (A, C, E) Hematoxylin-Eosin staining. (B, D, F) reticulin staining.

In this context, we focused on CCR2 expression in ET, prePMF and overtPMF. Figure 60 and figure 61 report the bone marrow histopathological analysis and dot plots obtained by flow cytometry assay of a representative true-ET, prePMF and overtPMF patients, respectively.

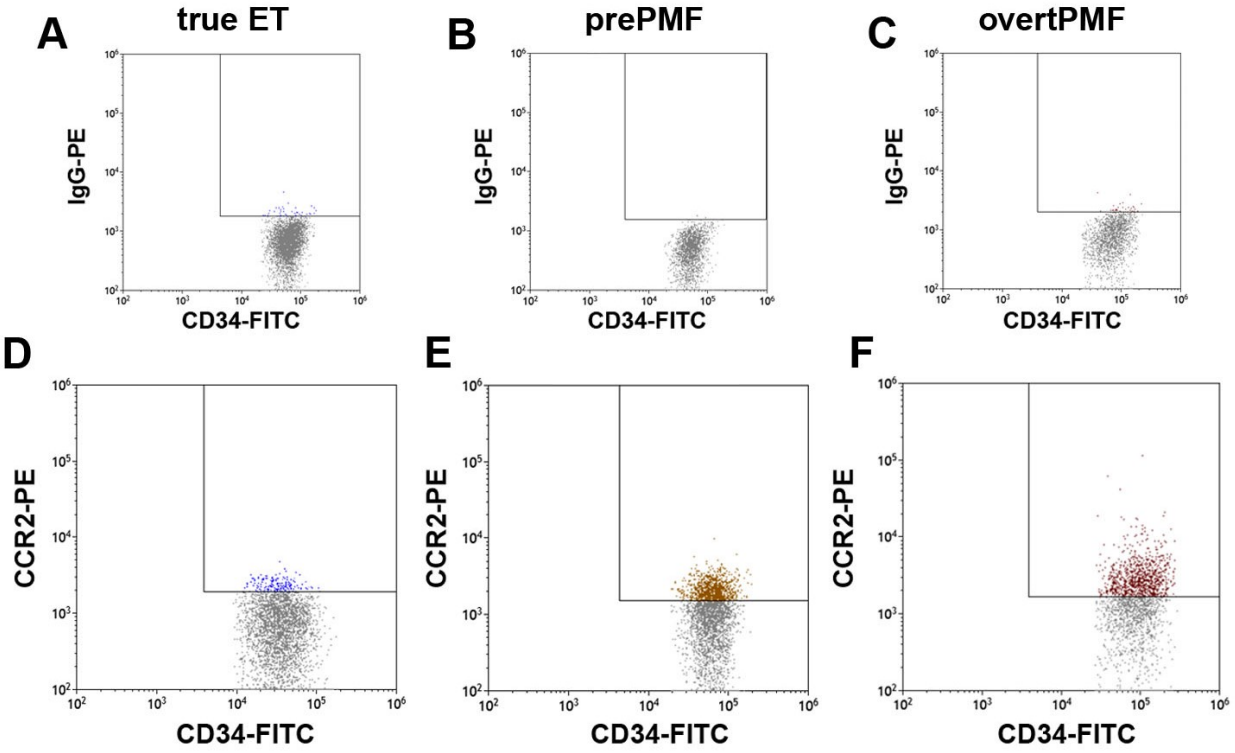

Figure 61. Flow cytometry detection of CCR2-expressing CD34⁺ cells in trueET, prePMF and overtPMF. CCR2 evaluation on CD34⁺ cells by flow cytometry in a representative trueET (A, D), prePMF (B, E) and overtPMF patients (C, F). A-C) Dot plots representative for true ET, a preMF and an overtPMF isotype controls (CD34⁺IgG-PE⁺/CD34⁺ cells). D-F) Dot plots showing the percentages of CD34⁺CCR2⁺/CD34⁺ cells (4.49%, 9.33% and 61.32% in trueET, prePMF and overtPMF, respectively).

As previously described, the percentage of CCR2-expressing CD34⁺ cells is significantly higher in prePMF as compared to ET (Figure 61, panels D, E; Figure 62, panel A). Therefore, we applied the receiver-operating characteristic (ROC) curve analysis of flow cytometry evaluation of CCR2-expressing CD34⁺ cells to measure diagnostic accuracy of the test and calculate the optimal cut-off value (Figure 62, panels B, C).

The ROC curve shows an area under the curve (AUC) of 0.8769 [CI of 95%: 0.7563–0.9976] (*P*=0.0003) (Figure 62, panels B, C). The assay showed an optimal cut-off value of 5.595 with a specificity of 80% and a sensitivity of 84.62%, a positive predictive value (PPV) of 69.2% and a negative predictive value (NPV) of 80% (Figure 62, panel C). These data indicate that the flow cytometry evaluation of CD34⁺CCR2⁺ has very good diagnostic accuracy (Haley et al., 1982) in discriminating true-ET from prePMF.

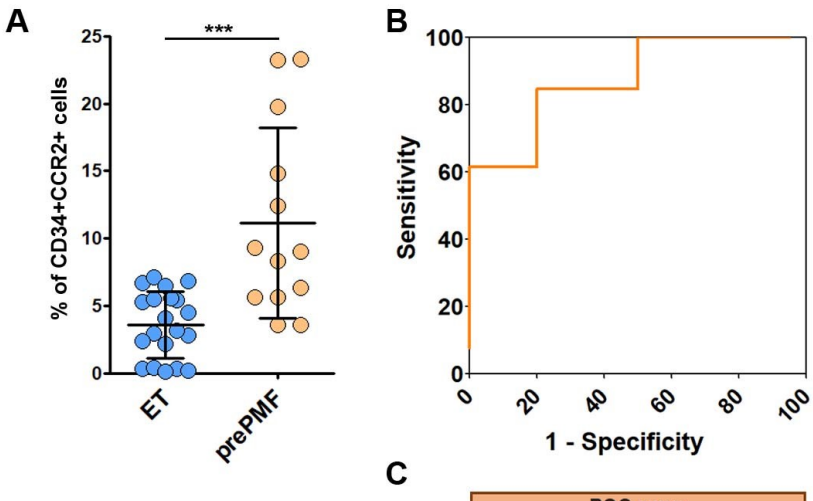

C

ROC curve	
AUC [95% C.I.]	0.8769 [0.7563-0.9976]
P value	0.0003
Cut-off	5.595
Sensitivity	84.62%
Specificity	80%
PPV	69.2%
NPV	80%

Figure 62. Diagnostic accuracy of flow cytometry evaluation of CCR2 expression on CD34+ cells in ET *vs*. prePMF. A) Scatter plot showing the percentage of $CD34^+CCR2^+/CD34^+$ cells in ET (N=22) and prePMF (N=15). Data are showed as single percentage and mean ± SD ($P<0.001$, Mann-Whitney test). B) ROC curve of FCM analysis of $CD34^+CCR2^+/CD34^+$ cells in ET and prePMF patients. C) Summary table reporting: Area under the curve (AUC), confidential interval (CI), P value (P), cut-off value, sensitivity, specificity, positive predictive value (PPV) and negative predictive value (NPV) of FCM detection of $CD34^+CCR2^+/CD34^+$ cells in ET *vs.* prePMF.

Moreover, we asked whether the flow cytometry evaluation of CCR2 on $CD34^+$ cells could be effective also in distinguishing PMF subtypes, verifying the diagnostic accuracy of CCR2-expressing CD34+ in discriminating prePMF *vs*. overtPMF.

As previously shown, overtPMF patients report a significantly higher expression of CCR2 as compared to prePMF ($P=0.02$) (Figure 61, panels E, F; Figure 63, panel A). The receiver-operating characteristic (ROC) curve analysis shows an area under the curve (AUC) of 0.7863 [CI of 95%: 0.5928–0.9798] ($P=0.02533$) (Figure 63, panels B, C).

The FCM assay showed an optimal cut-off value of 9.970 with a specificity of 61.4% and a sensitivity of 100%, a positive predictive value (PPV) of 64.3% and a negative predictive value (NPV) of 100% (Figure 63, panel C). These data indicate that the flow cytometry evaluation of $CD34^+CCR2^+$ has good diagnostic accuracy (Haley et al., 1982) in discriminating prePMF from overtPMF.

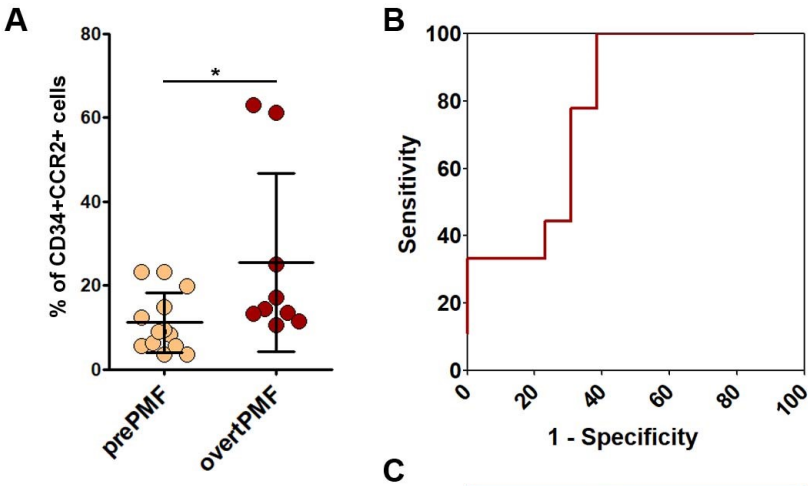

C

ROC curve	
AUC [95% C.I.]	0.7863 [0.5928-0.9798]
P value	0.02533
Cut-off	9.970
Sensitivity	100%
Specificity	61.4%
PPV	64.3%
NPV	100%

Figure 63. Diagnostic accuracy of flow cytometry evaluation of CCR2 expression on CD34+ cells in ET *vs*. prePMF. A) Scatter plot showing the percentage of $CD34^+CCR2^+/CD34^+$ cells in prePMF (N=13) and overtPMF (N=9). Data are showed as single percentage and mean ± SD (*P*=0.02, Mann-Whitney test). B) ROC curve of FCM analysis of $CD34^+CCR2^+/CD34^+$ cells in prePMF and overtPMF patients. C) Summary table reporting: Area under the curve (AUC), confidential interval (CI), P value (P), cut-off value, sensitivity, specificity, positive predictive value (PPV) and negative predictive value (NPV) of FCM detection of $CD34^+CCR2^+/CD34^+$ cells in prePMF *vs.* overtPMF.

Discussion

PMF is the most aggressive myeloproliferative neoplasm (MPNs), with a complex and multifactorial pathogenesis. It is considered a “classic” multistage clonal disorder triggered by somatic mutations, defined driver mutations, which confer a proliferative advantage to a multipotent hematopoietic stem cell defective for MK differentiation. However, PMF mutational landscape is extremely complex, and disease phenotype is generally the result of the combination of several genetic events. In this context, evidence from epidemiological and familial studies (Rumi et al., 2007) strongly suggest that genetic predisposition, such host genetic variants or single nucleotide polymorphisms (SNPs), may influence not only the disease onset but also the evolution. Host genetic variants in cytokine/chemokine genes have recently emerged. MPNs, especially PMF, are considered the paradigm of “onco-inflammation” disorders.

Chronic inflammation contributes to both local (bone marrow fibrosis) and systemic (constitutional symptoms, thrombosis) complications (Hasselbach, 2013; Jutzi and Mullally 2020). Moreover, inflammation, fueled by the neoplastic clone, exacerbates tumor genetic instability, generating a permissive milieu for clonal expansion in a self-perpetuating vicious cycle defined by Hasselbalch as “the human inflammation model for cancer development” (Hasselbalch, 2013). Indeed, driver mutations constitutively activate the JAK/STAT pathway (Coffer et al., 2000), which is involved in the production of pro-inflammatory mediators. A number of studies have investigated bone marrow and circulating cytokines levels, as well as cytokine gene expression profile in MPNs (recently reviewed by Masselli et al., 2020), depicting MPN patients as “dysfunctional cytokine producers”. Among MPNs, PMF is characterized by the highest inflammatory burden and a peculiar “fibrogenic cytokine signature”. Indeed, pro-inflammatory and pro-fibrogenic cytokines/chemokines levels have been found significantly increased in plasma of PMF patients as compared to other MPNs and to healthy subjects (Panteli et al., 2005; Tefferi et al., 2011; Vaidya et al., 2012; Cacemiro et al., 2018; Wong et al., 2018). Elevated levels of some of these cytokines also correlated to PMF adverse phenotype and predicted therapy response (Pardanani et al., 2011).

In this context, host genetic variants in cytokines and chemokines genes contribute to explain the phenotypic pleiotropy and different clinical outcomes observed in patients who share the same somatic mutations (McMullin and Anderson, 2020). However, how these gene variants can predetermine the nature and extent of the host inflammatory response to the mutated clone and how they can affect the disease phenotype, clinical outcome or even therapy response, is still unclear.

Here, we investigate the role of CCL2 in PMF. CCL2 is one of the most potent pro-inflammatory and pro-fibrogenic chemokine, known to be elevated in plasma of PMF patients. CCL2 expression levels are highly variable among individuals, due to genetic variants, as SNPs, in the cis-regulatory regions of *CCL2* gene (McDermott et al., 2005).

Here, we focused on the rs1024611 SNP of *CCL2,* located within the enhancer sequence of the gene. The SNP rs1024611 consists of a substitution from A to G in position -2518, responsible for

the constitutively activation of the transcriptional activity of the gene and therefore for the increased expression of CCL2 by mononuclear cells upon inflammatory stimulus (Rovin et al., 1999). This SNP of *CCL2* has been widely investigated in pathological conditions typified by chronic inflammation and organ fibrosis (Colobran et al., 2007). We recently studied the rs1024611 SNP of *CCL2* in MPNs and we demonstrated that patients with post-PV/ET MF are enriched in polymorphic subjects, and its presence is associated with adverse clinical features (Masselli et al., 2018).

Here we investigate the contribution of this SNP to demographical, clinical, and biological characteristics as well as its impact on disease outcome, in a large cohort of 773 well-characterized PMF patients. Consistently with our previous data, genotype frequencies were in Hardy–Weinberg equilibrium both in PMF and CTRL cohorts (Masselli et al., 2018). Overall PMF population showed similar genotypic and allelic frequencies of control subjects. Therefore, we could assert that the rs1024611 SNP of CCL2 does not represent a major host predisposing factor for PMF. Interestingly, the number of subjects carrying a homozygous genotype was significantly higher in PMF males *vs*. PMF females and *vs*. CTRL males, suggesting that G/G genotype is associated with the male gender in PMF. These data indicate genetic background interplay between *CCL2* variants and gender. Indeed, the fact that the homozygosity for the SNP represents a host predisposing factor for PMF only in the male cohort could be due to a sex-related background that elicits (in males) or mitigates (in females) the effects of the SNP. In this context, the underlying mechanisms remain unclear, although sex chromosome complement/aberrations/aneuploidy, sex hormones, immune-competence, and gene expression may all be involved in gender discrepancies. Several studies have suggested that sexual dimorphism also occurs at the epigenetic level; indeed, sex may influence cell transcriptome, methylome and DNA accessibility, independently from the well-characterized phenomenon of X-chromosome inactivation (Shepherd et al., 2021).

Moreover, PMF patients carrying two copies of the G-allele (G/G) were slightly older as compared to A/A and A/G PMF patients. This result is consistent with the concept of “inflammageing” (Ferrucci and Fabbri, 2018); indeed older age is a condition associated with a chronic, low-grade, subclinical inflammatory state. Recently, Barosi and co-workers demonstrated that older age (≥52 years) correlates with a higher inflammatory burden and a phenotype of severe disease in PMF (Barosi et al., 2017).

Genotype-phenotype correlation revealed that G/G PMF displayed similar hematologic characteristics of A/A and A/G at the time of diagnosis. Moreover, the G/G cohort was not significantly enriched in adverse molecular features, such as the triple-negativity or HMR mutations. Of note, despite the same clinical phenotype at the time of disease onset, patients homozygous for the rs1024611 SNP showed a significantly reduced overall survival (in terms of time to death and time to fatality endpoint) as compared to the other genotypes. The univariate and

multivariate analyses demonstrated that the rs1024611 G/G genotype represents a high-risk variant and an independent prognostic factor for reduced survival in PMF.
Genotyping of PMF patients for the rs1024611 SNP of *CCL2* may configure as a novel biomarker to identify, at the time of diagnosis, those patients, with higher risk of unfavourable disease course and poor clinical outcome, who could benefit from close monitoring and personalized therapeutic strategies.

The main limitation of our approach is the lack of a validation cohort of PMF patients, to verify the prognostic accuracy of the rs1024611 SNP of CCL2. Further studies are required to confirm our results with an independent validation set of patients and to translate our results to daily clinical practice.

Given the clinical impact of the G/G genotype on PMF patient survival, we sought to investigate the functional role of the rs1024611 SNP of *CCL2* as well as the biological role CCL2/CCR2 chemokine system in PMF cells.
Firstly, we evaluated CCL2 basal expression levels in PMF patients, demonstrating, consistently with data by Tefferi's research group, that MNCs from PMF patients showed significant higher levels (both mRNA and protein) of CCL2 as compared to healthy subjects. In addition, overtPMF patients, characterized by a more severe disease, overexpressed the chemokine as compared to HD and prePMF.
Then, we investigated the effect of the rs1024611 SNP on CCL2 expression, and we demonstrated that G/G PMF patients are the highest CCL2 producers. Indeed, upon inflammatory stimulation G/G patients significantly overexpressed the chemokine as compared to the other genotypes, suggesting a "dose dependent" effect of the G allele on CCL2 expression. These results were consistent with data from Rovin and co-workers obtained from MNCs of healthy subjects (Rovin et al., 1999).
We then asked whether immunomodulatory therapy could interfere with the CCL2 expression, and we evaluated the capacity of producing CCL2 in response to pro-inflammatory stimulation in MNCs from patients before and after therapy with ruxolitinib. Ruxolitinib is a JAK1/2 inhibitor, which represents the first-line therapy for symptomatic intermediate- to high-risk MF patients, who are not eligible for hematopoietic stem cell transplantation. Ruxolitinib has demonstrated efficacy in reducing splenomegaly and the constitutional symptom burden, mainly acting on the disease-related cytokine storm (Cervantes et al., 2013; Harrison et al., 2016). Here, we demonstrated that ruxolinitib significantly reduceed MNCs capacity to express CCL2 upon IL1-β stimulation. Of note, G/G PMF patients appear the most sensitive patients to immunomodulatory therapy.
Then we asked whether hematopoietic stem cells could represent a putative target of CCL2. CCL2 exerts its biological functions by preferentially binding its cognate receptor CCR2. CCR2 is a G-

protein-coupled seven-transmembrane receptor, expressed on several cell types. The binding of CCL2 to CCR2 induces the activation of downstream cascades, which include G-proteins, MAPK/ERK, PI3K/Akt and JAK/STAT pathways (Haung et al., 2020). Abnormal activation of the CCL2/CCR2 chemokine system has been observed in different type of neoplastic cells as breast (Qian et al., 2011), prostate (Roca et al., 2008), colorectal (Chun et al., 2015), liver (Li et al., 2017), and pancreatic (Sanford et al., 2013) cancers. In these solid tumors, the activation of CCL2/CCR2 chemokine system promotes cancer cells to evade the immune system and regulates the initial stage of metastatic process, driving cell migration to secondary sites and boosting neoplastic cell invasion and neo-angiogenesis (Lim et al., 2016). Moreover, the CCL2/CCR2 axis has been widely described in fibrotic disorders including lung, liver and colon fibrosis, and others multi-organ fibrotic disease (Seki et al., 2009; Moore et al., 2001; Kuroda et al., 2019). However, little is known on the CCL2/CCR2 chemokine system in hematologic neoplasms. Therefore, we investigated this system in PMF, which is typified by chronic inflammation and bone marrow fibrosis.

We evaluated CCR2 expression by flow cytometry in primary hematopoietic progenitors ($CD34^+$ cells) from MPNs, healthy subjects and in HEL cell line. We found that PMF $CD34^+$ cells selectively overexpressed CCR2 as compared to HD, in which CCR2 is virtually absent. Moreover, CCR2 expression appears to be a peculiar feature of PMF hematopoietic progenitors, indeed PMF $CD34^+$ cells overexpressed the receptor as compared not only to HD but also to other MPN subtypes, such as ET and PV, which shared the same somatic mutations. HEL cells, which are widely considered a cell model of MF, displayed an intermediate expression of CCR2. Therefore, we demonstrate for the first time that CCR2 overexpression is a unique characteristic of PMF hematopoietic progenitors.

Interestingly, we here found that overtPMF significantly overexpress CCR2 as compared to prePMF, envisioning CCR2 expression on $CD34^+$ cells as a marker of bone marrow fibrosis (independently of rs1024611 SNP).

Moreover, we demonstrated that the pro-inflammatory cytokines and CCL2 itself are not capable of inducing CCR2 expression on primary CD34+ cells from PV/ET (carrying driver mutations) or in the *JAK2*V617Fpos HEL cell line. Despite the small sample size, CCR2 expression is not regulated by pro-inflammatory milieu or by an autocrine loop. We can speculate that other mechanisms could directly or indirectly act on CCR2 transcriptional regulation. The transcriptional activity of hCCR2 was modulated by clustered tissue-specific *cis*-regulatory elements, which include GATA consensus sequences (Yamamoto et al., 1999). Among the members of GATA transcription factors, GATA1 has been associated to several hematologic disorders typified by bone marrow fibrosis and altered MK differentiation (Migliaccio et al., 2005; Katsumare et al., 2017). GATA-1^{low} mice, which show a marked reduced GATA1 expression, development a progressive bone marrow fibrosis and a phenotype resembling human MF; thus, they are considered a well-established murine model of MF (Vannucchi et al., 2002; Vannucchi et al., 2005). Vannucchi and colleagues

demonstrated that megakaryocytes from MF patients expressed low levels of GATA1 (Vannucchi et al., 2005). Furthermore, GATA1 was found markedly reduced in prePMF as compared to ET and PV, and PMF disease evolution and bone marrow fibrosis progression were accompanied by a further reduction of GATA1 expression (Sangiorgio et al., 2021). We speculate therefore that GATA1 could act as a negative transcription factor for CCR2 gene expression. This promising hypothesis will be verified in further experiments to reveal the mechanism that led to CCR2 overexpression in PMF $CD34^+$ cells.

Subsequently, we investigated which signalling pathways could be activated downstream CCL2/CCR2 axis activation. Of note, when PMF $CD34^+$ were *ex vivo* stimulated with rhCCL2, a significant phosphorylation of Akt was detected. As we expected, primary $CD34^+$ cells from healthy subjects that lack of CCR2, do not display CCL2-mediated phosphorylation of Akt or of other signaling pathways. The selective activation of Akt-mediated signaling is consistent with what has been described in solid tumors such as ovarian, breast and prostate cancer (Mizutani et al, 2009; Sun et al, 2020; Lim et al, 2016). In solid tumors, Akt activation supports cell proliferation by acting on diverse downstream factors involved in controlling the G1/S and G2/M transitions in cell cycle and cooperated with mTORC1 to promote cell proliferation (Gao et al., 2003; Chang et al., 2003). Moreover, AKT hyperactivation contributes to DNA damage accumulation and genome instability, indeed neoplastic cells expressing constitutively active AKT can avoid apoptosis and overcome checkpoint-dependent cell cycle arrest, accumulating potential cancer-related mutations (Xu et al., 2012). Here, we demonstrate that CCL2/CCR2 chemokine system is selectively activated in PMF, and its activation boosts pro-survival and proliferative signals, induced by driver mutations, in PMF neoplastic cells through the phosphorylation of Akt.

Then, we asked whether ruxolitinib could also affect CCR2 expression on PMF $CD34^+$ cells.

We evaluated CCR2 expression on $CD34^+$ cells by flow cytometry in PMF patients before and after 1, 3 and 9 months from ruxolitinib start and we observed a significant and stable reduction of CCR2 surface expression. Together with data on CCL2 expression, we demonstrate an additional mechanism of action of ruxolitinib that could potentially turn off the CCL2/CCR2 chemokine system in PMF.

Eventually, we evaluated the diagnostic accuracy of CCR2-expressing hematopoietic progenitors in discriminating ET vs. prePMF and prePMF vs. overtPMF. Differential diagnosis of PMF is based on the 2016 WHO-criteria and the composite assessment of clinical, histopathological, genetic and laboratory parameters. MF is the most aggressive subtype among MPNs, typified by a poorer outcome and a more reduced survival as compared to ET and PV. Therefore, an accurate and timely diagnosis is pivotal for the management and the correct therapeutic approach of MF patients.

However, in some cases, differential diagnosis is challenging as driver mutations are not disease specific, MPN subtypes often share the same mutational profile and often the same laboratory

parameters and clinical manifestation (i.e., isolated thrombocytosis in asymptomatic patient).

Bone marrow histology currently represents the key diagnostic procedure to discriminate among MPN entities. BM fibrosis represents a reactive and progressive phenomenon typified by the presence of increased collagen and reticulin fibers arranged in a disorderly manner. Histologically, fibrosis is assessed by reticulin and collagen (trichrome) stainings of bone marrow trephine biopsy, and classification criteria have been drawn up by the European consensus system (Thiele et al., 2005; Thiele et al., 2005). The methodology used in reporting bone marrow fibrosis and the integration of bone marrow biopsy data in clinical algorithm are still under debate. Indeed, traditional grading systems are semi-quantitative, and the main limitations are represented by the lack of standardization, the subjectivity of the operators' evaluation, and the heterogeneity of samples (Zahr et al., 2016). Moreover, in some cases the evaluation of bone marrow biopsy results problematic and ambiguous also for expert pathologists. For instance, the diagnosis between prePMF and true-ET is often critical, as prePMF frequently mimics ET phenotype showing similar initial clinical presentation and mutational profile. Although prePMF and ET can be similar at disease onset, prePMF is typified by reduced survival and a higher risk of blast transformation as compared to ET (Vainchenker et al, 2017). Additionally, prePMF an overtPMF represent two different pathological entities; overtPMF is enriched in adverse clinical and molecular features, severe symptoms (splenomegaly and extramedullary hematopoiesis) and poor prognosis (Nazha et al., 2013; Lekovic et al., 2014).

Given the peculiar expression of CCR2 in PMF, we evaluated whether flow cytometry detection of CCR2-expressing $CD34^+$ cells could be used as non-invasive diagnostic tool in support of bone marrow biopsy histopathological analysis for the differential diagnosis of (i) true ET *vs*. prePMF and (ii) prePMF *vs.* overtPMF.

ROC curve analysis of flow cytometry evaluation of CCR2-expressing $CD34^+$ cells in ET *vs.* prePMF showed a very good diagnostic accuracy (AUC of 0.8769, CI of 95%: 0.7563-0.9976, P=0.0003) (Haley et al., 1982). The identified cut-off value of 5.595 has a sensitivity of 84.6% and specificity of 80% in discriminating "true" ET from pre-fibrotic PMF. At the same time, ROC curve analysis of flow cytometry evaluation of CCR2-expressing $CD34^+$ cells in prePMF *vs*. overtPMF shows a cut-off value of 9.970 with a sensitivity of 100% and specificity of 61% in discriminating prePMF from overtPMF, with NPV of 100%, overall demonstrating a good diagnostic performance (AUC of 0.7863, CI of 95%: 0.5928-0.9798, P=0.02) (Haley et al., 1982).

Although we are aware that these data need to be validated in a larger cohort of patients and that the protocol needs standardization to be used in clinical practice, our results pinpoint CCR2-expression on $CD34^+$ cells as a novel diagnostic biomarker in MPNs. Moreover, flow cytometry shows some relevant advantages as compared to other diagnostic tools, allowing a rapid and complete characterization in a single-shot analysis. Bone marrow histopathology instead required at least 10 days. Therefore, the evaluation of CCR2-expressing CD34+ by flow cytometry could

rapidly offer an immediate diagnostic indication to physician before the morphological results of bone marrow histology. Moreover, this biomarker could also be used to assess disease progression or to monitor the impact of therapy on marrow histology as a surrogate endpoint of treatment efficacy.

Collectively, we described for the first time the biological role of the rs1024611 SNP of CCL2 and the CCL2/CCR2 chemokine system in PMF. Our data suggest the rs1024611 SNP genotyping as a potential novel strategy for risk stratification of patients, with the extremely important advantage of not being influenced, as a germinal variant, by clonal evolution or by therapy.

According to our results, the poor outcome and reduced survival observed in G/G patients are the result of the interaction between host genetic predisposition and the peculiar expression of CCR2 on the neoplastic clone. When the PMF CCR2-expressing clone arises in a host genetic background characterized by CCL2 overproduction, such as in G/G individuals, the selective activation of the CCL2/CCR2 chemokine system markedly boosts pro-survival and proliferative signals, induced by driver mutations, in PMF hematopoietic progenitors. This mechanism cannot occur in healthy subjects and PV or ET, in whom CCL2 levels are likely modulated in a similar way by the rs1024611 SNP, but chemokine levels are irrelevant for $CD34^+$ cells proliferation, since HD and PV/ET $CD34^+$ cells do not express (or express at very low levels) CCR2.

On the other hand, our data pave the way for a novel and rapid diagnostic strategy, based on the evaluation of CCR2 expression in $CD34^+$ cells by flow cytometry to discriminate between trueET *vs.* prePMF and prePMF *vs.* overtPMF.

Finally, we provide the biologic rationale for novel therapeutic strategy based on CCL2/CCR2 axis inhibition in PMF, demonstrating an addition mechanism underlying the anti-inflammatory effects of ruxolitinib, via the simultaneous down-modulation of CCL2 production and CCR2 expression in PMF hematopoietic progenitors.

List of publications on peer reviewed international scientific journals during my PhD

- **Pozzi G**, Gobbi G, Masselli E, Carubbi C, Presta V, Ambrosini L, Vitale M, Mirandola P. Buffering Adaptive Immunity by Hydrogen Sulfide. Cells. 2022; 11(3):325,
- **Pozzi G***, Masselli E*, Gobbi G, Mirandola P, Taborda-Barata L, Ampollini L, Carbognani P, Micheloni C, Corazza F, Galli D, Carubbi C, Vitale M. Hydrogen Sulfide Inhibits TMPRSS2 in Human Airway Epithelial Cells: Implications for SARS-CoV-2 Infection. Biomedicines. 2021; 9(9):1273, ***co-first authors,**
- Masselli E, Pozzi G, Carubbi C, Vitale M. The Genetic Makeup of Myeloproliferative Neoplasms: Role of Germline Variants in Defining Disease Risk, Phenotypic Diversity and Outcome. Cells. 2021 10(10):2597,
- Chiu M, Taurino G, Dander E, Bardelli D, Fallati A, Andreoli R, Bianchi MG, Carubbi C, **Pozzi G**, Galuppo L, Mirandola P, Rizzari C, Tardito S, Biondi A, D'Amico G, Bussolati O. ALL blasts drive primary mesenchymal stromal cells to increase asparagine availability during asparaginase treatment. Blood Adv. 2021;5(23):5164-5178,
- Masselli E, Carubbi C, **Pozzi G**, Percesepe A, Campanelli R, Villani L, Gobbi G, Bonomini S, Roti G, Rosti V, Massa M, Barosi G, Vitale M. Impact of the rs1024611 Polymorphism of CCL2 on the Pathophysiology and Outcome of Primary Myelofibrosis. Cancers. 2021; 13(11):2552,
- Galli D, Carubbi C, Masselli E, Vaccarezza M, Presta V, **Pozzi G**, Ambrosini L, Gobbi G, Vitale M, Mirandola P. Physical Activity and Redox Balance in the Elderly: Signal Transduction Mechanisms. Applied Sciences. 2021; 11(5):2228,
- Masselli E*, **Pozzi G***, Gobbi G, Merighi S, Gessi S, Vitale M, Carubbi C. Cytokine Profiling in Myeloproliferative Neoplasms: Overview on Phenotype Correlation, Outcome Prediction, and Role of Genetic Variants. Cells. 2020 Sep 21;9(9):2136. ***co-first authors,**
- Masselli E, Vaccarezza M, Carubbi C, **Pozzi G**, Presta V, Mirandola P, Vitale M. NK cells: A double edge sword against SARS-CoV-2. Adv Biol Regul. 2020 Aug; 77:100737,
- Masselli E*, **Pozzi G*,** Vaccarezza M, Mirandola P, Galli D, Vitale M, Carubbi C, Gobbi G. ROS in Platelet Biology: Functional Aspects and Methodological Insights. Int J Mol Sci. 2020 Jul 9;21(14):4866. ***co-first authors,**
- Spigoni V, Fantuzzi F, Carubbi C, Pozzi G, Masselli E, Gobbi G, Solini A, Bonadonna RC, Dei Cas A. Sodium-glucose cotransporter 2 inhibitors antagonize lipotoxicity in human myeloid angiogenic cells and ADP-dependent activation in human platelets: potential relevance to prevention of cardiovascular events. Cardiovasc Diabetol. 2020 Apr 7;19(1):46,
- Presta V, Galuppo L, Mirandola P, Galli D, **Pozzi G**, Zoni R, Capici S, Colucci ME, Veronesi L, Ambrosini L, Gobbi G, Vitale M, Pasquarella C. One-shoulder carrying school backpack strongly affects gait swing phase and pelvic tilt: a case study. Acta Biomed. 2020 Apr 10;91(3-S):168-170,
- Gobbi G, Carubbi C, Tagliazucchi GM, Masselli E, Mirandola P, Pigazzani F, Crocamo A,

Notarangelo MF, Suma S, Paraboschi E, Maglietta G, Nagalla S, **Pozzi G**, Galli D, Vaccarezza M, Fortina P, Addya S, Ertel A, Bray P, Duga S, Berzuini C, Vitale M, Ardissino D. Sighting acute myocardial infarction through platelet gene expression. Sci Rep. 2019 Dec 20;9(1):19574,

- Carubbi C, Masselli E, Calabrò E, Bonati E, Galeone C, Andreoli R, Goldoni M, Corradi M, Sverzellati N, **Pozzi G**, Banchini A, Pastorino U, Vitale M. Sulphurous thermal water inhalation impacts respiratory metabolic parameters in heavy smokers. Int J Biometeorol. 2019;63(9):1209-1216,
- Carubbi C, Masselli E, **Pozzi G**, Mattioli M, Martini S, Goldoni M, Aloe R, Cervellin G, Vitale M, Gobbi G. Combination of Platelet expression of PKCepsilon and cardiac troponin-I for early diagnosis of chest pain patients in the emergency department. Sci Rep. 2019 Feb 14;9(1):2125.

Part I: References

- Abbas A, Aukrust P, Dahl TB, Bjerkeli V, Sagen EB, Michelsen A, Russell D, Krohg-Sørensen K, Holm S, Skjelland M, Halvorsen B. High levels of S100A12 are associated with recent plaque symptomatology in patients with carotid atherosclerosis. Stroke. 2012;43(5):1347-53.
- Aimo A, Gaggin HK, Barison A, Emdin M, Januzzi JL Jr. Imaging, biomarker, and clinical predictors of cardiac remodeling in heart failure with reduced ejection fraction. JACC Heart Fail. 2019;7(9):782-794.
- Akita Y. Protein kinase C-epsilon (PKC-epsilon): its unique structure and function. J Biochem. 2002;132(6):847-52.
- Anderson JL, Morrow DA. Acute Myocardial Infarction. N Engl J Med. 2017;376(21):2053-2064
- Antman EM, Anbe DT, Armstrong PW, Bates ER, Green LA, Hand M, Hochman JS, Krumholz HM, Kushner FG, Lamas GA, Mullany CJ, Ornato JP, Pearle DL, Sloan MA, Smith SC Jr; American College of Cardiology; American Heart Association; Canadian Cardiovascular Society. ACC/AHA guidelines for the management of patients with ST-elevation myocardial infarction--executive summary. A report of the American College of Cardiology/American Heart Association Task Force on Practice Guidelines (Writing Committee to revise the 1999 guidelines for the management of patients with acute myocardial infarction). J Am Coll Cardiol. 2004;44(3):671-719.
- Babuin L, Jaffe AS. Troponin: the biomarker of choice for the detection of cardiac injury. CMAJ. 2005;173(10):1191-202.
- Backus BE, Six AJ, Kelder JC, Bosschaert MA, Mast EG, Mosterd A, Veldkamp RF, Wardeh AJ, Tio R, Braam R, Monnink SH, van Tooren R, Mast TP, van den Akker F, Cramer MJ, Poldervaart JM, Hoes AW, Doevendans PA. A prospective validation of the HEART score for chest pain patients at the emergency department. Int J Cardiol. 2013;168(3):2153-8.
- Ballen KK, Ritchie AJ, Murphy C, Handin RI, Ewenstein BM. Expression and activation of protein kinase C isoforms in a human megakaryocytic cell line. Exp Hematol. 1996;24(13):1501-8.
- Basatemur GL, Jørgensen HF, Clarke MCH, Bennett MR, Mallat Z. Vascular smooth muscle cells in atherosclerosis. Nat Rev Cardiol. 2019;16(12):727-744.
- Bassini A, Zauli G, Migliaccio G, Migliaccio AR, Pascuccio M, Pierpaoli S, Guidotti L, Capitani S, Vitale M. Lineage-restricted expression of protein kinase C isoforms in hematopoiesis. Blood. 1999;93(4):1178-88.
- Bentzon JF, Otsuka F, Virmani R, Falk E. Mechanisms of plaque formation and rupture. Circ Res. 2014;114(12):1852-66.
- Bentzon JF, Sondergaard CS, Kassem M, Falk E. Smooth muscle cells healing atherosclerotic plaque disruptions are of local, not blood, origin in apolipoprotein E knockout mice. Circulation 2007;116: 205361.
- Bodor GS, Survant L, Voss EM, et al. Cardiac troponin T composition in normal and regenerating human skeletal muscle. Clin Chem 1997;43: 476-84.
- Bongiovanni D, Santamaria G, Klug M, Santovito D, Felicetta A, Hristov M, von Scheidt M, Aslani M, Cibella J, Weber C, Moretti A, Laugwitz KL, Peano C, Bernlochner I. Transcriptome Analysis of Reticulated Platelets Reveals a Prothrombotic Profile. Thromb Haemost. 2019;119(11):1795-1806
- Borissoff JI, Spronk HM, ten Cate H. The hemostatic system as a modulator of atherosclerosis. N Engl J Med. 2011;364(18):1746-60.
- Bourgon R, Gentleman R, Huber W. Independent filtering increases detection power for high-throughput experiments. Proc Natl Acad Sci U S A. 2010;107(21):9546-51.
- Bugert P, Dugrillon A, Günaydin A, Eichler H, Klüter H. Messenger RNA profiling of human platelets by microarray hybridization. Thromb Haemost. 2003;90(4):738-48.
- Burke AP, Kolodgie FD, Farb A, et al. Healed plaque ruptures and sudden coronary death: evidence that subclinical rupture has a role in plaque progression. Circulation 2001;103: 934-40.

- Bynagari-Settipalli YS, Lakhani P, Jin J, et al. Protein kinase C isoform ε negatively regulates ADP-induced calcium mobilization and thromboxane generation in platelets. Arterioscler Thromb Vasc Biol. 2012;32(5):1211-1219.
- Cai XY, Lu L, Wang YN, Jin C, Zhang RY, Zhang Q, Chen QJ, Shen WF. Association of increased S100B, S100A6 and S100P in serum levels with acute coronary syndrome and also with the severity of myocardial infarction in cardiac tissue of rat models with ischemia-reperfusion injury. Atherosclerosis. 2011;217(2):536-42.
- Canto JG, Rogers WJ, Goldberg RJ, Peterson ED, Wenger NK, Vaccarino V, Kiefe CI, Frederick PD, Sopko G, Zheng ZJ; NRMI Investigators. Association of age and sex with myocardial infarction symptom presentation and in-hospital mortality. JAMA. 2012;307(8):813-22.
- Carlton EW, Cullen L, Than M, Gamble J, Khattab A, Greaves K. A novel diagnostic protocol to identify patients suitable for discharge after a single high-sensitivity troponin. Heart. 2015;101(13):1041-6.
- Carubbi C, Masselli E, Gesi M, Galli D, Mirandola P, Vitale M, Gobbi G. Cytofluorimetric platelet analysis. Semin Thromb Hemost. 2014;40(1):88-98.
- Carubbi C, Masselli E, Martini S, et al. Human thrombopoiesis depends on Protein kinase Cδ/protein kinase Cε functional couple. *Haematologica*. 2016;101(7):812-820.
- Carubbi C, Masselli E, Nouvenne A, Russo D, Galli D, Mirandola P, Gobbi G, Vitale M. Laboratory diagnostics of inherited platelet disorders. Clin Chem Lab Med. 2014;52(8):1091-106.
- Carubbi C, Masselli E, Vitale M. Flow Cytometry. 2017 In: Gresele P., Kleiman N., Lopez J., Page C. (eds) Platelets in Thrombotic and Non-Thrombotic Disorders.
- Carubbi C, Mirandola P, Mattioli M, et al. Protein kinase C ε expression in platelets from patients with acute myocardial infarction. *PLoS One*. 2012;7(10):e46409.
- Cervellin G, Mattiuzzi C, Bovo C, Lippi G. Diagnostic algorithms for acute coronary syndrome-is one better than another?. Ann Transl Med 2016; 4 (10) 193.
- Cesari F, Marcucci R, Gori AM, Caporale R, Fanelli A, Casola G, Balzi D, Barchielli A, Valente S, Giglioli C, Gensini GF, Abbate R. Reticulated platelets predict cardiovascular death in acute coronary syndrome patients. Insights from the AMI-Florence 2 Study. Thromb Haemost. 2013;109(5):846-53.
- Chang Y, Bluteau D, Debili N, Vainchenker W. From hematopoietic stem cells to platelets. J Thromb Haemost. 2007;5 Suppl 1:318-27.
- Chen S, Du C, Shen M, Zhao G, Xu Y, Yang K, Wang X, Li F, Zeng D, Chen F, Wang S, Chen M, Wang C, He T, Wang F, Wang A, Cheng T, Su Y, Zhao J, Wang J. Sympathetic stimulation facilitates thrombopoiesis by promoting megakaryocyte adhesion, migration, and proplatelet formation. Blood. 2016;127(8):1024-35.
- Chiesa M, Piacentini L, Bono E, Milazzo V, Campodonico J, Marenzi G, Colombo GI. Whole blood transcriptome profile at hospital admission discriminates between patients with ST-segment elevation and non-ST-segment elevation acute myocardial infarction. Sci Rep. 2020;10(1):8731.
- Chu SG, Becker RC, Berger PB, Bhatt DL, Eikelboom JW, Konkle B, Mohler ER, Reilly MP, Berger JS. Mean platelet volume as a predictor of cardiovascular risk: a systematic review and meta-analysis. J Thromb Haemost. 2010;8(1):148-56.
- Cifuni SM, Wagner DD, Bergmeier W. CalDAG-GEFI and protein kinase C represent alternative pathways leading to activation of integrin alphaIIbbeta3 in platelets. Blood. 2008;112(5):1696-703.
- Clément M, Basatemur G, Masters L, Baker L, Bruneval P, Iwawaki T, Kneilling M, Yamasaki S, Goodall J, Mallat Z. Necrotic Cell Sensor Clec4e Promotes a Proatherogenic Macrophage Phenotype Through Activation of the Unfolded Protein Response. Circulation. 2016;134(14):1039-1051.
- Collins T, Cybulsky MI. NF-kappaB: pivotal mediator or innocent bystander in atherogenesis? J Clin Invest. 2001;107(3):255-64.
- Colombo G, Gertow K, Marenzi G, Brambilla M, De Metrio M, Tremoli E, Camera M. Gene expression profiling reveals multiple differences in platelets from patients with stable angina or non-ST elevation acute coronary syndrome. Thromb Res. 2011;128(2):161-8.

- Cybulsky MI, Gimbrone MA Jr. Endothelial expression of a mononuclear leukocyte adhesion molecule during atherogenesis. Science. 1991;251(4995):788-91.
- Di Marcantonio D, Galli D, Carubbi C, Gobbi G, Queirolo V, Martini S, Merighi S, Vaccarezza M, Maffulli N, Sykes SM, Vitale M, Mirandola P. PKCε as a novel promoter of skeletal muscle differentiation and regeneration. Exp Cell Res. 2015;339(1):10-9.
- Dong ZM, Chapman SM, Brown AA, Frenette PS, Hynes RO, Wagner DD. The combined role of P- and E-selectins in atherosclerosis. J Clin Invest. 1998;102(1):145-52.
- Durgan J, Cameron AJ, Saurin AT, Hanrahan S, Totty N, Messing RO, Parker PJ. The identification and characterization of novel PKCepsilon phosphorylation sites provide evidence for functional cross-talk within the PKC superfamily. Biochem J. 2008;411(2):319-31.
- Eggers KM, Lindahl B. Application of Cardiac Troponin in Cardiovascular Diseases Other Than Acute Coronary Syndrome. Clin Chem. 2017;63(1):223-235.
- Eggers KM, Lindahl B. Impact of Sex on Cardiac Troponin Concentrations-A Critical Appraisal. Clin Chem. 2017;63(9):1457-1464.
- Eichbaum FW. 'Wavy' myocardial fibers in spontaneous and experimental adrenergic cardiopathies. Cardiology. 1975;60(6):358-65.
- Eicher JD, Wakabayashi Y, Vitseva O, Esa N, Yang Y, Zhu J, Freedman JE, McManus DD, Johnson AD. Characterization of the platelet transcriptome by RNA sequencing in patients with acute myocardial infarction. Platelets. 2016;27(3):230-9.
- Ekelund U, Akbarzadeh M, Khoshnood A, Björk J, Ohlsson M. Likelihood of acute coronary syndrome in emergency department chest pain patients varies with time of presentation. BMC Res Notes. 2012;5: 420.
- Elalamy I, Chakroun T, Gerotziafas GT, Petropoulou A, Robert F, Karroum A, Elgrably F, Samama MM, Hatmi M. Circulating platelet-leukocyte aggregates: a marker of microvascular injury in diabetic patients. Thromb Res. 2008;121(6):843-8.
- Erbel R, Aboyans V, Boileau C, Bossone E, Bartolomeo RD, Eggebrecht H, Evangelista A, Falk V, Frank H, Gaemperli O, Grabenwöger M, Haverich A, Iung B, Manolis AJ, Meijboom F, Nienaber CA, Roffi M, Rousseau H, Sechtem U, Sirnes PA, Allmen RS, Vrints CJ; ESC Committee for Practice Guidelines. 2014 ESC Guidelines on the diagnosis and treatment of aortic diseases: Document covering acute and chronic aortic diseases of the thoracic and abdominal aorta of the adult. The Task Force for the Diagnosis and Treatment of Aortic Diseases of the European Society of Cardiology (ESC). Eur Heart J. 2014;35(41):2873-926.
- Eslin DE, Zhang C, Samuels KJ, Rauova L, Zhai L, Niewiarowski S, Cines DB, Poncz M, Kowalska MA. Transgenic mice studies demonstrate a role for platelet factor 4 in thrombosis: dissociation between anticoagulant and antithrombotic effect of heparin. Blood. 2004;104(10):3173-80.
- Facchinetti V, Ouyang W, Wei H, Soto N, Lazorchak A, Gould C, Lowry C, Newton AC, Mao Y, Miao RQ, Sessa WC, Qin J, Zhang P, Su B, Jacinto E. The mammalian target of rapamycin complex 2 controls folding and stability of Akt and protein kinase C. EMBO J. 2008;27(14):1932-43.
- Falk E. Unstable angina with fatal outcome: dynamic coronary thrombosis leading to infarction and/or sudden death. Autopsy evidence of recur- rent mural thrombosis with peripheral embolization culminating in total vascular occlusion. Circulation. 1985;71: 699–708.
- Fallon EM, Roques J. Acute chest pain. AACN Clin Issues. 1997;8(3):383-97.
- Ferroni P, Basili S, Falco A, Davì G. Platelet activation in type 2 diabetes mellitus. J Thromb Haemost. 2004;2(8):1282-91.
- Fink L, Hölschermann H, Kwapiszewska G, Muyal JP, Lengemann B, Bohle RM, Santoso S. Characterization of platelet-specific mRNA by real-time PCR after laser-assisted microdissection. Thromb Haemost. 2003;90(4):749-56.
- Fishbein MC, Maclean D, Maroko PR. The histopathologic evolution of myocardial infarction. Chest. 1978;73(6):843-9.
- Foreman RD. Mechanisms of cardiac pain. Annu Rev Physiol. 1999;61: 143-67.
- Frangogiannis NG. Regulation of the inflammatory response in cardiac repair. Circ Res. 2012;110(1):159-73.

- Freishtat RJ, Natale J, Benton AS, Cohen J, Sharron M, Wiles AA, Ngor WM, Mojgani B, Bradbury M, Degnan A, Sachdeva R, Debiase LM, Ghimbovschi S, Chow M, Bunag C, Kristosturyan E, Hoffman EP. Sepsis alters the megakaryocyte-platelet transcriptional axis resulting in granzyme B-mediated lymphotoxicity. Am J Respir Crit Care Med. 2009 Mar 15;179(6): 467-73.
- Fries GR, Gassen NC, Rein T. The FKBP51 Glucocorticoid Receptor Co-Chaperone: Regulation, Function, and Implications in Health and Disease. Int J Mol Sci. 2017;18(12):2614.
- Frossard M, Fuchs I, Leitner JM, Hsieh K, Vlcek M, Losert H, Domanovits H, Schreiber W, Laggner AN, Jilma B. Platelet function predicts myocardial damage in patients with acute myocardial infarction. Circulation. 2004;110(11):1392-7.
- Fu S, Zhao H, Shi J, Abzhanov A, Crawford K, Ohno-Machado L, Zhou J, Du Y, Kuo WP, Zhang J, Jiang M, Jin JG. Peripheral arterial occlusive disease: global gene expression analyses suggest a major role for immune and inflammatory responses. BMC Genomics. 2008; 9: 369.
- Furman MI, Benoit SE, Barnard MR, Valeri CR, Borbone ML, Becker RC, Hechtman HB, Michelson AD. Increased platelet reactivity and circulating monocyte-platelet aggregates in patients with stable coronary artery disease. J Am Coll Cardiol. 1998;31(2):352-8.
- Galli D, Gobbi G, Carrubbi C, Di Marcantonio D, Benedetti L, De Angelis MG, Meschi T, Vaccarezza M, Sampaolesi M, Mirandola P, Vitale M. The role of PKCε-dependent signaling for cardiac differentiation. Histochem Cell Biol. 2013;139(1):35-46.
- Garg P, Morris P, Fazlanie AL, Vijayan S, Dancso B, Dastidar AG, Plein S, Mueller C, Haaf P. Cardiac biomarkers of acute coronary syndrome: from history to high-sensitivity cardiac troponin. Intern Emerg Med. 2017;12(2):147-155.
- Gawaz M, Brand K, Dickfeld T, Pogatsa-Murray G, Page S, Bogner C, Koch W, Schömig A, Neumann F. Platelets induce alterations of chemotactic and adhesive properties of endothelial cells mediated through an interleukin-1-dependent mechanism. Implications for atherogenesis. Atherosclerosis. 2000;148(1):75-85.
- Gawaz M. Role of platelets in coronary thrombosis and reperfusion of ischemic myocardium. Cardiovasc Res. 2004;61(3):498-511.
- Ghafoor M, Kamal M, Nadeem U, Husain AN. Educational Case: Myocardial Infarction: Histopathology and Timing of Changes. Acad Pathol. 2020;7: 2374289520976639.
- Giorgione JR, Lin JH, McCammon JA, Newton AC. Increased membrane affinity of the C1 domain of protein kinase Cdelta compensates for the lack of involvement of its C2 domain in membrane recruitment. *J Biol Chem*. 2006;281(3):1660-1669.
- Gkaliagkousi E, Passacquale G, Douma S, Zamboulis C, Ferro A. Platelet activation in essential hypertension: implications for antiplatelet treatment. Am J Hypertens. 2010;23(3):229-36.
- Gleissner CA. Macrophage Phenotype Modulation by CXCL4 in Atherosclerosis. Front Physiol. 2012;3: 1
- Gnatenko DV, Dunn JJ, McCorkle SR, Weissmann D, Perrotta PL, Bahou WF. Transcript profiling of human platelets using microarray and serial analysis of gene expression. Blood 2003; 101.:2285–93
- Gnatenko DV, Dunn JJ, Schwedes J, Bahou WF. Transcript profiling of human platelets using microarray and serial analysis of gene expression (SAGE). Methods Mol Biol. 2009; 496: 245-72.
- Gobbi G, Di Marcantonio D, Micheloni C, Carubbi C, Galli D, Vaccarezza M, Bucci G, Vitale M, Mirandola P. TRAIL up-regulation must be accompanied by a reciprocal PKCε down-regulation during differentiation of colonic epithelial cell: implications for colorectal cancer cell differentiation. J Cell Physiol. 2012; 227(2): 630-8.
- Gobbi G, Mirandola P, Sponzilli I, Micheloni C, Malinverno C, Cocco L, Vitale M. Timing and expression level of protein kinase C epsilon regulate the megakaryocytic differentiation of human CD34 cells. Stem Cells. 2007;25(9):2322-9.
- Goldfarb AN, Delehanty LL, Wang D, Racke FK, Hussaini IM. Stromal inhibition of megakaryocytic differentiation correlates with blockade of signaling by protein kinase C-epsilon and ERK/MAPK. J Biol Chem. 2001;276(31): 29526-30.

- Gonzalez-Porras JR, Martin-Herrero F, Gonzalez-Lopez TJ, Olazabal J, Diez-Campelo M, Pabon P, Alberca I, San Miguel JF. The role of immature platelet fraction in acute coronary syndrome. Thromb Haemost. 2010;103(1):247-9.
- Goodacre S, Cross E, Arnold J, Angelini K, Capewell S, Nicholl J. The health care burden of acute chest pain. Heart. 2005;91(2): 229-30.
- Goyette J, Yan WX, Yamen E, Chung YM, Lim SY, Hsu K, Rahimi F, Di Girolamo N, Song C, Jessup W, Kockx M, Bobryshev YV, Freedman SB, Geczy CL. Pleiotropic roles of S100A12 in coronary atherosclerotic plaque formation and rupture. J Immunol. 2009;183(1):593-603.
- Gorin MA, Pan Q. Protein kinase C epsilon: an oncogene and emerging tumor biomarker. Mol Cancer. 2009; 8:9.
- Graness A, Adomeit A, Heinze R, Wetzker R, Liebmann C. A novel mitogenic signaling pathway of bradykinin in the human colon carcinoma cell line SW-480 involves sequential activation of a Gq/11 protein, phosphatidylinositol 3-kinase beta, and protein kinase Cepsilon. J Biol Chem. 1998;273(48):32016-22.
- Gremmel T, Ay C, Riedl J, Kopp CW, Eichelberger B, Koppensteiner R, Panzer S. Platelet-specific markers are associated with monocyte-platelet aggregate formation and thrombin generation potential in advanced atherosclerosis. Thromb Haemost. 2016;115(3):615-21.
- Griner EM, Kazanietz MG. Protein kinase C and other diacylglycerol effectors in cancer. Nat Rev Cancer. 2007;7(4):281-94.
- Gulati M, Levy PD, Mukherjee D, Amsterdam E, Bhatt DL, Birtcher KK, Blankstein R, Boyd J, Bullock-Palmer RP, Conejo T, Diercks DB, Gentile F, Greenwood JP, Hess EP, Hollenberg SM, Jaber WA, Jneid H, Joglar JA, Morrow DA, O'Connor RE, Ross MA, Shaw LJ. 2021 AHA/ACC/ASE/CHEST/SAEM/SCCT/SCMR Guideline for the Evaluation and Diagnosis of Chest Pain: A Report of the American College of Cardiology/American Heart Association Joint Committee on Clinical Practice Guidelines. Circulation. 2021;144(22): e368-e454.
- Handagama P, Rappolee DA, Werb Z, Levin J, Bainton DF. Platelet alpha-granule fibrinogen, albumin, and immunoglobulin G are not synthesized by rat and mouse megakaryocytes. J Clin Invest. 1990;86(4):1364-8.
- Hanley JA, McNeil BJ. The meaning and use of the area under a receiver operating characteristic (ROC) curve. Radiology. 1982;143(1):29-36.
- Harper MT, Poole AW. Diverse functions of protein kinase C isoforms in platelet activation and thrombus formation. J Thromb Haemost. 2010;8(3):454-62.
- Healy AM, Pickard MD, Pradhan AD, Wang Y, Chen Z, Croce K, et al. Platelet expression profiling and clinical validation of myeloid-related protein-14 as a novel determinant of cardiovascular events. Circulation 2006;113: 2278–84.
- Heusch G. The Coronary Circulation as a Target of Cardioprotection. Circ Res. 2016;118(10):1643-58.
- Hoffmann JJ. Reticulated platelets: analytical aspects and clinical utility. Clin Chem Lab Med. 2014;52(8):1107-17.
- Ibanez B, James S, Agewall S, Antunes MJ, Bucciarelli-Ducci C, Bueno H, Caforio ALP, Crea F, Goudevenos JA, Halvorsen S, Hindricks G, Kastrati A, Lenzen MJ, Prescott E, Roffi M, Valgimigli M, Varenhorst C, Vranckx P, Widimský P; ESC Scientific Document Group. 2017 ESC Guidelines for the management of acute myocardial infarction in patients presenting with ST-segment elevation: The Task Force for the management of acute myocardial infarction in patients presenting with ST-segment elevation of the European Society of Cardiology (ESC). Eur Heart J. 2018;39(2):119-177.
- Italiano JE Jr, Lecine P, Shivdasani RA, Hartwig JH. Blood platelets are assembled principally at the ends of proplatelet processes produced by differentiated megakaryocytes. J Cell Biol. 1999;147(6):1299-312
- Italiano JE Jr, Mairuhu AT, Flaumenhaft R. Clinical relevance of microparticles from platelets and megakaryocytes. Curr Opin Hematol. 2010;17(6):578-84.
- Jaffe AS, Babuin L, Apple FS. Biomarkers in acute cardiac disease: the present and the future. J Am Coll Cardiol. 2006;48(1):1-11.

- Jaffe AS. Chasing troponin: how low can you go if you can see the rise? J Am Coll Cardiol. 2006;48(9):1763-4.
- Jawien A, Bowen-Pope DF, Lindner V, Schwartz SM, Clowes AW. Platelet-derived growth factor promotes smooth muscle migration and intimal thickening in a rat model of balloon angioplasty. *J Clin Invest*. 1992;89(2):507-511.
- Jennings RB, Ganote CE, Reimer KA. Ischemic tissue injury. Am J Pathol. 1975;81(1):179-98.
- Jespersen L, Hvelplund A, Abildstrøm SZ, Pedersen F, Galatius S, Madsen JK, Jørgensen E, Kelbæk H, Prescott E. Stable angina pectoris with no obstructive coronary artery disease is associated with increased risks of major adverse cardiovascular events. Eur Heart J. 2012;33(6):734-44.
- Jin J, Quinton TM, Zhang J, Rittenhouse SE, Kunapuli SP. Adenosine diphosphate (ADP)-induced thromboxane A (2) generation in human platelets requires coordinated signaling through integrin alpha(IIb)beta(3) and ADP receptors. Blood. 2002;99(1):193-8.
- Junt T, Schulze H, Chen Z, Massberg S, Goerge T, Krueger A, Wagner DD, Graf T, Italiano JE Jr, Shivdasani RA, von Andrian UH. Dynamic visualization of thrombopoiesis within bone marrow. Science. 2007;317(5845):1767-70.
- Kamath S, Blann AD, Lip GY. Platelet activation: assessment and quantification. Eur Heart J. 2001 Sep;22(17):1561-71.
- Kamei M, Carman CV. New observations on the trafficking and diapedesis of monocytes. Curr Opin Hematol. 2010;17(1):43-52.
- Kannel WB, Feinleib M. Natural history of angina pectoris in the Framingham Study: prognosis and survival. Am J Cardiol.1972;.29: 154–163.
- Kaplanski G, Farnarier C, Kaplanski S, Porat R, Shapiro L, Bongrand P, Dinarello CA. Interleukin-1 induces interleukin-8 secretion from endothelial cells by a juxtacrine mechanism. Blood. 1994;84(12):4242-8.
- Karpatkin S. Heterogeneity of human platelets. II. Functional evidence suggestive of young and old platelets. J Clin Invest. 1969;48(6):1083-7.
- Katrukha IA. Human cardiac troponin complex. Structure and functions. Biochemistry (Mosc). 2013;78(13):1447-65.
- Kaushansky K. Lineage-specific hematopoietic growth factors. N Engl J Med. 2006;354(19):2034-45
- Kaushansky K. Thrombopoiesis. Semin Hematol. 2015;52(1):4-11.
- Kienast J, Schmitz G. Flow cytometric analysis of thiazole orange uptake by platelets: a diagnostic aid in the evaluation of thrombocytopenic disorders. Blood. 1990;75(1):116-21.
- Kim J, Ghasemzadeh N, Eapen DJ, Chung NC, Storey JD, Quyyumi AA, Gibson G. Gene expression profiles associated with acute myocardial infarction and risk of cardiovascular death. Genome Med. 2014;6(5):40.
- Knowlman T, Greenslade JH, Parsonage W, Hawkins T, Ruane L, Martin P, Prasad S, Lancini D, Cullen L. The association of electrocardiographic abnormalities and acute coronary syndrome in emergency patients with chest pain. Acad Emerg Med. 2017;24(3):344-352.
- Konopatskaya O, Matthews SA, Harper MT, Gilio K, Cosemans JM, Williams CM, Navarro MN, Carter DA, Heemskerk JW, Leitges M, Cantrell D, Poole AW. Protein kinase C mediates platelet secretion and thrombus formation through protein kinase D2. Blood. 2011;118(2):416-24.
- Konopka A, Spychalska J, Sitkiewicz D, Zdebska E, Pilichowska I, Piotrowski W, Stepińska J. Expression of platelet surface receptors and early changes in platelet function in patients with STEMI treated with abciximab and clopidogrel versus clopidogrel alone. Am J Cardiovasc Drugs. 2007;7(6):433-9.
- Konstantinides SV, Torbicki A, Agnelli G, Danchin N, Fitzmaurice D, Galiè N, Gibbs JS, Huisman MV, Humbert M, Kucher N, Lang I, Lankeit M, Lekakis J, Maack C, Mayer E, Meneveau N, Perrier A, Pruszczyk P, Rasmussen LH, Schindler TH, Svitil P, Vonk Noordegraaf A, Zamorano JL, Zompatori M; Task Force for the Diagnosis and Management of Acute Pulmonary Embolism of the European Society of Cardiology (ESC). 2014 ESC guidelines on the diagnosis and management of acute pulmonary embolism. Eur Heart J. 2014;35(43):3033-69, 3069a-3069k.

- Konstantinidis K, Whelan RS, Kitsis RN. Mechanisms of cell death in heart disease. Arterioscler Thromb Vasc Biol. 2012;32(7):1552-62.
- Koupenova M, Clancy L, Corkrey HA, Freedman JE. Circulating Platelets as Mediators of Immunity, Inflammation, and Thrombosis. Circ Res. 2018;19;122(2):337-351.
- Kragel AH, Reddy SG, Wittes JT, Roberts WC. Morphometric analysis of the composition of atherosclerotic plaques in the four major epicardial coronary arteries in acute myocardial infarction and in sudden coronary death. Circulation. 1989;80(6):1747-56.
- Kramer MC, Rittersma SZ, de Winter RJ, Ladich ER, Fowler DR, Liang YH, Kutys R, Carter-Monroe N, Kolodgie FD, van der Wal AC, Virmani R. Relationship of thrombus healing to underlying plaque morphology in sudden coronary death. J Am Coll Cardiol. 2010;55(2):122-32.
- Lee SH, Ihn HJ, Park EK, Kim JE. S100 Calcium-Binding Protein P Secreted from Megakaryocytes Promotes Osteoclast Maturation. Int J Mol Sci. 2021;22(11):6129.
- Lenfant C. Chest pain of cardiac and noncardiac origin. Metabolism. 2010;59 Suppl 1: S41-6.
- Lentz BR. Exposure of platelet membrane phosphatidylserine regulates blood coagulation. Prog Lipid Res. 2003;42(5):423-38.
- Lev EI, Estrov Z, Aboulfatova K, et al. Potential role of activated platelets in homing of human endothelial progenitor cells to subendothelial matrix. Thromb Haemost 2006;96:498-504.
- Li Z, Delaney MK, O'Brien KA, Du X. Signaling during platelet adhesion and activation. Arterioscler Thromb Vasc Biol. 2010;30(12):2341-9.
- Libby P. Inflammation in atherosclerosis. Nature. 2002; 420: 868–874.
- Lindemann S, Krämer B, Seizer P, Gawaz M. Platelets, inflammation, and atherosclerosis. J Thromb Haemost. 2007;5 Suppl 1:203-11.
- Lippi G, Franchini M, Targher G. Arterial thrombus formation in cardiovascular disease. Nat Rev Cardiol. 2011;8(9):502-12.
- Lisman T, Weeterings C, de Groot PG. Platelet aggregation: involvement of thrombin and fibrin(ogen). Front Biosci. 2005;10:2504-17.
- Londin ER, Hatzimichael E, Loher P, Edelstein L, Shaw C, Delgrosso K, Fortina P, Bray PF, McKenzie SE, Rigoutsos I. The human platelet: strong transcriptome correlations among individuals associate weakly with the platelet proteome. Biol Direct. 2014; 9:3.
- Long MW, Williams N, Ebbe S. Immature megakaryocytes in the mouse: physical characteristics, cell cycle status, and in vitro responsiveness to thrombopoietic stimulatory factor. Blood. 1982;59(3):569-75.
- Macaulay IC, Carr P, Gusnanto A, Ouwehand WH, Fitzgerald D, Watkins NA. Platelet genomics and proteomics in human health and disease. J Clin Invest. 2005;115(12):3370-7.
- Machlus KR, Italiano JE Jr. The incredible journey: From megakaryocyte development to platelet formation. J Cell Biol. 2013;201(6):785-96.
- Mackay HJ, Twelves CJ. Targeting the protein kinase C family: are we there yet? Nat Rev Cancer. 2007;7(7):554-62.
- Macrae AR, Kavsak PA, Lustig V, Bhargava R, Vandersluis R, Palomaki GE, Yerna MJ, Jaffe AS. Assessing the requirement for the 6-hour interval between specimens in the American Heart Association Classification of Myocardial Infarction in Epidemiology and Clinical Research Studies. Clin Chem. 2006;52(5):812-8.
- Mair J, Lindahl B, Hammarsten O, et al. How is cardiac troponin released from injured myocardium? *Eur Heart J Acute Cardiovasc Care* 2018; 7: 553–560.
- Martini S, Pozzi G, Carubbi C, Masselli E, Galli D, Di Nuzzo S, Banchini A, Gobbi G, Vitale M, Mirandola P. PKCε promotes human Th17 differentiation: Implications in the pathophysiology of psoriasis. Eur J Immunol. 2018;48(4):644-654.
- Massberg S, Brand K, Grüner S, Page S, Müller E, Müller I, Bergmeier W, Richter T, Lorenz M, Konrad I, Nieswandt B, Gawaz M. A critical role of platelet adhesion in the initiation of atherosclerotic lesion formation. J Exp Med. 2002;196(7):887-96.
- Masselli E, Carubbi C, Gobbi G, Mirandola P, Galli D, Martini S, Bonomini S, Crugnola M, Craviotto L, Aversa F, Vitale M. Protein kinase Cε inhibition restores megakaryocytic differentiation of

hematopoietic progenitors from primary myelofibrosis patients. Leukemia. 2015;29(11):2192-201.
- Masselli E, Carubbi C, Pozzi G, Martini S, Aversa F, Galli D, Gobbi G, Mirandola P, Vitale M. Platelet expression of PKCepsilon oncoprotein in myelofibrosis is associated with disease severity and thrombotic risk. Ann Transl Med. 2017;5(13):273.
- Masselli E, Pozzi G, Vaccarezza M, Mirandola P, Galli D, Vitale M, Carubbi C, Gobbi G. ROS in Platelet Biology: Functional Aspects and Methodological Insights. Int J Mol Sci. 2020;21(14):4866.
- May F, Hagedorn I, Pleines I, Bender M, Vögtle T, Eble J, Elvers M, Nieswandt B. CLEC-2 is an essential platelet-activating receptor in hemostasis and thrombosis. Blood. 2009;114(16):3464-72.
- McRedmond JP, Park SD, Reilly DF, Coppinger JA, Maguire PB, Shields DC, Fitzgerald DJ. Integration of proteomics and genomics in platelets: a profile of platelet proteins and platelet-specific genes. Mol Cell Proteomics. 2004;3(2):133-44.
- Meadows TA, Bhatt DL. Clinical aspects of platelet inhibitors and thrombus formation. Circ Res. 2007;100(9):1261-75.
- Mehta LS, Beckie TM, DeVon HA, Grines CL, Krumholz HM, Johnson MN, Lindley KJ, Vaccarino V, Wang TY, Watson KE, Wenger NK; American Heart Association Cardiovascular Disease in Women and Special Populations Committee of the Council on Clinical Cardiology, Council on Epidemiology and Prevention, Council on Cardiovascular and Stroke Nursing, and Council on Quality of Care and Outcomes Research. Acute Myocardial Infarction in Women: A Scientific Statement From the American Heart Association. Circulation. 2016;133(9):916-47.
- Mehta RH, Rathore SS, Radford MJ, Wang Y, Wang Y, Krumholz HM. Acute myocardial infarction in the elderly: differences by age. J Am Coll Cardiol. 2001;38(3):736-41.
- Meijer B, Gearry RB, Day AS. The role of S100A12 as a systemic marker of inflammation. Int J Inflam. 2012; 2012: 907078.
- Mérida I, Arranz-Nicolás J, Rodríguez-Rodríguez C, Ávila-Flores A. Diacylglycerol kinase control of protein kinase C. Biochem J. 2019;476(8):1205-1219.
- Mestas J, Ley K. Monocyte-endothelial cell interactions in the development of atherosclerosis. Trends Cardiovasc Med. 2008;18(6):228-32.
- Michaud K, Basso C, d'Amati G, Giordano C, Kholová I, Preston SD, Rizzo S, Sabatasso S, Sheppard MN, Vink A, van der Wal AC; Association for European Cardiovascular Pathology (AECVP). Diagnosis of myocardial infarction at autopsy: AECVP reappraisal in the light of the current clinical classification. Virchows Arch. 2020;476(2):179-194.
- Millett ERC, Peters SAE, Woodward M. Sex differences in risk factors for myocardial infarction: cohort study of UK Biobank participants. BMJ. 2018;363: k4247.
- Mittelmark MB, Psaty BM, Rautaharju PM, Fried LP, Borhani NO, Tracy RP, Gardin JM, O'Leary DH. Prevalence of cardiovascular diseases among older adults: the Cardiovascular Health Study. Am J Epidemiol. 1993; 137: 311–317.
- Mockel M, Searle J, Muller R, Slagman A, Storchmann H, Oestereich P, Wyrwich W, Ale-Abaei A, Vollert JO, Koch M, Somasundaram R. Chief complaints in medical emergencies: do they relate to underlying disease and outcome? The Charité Emergency Medicine Study (CHARITEM). Eur J Emerg Med. 2013;20(2):103-8.
- Montalescot G, Sechtem U, Achenbach S, Andreotti F, Arden C, Budaj A, Bugiardini R, Crea F, Cuisset T, Di Mario C, Ferreira JR, Gersh BJ, Gitt AK, Hulot JS, Marx N, Opie LH, Pfisterer M, Prescott E, Ruschitzka F, Sabaté M, Senior R, Taggart DP, van der Wall EE, Vrints CJ; ESC Committee for Practice Guidelines, Zamorano JL, Achenbach S, Baumgartner H, Bax JJ, Bueno H, Dean V, Deaton C, Erol C, Fagard R, Ferrari R, Hasdai D, Hoes AW, Kirchhof P, Knuuti J, Kolh P, Lancellotti P, Linhart A, Nihoyannopoulos P, Piepoli MF, Ponikowski P, Sirnes PA, Tamargo JL, Tendera M, Torbicki A, Wijns W, Windecker S; Document Reviewers, Knuuti J, Valgimigli M, Bueno H, Claeys MJ, Donner-Banzhoff N, Erol C, Frank H, Funck-Brentano C, Gaemperli O, Gonzalez-Juanatey JR, Hamilos M, Hasdai D, Husted S, James SK, Kervinen K, Kolh P, Kristensen SD, Lancellotti P, Maggioni AP, Piepoli MF, Pries AR, Romeo F, Rydén L, Simoons ML, Sirnes PA, Steg PG, Timmis A, Wijns W, Windecker S, Yildirir A, Zamorano JL. 2013 ESC guidelines on the

management of stable coronary artery disease: the Task Force on the management of stable coronary artery disease of the European Society of Cardiology. Eur Heart J. 2013;34(38):2949-3003.

- Moore KJ, Tabas I. Macrophages in the pathogenesis of atherosclerosis. Cell. 2011;145(3):341-55
- Moriya S, Kazlauskas A, Akimoto K, Hirai S, Mizuno K, Takenawa T, Fukui Y, Watanabe Y, Ozaki S, Ohno S. Platelet-derived growth factor activates protein kinase C epsilon through redundant and independent signaling pathways involving phospholipase C gamma or phosphatidylinositol 3-kinase. Proc Natl Acad Sci U S A. 1996;93(1):151-5.
- Moroi M, Jung SM, Shinmyozu K, Tomiyama Y, Ordinas A, Diaz-Ricart M. Analysis of platelet adhesion to a collagen-coated surface under flow conditions: the involvement of glycoprotein VI in the platelet adhesion. Blood. 1996;88(6):2081-92.
- Morrow DA. Cardiovascular risk prediction in patients with stable and unstable coronary heart disease. Circulation. 2010;121(24):2681-91.
- Mozaffarian D, Benjamin EJ, Go AS, Arnett DK, Blaha MJ, Cushman M, Das SR, de Ferranti S, Després JP, Fullerton HJ, Howard VJ, Huffman MD, Isasi CR, Jiménez MC, Judd SE, Kissela BM, Lichtman JH, Lisabeth LD, Liu S, Mackey RH, Magid DJ, McGuire DK, Mohler ER 3rd, Moy CS, Muntner P, Mussolino ME, Nasir K, Neumar RW, Nichol G, Palaniappan L, Pandey DK, Reeves MJ, Rodriguez CJ, Rosamond W, Sorlie PD, Stein J, Towfighi A, Turan TN, Virani SS, Woo D, Yeh RW, Turner MB; American Heart Association Statistics Committee; Stroke Statistics Subcommittee. Heart Disease and Stroke Statistics-2016 Update: A Report From the American Heart Association. Circulation. 2016;133(4):e38-360.
- Muller JE, Stone PH, Turi ZG, Rutherford JD, Czeisler CA, Parker C, Poole WK, Passamani E, Roberts R, Robertson T. Circadian variation in the frequency of onset of acute myocardial infarction. N Engl J Med. 1985; 313: 1315–1322.
- Muse ED, Kramer ER, Wang H, Barrett P, Parviz F, Novotny MA, Lasken RS, Jatkoe TA, Oliveira G, Peng H, Lu J, Connelly MC, Schilling K, Rao C, Torkamani A, Topol EJ. A Whole Blood Molecular Signature for Acute Myocardial Infarction. Sci Rep. 2017;7(1):12268.
- Nagalla S, Shaw C, Kong X, Kondkar AA, Edelstein LC, Ma L, Chen J, McKnight GS, López JA, Yang L, Jin Y, Bray MS, Leal SM, Dong JF, Bray PF. Platelet microRNA-mRNA coexpression profiles correlate with platelet reactivity. Blood. 2011;117(19):5189-97.
- Nagy B Jr, Bhavaraju K, Getz T, Bynagari YS, Kim S, Kunapuli SP. Impaired activation of platelets lacking protein kinase C-theta isoform. Blood. 2009;113(11):2557-67.
- Nanni L, Romualdi C, Maseri A, Lanfranchi G. Differential gene expression profiling in genetic and multifactorial cardiovascular diseases. J Mol Cell Cardiol. 2006;41(6):934-48.
- Newton AC. Protein kinase C: structure, function, and regulation. J Biol Chem. 1995;270(48):28495-8.
- Nieswandt B, Pleines I, Bender M. Platelet adhesion and activation mechanisms in arterial thrombosis and ischaemic stroke. J Thromb Haemost. 2011;9 Suppl 1:92-104.
- Nishimura S, Nagasaki M, Kunishima S, Sawaguchi A, Sakata A, Sakaguchi H, Ohmori T, Manabe I, Italiano JE Jr, Ryu T, Takayama N, Komuro I, Kadowaki T, Eto K, Nagai R. IL-1α induces thrombopoiesis through megakaryocyte rupture in response to acute platelet needs. J Cell Biol. 2015;209(3):453-66.
- Nishizuka Y. The molecular heterogeneity of protein kinase C and its implications for cellular regulation. Nature. 1988;334(6184):661-5.
- Okafor ON, Gorog DA. Endogenous fibrinolysis: an important mediator of thrombus formation and cardiovascular risk. J Am Coll Cardiol 2015; 65: 1683-99.
- Ono Y, Fujii T, Ogita K, Kikkawa U, Igarashi K, Nishizuka Y. The structure, expression, and properties of additional members of the protein kinase C family. J Biol Chem. 1988;263(14):6927-32.
- Pagler TA, Wang M, Mondal M, Murphy AJ, Westerterp M, Moore KJ, Maxfield FR, Tall AR. Deletion of ABCA1 and ABCG1 impairs macrophage migration because of increased Rac1 signaling. Circ Res. 2011;108(2):194-200
- Panteghini M. Assay-related issues in the measurement of cardiac troponins. Clin Chim Acta. 2009;402(1-2):88-93.

- Parikh NI, Gona P, Larson MG, Fox CS, Benjamin EJ, Murabito JM, O'Donnell CJ, Vasan RS, Levy D. Long-term trends in myocardial infarction incidence and case fatality in the National Heart, Lung, and Blood Institute's Framingham Heart study. Circulation. 2009;119(9):1203-10.
- Parker PJ, Lockwood N, Davis K, Kelly JR, Soliman TN, Pardo AL, Marshall JJT, Redmond JM, Vitale M, Silvia Martini. A cancer-associated, genome protective programme engaging PKCε. Adv Biol Regul. 2020;78: 100759.
- Patel SR, Hartwig JH, Italiano JE Jr. The biogenesis of platelets from megakaryocyte proplatelets. J Clin Invest. 2005;115(12):3348-54.
- Paul GK, Sen B, Bari MA, Rahman Z, Jamal F, Bari MS, Sazidur SR. Correlation of platelet count and acute ST-elevation in myocardial infarction. Mymensingh Med J. 2010;19(3):469-73.
- Pears CJ, Thornber K, Auger JM, Hughes CE, Grygielska B, Protty MB, Pearce AC, Watson SP. Differential roles of the PKC novel isoforms, PKCdelta and PKCepsilon, in mouse and human platelets. PLoS One. 2008;3(11): e3793.
- Polanowska-Grabowska R, Simon CG Jr, Gear AR. Platelet adhesion to collagen type I, collagen type IV, von Willebrand factor, fibronectin, laminin and fibrinogen: rapid kinetics under shear. Thromb Haemost. 1999;81(1): 118-23.
- Pope JH, Aufderheide TP, Ruthazer R, Woolard RH, Feldman JA, Beshansky JR, Griffith JL, Selker HP. Missed diagnoses of acute cardiac ischemia in the emergency department. N Engl J Med. 2000;342(16):1163-70.
- Puelacher C, Gugala M, Adamson PD, Shah A, Chapman AR, Anand A, Sabti Z, Boeddinghaus J, Nestelberger T, Twerenbold R, Wildi K, Badertscher P, Rubini Gimenez M, Shrestha S, Sazgary L, Mueller D, Schumacher L, Kozhuharov N, Flores D, du Fay de Lavallaz J, Miro O, Martín-Sánchez FJ, Morawiec B, Fahrni G, Osswald S, Reichlin T, Mills NL, Mueller C. Incidence and outcomes of unstable angina compared with non-ST-elevation myocardial infarction. Heart. 2019;105(18):1423-1431.
- Radico F, Cicchitti V, Zimarino M, De Caterina R. Angina pectoris and myocardial ischemia in the absence of obstructive coronary artery disease: practical considerations for diagnostic tests. JACC Cardiovasc Interv. 2014;7(5):453-63.
- Reimer KA, Jennings RB. The "wavefront phenomenon" of myocardial ischemic cell death. II. Transmural progression of necrosis within the framework of ischemic bed size (myocardium at risk) and collateral flow. Lab Invest. 1979;40(6):633-44.
- Reimer KA, Jennings RB, Tatum AH. Pathobiology of acute myocardial ischemia: metabolic, functional and ultrastructural studies. Am J Cardiol. 1983;52(2):72A-81A.
- Rinder HM, Schuster JE, Rinder CS, Wang C, Schweidler HJ, Smith BR. Correlation of thrombosis with increased platelet turnover in thrombocytosis. Blood. 1998;91(4):1288-94.
- Roffi M, Chew DP, Mukherjee D, Bhatt DL, White JA, Heeschen C, Hamm CW, Moliterno DJ, Califf RM, White HD, Kleiman NS, Théroux P, Topol EJ. Platelet glycoprotein IIb/IIIa inhibitors reduce mortality in diabetic patients with non-ST-segment-elevation acute coronary syndromes. Circulation. 2001;104(23): 2767-71.
- Roffi M, Patrono C, Collet JP, Mueller C, Valgimigli M, Andreotti F, Bax JJ, Borger MA, Brotons C, Chew DP, Gencer B, Hasenfuss G, Kjeldsen K, Lancellotti P, Landmesser U, Mehilli J, Mukherjee D, Storey RF, Windecker S; ESC Scientific Document Group. 2015 ESC Guidelines for the management of acute coronary syndromes in patients presenting without persistent ST-segment elevation: Task Force for the Management of Acute Coronary Syndromes in Patients Presenting without Persistent ST-Segment Elevation of the European Society of Cardiology (ESC). Eur Heart J. 2016;37(3):267-315
- Roffi M, Patrono C, Collet JP, Mueller C, Valgimigli M, Andreotti F, Bax JJ, Borger MA, Brotons C, Chew DP, Gencer B, Hasenfuss G, Kjeldsen K, Lancellotti P, Landmesser U, Mehilli J, Mukherjee D, Storey RF, Windecker S; ESC Scientific Document Group. 2015 ESC Guidelines for the management of acute coronary syndromes in patients presenting without persistent ST-segment elevation: Task Force for the Management of Acute Coronary Syndromes in Patients Presenting

without Persistent ST-Segment Elevation of the European Society of Cardiology (ESC). Eur Heart J. 2016;37(3):267-315.

- Russo G, Zegar C, Giordano A. Advantages and limitations of microarray technology in human cancer. Oncogene. 2003;22(42): 6497-507.
- Sachais BS, Kuo A, Nassar T, Morgan J, Kariko K, Williams KJ, Feldman M, Aviram M, Shah N, Jarett L, Poncz M, Cines DB, Higazi AA. Platelet factor 4 binds to low-density lipoprotein receptors and disrupts the endocytic machinery, resulting in retention of low-density lipoprotein on the cell surface. Blood. 2002;99(10):3613-22.
- Sagris M, Antonopoulos AS, Theofilis P, Oikonomou E, Siasos G, Tsalamandris S, Antoniades C, Brilakis ES, Kaski JC, Tousoulis D. Risk factors profile of young and older patients with Myocardial Infarction. Cardiovasc Res. 2021: cvab264.
- Saurin AT, Durgan J, Cameron AJ, Faisal A, Marber MS, Parker PJ. The regulated assembly of a PKCepsilon complex controls the completion of cytokinesis. Nat Cell Biol. 2008;10(8):891-901.
- Schaap D, Parker PJ. Expression, purification, and characterization of protein kinase C-epsilon. J Biol Chem. 1990;265(13):7301-7.
- Schechtman D, Mochly-Rosen D. Adaptor proteins in protein kinase C-mediated signal transduction. Oncogene. 2001;20(44):6339-47.
- Sharaf BL, Pepine CJ, Kerensky RA, Reis SE, Reichek N, Rogers WJ, Sopko G, Kelsey SF, Holubkov R, Olson M, Miele NJ, Williams DO, Merz CN; WISE Study Group. Detailed angiographic analysis of women with suspected ischemic chest pain (pilot phase data from the NHLBI-sponsored Women's Ischemia Syndrome Evaluation [WISE] Study Angiographic Core Laboratory). Am J Cardiol. 2001;87(8):937-41; A3.
- Shattil SJ, Cunningham M, Hoxie JA. Detection of activated plate- lets in whole blood using activation-dependent monoclonal anti- bodies and flow cytometry. Blood 1987;70(1):307–315.
- Shaw LJ, Shaw RE, Merz CN, Brindis RG, Klein LW, Nallamothu B, Douglas PS, Krone RJ, McKay CR, Block PC, Hewitt K, Weintraub WS, Peterson ED; American College of Cardiology-National Cardiovascular Data Registry Investigators. Impact of ethnicity and gender differences on angiographic coronary artery disease prevalence and in-hospital mortality in the American College of Cardiology-National Cardiovascular Data Registry. Circulation. 2008;117(14):1787-801.
- Shirai Y, Kashiwagi K, Yagi K, Sakai N, Saito N. Distinct effects of fatty acids on translocation of gamma- and epsilon-subspecies of protein kinase C. J Cell Biol. 1998;143(2):511-21.
- Stary HC, Chandler AB, Glagov S, Guyton JR, Insull W, Rosenfeld ME, Schaffer SA, Schwartz CJ, Wagner WD, Wissler RW. A definition of initial, fatty streak, and intermediate lesions of atherosclerosis. A report from the Committee on Vascular Lesions of the Council on Arteriosclerosis, American Heart Association. Arterioscler Thromb. 1994; 14:840–856.
- Stary HC. Natural history and histological classification of atherosclerotic lesions: an update. Arterioscler Thromb Vasc Biol. 2000;20: 1177–1178.
- Stenberg PE, McEver RP, Shuman MA, Jacques YV, Bainton DF. A platelet alpha-granule membrane protein (GMP-140) is expressed on the plasma membrane after activation. J Cell Biol 1985;101(3): 880–886.
- Stepinska J, Lettino M, Ahrens I, Bueno H, Garcia-Castrillo L, Khoury A, Lancellotti P, Mueller C, Muenzel T, Oleksiak A, Petrino R, Guimenez MR, Zahger D, Vrints CJ, Halvorsen S, de Maria E, Lip GY, Rossini R, Claeys M, Huber K. Diagnosis and risk stratification of chest pain patients in the emergency department: focus on acute coronary syndromes. A position paper of the Acute Cardiovascular Care Association. Eur Heart J Acute Cardiovasc Care. 2020;9(1):76-89.
- Tabas I, Williams KJ, Borén J. Subendothelial lipoprotein retention as the initiating process in atherosclerosis: update and therapeutic implications. Circulation. 2007;116(16):1832-44.
- Takahashi M, Mukai H, Oishi K, Isagawa T, Ono Y. Association of immature hypophosphorylated protein kinase cepsilon with an anchoring protein CG-NAP. J Biol Chem. 2000;275(44):34592-6.
- Thygesen K, Alpert JS, Jaffe AS, Chaitman BR, Bax JJ, Morrow DA, White HD; Executive Group on behalf of the Joint European Society of Cardiology (ESC)/American College of Cardiology (ACC)/American Heart Association (AHA)/World Heart Federation (WHF) Task Force for the

Universal Definition of Myocardial Infarction. Fourth Universal Definition of Myocardial Infarction (2018). J Am Coll Cardiol. 2018;72(18):2231-2264.

- Thygesen K, Alpert JS, White HD; Joint ESC/ACCF/AHA/WHF Task Force for the Redefinition of Myocardial Infarction. Universal definition of myocardial infarction. Eur Heart J. 2007;28(20):2525-38
- Timmers L, Pasterkamp G, de Hoog VC, Arslan F, Appelman Y, de Kleijn DP. The innate immune response in reperfused myocardium. Cardiovasc Res. 2012;94(2):276-83.
- Tong M, Seth P, Penington DG. Proplatelets and stress platelets. Blood. 1987;69: 522–528.
- Twerenbold R, Boeddinghaus J, Nestelberger T, Wildi K, Rubini Gimenez M, Badertscher P, Mueller C. Clinical Use of High-Sensitivity Cardiac Troponin in Patients With Suspected Myocardial Infarction. J Am Coll Cardiol. 2017;70(8):996-1012.
- Van Gelder RN, von Zastrow ME, Yool A, Dement WC, Barchas JD, Eberwine JH. Amplified RNA synthesized from limited quantities of heterogeneous cDNA. Proc Natl Acad Sci USA. 1990;87(5):1663-1667.
- Vandesompele J, De Preter K, Pattyn F, Poppe B, Van Roy N, De Paepe A, Speleman F. Accurate normalization of real-time quantitative RT-PCR data by geometric averaging of multiple internal control genes. Genome Biol. 2002;3(7): RESEARCH0034.
- Varga-Szabo D, Pleines I, Nieswandt B. Cell adhesion mechanisms in platelets. Arterioscler Thromb Vasc Biol. 2008;28(3):403-12.
- Vergallo R, Crea F. Atherosclerotic Plaque Healing. N Engl J Med. 2020;383(9):846-857.
- Vergallo R, Porto I, D'Amario D, et al. Coronary atherosclerotic phenotype and plaque healing in patients with recurrent acute coronary syndromes compared with patients with longterm clinical stability: an in vivo optical coherence tomography study. JAMA Cardiol 2019;4:321-9.
- Vernon ST, Coffey S, D'Souza M, Chow CK, Kilian J, Hyun K, Shaw JA, Adams M, Roberts-Thomson P, Brieger D, Figtree GA. ST-Segment-Elevation Myocardial Infarction (STEMI) Patients Without Standard Modifiable Cardiovascular Risk Factors-How Common Are They, and What Are Their Outcomes? J Am Heart Assoc. 2019;8(21): e013296.
- Viemann D, Strey A, Janning A, Jurk K, Klimmek K, Vogl T, Hirono K, Ichida F, Foell D, Kehrel B, Gerke V, Sorg C, Roth J. Myeloid-related proteins 8 and 14 induce a specific inflammatory response in human microvascular endothelial cells. Blood. 2005;105(7):2955-62.
- Vinholt PJ. The role of platelets in bleeding in patients with thrombocytopenia and hematological disease. Clin Chem Lab Med. 2019;57(12):1808-1817.
- Virchow RLK. Archiv fuer pathologische Anatomie und Physiologie und fuer klinische Medizin. 2; 1849:303-309 [Translated in: Ackerknecht, E.H. Rudolf Virchow. Doctor, Statesman, Anthropologist. Madison, University of Wisconsin, 1953, pp 15].
- Virmani R, Burke AP, Kolodgie FD, Farb A. Vulnerable plaque: the pathology of unstable coronary lesions. J Interv Cardiol. 2002;15(6):439-46.
- Virmani R, Kolodgie FD, Burke AP, Farb A, Schwartz SM. Lessons from sudden coronary death: a comprehensive morphological classification scheme for atherosclerotic lesions. Arterioscler Thromb Vasc Biol. 2000; 20: 1262–1275.
- Wang K, Asinger RW, Marriott HJ. ST-segment elevation in conditions other than acute myocardial infarction. N Engl J Med. 2003;349(22):2128-35.
- Wang N, Tall AR. Cholesterol in platelet biogenesis and activation. Blood. 2016;127(16):1949-53.
- Wang Y, Fang C, Gao H, Bilodeau ML, Zhang Z, Croce K, Liu S, Morooka T, Sakuma M, Nakajima K, Yoneda S, Shi C, Zidar D, Andre P, Stephens G, Silverstein RL, Hogg N, Schmaier AH, Simon DI. Platelet-derived S100 family member myeloid-related protein-14 regulates thrombosis. J Clin Invest. 2014;124(5):2160-71.
- Welch RD, Zalenski RJ, Frederick PD, Malmgren JA, Compton S, Grzybowski M, Thomas S, Kowalenko T, Every NR; National Registry of Myocardial Infarction 2 and 3 Investigators. Prognostic value of a normal or nonspecific initial electrocardiogram in acute myocardial infarction. JAMA. 2001;286(16):1977-84.

- Westman PC, Lipinski MJ, Luger D, Waksman R, Bonow RO, Wu E, Epstein SE. Inflammation as a Driver of Adverse Left Ventricular Remodeling After Acute Myocardial Infarction. J Am Coll Cardiol. 2016;67(17):2050-60.
- Weyrich AS, Dixon DA, Pabla R, Elstad MR, McIntyre TM, Prescott SM, Zimmerman GA. Signal-dependent translation of a regulatory protein, Bcl-3, in activated human platelets. Proc Natl Acad Sci USA. 1998;95(10):5556-61.
- Weyrich AS, Lindemann S, Tolley ND, Kraiss LW, Dixon DA, Mahoney TM, Prescott SP, McIntyre TM, Zimmerman GA. Change in protein phenotype without a nucleus: translational control in platelets. Semin Thromb Hemost. 2004;30(4):491-8.
- White HD, Norris RM, Brown MA, Brandt PW, Whitlock RM, Wild CJ. Left ventricular end-systolic volume as the major determinant of survival after recovery from myocardial infarction. Circulation. 1987;76(1):44-51.
- Widimsky P, Wijns W, Fajadet J, de Belder M, Knot J, Aaberge L, Andrikopoulos G, Baz JA, Betriu A, Claeys M, Danchin N, Djambazov S, Erne P, Hartikainen J, Huber K, Kala P, Klinceva M, Kristensen SD, Ludman P, Ferre JM, Merkely B, Milicic D, Morais J, Noc M, Opolski G, Ostojic M, Radovanovic D, De Servi S, Stenestrand U, Studencan M, Tubaro M, Vasiljevic Z, Weidinger F, Witkowski A, Zeymer U; European Association for Percutaneous Cardiovascular Interventions. Reperfusion therapy for ST elevation acute myocardial infarction in Europe: description of the current situation in 30 countries. Eur Heart J. 2010;31(8):943-57.
- Willoughby S, Holmes A, Loscalzo J. Platelets and cardiovascular disease. Eur J Cardiovasc Nurs. 2002;1(4):273-88.
- Xu XR, Carrim N, Neves MA, McKeown T, Stratton TW, Coelho RM, Lei X, Chen P, Xu J, Dai X, Li BX, Ni H. Platelets and platelet adhesion molecules: novel mechanisms of thrombosis and anti-thrombotic therapies. Thromb J. 2016;14(Suppl 1): 29.
- Yoshioka A, Shirakawa R, Nishioka H, Tabuchi A, Higashi T, Ozaki H, Yamamoto A, Kita T, Horiuchi H. Identification of protein kinase Calpha as an essential, but not sufficient, cytosolic factor for Ca2+-induced alpha- and dense-core granule secretion in platelets. J Biol Chem. 2001;276(42):39379-85
- Youssefian T, Cramer EM. Megakaryocyte dense granule components are sorted in multivesicular bodies. Blood. 2000;95(12):4004-7.
- Yusuf S, Mehta SR, Zhao F, Gersh BJ, Commerford PJ, Blumenthal M, Budaj A, Wittlinger T, Fox KA; Clopidogrel in Unstable angina to prevent Recurrent Events Trial Investigators. Early and late effects of clopidogrel in patients with acute coronary syndromes. Circulation. 2003;107(7):966-72.
- Zannas AS, Jia M, Hafner K, Baumert J, Wiechmann T, Pape JC, Arloth J, Ködel M, Martinelli S, Roitman M, Röh S, Haehle A, Emeny RT, Iurato S, Carrillo-Roa T, Lahti J, Räikkönen K, Eriksson JG, Drake AJ, Waldenberger M, Wahl S, Kunze S, Lucae S, Bradley B, Gieger C, Hausch F, Smith AK, Ressler KJ, Müller-Myhsok B, Ladwig KH, Rein T, Gassen NC, Binder EB. Epigenetic upregulation of FKBP5 by aging and stress contributes to NF-κB-driven inflammation and cardiovascular risk. Proc Natl Acad Sci USA. 2019;116(23):11370-11379.
- Zimmet J, Ravid K. Polyploidy: occurrence in nature, mechanisms, and significance for the megakaryocyte-platelet system. Exp Hematol. 2000;28(1):3-16.Agarwal A, Morrone K, Bartenstein M, Zhao ZJ, Verma A, Goel S. Bone marrow fibrosis in primary myelofibrosis: pathogenic mechanisms and the role of TGF-β. Stem Cell Investig. 2016;3: 5.

Part II: References

- Agarwal A, Morrone K, Bartenstein M, Zhao ZJ, Verma A, Goel S. Bone marrow fibrosis in primary myelofibrosis: pathogenic mechanisms and the role of TGF-β. Stem Cell Investig. 2016;3: 5.
- Alshemmari SH, Rajan R, Emadi A. Molecular Pathogenesis and Clinical Significance of Driver Mutations in Primary Myelofibrosis: A Review. Med Princ Pract. 2016;25(6):501–509.
- Alshemmari SH, Rajan R, Emadi A. Molecular Pathogenesis and Clinical Significance of Driver Mutations in Primary Myelofibrosis: A Review. Med Princ Pract. 2016;25(6):501-509.
- Araki M, Yang Y, Masubuchi N, Hironaka Y, Takei H, Morishita S, Mizukami Y, Kan S, Shirane S, Edahiro Y, Sunami Y, Ohsaka A, Komatsu N. Activation of the thrombopoietin receptor by mutant calreticulin in CALR-mutant myeloproliferative neoplasms. Blood. 2016;127(10):1307-16.
- Arber DA, Orazi A, Hasserjian R, Thiele J, Borowitz MJ, Le Beau MM, Bloomfield CD, Cazzola M, Vardiman JW. The 2016 revision to the World Health Organization classification of myeloid neoplasms and acute leukemia. Blood. 2016;127(20):2391-405.
- Balduini A, Badalucco S, Pugliano MT, Baev D, De Silvestri A, Cattaneo M, Rosti V, Barosi G. In vitro megakaryocyte differentiation and proplatelet formation in Ph-negative classical myeloproliferative neoplasms: distinct patterns in the different clinical phenotypes. PLoS One. 2011;6(6):e21015.
- Bao EL, Nandakumar SK, Liao X, Bick AG, Karjalainen J, Tabaka M, Gan OI, Havulinna AS, Kiiskinen TTJ, Lareau CA, de Lapuente Portilla AL, Li B, Emdin C, Codd V, Nelson CP, Walker CJ, Churchhouse C, de la Chapelle A, Klein DE, Nilsson B, Wilson PWF, Cho K, Pyarajan S, Gaziano JM, Samani NJ; FinnGen; 23andMe Research Team, Regev A, Palotie A, Neale BM, Dick JE, Natarajan P, O'Donnell CJ, Daly MJ, Milyavsky M, Kathiresan S, Sankaran VG. Inherited myeloproliferative neoplasm risk affects haematopoietic stem cells. Nature. 2020;586(7831):769-775.
- Barbui T, Carobbio A, Finazzi G, Guglielmelli P, Salmoiraghi S, Rosti V, Rambaldi A, Vannucchi AM, Barosi G. Elevated C-reactive protein is associated with shortened leukemia-free survival in patients with myelofibrosis. Leukemia. 2013;27(10):2084-6.
- Barbui T, Carobbio A, Finazzi G, Vannucchi AM, Barosi G, Antonioli E, Guglielmelli P, Pancrazzi A, Salmoiraghi S, Zilio P, Ottomano C, Marchioli R, Cuccovillo I, Bottazzi B, Mantovani A, Rambaldi A; AGIMM and IIC Investigators. Inflammation and thrombosis in essential thrombocythemia and polycythemia vera: different role of C-reactive protein and pentraxin 3. Haematologica. 2011;96(2):315-8.
- Barbui T, Thiele J, Gisslinger H, Kvasnicka HM, Vannucchi AM, Guglielmelli P, Orazi A, Tefferi A. The 2016 WHO classification and diagnostic criteria for myeloproliferative neoplasms: document summary and in-depth discussion. Blood Cancer J. 2018;8(2):15.
- Barone M, Catani L, Ricci F, Romano M, Forte D, Auteri G, Bartoletti D, Ottaviani E, Tazzari PL, Vianelli N, Cavo M, Palandri F. The role of circulating monocytes and JAK inhibition in the infectious-driven inflammatory response of myelofibrosis. Oncoimmunology. 2020;9(1):1782575.
- Barosi G, Campanelli R, Catarsi P, De Amici M, Abbà C, Viarengo G, Villani L, Gale RP, Rosti V, Massa M. Plasma sIL-2Rα levels are associated with disease progression in myelofibrosis with $JAK2^{V617F}$ but not CALR mutation. Leuk Res. 2020;90: 106319.
- Barosi G, Massa M, Campanelli R, Fois G, Catarsi P, Viarengo G, Villani L, Poletto V, Bosoni T, Magrini U, Gale RP, Rosti V. Primary myelofibrosis: Older age and high JAK2V617F allele burden are associated with elevated plasma high-sensitivity C-reactive protein levels and a phenotype of progressive disease. Leuk Res. 2017;60:18-23.
- Barosi G. Myelofibrosis with myeloid metaplasia: diagnostic definition and prognostic classification for clinical studies and treatment guidelines. J Clin Oncol. 1999;17(9):2954-70.
- Bartoli C, Civatte M, Pellissier JF, Figarella-Branger D. CCR2A and CCR2B, the two isoforms of the monocyte chemoattractant protein-1 receptor are up-regulated and expressed by different cell subsets in idiopathic inflammatory myopathies. Acta Neuropathol. 2001;102(4):385-92.

- Bauermeister DE. Quantitation of bone marrow reticulin - a normal range. Am J Clin Pathol 1971;56:24–31.
- Beauchemin H, Shooshtharizadeh P, Pinder J, Dellaire G, Möröy T. Dominant negative Gfi1b mutations cause moderate thrombocytopenia and an impaired stress thrombopoiesis associated with mild erythropoietic abnormalities in mice. Haematologica. 2020;105(10):2457-2470.
- Biswas SK, Sodhi A. Tyrosine phosphorylation-mediated signal transduction in MCP-1-induced macrophage activation: role for receptor dimerization, focal adhesion protein complex and JAK/STAT pathway. Int Immunopharmacol. 2002;2(8):1095-107.
- Bjørn ME, Hasselbalch HC. The Role of Reactive Oxygen Species in Myelofibrosis and Related Neoplasms. Mediators Inflamm. 2015;2015: 648090.
- Blank U, Karlsson S. The role of Smad signaling in hematopoiesis and translational hematology. Leukemia. 2011;25(9):1379–1388.
- Bogani C, Ponziani V, Guglielmelli P, Desterke C, Rosti V, Bosi A, Le Bousse-Kerdilès MC, Barosi G, Vannucchi AM; Myeloproliferative Disorders Research Consortium. Hypermethylation of CXCR4 promoter in CD34+ cells from patients with primary myelofibrosis. Stem Cells. 2008;26(8):1920-30.
- Boring L, Gosling J, Cleary M, Charo IF. Decreased lesion formation in CCR2-/- mice reveals a role for chemokines in the initiation of atherosclerosis. Nature. 1998;394(6696):894-7.
- Bottazzi B, Riboli E, Mantovani A. Aging, inflammation and cancer. Semin Immunol. 2018; 40:74-82.
- Bourantas KL, Hatzimichael EC, Makis AC, Chaidos A, Kapsali ED, Tsiara S, Mavridis A. Serum beta-2-microglobulin, TNF-alpha and interleukins in myeloproliferative disorders. Eur J Haematol. 1999;63(1):19-25.
- Brody SL, Gunsten SP, Luehmann HP, Sultan DH, Hoelscher M, Heo GS, Pan J, Koenitzer JR, Lee EC, Huang T, Mpoy C, Guo S, Laforest R, Salter A, Russell TD, Shifren A, Combadiere C, Lavine KJ, Kreisel D, Humphreys BD, Rogers BE, Gierada DS, Byers DE, Gropler RJ, Chen DL, Atkinson JJ, Liu Y. Chemokine Receptor 2-targeted Molecular Imaging in Pulmonary Fibrosis. A Clinical Trial. Am J Respir Crit Care Med. 2021;203(1):78-89.
- Burns K, Duggan B, Atkinson EA, Famulski KS, Nemer M, Bleackley RC, Michalak M. Modulation of gene expression by calreticulin binding to the glucocorticoid receptor. Nature. 1994;367(6462):476-80.
- Cabagnols X, Defour JP, Ugo V, Ianotto JC, Mossuz P, Mondet J, Girodon F, Alexandre JH, Mansier O, Viallard JF, Lippert E, Murati A, Mozziconacci MJ, Saussoy P, Vekemans MC, Knoops L, Pasquier F, Ribrag V, Solary E, Plo I, Constantinescu SN, Casadevall N, Vainchenker W, Marzac C, Bluteau O. Differential association of calreticulin type 1 and type 2 mutations with myelofibrosis and essential thrombocytemia: relevance for disease evolution. Leukemia. 2015;29(1):249-52.
- Cacemiro MDC, Cominal JG, Tognon R, Nunes NS, Simões BP, Figueiredo-Pontes LL, Catto LFB, Traina F, Souto EX, Zambuzi FA, Frantz FG, Castro FA. Philadelphia-negative myeloproliferative neoplasms as disorders marked by cytokine modulation. Hematol Transfus Cell Ther. 2018;40(2):120-131.
- Campanelli R, Rosti V, Villani L, Castagno M, Moretti E, Bonetti E, Bergamaschi G, Balduini A, Barosi G, Massa M. Evaluation of the bioactive and total transforming growth factor β1 levels in primary myelofibrosis. Cytokine. 2011;53(1):100-6.
- Caramazza D, Begna KH, Gangat N, Vaidya R, Siragusa S, Van Dyke DL, Hanson C, Pardanani A, Tefferi A. Refined cytogenetic-risk categorization for overall and leukemia-free survival in primary myelofibrosis: a single center study of 433 patients. Leukemia. 2011;25(1):82-8.
- Ceglia I, Dueck AC, Masiello F, Martelli F, He W, Federici G, Petricoin EF 3rd, Zeuner A, Iancu-Rubin C, Weinberg R, Hoffman R, Mascarenhas J, Migliaccio AR. Preclinical rationale for TGF-β inhibition as a therapeutic target for the treatment of myelofibrosis. Exp Hematol. 2016;44(12):1138-1155.e4.
- Cervantes F, Dupriez B, Pereira A, Passamonti F, Reilly JT, Morra E, Vannucchi AM, Mesa RA, Demory JL, Barosi G, Rumi E, Tefferi A. New prognostic scoring system for primary myelofibrosis based on a study of the International Working Group for Myelofibrosis Research and Treatment. Blood. 2009;113(13):2895-901.

- Cervantes F, Pereira A, Esteve J, Rafel M, Cobo F, Rozman C, Montserrat E. Identification of 'short-lived' and 'long-lived' patients at presentation of idiopathic myelofibrosis. Br J Haematol. 1997;97(3):635-40.
- Cervantes F, Vannucchi AM, Kiladjian JJ, Al-Ali HK, Sirulnik A, Stalbovskaya V, McQuitty M, Hunter DS, Levy RS, Passamonti F, Barbui T, Barosi G, Harrison CN, Knoops L, Gisslinger H; COMFORT-II investigators. Three-year efficacy, safety, and survival findings from COMFORT-II, a phase 3 study comparing ruxolitinib with best available therapy for myelofibrosis. Blood. 2013;122(25):4047-53.
- Chang F, Lee JT, Navolanic PM, Steelman LS, Shelton JG, Blalock WL, Franklin RA, McCubrey JA. Involvement of PI3K/Akt pathway in cell cycle progression, apoptosis, and neoplastic transformation: a target for cancer chemotherapy. Leukemia. 2003;17(3):590-603.
- Charo IF, Myers SJ, Herman A, Franci C, Connolly AJ, Coughlin SR. Molecular cloning and functional expression of two monocyte chemoattractant protein 1 receptors reveals alternative splicing of the carboxyl-terminal tails. Proc Natl Acad Sci U S A. 1994;91(7):2752-2756.
- Chen E, Schneider RK, Breyfogle LJ, Rosen EA, Poveromo L, Elf S, Ko A, Brumme K, Levine R, Ebert BL, Mullally A. Distinct effects of concomitant Jak2V617F expression and Tet2 loss in mice promote disease progression in myeloproliferative neoplasms. Blood. 2015;125(2):327-35.
- Chen L, Deng H, Cui H, Fang J, Zuo Z, Deng J, Li Y, Wang X, Zhao L. Inflammatory responses and inflammation-associated diseases in organs. Oncotarget. 2017;9(6):7204-7218.
- Chou JM, Li CY, Tefferi A. Bone marrow immunohistochemical studies of angiogenic cytokines and their receptors in myelofibrosis with myeloid metaplasia. Leuk Res. 2003;27(6):499-504.
- Chun E, Lavoie S, Michaud M, Gallini CA, Kim J, Soucy G, Odze R, Glickman JN, Garrett WS. CCL2 Promotes Colorectal Carcinogenesis by Enhancing Polymorphonuclear Myeloid-Derived Suppressor Cell Population and Function. Cell Rep. 2015;12(2):244-57.
- Cignetti A, Vallario A, Roato I, Circosta P, Strola G, Scielzo C, Allione B, Garetto L, Caligaris-Cappio F, Ghia P. The characterization of chemokine production and chemokine receptor expression reveals possible functional crosstalks in AML blasts with monocytic differentiation. Exp Hematol. 2003;31(6):495-503.
- Ciurea SO, Merchant D, Mahmud N, Ishii T, Zhao Y, Hu W, Bruno E, Barosi G, Xu M, Hoffman R. Pivotal contributions of megakaryocytes to the biology of idiopathic myelofibrosis. Blood. 2007;110(3):986-93.
- Cochran BH, Reel AC, Stiles CD. Molecular cloning of gene sequences regulated by platelet-derived growth factor. Cell 1983;33: 939-47.
- Codd V, Nelson CP, Albrecht E, Mangino M, Deelen J, Buxton JL, Hottenga JJ, Fischer K, Esko T, Surakka I, Broer L, Nyholt DR, Mateo Leach I, Salo P, Hägg S, Matthews MK, Palmen J, Norata GD, O'Reilly PF, Saleheen D, Amin N, Balmforth AJ, Beekman M, de Boer RA, Böhringer S, Braund PS, Burton PR, de Craen AJ, Denniff M, Dong Y, Douroudis K, Dubinina E, Eriksson JG, Garlaschelli K, Guo D, Hartikainen AL, Henders AK, Houwing-Duistermaat JJ, Kananen L, Karssen LC, Kettunen J, Klopp N, Lagou V, van Leeuwen EM, Madden PA, Mägi R, Magnusson PK, Männistö S, McCarthy MI, Medland SE, Mihailov E, Montgomery GW, Oostra BA, Palotie A, Peters A, Pollard H, Pouta A, Prokopenko I, Ripatti S, Salomaa V, Suchiman HE, Valdes AM, Verweij N, Viñuela A, Wang X, Wichmann HE, Widen E, Willemsen G, Wright MJ, Xia K, Xiao X, van Veldhuisen DJ, Catapano AL, Tobin MD, Hall AS, Blakemore AI, van Gilst WH, Zhu H; CARDIoGRAM consortium, Erdmann J, Reilly MP, Kathiresan S, Schunkert H, Talmud PJ, Pedersen NL, Perola M, Ouwehand W, Kaprio J, Martin NG, van Duijn CM, Hovatta I, Gieger C, Metspalu A, Boomsma DI, Jarvelin MR, Slagboom PE, Thompson JR, Spector TD, van der Harst P, Samani NJ. Identification of seven loci affecting mean telomere length and their association with disease. Nat Genet. 2013;45(4):422-7, 427e1-2.
- Coffer PJ, Koenderman L, de Groot RP. The role of STATs in myeloid differentiation and leukemia. Oncogene. 2000;19(21):2511-22.
- Colobran R, Pujol-Borrell R, Armengol MP, Juan M. The chemokine network. II. On how polymorphisms and alternative splicing increase the number of molecular species and configure intricate patterns of disease susceptibility. Clin Exp Immunol. 2007;150: 1–12.

- Cominal JG, Cacemiro MDC, Berzoti-Coelho MG, Pereira IEG, Frantz FG, Souto EX, Covas DT, de Figueiredo-Pontes LL, Oliveira MC, Malmegrim KCR, de Castro FA. Bone marrow soluble mediator signatures of patients with Philadelphia chromosome-negative myeloproliferative neoplasms. Front Oncol. 2021;11: 665037.
- Craver BM, Ramanathan G, Hoang S, Chang X, Mendez Luque LF, Brooks S, Lai HY, Fleischman AG. N-acetylcysteine inhibits thrombosis in a murine model of myeloproliferative neoplasm. Blood Adv. 2020;4(2):312-321.
- Dameshek W. Some speculations on the myeloproliferative syndromes. Blood. 1951;6: 372–5.
- de Lemos JA, Morrow DA, Sabatine MS, Murphy SA, Gibson CM, Antman EM, McCabe CH, Cannon CP, Braunwald E. Association between plasma levels of monocyte chemoattractant protein-1 and long-term clinical outcomes in patients with acute coronary syndromes. Circulation. 2003;107(5): 690-5.
- Deininger M, Radich J, Burn TC, Huber R, Paranagama D, Verstovsek S. The effect of long-term ruxolitinib treatment on JAK2p.V617F allele burden in patients with myelofibrosis. Blood 2015; 126: 1551–1554.
- Derijk RH, Schaaf MJ, Turner G, Datson NA, Vreugdenhil E, Cidlowski J, de Kloet ER, Emery P, Sternberg EM, Detera-Wadleigh SD. A human glucocorticoid receptor gene variant that increases the stability of the glucocorticoid receptor beta-isoform mRNA is associated with rheumatoid arthritis. J Rheumatol. 2001;28(11):2383-8.
- Duggan MA, Anderson WF, Altekruse S, Penberthy L, Sherman ME. The Surveillance, Epidemiology, and End Results (SEER) Program and Pathology: Toward Strengthening the Critical Relationship. Am J Surg Pathol. 2016;40(12): e94-e102.
- Durham GA, Williams JJL, Nasim MT, Palmer TM. Targeting SOCS Proteins to Control JAK-STAT Signalling in Disease. Trends Pharmacol Sci. 2019;40(5):298-308.
- Dvorak HF. Tumors: wounds that do not heal. Similarities between tumor stroma generation and wound healing. N Engl J Med. 1986;315(26):1650-9.
- Ekert JE, Murray LA, Das AM, Sheng H, Giles-Komar J, Rycyzyn MA. Chemokine (C-C motif) ligand 2 mediates direct and indirect fibrotic responses in human and murine cultured fibrocytes. Fibrogenesis Tissue Repair. 2011;4(1):23.
- Elena C, Passamonti F, Rumi E, Malcovati L, Arcaini L, Boveri E, Merli M, Pietra D, Pascutto C, Lazzarino M. Red blood cell transfusion-dependency implies a poor survival in primary myelofibrosis irrespective of IPSS and DIPSS. Haematologica. 2011;96(1):167-70.
- Elf S, Abdelfattah NS, Chen E, Perales-Patón J, Rosen EA, Ko A, Peisker F, Florescu N, Giannini S, Wolach O, Morgan EA, Tothova Z, Losman JA, Schneider RK, Al-Shahrour F, Mullally A. Mutant Calreticulin Requires Both Its Mutant C-terminus and the Thrombopoietin Receptor for Oncogenic Transformation. Cancer Discov. 2016;6(4):368-81.
- Erba BG, Gruppi C, Corada M, Pisati F, Rosti V, Bartalucci N, Villeval JL, Vannucchi AM, Barosi G, Balduini A, Dejana E. Endothelial-to-Mesenchymal Transition in Bone Marrow and Spleen of Primary Myelofibrosis. Am J Pathol. 2017;187(8):1879-1892.
- Estrov Z, Kurzrock R, Wetzler M, Kantarjian H, Blake M, Harris D, Gutterman JU, Talpaz M. Suppression of chronic myelogenous leukemia colony growth by interleukin-1 (IL-1) receptor antagonist and soluble IL-1 receptors: a novel application for inhibitors of IL-1 activity. Blood. 1991;78(6):1476-84.
- Falanga A, Marchetti M. Thrombosis in myeloproliferative neoplasms. Semin Thromb Hemost. 2014;40(3):348-58.
- Ferreira MA, Hottenga JJ, Warrington NM, Medland SE, Willemsen G, Lawrence RW, Gordon S, de Geus EJ, Henders AK, Smit JH, Campbell MJ, Wallace L, Evans DM, Wright MJ, Nyholt DR, James AL, Beilby JP, Penninx BW, Palmer LJ, Frazer IH, Montgomery GW, Martin NG, Boomsma DI. Sequence variants in three loci influence monocyte counts and erythrocyte volume. Am J Hum Genet. 2009;85(5):745-9.
- Ferrer-Marín F, Arroyo AB, Bellosillo B, Cuenca EJ, Zamora L, Hernández-Rivas JM, Hernández-Boluda JC, Fernandez-Rodriguez C, Luño E, García Hernandez C, Kerguelen A, Fiallo-Suárez DV,

Gómez-Casares MT, Ayala R, Vélez P, Boqué C, García-Gutierrez V, Arrizabalaga B, Estrada N, Cifuentes R, Arcas I, de Los Reyes-García AM, Besses C, Vicente V, Alvarez-Larrán A, Teruel-Montoya R, González-Conejero R, Martínez C; GEMFIN Group. miR-146a rs2431697 identifies myeloproliferative neoplasm patients with higher secondary myelofibrosis progression risk. Leukemia. 2020;34(10):2648-2659.

- Ferrucci L, Fabbri E. Inflammageing: chronic inflammation in ageing, cardiovascular disease, and frailty. Nat Rev Cardiol. 2018;15(9):505-522.
- Fisher DAC, Fowles JS, Zhou A, Oh ST. Inflammatory Pathophysiology as a Contributor to Myeloproliferative Neoplasms. Front Immunol. 2021;12: 683401.
- Fisher DAC, Malkova O, Engle EK, Miner CA, Fulbright MC, Behbehani GK, Collins TB, Bandyopadhyay S, Zhou A, Nolan GP, Oh ST. Mass cytometry analysis reveals hyperactive NF Kappa B signaling in myelofibrosis and secondary acute myeloid leukemia. Leukemia. 2017;31(9):1962-1974.
- Fleischman AG. Inflammation as a Driver of Clonal Evolution in Myeloproliferative Neoplasm. Mediators Inflamm. 2015; 2015:606819.
- Freter RR, Alberta JA, Hwang GY, Wrentmore AL, Stiles CD. Platelet-derived growth factor induction of the immediate-early gene MCP-1 is mediated by NF-kappaB and a 90-kDa phosphoprotein coactivator. J Biol Chem. 1996;271(29):17417-24.
- Funakoshi-Tago M, Pelletier S, Moritake H, Parganas E, Ihle JN. Jak2 FERM domain interaction with the erythropoietin receptor regulates Jak2 kinase activity. Mol Cell Biol. 2008;28(5):1792-801.
- Gangat N, Caramazza D, Vaidya R, George G, Begna K, Schwager S, Van Dyke D, Hanson C, Wu W, Pardanani A, Cervantes F, Passamonti F, Tefferi A. DIPSS plus: a refined Dynamic International Prognostic Scoring System for primary myelofibrosis that incorporates prognostic information from karyotype, platelet count, and transfusion status. J Clin Oncol. 2011;29(4):392-7.
- Gao N, Zhang Z, Jiang BH, Shi X. Role of PI3K/AKT/mTOR signaling in the cell cycle progression of human prostate cancer. Biochem Biophys Res Commun. 2003;310(4):1124-32.
- Gardai SJ, McPhillips KA, Frasch SC, et al: Cell-surface calreticulin initiates clearance of viable or apoptotic cells through trans-activa- tion of LRP on the phagocyte. Cell 2005;123: 321–334.
- Geyer HL, Kosiorek H, Dueck AC, Scherber R, Slot S, Zweegman S, Te Boekhorst PA, Senyak Z, Schouten HC, Sackmann F, Fuentes AK, Hernández-Maraver D, Pahl HL, Griesshammer M, Stegelmann F, Döhner K, Lehmann T, Bonatz K, Reiter A, Boyer F, Etienne G, Ianotto JC, Ranta D, Roy L, Cahn JY, Harrison CN, Radia D, Muxi P, Maldonado N, Besses C, Cervantes F, Johansson PL, Barbui T, Barosi G, Vannucchi AM, Paoli C, Passamonti F, Andreasson B, Ferrari ML, Rambaldi A, Samuelsson J, Cannon K, Birgegard G, Xiao Z, Xu Z, Zhang Y, Sun X, Xu J, Kiladjian JJ, Zhang P, Gale RP, Mesa RA. Associations between gender, disease features and symptom burden in patients with myeloproliferative neoplasms: an analysis by the MPN QOL International Working Group. Haematologica. 2017;102(1):85-93.
- Ghoreschi K, Laurence A, O'Shea JJ. Janus kinases in immune cell signaling. Immunol Rev. 2009;228(1):273-287.
- Giaccherini M, Macauda A, Sgherza N, Sainz J, Gemignani F, Maldonado JMS, Jurado M, Tavano F, Mazur G, Jerez A, Góra-Tybor J, Gołos A, Mohedo FH, Lopez JM, Várkonyi J, Spadano R, Butrym A, Canzian F, Campa D. Genetic polymorphisms associated with telomere length and risk of developing myeloproliferative neoplasms. Blood Cancer J. 2020;10(8):89.
- Gianelli U, Vener C, Bossi A. The European Consensus on grading of bone marrow fibrosis allows a better prognostication of patients with primary myelofibrosis. Mod Pathol. 2012; 25(9):1193-1202.
- Greiner G, Witzeneder N, Berger A, Schmetterer K, Eisenwort G, Schiefer AI, Roos S, Popow-Kraupp T, Müllauer L, Zuber J, Sexl V, Kenner L, Sperr WR, Valent P, Mayerhofer M, Hoermann G. CCL2 is a KIT D816V-dependent modulator of the bone marrow microenvironment in systemic mastocytosis. Blood. 2017;129(3):371-382.
- Grewal IS, Rutledge BJ, Fiorillo JA, Gu L, Gladue RP, Flavell RA, Rollins BJ. Transgenic monocyte chemoattractant protein-1 (MCP-1) in pancreatic islets produces monocyte-rich insulitis without

diabetes: abrogation by a second transgene expressing systemic MCP-1. J Immunol 1997;159: 401-8.

- Gschwandtner M, Derler R, Midwood KS. More Than Just Attractive: How CCL2 Influences Myeloid Cell Behavior Beyond Chemotaxis. Front Immunol. 2019;10: 2759.
- Gu W, Yao L, Li L, Zhang J, Place AT, Minshall RD, Liu G. ICAM-1 regulates macrophage polarization by suppressing MCP-1 expression via miR-124 upregulation. Oncotarget. 2017;8(67):111882-111901.
- Guglielmelli P, Biamonte F, Score J, Hidalgo-Curtis C, Cervantes F, Maffioli M, Fanelli T, Ernst T, Winkelman N, Jones AV, Zoi K, Reiter A, Duncombe A, Villani L, Bosi A, Barosi G, Cross NC, Vannucchi AM. EZH2 mutational status predicts poor survival in myelofibrosis. Blood. 2011;118(19):5227-34.
- Guglielmelli P, Lasho TL, Rotunno G, Mudireddy M, Mannarelli C, Nicolosi M, Pacilli A, Pardanani A, Rumi E, Rosti V, Hanson CA, Mannelli F, Ketterling RP, Gangat N, Rambaldi A, Passamonti F, Barosi G, Barbui T, Cazzola M, Vannucchi AM, Tefferi A. MIPSS70: Mutation-Enhanced International Prognostic Score System for Transplantation-Age Patients With Primary Myelofibrosis. J Clin Oncol. 2018;36(4):310-318.
- Guglielmelli P, Lasho TL, Rotunno G, Score J, Mannarelli C, Pancrazzi A, Biamonte F, Pardanani A, Zoi K, Reiter A, Duncombe A, Fanelli T, Pietra D, Rumi E, Finke C, Gangat N, Ketterling RP, Knudson RA, Hanson CA, Bosi A, Pereira A, Manfredini R, Cervantes F, Barosi G, Cazzola M, Cross NC, Vannucchi AM, Tefferi A. The number of prognostically detrimental mutations and prognosis in primary myelofibrosis: an international study of 797 patients. Leukemia. 2014 Sep;28(9):1804-10.
- Gunn MD, Nelken NA, Liao X, Williams LT. Monocyte chemoattractant protein-1 is sufficient for the chemotaxis of monocytes and lymphocytes in transgenic mice but requires an additional stimulus for inflammatory activation. J Immunol, 1997;158:376-83.
- Haan S, Margue C, Engrand A, Rolvering C, Schmitz-Van de Leur H, Heinrich PC, Behrmann I, Haan C. Dual role of the Jak1 FERM and kinase domains in cytokine receptor binding and in stimulation-dependent Jak activation. J Immunol. 2008;180(2):998-1007.
- Hanley JA, McNeil BJ. The meaning and use of the area under a receiver operating characteristic (ROC) curve. Radiology. 1982;143(1):29-36.
- Hao Q, Vadgama JV, Wang P. CCL2/CCR2 signaling in cancer pathogenesis. Cell Commun Signal. 2020;18(1):82.
- Harrison CN, Vannucchi AM, Kiladjian JJ, Al-Ali HK, Gisslinger H, Knoops L, Cervantes F, Jones MM, Sun K, McQuitty M, Stalbovskaya V, Gopalakrishna P, Barbui T. Long-term findings from COMFORT-II, a phase 3 study of ruxolitinib vs best available therapy for myelofibrosis. Leukemia. 2016;30(8):1701-7.
- Hasselbalch HC. Chronic inflammation as a promotor of mutagenesis in essential thrombocythemia, polycythemia vera and myelofibrosis. A human inflammation model for cancer development? Leuk Res. 2013;37(2):214-20.
- Hasselbalch HC. Idiopathic myelofibrosis--an update with particular reference to clinical aspects and prognosis. Int J Clin Lab Res.1993;23: 124-38.
- Hasselbalch HC. The role of cytokines in the initiation and progression of myelofibrosis. Cytokine Growth Factor Rev. 2013;24(2):133-45.
- Hermouet S, Vilaine M. The JAK2 46/1 haplotype: a marker of inappropriate myelomonocytic response to cytokine stimulation, leading to increased risk of inflammation, myeloid neoplasm, and impaired defense against infection? Haematologica. 2011;96(11):1575-9.
- Hinds DA, Barnholt KE, Mesa RA, Kiefer AK, Do CB, Eriksson N, Mountain JL, Francke U, Tung JY, Nguyen HM, Zhang H, Gojenola L, Zehnder JL, Gotlib J. Germ line variants predispose to both JAK2 V617F clonal hematopoiesis and myeloproliferative neoplasms. Blood. 2016;128(8):1121-8.
- Ho CL, Lasho TL, Butterfield JH, Tefferi A. Global cytokine analysis in myeloproliferative disorders. Leuk Res. 2007;31(10):1389-92.

- Hsu HC, Tsai WH, Jiang ML, Ho CH, Hsu ML, Ho CK, Wang SY. Circulating levels of thrombopoietic and inflammatory cytokines in patients with clonal and reactive thrombocytosis. J Lab Clin Med. 1999;134(4):392-7.
- Hua Y, Bergers G. Tumors vs. Chronic Wounds: An Immune Cell's Perspective. Front Immunol. 2019;10:2178.
- Huang C, Foster SR, Shah AD, Kleifeld O, Canals M, Schittenhelm RB, Stone MJ. Phosphoproteomic characterization of the signaling network resulting from activation of the chemokine receptor CCR2. J Biol Chem. 2020;295(19):6518-6531.
- Hussein K, Pardanani AD, Van Dyke DL, Hanson CA, Tefferi A. International Prognostic Scoring System-independent cytogenetic risk categorization in primary myelofibrosis. Blood. 2010;115(3):496-9.
- Jäger R, Gisslinger H, Fuchs E, Bogner E, Milosevic Feenstra JD, Weinzierl J, Schischlik F, Gisslinger B, Schalling M, Zörer M, Krejcy K, Klade C, Kralovics R. Germline genetic factors influence the outcome of interferon-α therapy in polycythemia vera. Blood. 2021;137(3):387-391.
- James C, Ugo V, Le Couédic JP, Staerk J, Delhommeau F, Lacout C, Garçon L, Raslova H, Berger R, Bennaceur-Griscelli A, Villeval JL, Constantinescu SN, Casadevall N, Vainchenker W. A unique clonal JAK2 mutation leading to constitutive signalling causes polycythaemia vera. Nature. 2005;434(7037):1144-8.
- Jia R, Kralovics R. Progress in elucidation of molecular pathophysiology of myeloproliferative neoplasms and its application to therapeutic decisions. Int J Hematol. 2020;111(2):182-191.
- Jiang Y, Valente AJ, Williamson MJ, Zhang L, Graves DT. Post-translational modification of a monocyte-specific chemoattractant synthesized by glioma, osteosarcoma, and vascular smooth muscle cells. J Biol Chem 1990;265: 18318, 21.
- Jutzi JS, Mullally A. Remodeling the Bone Marrow Microenvironment - A Proposal for Targeting Pro-inflammatory Contributors in MPN. Front Immunol. 2020;11: 2093.
- Karantanos T, Chaturvedi S, Braunstein EM, Spivak J, Resar L, Karanika S, Williams DM, Rogers O, Gocke CD, Moliterno AR. Sex determines the presentation and outcomes in MPN and is related to sex-specific differences in the mutational burden. Blood Adv. 2020;4(12):2567-2576.
- Katsumura KR, Bresnick EH; GATA Factor Mechanisms Group. The GATA factor revolution in hematology. Blood. 2017;129(15):2092-2102.
- Kilpivaara O, Mukherjee S, Schram AM, Wadleigh M, Mullally A, Ebert BL, Bass A, Marubayashi S, Heguy A, Garcia-Manero G, Kantarjian H, Offit K, Stone RM, Gilliland DG, Klein RJ, Levine RL. A germline JAK2 SNP is associated with predisposition to the development of JAK2(V617F)-positive myeloproliferative neoplasms. Nat Genet. 2009;41(4):455-9.
- Klampfl T, Gisslinger H, Harutyunyan AS, Nivarthi H, Rumi E, Milosevic JD, Them NC, Berg T, Gisslinger B, Pietra D, Chen D, Vladimer GI, Bagienski K, Milanesi C, Casetti IC, Sant'Antonio E, Ferretti V, Elena C, Schischlik F, Cleary C, Six M, Schalling M, Schönegger A, Bock C, Malcovati L, Pascutto C, Superti-Furga G, Cazzola M, Kralovics R. Somatic mutations of calreticulin in myeloproliferative neoplasms. N Engl J Med. 2013;369(25):2379-90.
- Kleppe et al., M, Kwak M, Koppikar P, Riester M, Keller M, Bastian L, Hricik T, Bhagwat N, McKenney AS, Papalexi E, Abdel-Wahab O, Rampal R, Marubayashi S, Chen JJ, Romanet V, Fridman JS, Bromberg J, Teruya-Feldstein J, Murakami M, Radimerski T, Michor F, Fan R, Levine RL. JAK-STAT pathway activation in malignant and nonmalignant cells contributes to MPN pathogenesis and therapeutic response. Cancer Discov. 2015;5(3):316-31.
- Ko J, Yun CY, Lee JS, Kim JH, Kim IS. p38 MAPK and ERK activation by 9-cis-retinoic acid induces chemokine receptors CCR1 and CCR2 expression in human monocytic THP-1 cells. Exp Mol Med. 2007;39(2):129-38.
- Kramer F, Dernedde J, Mezheyeuski A, Tauber R, Micke P, Kappert K. Platelet-derived growth factor receptor β activation and regulation in murine myelofibrosis. Haematologica. 2020;105(8):2083-2094.
- Kröger N, Holler E, Kobbe G. Allogeneic stem cell transplantation after reduced-intensity conditioning in patients with myelofibrosis: a prospective, multicentre study of the Chronic Leukemia

Working Party of the European Group for Blood and Marrow Transplantation. Blood. 2009; 114(26):5264-5270.

- Kröger NM, Deeg JH, Olavarria E. Indication and management of allogeneic stem cell transplantation in primary myelofibrosis: a consensus process by an EBMT/ELN international working group. Leukemia. 2015; 29(11):2126-2133.
- Kurihara T, Warr G, Loy J, Bravo R. Defects in macrophage recruitment and host defense in mice lacking the CCR2 chemokine receptor. J Exp Med 1997;186: 1757-62.
- Kuroda N, Masuya M, Tawara I, Tsuboi J, Yoneda M, Nishikawa K, Kageyama Y, Hachiya K, Ohishi K, Miwa H, Yamada R, Hamada Y, Tanaka K, Kato T, Takei Y, Katayama N. Infiltrating $CCR2^{+}$ monocytes and their progenies, fibrocytes, contribute to colon fibrosis by inhibiting collagen degradation through the production of TIMP-1. Sci Rep. 2019;9(1):8568.
- Landskron G, De la Fuente M, Thuwajit P, Thuwajit C, Hermoso MA. Chronic inflammation and cytokines in the tumor microenvironment. J Immunol Res. 2014;2014: 149185.
- Le Bousse-Kerdilès MC, Martyré MC. Dual implication of fibrogenic cytokines in the pathogenesis of fibrosis and myeloproliferation in myeloid metaplasia with myelofibrosis. Ann Hematol. 1999;78(10):437-44.
- Le Bousse-Kerdilès MC. Primary myelofibrosis and the "bad seeds in bad soil" concept. Fibrogenesis Tissue Repair. 2012 Jun 6;5(Suppl 1): S20.
- Legdeur MC, Beelen RH, Schuurhuis GJ, et al. A functional study on the migration of human monocytes to human leukemic cell lines and the role of monocyte chemoattractant protein-1. Leukemia. 1997;11: 1904–1908.
- Lekovic D, Gotic M, Perunicic-Jovanovic M. Contribution of comorbidities and grade of bone marrow fibrosis to the prognosis of survival in patients with primary myelofibrosis. Med Oncol. 2014; 31(3):869.
- Li X, Yao W, Yuan Y, Chen P, Li B, Li J, Chu R, Song H, Xie D, Jiang X, Wang H. Targeting of tumour-infiltrating macrophages via CCL2/CCR2 signalling as a therapeutic strategy against hepatocellular carcinoma. Gut. 2017 Jan;66(1):157-167.
- Li YS, Kolattukudy PE. Functional role of the cis-acting elements in human monocyte chemotactic protein-1 gene in the regulation of its expression by phorbol ester in human glioblastoma cells. Mol Cell Biochem. 1994 Dec 21;141(2):121-8.
- Lim SY, Yuzhalin AE, Gordon-Weeks AN, Muschel RJ. Targeting the CCL2-CCR2 signaling axis in cancer metastasis. Oncotarget. 2016;7(19):28697-710.
- Lindgren M, Samuelsson J, Nilsson L, Knutsen H, Ghanima W, Westin J, Johansson PL, Andréasson B. Genetic variation in IL28B (IFNL3) and response to interferon-alpha treatment in myeloproliferative neoplasms. Eur J Haematol. 2018;100(5):419-425.
- López-Cotarelo P, Gómez-Moreira C, Criado-García O, Sánchez L, Rodríguez-Fernández JL. Beyond Chemoattraction: Multifunctionality of Chemokine Receptors in Leukocytes. Trends Immunol. 2017;38(12):927-941.
- Lugo TG, Pendergast AM, Muller AJ, Witte ON. Tyrosine kinase activity and transformation potency of bcr-abl oncogene products. Science. 1990;247: 1079–82.
- Lussana F, Carobbio A, Salmoiraghi S, Guglielmelli P, Vannucchi AM, Bottazzi B, Leone R, Mantovani A, Barbui T, Rambaldi A. Driver mutations (JAK2V617F, MPLW515L/K or CALR), pentraxin-3 and C-reactive protein in essential thrombocythemia and polycythemia vera. J Hematol Oncol. 2017;10(1):54.
- Macanas-Pirard P, Quezada T, Navarrete L, Broekhuizen R, Leisewitz A, Nervi B, Ramírez PA. The CCL2/CCR2 Axis Affects Transmigration and Proliferation but Not Resistance to Chemotherapy of Acute Myeloid Leukemia Cells. PLoS One. 2017;12(1): e0168888.
- Malara A, Abbonante V, Zingariello M, Migliaccio A, Balduini A. Megakaryocyte Contribution to Bone Marrow Fibrosis: many Arrows in the Quiver. Mediterr J Hematol Infect Dis. 2018;10(1): e2018068.
- Mantovani A. The chemokine system: redundancy for robust outputs. Immunol. Today. 1999; 20: 254-257.

- Marty C, Lacout C, Droin N, Le Couédic JP, Ribrag V, Solary E, Vainchenker W, Villeval JL, Plo I. A role for reactive oxygen species in JAK2 V617F myeloproliferative neoplasm progression. Leukemia. 2013;27(11):2187-95.
- Masselli E, Carubbi C, Gobbi G, Mirandola P, Galli D, Martini S, Bonomini S, Crugnola M, Craviotto L, Aversa F, Vitale M. Protein kinase Cε inhibition restores megakaryocytic differentiation of hematopoietic progenitors from primary myelofibrosis patients. Leukemia. 2015;29(11):2192-201.
- Masselli E, Carubbi C, Pozzi G, Martini S, Aversa F, Galli D, Gobbi G, Mirandola P, Vitale M. Platelet expression of PKCepsilon oncoprotein in myelofibrosis is associated with disease severity and thrombotic risk. Ann Transl Med. 2017;5(13):273.
- Masselli E, Pozzi G, Carubbi C, Vitale M. The Genetic Makeup of Myeloproliferative Neoplasms: Role of Germline Variants in Defining Disease Risk, Phenotypic Diversity and Outcome. Cells. 2021;10(10):2597.
- Masselli E, Pozzi G, Gobbi G, Merighi S, Gessi S, Vitale M, Carubbi C. Cytokine Profiling in Myeloproliferative Neoplasms: Overview on Phenotype Correlation, Outcome Prediction, and Role of Genetic Variants. Cells. 2020;9(9):2136.
- McDermott DH, Yang Q, Kathiresan S, Cupples LA, Massaro JM, Keaney JF Jr, Larson MG, Vasan RS, Hirschhorn JN, O'Donnell CJ, Murphy PM, Benjamin EJ. CCL2 polymorphisms are associated with serum monocyte chemoattractant protein-1 levels and myocardial infarction in the Framingham Heart Study. Circulation. 2005;112(8):1113-20.
- McMullin MF, Anderson LA. Aetiology of Myeloproliferative Neoplasms. Cancers (Basel). 2020;12(7):1810.
- Melgarejo E, Medina MA, Sánchez-Jiménez F, Urdiales JL. Monocyte chemoattractant protein-1: a key mediator in inflammatory processes. Int J Biochem Cell Biol. 2009;41(5):998-1001.
- Mesa RA, Schwager S, Radia D, Cheville A, Hussein K, Niblack J, Pardanani AD, Steensma DP, Litzow MR, Rivera CE, Camoriano J, Verstovsek S, Sloan J, Harrison C, Kantarjian H, Tefferi A. The Myelofibrosis Symptom Assessment Form (MFSAF): an evidence-based brief inventory to measure quality of life and symptomatic response to treatment in myelofibrosis. Leuk Res. 2009;33(9):1199-203.
- Mesa RA, Verstovsek S, Cervantes F, Barosi G, Reilly JT, Dupriez B, Levine R, Le Bousse-Kerdiles MC, Wadleigh M, Campbell PJ, Silver RT, Vannucchi AM, Deeg HJ, Gisslinger H, Thomas D, Odenike O, Solberg LA, Gotlib J, Hexner E, Nimer SD, Kantarjian H, Orazi A, Vardiman JW, Thiele J, Tefferi A; International Working Group for Myelofibrosis Research and Treatment (IWG-MRT). Primary myelofibrosis (PMF), post polycythemia vera myelofibrosis (post-PV MF), post essential thrombocythemia myelofibrosis (post-ET MF), blast phase PMF (PMF-BP): Consensus on terminology by the international working group for myelofibrosis research and treatment (IWG-MRT). Leuk Res. 2007 Jun;31(6):737-40.
- Michiels JJ, De Raeve H, Berneman Z, Van Bockstaele D, Hebeda K, Lam K, Schroyens W. The 2001 World Health Organization and updated European clinical and pathological criteria for the diagnosis, classification, and staging of the Philadelphia chromosome-negative chronic myeloproliferative disorders. Semin Thromb Hemost. 2006;32(4 Pt 2):307-40.
- Migliaccio AR, Rana RA, Vannucchi AM, Manzoli FA. Role of GATA-1 in normal and neoplastic hemopoiesis. Ann N Y Acad Sci. 2005;1044: 142-58.
- Moore BB, Paine R 3rd, Christensen PJ, Moore TA, Sitterding S, Ngan R, Wilke CA, Kuziel WA, Toews GB. Protection from pulmonary fibrosis in the absence of CCR2 signaling. J Immunol. 2001;167(8):4368-77.
- Moser B, Wolf M, Walz A, Loetscher P. Chemokines: multiple levels of leukocyte migration control. Trends Immunol. 2004;25(2):75-84.
- Mui AL. The role of STATs in proliferation, differentiation, and apoptosis. Cell Mol Life Sci. 1999;55(12):1547-58.
- Nakatsumi H, Matsumoto M, Nakayama KI. Noncanonical Pathway for Regulation of CCL2 Expression by an mTORC1-FOXK1 Axis Promotes Recruitment of Tumor-Associated Macrophages. Cell Rep. 2017;21(9):2471-2486.

- Nangalia J, Massie CE, Baxter EJ, Nice FL, Gundem G, Wedge DC, Avezov E, Li J, Kollmann K, Kent DG, Aziz A, Godfrey AL, Hinton J, Martincorena I, Van Loo P, Jones AV, Guglielmelli P, Tarpey P, Harding HP, Fitzpatrick JD, Goudie CT, Ortmann CA, Loughran SJ, Raine K, Jones DR, Butler AP, Teague JW, O'Meara S, McLaren S, Bianchi M, Silber Y, Dimitropoulou D, Bloxham D, Mudie L, Maddison M, Robinson B, Keohane C, Maclean C, Hill K, Orchard K, Tauro S, Du MQ, Greaves M, Bowen D, Huntly BJP, Harrison CN, Cross NCP, Ron D, Vannucchi AM, Papaemmanuil E, Campbell PJ, Green AR. Somatic CALR mutations in myeloproliferative neoplasms with nonmutated JAK2. N Engl J Med. 2013;369(25):2391-2405.
- Nazha A, Estrov Z, Cortes J, Bueso-Ramos CE, Kantarjian H, Verstovsek S. Prognostic implications and clinical characteristics associated with bone marrow fibrosis in patients with myelofibrosis. Leuk Lymphoma. 2013; 54(11):2537-2539.
- Nelken NA, Coughlin SR, Gordon D, Wilcox JN. Monocyte chemoattractant protein-1 in human atheromatous plaques. J Clin Invest. 1991 Oct;88(4):1121-7.
- Nio Y, Yamauchi T, Iwabu M, Okada-Iwabu M, Funata M, Yamaguchi M, Ueki K, Kadowaki T. Monocyte chemoattractant protein-1 (MCP-1) deficiency enhances alternatively activated M2 macrophages and ameliorates insulin resistance and fatty liver in lipoatrophic diabetic A-ZIP transgenic mice. Diabetologia. 2012;55(12):3350-8.
- Nomiyama H, Mera A, Ohneda O, Miura R, Suda T, Yoshie O. Organization of the chemokine genes in the human and mouse major clusters of CC and CXC chemokines: diversification between the two species. Genes Immun. 2001;2(2):110-3.
- Nowell PC, Hungerford DA. Chromosome studies on normal and leukemic human leukocytes. J Natl Cancer Inst 1960;25:85–109.
- O'Hayre M, Salanga CL, Handel TM, Allen SJ. Chemokines and cancer: migration, intracellular signaling and intercellular communication in the microenvironment. Biochem J 2008; 409:635–49.
- Øbro NF, Grinfeld J, Belmonte M, Irvine M, Shepherd MS, Rao TN, Karow A, Riedel LM, Harris OB, Baxter EJ, Nangalia J, Godfrey A, Harrison CN, Li J, Skoda RC, Campbell PJ, Green AR, Kent DG. Longitudinal Cytokine Profiling Identifies GRO-α and EGF as Potential Biomarkers of Disease Progression in Essential Thrombocythemia. Hemasphere. 2020;4(3): e371.
- O'Connor T, Borsig L, Heikenwalder M. CCL2-CCR2 Signaling in Disease Pathogenesis. Endocr Metab Immune Disord Drug Targets. 2015;15(2):105-18.
- Oddsson A, Kristinsson SY, Helgason H, Gudbjartsson DF, Masson G, Sigurdsson A, Jonasdottir A, Jonasdottir A, Steingrimsdottir H, Vidarsson B, Reykdal S, Eyjolfsson GI, Olafsson I, Onundarson PT, Runarsson G, Sigurdardottir O, Kong A, Rafnar T, Sulem P, Thorsteinsdottir U, Stefansson K. The germline sequence variant rs2736100_C in TERT associates with myeloproliferative neoplasms. Leukemia. 2014;28(6):1371-4.
- Ortmann CA, Kent DG, Nangalia J, Silber Y, Wedge DC, Grinfeld J, Baxter EJ, Massie CE, Papaemmanuil E, Menon S, Godfrey AL, Dimitropoulou D, Guglielmelli P, Bellosillo B, Besses C, Döhner K, Harrison CN, Vassiliou GS, Vannucchi A, Campbell PJ, Green AR. Effect of mutation order on myeloproliferative neoplasms. N Engl J Med. 2015;372(7):601-612.
- Panteli KE, Hatzimichael EC, Bouranta PK, Katsaraki A, Seferiadis K, Stebbing J, Bourantas KL. Serum interleukin (IL)-1, IL-2, sIL-2Ra, IL-6 and thrombopoietin levels in patients with chronic myeloproliferative diseases. Br J Haematol. 2005;130(5):709-15.
- Papadantonakis N, Matsuura S, Ravid K. Megakaryocyte pathology and bone marrow fibrosis: the lysyl oxidase connection. Blood 2012; 120: 1774–1781.
- Parashar Y, Kushwaha R, Kumar A, Agarwal K, Singh US, Jain M, Verma SP, Tripathi AK. Haemostatic Profile in Patients of Myeloproliferative Neoplasms-A Tertiary Care Centre Experience. J Clin Diagn Res. 2016;10(11):EC01-EC04.
- Pardanani A, Begna K, Finke C, Lasho T, Tefferi A. Circulating levels of MCP-1, sIL-2R, IL-15, and IL-8 predict anemia response to pomalidomide therapy in myelofibrosis. Am J Hematol. 2011 Apr;86(4):343-5.
- Pardanani A, Lasho TL, Finke CM, Mai M, McClure RF, Tefferi A. IDH1 and IDH2 mutation analysis in chronic- and blast-phase myeloproliferative neoplasms. Leukemia. 2010;24(6):1146-51.

- Pardanani AD, Levine RL, Lasho T, Pikman Y, Mesa RA, Wadleigh M, Steensma DP, Elliott MA, Wolanskyj AP, Hogan WJ, McClure RF, Litzow MR, Gilliland DG, Tefferi A. MPL515 mutations in myeloproliferative and other myeloid disorders: a study of 1182 patients. Blood. 2006;108(10):3472-6.
- Passamonti F, Cervantes F, Vannucchi AM, Morra E, Rumi E, Pereira A, Guglielmelli P, Pungolino E, Caramella M, Maffioli M, Pascutto C, Lazzarino M, Cazzola M, Tefferi A. A dynamic prognostic model to predict survival in primary myelofibrosis: a study by the IWG-MRT (International Working Group for Myeloproliferative Neoplasms Research and Treatment). Blood. 2010;115(9):1703-8.
- Passamonti F, Elena C, Schnittger S, Skoda RC, Green AR, Girodon F, Kiladjian JJ, McMullin MF, Ruggeri M, Besses C, Vannucchi AM, Lippert E, Gisslinger H, Rumi E, Lehmann T, Ortmann CA, Pietra D, Pascutto C, Haferlach T, Cazzola M. Molecular and clinical features of the myeloproliferative neoplasm associated with JAK2 exon 12 mutations. Blood. 2011;117(10):2813-6.
- Pham MH, Bonello GB, Castiblanco J, Le T, Sigala J, He W, Mummidi S. The rs1024611 regulatory region polymorphism is associated with CCL2 allelic expression imbalance. PLoS One. 2012;7(11): e49498.
- Pikman Y, Lee BH, Mercher T, McDowell E, Ebert BL, Gozo M, Cuker A, Wernig G, Moore S, Galinsky I, DeAngelo DJ, Clark JJ, Lee SJ, Golub TR, Wadleigh M, Gilliland DG, Levine RL. MPLW515L is a novel somatic activating mutation in myelofibrosis with myeloid metaplasia. PLoS Med. 2006;3(7): e270.
- Pilling D, Fan T, Huang D, Kaul B, Gomer RH. Identification of markers that distinguish monocyte-derived fibrocytes from monocytes, macrophages, and fibroblasts. PLoS One. 2009;4(10): e7475.
- Ping D, Jones PL, Boss JM. TNF regulates the in vivo occupancy of both distal and proximal regulatory regions of the MCP-1/JE gene. Immunity. 1996;4(5):455-69.
- Pizzi M, Silver RT, Barel A, Orazi A. Recombinant interferon-alpha in myelofibrosis reduces bone marrow fibrosis, improves its morphology and is associated with clinical response. Mod Pathol. 2015; 28: 1315–1323.
- Poletto V, Rosti V, Villani L, Catarsi P, Carolei A, Campanelli R, Massa M, Martinetti M, Viarengo G, Malovini A, Migliaccio AR, Barosi G. A3669G polymorphism of glucocorticoid receptor is a susceptibility allele for primary myelofibrosis and contributes to phenotypic diversity and blast transformation. Blood. 2012;120(15):3112-7.
- Pourcelot E, Trocme C, Mondet J, Bailly S, Toussaint B, Mossuz P. Cytokine profiles in polycythemia vera and essential thrombocythemia patients: clinical implications. Exp Hematol. 2014;42(5):360-8.
- Pritchard MA, Baker E, Callen DF, Sutherland GR, Wilks AF. Two members of the JAK family of protein tyrosine kinases map to chromosomes 1p31.3 and 9p24. Mamm Genome. 1992;3: 36–8.
- Proudfoot AE, Handel TM, Johnson Z, Lau EK, LiWang P, Clark-Lewis I, Borlat F, Wells TN, Kosco-Vilbois MH. Glycosaminoglycan binding and oligomerization are essential for the in vivo activity of certain chemokines. Proc Natl Acad Sci U S A. 2003;100(4):1885-90.
- Qian BZ, Li J, Zhang H, Kitamura T, Zhang J, Campion LR, Kaiser EA, Snyder LA, Pollard JW. CCL2 recruits inflammatory monocytes to facilitate breast-tumour metastasis. Nature. 2011;475(7355):222-5.
- Quivoron C, Couronné L, Della Valle V, Lopez CK, Plo I, Wagner-Ballon O, Do Cruzeiro M, Delhommeau F, Arnulf B, Stern MH, Godley L, Opolon P, Tilly H, Solary E, Duffourd Y, Dessen P, Merle-Beral H, Nguyen-Khac F, Fontenay M, Vainchenker W, Bastard C, Mercher T, Bernard OA. TET2 inactivation results in pleiotropic hematopoietic abnormalities in mouse and is a recurrent event during human lymphomagenesis. Cancer Cell. 2011;20(1):25-38.
- Raghu G, Martinez FJ, Brown KK, Costabel U, Cottin V, Wells AU, Lancaster L, Gibson KF, Haddad T, Agarwal P, Mack M, Dasgupta B, Nnane IP, Flavin SK, Barnathan ES. CC-chemokine ligand 2 inhibition in idiopathic pulmonary fibrosis: a phase 2 trial of carlumab. Eur Respir J. 2015;46(6):1740-50.
- Rampal R, Ahn J, Abdel-Wahab O, Nahas M, Wang K, Lipson D, Otto GA, Yelensky R, Hricik T, McKenney AS, Chiosis G, Chung YR, Pandey S, van den Brink MR, Armstrong SA, Dogan A,

Intlekofer A, Manshouri T, Park CY, Verstovsek S, Rapaport F, Stephens PJ, Miller VA, Levine RL. Genomic and functional analysis of leukemic transformation of myeloproliferative neoplasms. Proc Natl Acad Sci U S A. 2014;111(50): E5401-10.

- Rampal R, Al-Shahrour F, Abdel-Wahab O, Patel JP, Brunel JP, Mermel CH, Bass AJ, Pretz J, Ahn J, Hricik T, Kilpivaara O, Wadleigh M, Busque L, Gilliland DG, Golub TR, Ebert BL, Levine RL. Integrated genomic analysis illustrates the central role of JAK-STAT pathway activation in myeloproliferative neoplasm pathogenesis. Blood. 2014;123(22): e123-33.
- Roca H, Varsos Z, Pienta KJ. CCL2 protects prostate cancer PC3 cells from autophagic death via phosphatidylinositol 3-kinase/AKT-dependent survivin up-regulation. J Biol Chem. 2008; 283(36):25057-73.
- Rollins BJ, Stier P, Ernst T, Wong GG. The human homolog of the JE gene encodes a monocyte secretory protein. Mol Cell Biol. 1989;9(11):4687-95.
- Rollins BJ. Chemokines. Blood. 1997;90(3):909-28.
- Rovin BH, Lu L, Saxena R. A novel polymorphism in the MCP-1 gene regulatory region that influences MCP-1 expression. Biochem Biophys Res Commun. 1999;259: 344–8.
- Rudd MF, Sellick GS, Webb EL, Catovsky D, Houlston RS. Variants in the ATM-BRCA2-CHEK2 axis predispose to chronic lymphocytic leukemia. Blood. 2006;108(2):638-44.
- Rumi E, Cazzola M. Diagnosis, risk stratification, and response evaluation in classical myeloproliferative neoplasms. Blood. 2017;129(6):680-692.
- Rumi E, Passamonti F, Della Porta MG, Elena C, Arcaini L, Vanelli L, Del Curto C, Pietra D, Boveri E, Pascutto C, Cazzola M, Lazzarino M. Familial chronic myeloproliferative disorders: clinical phenotype and evidence of disease anticipation. J Clin Oncol. 2007;25(35):5630-5.
- Rumi E, Pietra D, Ferretti V, Klampfl T, Harutyunyan AS, Milosevic JD, Them NC, Berg T, Elena C, Casetti IC, Milanesi C, Sant'antonio E, Bellini M, Fugazza E, Renna MC, Boveri E, Astori C, Pascutto C, Kralovics R, Cazzola M; Associazione Italiana per la Ricerca sul Cancro Gruppo Italiano Malattie Mieloproliferative Investigators. JAK2 or CALR mutation status defines subtypes of essential thrombocythemia with substantially different clinical course and outcomes. Blood. 2014;123(10):1544-51.
- Rumi E, Pietra D, Guglielmelli P, Bordoni R, Casetti I, Milanesi C, Sant'Antonio E, Ferretti V, Pancrazzi A, Rotunno G, Severgnini M, Pietrelli A, Astori C, Fugazza E, Pascutto C, Boveri E, Passamonti F, De Bellis G, Vannucchi A, Cazzola M; Associazione Italiana per la Ricerca sul Cancro Gruppo Italiano Malattie Mieloproliferative. Acquired copy-neutral loss of heterozygosity of chromosome 1p as a molecular event associated with marrow fibrosis in MPL-mutated myeloproliferative neoplasms. Blood. 2013;121(21):4388-95.
- Rumi E, Pietra D, Pascutto C, Guglielmelli P, Martínez-Trillos A, Casetti I, Colomer D, Pieri L, Pratcorona M, Rotunno G, Sant'Antonio E, Bellini M, Cavalloni C, Mannarelli C, Milanesi C, Boveri E, Ferretti V, Astori C, Rosti V, Cervantes F, Barosi G, Vannucchi AM, Cazzola M; Associazione Italiana per la Ricerca sul Cancro Gruppo Italiano Malattie Mieloproliferative Investigators. Clinical effect of driver mutations of JAK2, CALR, or MPL in primary myelofibrosis. Blood. 2014;124(7):1062-9.
- Saint-Martin C, Leroy G, Delhommeau F, Panelatti G, Dupont S, James C, Plo I, Bordessoule D, Chomienne C, Delannoy A, Devidas A, Gardembas-Pain M, Isnard F, Plumelle Y, Bernard O, Vainchenker W, Najman A, Bellanné-Chantelot C; French Group of Familial Myeloproliferative Disorders. Analysis of the ten-eleven translocation 2 (TET2) gene in familial myeloproliferative neoplasms. Blood. 2009;114(8):1628-32.
- Sanford DE, Belt BA, Panni RZ, Mayer A, Deshpande AD, Carpenter D, Mitchem JB, Plambeck-Suess SM, Worley LA, Goetz BD, Wang-Gillam A, Eberlein TJ, Denardo DG, Goedegebuure SP, Linehan DC. Inflammatory monocyte mobilization decreases patient survival in pancreatic cancer: a role for targeting the CCL2/CCR2 axis. Clin Cancer Res. 2013;19(13):3404-15.
- Sangiorgio VFI, Nam A, Chen Z, Orazi A, Tam W. GATA1 downregulation in prefibrotic and fibrotic stages of primary myelofibrosis and in the myelofibrotic progression of other myeloproliferative neoplasms. Leuk Res. 2021;100: 106495.

- Sankaran VG, Menne TF, Šćepanović D, Vergilio JA, Ji P, Kim J, Thiru P, Orkin SH, Lander ES, Lodish HF. MicroRNA-15a and -16-1 act via MYB to elevate fetal hemoglobin expression in human trisomy 13. Proc Natl Acad Sci USA. 2011;108(4):1519-24.
- Savage SA, Alter BP. Dyskeratosis congenita. Hematol Oncol Clin North Am. 2009;23(2):215-31.
- Scherber RM, Geyer HL, Mesa RA. Quality of life in MPN comes of age as a therapeutic target. Curr Hematol Malig Rep. 2014;9(4):324-30.
- Scott LM, Tong W, Levine RL, Scott MA, Beer PA, Stratton MR, Futreal PA, Erber WN, McMullin MF, Harrison CN, Warren AJ, Gilliland DG, Lodish HF, Green AR. JAK2 exon 12 mutations in polycythemia vera and idiopathic erythrocytosis. N Engl J Med. 2007;356(5):459-68.
- Scott LM, Tong W, Levine RL, Scott MA, Beer PA, Stratton MR, Futreal PA, Erber WN, McMullin MF, Harrison CN, Warren AJ, Gilliland DG, Lodish HF, Green AR. JAK2 exon 12 mutations in polycythemia vera and idiopathic erythrocytosis. N Engl J Med. 2007;356(5):459-68.
- Seki E, de Minicis S, Inokuchi S, Taura K, Miyai K, van Rooijen N, Schwabe RF, Brenner DA. CCR2 promotes hepatic fibrosis in mice. Hepatology. 2009;50(1):185-97.
- Shallis RM, Wang R, Davidoff A, Ma X, Podoltsev NA, Zeidan AM. Epidemiology of the classical myeloproliferative neoplasms: The four corners of an expansive and complex map. Blood Rev. 2020;42: 100706.
- Shepherd R, Cheung AS, Pang K, Saffery R, Novakovic B. Sexual Dimorphism in Innate Immunity: The Role of Sex Hormones and Epigenetics. Front Immunol. 2021;11: 604000.
- Shuai K, Liu B. Regulation of JAK-STAT signalling in the immune system. Nat Rev Immunol. 2003;3(11):900-11.
- Silvennoinen O, Hubbard SR. Molecular insights into regulation of JAK2 in myeloproliferative neoplasms. Blood. 2015;125(22):3388-92.
- Silvennoinen O, Ungureanu D, Niranjan Y, Hammaren H, Bandaranayake R, Hubbard SR. New insights into the structure and function of the pseudokinase domain in JAK2. Biochem Soc Trans. 2013;41(4):1002-7.
- Skoda RC, Duek A, Grisouard J. Pathogenesis of myeloproliferative neoplasms. Exp Hematol. 2015;43(8):599-608.
- Skov V, Larsen TS, Thomassen M, Riley CH, Jensen MK, Bjerrum OW, Kruse TA, Hasselbalch HC. Molecular profiling of peripheral blood cells from patients with polycythemia vera and related neoplasms: identification of deregulated genes of significance for inflammation and immune surveillance. Leuk Res. 2012;36(11):1387-92.
- Soranzo N, Spector TD, Mangino M, Kühnel B, Rendon A, Teumer A, Willenborg C, Wright B, Chen L, Li M, Salo P, Voight BF, Burns P, Laskowski RA, Xue Y, Menzel S, Altshuler D, Bradley JR, Bumpstead S, Burnett MS, Devaney J, Döring A, Elosua R, Epstein SE, Erber W, Falchi M, Garner SF, Ghori MJ, Goodall AH, Gwilliam R, Hakonarson HH, Hall AS, Hammond N, Hengstenberg C, Illig T, König IR, Knouff CW, McPherson R, Melander O, Mooser V, Nauck M, Nieminen MS, O'Donnell CJ, Peltonen L, Potter SC, Prokisch H, Rader DJ, Rice CM, Roberts R, Salomaa V, Sambrook J, Schreiber S, Schunkert H, Schwartz SM, Serbanovic-Canic J, Sinisalo J, Siscovick DS, Stark K, Surakka I, Stephens J, Thompson JR, Völker U, Völzke H, Watkins NA, Wells GA, Wichmann HE, Van Heel DA, Tyler-Smith C, Thein SL, Kathiresan S, Perola M, Reilly MP, Stewart AF, Erdmann J, Samani NJ, Meisinger C, Greinacher A, Deloukas P, Ouwehand WH, Gieger C. A genome-wide meta-analysis identifies 22 loci associated with eight hematological parameters in the HaemGen consortium. Nat Genet. 2009;41(11):1182-90.
- Spangrude GJ, Lewandowski D, Martelli F, Marra M, Zingariello M, Sancillo L, Rana RA, Migliaccio AR. P-Selectin Sustains Extramedullary Hematopoiesis in the Gata1 low Model of Myelofibrosis. Stem Cells. 2016;34(1):67-82.
- Stadhouders R, Aktuna S, Thongjuea S, Aghajanirefah A, Pourfarzad F, van Ijcken W, Lenhard B, Rooks H, Best S, Menzel S, Grosveld F, Thein SL, Soler E. HBS1L-MYB intergenic variants modulate fetal hemoglobin via long-range MYB enhancers. J Clin Invest. 2014;124(4):1699-710.

- Stankovic A, Slavic V, Stamenkovic B, Kamenov B, Bojanovic M, Mitrovic DR. Serum and synovial fluid concentrations of CCL2 (MCP-1) chemokine in patients suffering rheumatoid arthritis and osteoarthritis reflect disease activity. Bratisl Lek Listy. 2009;110(10):641-6.
- Stegelmann F, Bullinger L, Schlenk RF, Paschka P, Griesshammer M, Blersch C, Kuhn S, Schauer S, Döhner H, Döhner K. DNMT3A mutations in myeloproliferative neoplasms. Leukemia. 2011;25(7):1217-9.
- Suga M, Iyonaga K, Ichiyasu H, Saita N, Yamasaki H, Ando M. Clinical significance of MCP-1 levels in BALF and serum in patients with interstitial lung diseases. Eur Respir J. 1999;14(2):376-82.
- Swierczek SI, Yoon D, Bellanné-Chantelot C, Kim SJ, Saint-Martin C, Delhommeau F, Najman A, Prchal JT. Extent of hematopoietic involvement by TET2 mutations in JAK2V^{617}F polycythemia vera. Haematologica. 2011;96(5):775-8.
- Szuber N, Tefferi A. Driver mutations in primary myelofibrosis and their implications. Curr Opin Hematol. 2018;25(2):129-135.
- Tapper W, Jones AV, Kralovics R, Harutyunyan AS, Zoi K, Leung W, Godfrey AL, Guglielmelli P, Callaway A, Ward D, Aranaz P, White HE, Waghorn K, Lin F, Chase A, Baxter EJ, Maclean C, Nangalia J, Chen E, Evans P, Short M, Jack A, Wallis L, Oscier D, Duncombe AS, Schuh A, Mead AJ, Griffiths M, Ewing J, Gale RE, Schnittger S, Haferlach T, Stegelmann F, Döhner K, Grallert H, Strauch K, Tanaka T, Bandinelli S, Giannopoulos A, Pieri L, Mannarelli C, Gisslinger H, Barosi G, Cazzola M, Reiter A, Harrison C, Campbell P, Green AR, Vannucchi A, Cross NC. Genetic variation at MECOM, TERT, JAK2 and HBS1L-MYB predisposes to myeloproliferative neoplasms. Nat Commun. 201;6: 6691.
- Tashi T, Swierczek S, Prchal JT. Familial MPN Predisposition. Curr Hematol Malig Rep. 2017;12(5):442-447.
- Tefferi A, Barbui T. Polycythemia vera and essential thrombocythemia: 2017 update on diagnosis, risk-stratification, and management. Am J Hematol. 2017;92(1):94-108.
- Tefferi A, Guglielmelli P, Lasho TL, Rotunno G, Finke C, Mannarelli C, Belachew AA, Pancrazzi A, Wassie EA, Ketterling RP, Hanson CA, Pardanani A, Vannucchi AM. CALR and ASXL1 mutations-based molecular prognostication in primary myelofibrosis: an international study of 570 patients. Leukemia. 2014;28(7):1494-500.
- Tefferi A, Guglielmelli P, Nicolosi M, Mannelli F, Mudireddy M, Bartalucci N, Finke CM, Lasho TL, Hanson CA, Ketterling RP, Begna KH, Naseema Gangat, Pardanani A, Vannucchi AM. GIPSS: genetically inspired prognostic scoring system for primary myelofibrosis. Leukemia. 2018;32(7):1631-1642.
- Tefferi A, Lasho TL, Finke CM, Knudson RA, Ketterling R, Hanson CH, Maffioli M, Caramazza D, Passamonti F, Pardanani A. CALR vs JAK2 vs MPL-mutated or triple-negative myelofibrosis: clinical, cytogenetic and molecular comparisons. Leukemia. 2014;28(7):1472-7.
- Tefferi A, Lasho TL, Mudireddy M, Finke CM, Hanson CA, Ketterling RP, Gangat N, Pardanani A. The germline JAK2 GGCC (46/1) haplotype and survival among 414 molecularly-annotated patients with primary myelofibrosis. Am J Hematol. 2019;94(3):299-305.
- Tefferi A, Lasho TL, Patnaik MM, Finke CM, Hussein K, Hogan WJ, Elliott MA, Litzow MR, Hanson CA, Pardanani A. JAK2 germline genetic variation affects disease susceptibility in primary myelofibrosis regardless of V617F mutational status: nullizygosity for the JAK2 46/1 haplotype is associated with inferior survival. Leukemia. 2010;24(1):105-9.
- Tefferi A, Pardanani A, Lim KH, Abdel-Wahab O, Lasho TL, Patel J, Gangat N, Finke CM, Schwager S, Mullally A, Li CY, Hanson CA, Mesa R, Bernard O, Delhommeau F, Vainchenker W, Gilliland DG, Levine RL. TET2 mutations and their clinical correlates in polycythemia vera, essential thrombocythemia and myelofibrosis. Leukemia. 2009;23(5):905-11.
- Tefferi A, Pardanani A. Myeloproliferative Neoplasms: A Contemporary Review. JAMA SEP Oncol. 2015;1(1):97–105.
- Tefferi A, Siragusa S, Hussein K, Schwager SM, Hanson CA, Pardanani A, Cervantes F, Passamonti F. Transfusion-dependency at presentation and its acquisition in the first year of

diagnosis are both equally detrimental for survival in primary myelofibrosis--prognostic relevance is independent of IPSS or karyotype. Am J Hematol. 2010;85(1):14-7.

- Tefferi A, Vaidya R, Caramazza D, Finke C, Lasho T, Pardanani A. Circulating interleukin (IL)-8, IL-2R, IL-12, and IL-15 levels are independently prognostic in primary myelofibrosis: a comprehensive cytokine profiling study. J Clin Oncol. 2011;29(10):1356-63.
- Tefferi A. JAK inhibitors for myeloproliferative neoplasms: clarifying facts frommyths. Blood. 2012;119(12):2721-2730.
- Tefferi A. Myelofibrosis with Myeloid Metaplasia. N Engl J Med 2000;342: 1255–1265.
- Tefferi A. Primary myelofibrosis: 2019 update on diagnosis, risk-stratification, and management. Am J Hematol. 2018;93(12):1551-1560.
- Tefferi A: Novel mutations and their func- tional and clinical relevance in myeloprolif- erative neoplasms: JAK2, MPL, TET2, ASXL1, CBL, IDH and IKZF1. Leukemia 2010;24: 1128-1138.
- Thiele J, Kvasnicka HM, Diehl V. Standardization of bone marrow features—does it work in hematopathology for histological discrimination of different disease patterns? Histol Histopathol. 2005; 20: 633–644.
- Thiele J, Kvasnicka HM, Facchetti F, Franco V, van der Walt J, Orazi A. European consensus on grading bone marrow fibrosis and assessment of cellularity. Haematologica. 2005; 90: 1128–1132.
- Thiele J. Philadelphia chromosome-negative chronic myeloproliferative disease. Am J Clin Pathol. 2009;132(2):261-80.
- Thompson CAH, Wong JMY. Non-canonical Functions of Telomerase Reverse Transcriptase: Emerging Roles and Biological Relevance. Curr Top Med Chem. 2020;20(6):498-507.
- Timmers HT, Pronk GJ, Bos JL, van der Eb AJ. Analysis of the rat JE gene promoter identifies an AP-1 binding site essential for basal expression but not for TPA induction. Nucleic Acids Res. 1990;18(1):23-34.
- Titmarsh GJ, Duncombe AS, McMullin MF, O'Rorke M, Mesa R, De Vocht F, Horan S, Fritschi L, Clarke M, Anderson LA. How common are myeloproliferative neoplasms? A systematic review and meta-analysis. Am J Hematol. 2014;89(6):581-7.
- Trifa AP, Bănescu C, Bojan AS, Voina CM, Popa Ș, Vișan S, Ciubean AD, Tripon F, Dima D, Popov VM, Vesa ȘC, Andreescu M, Török-Vistai T, Mihăilă RG, Berbec N, Macarie I, Coliță A, Iordache M, Cătană AC, Farcaș MF, Tomuleasa C, Vasile K, Truică C, Todincă A, Pop-Muntean L, Manolache R, Bumbea H, Vlădăreanu AM, Gaman M, Ciufu CM, Popp RA. MECOM, HBS1L-MYB, THRB-RARB, JAK2, and TERT polymorphisms defining the genetic predisposition to myeloproliferative neoplasms: A study on 939 patients. Am J Hematol. 2018;93(1):100-106.
- Tripathi DK, Poluri KM. Molecular insights into kinase mediated signaling pathways of chemokines and their cognate G protein coupled receptors. Front Biosci (Landmark Ed). 2020; 25:1361-1385.
- Tsuruta-Kishino T, Koya J, Kataoka K, Narukawa K, Sumitomo Y, Kobayashi H, Sato T, Kurokawa M. Loss of p53 induces leukemic transformation in a murine model of Jak2 V617F-driven polycythemia vera. Oncogene. 2017;36(23):3300-3311.
- Ueda A, Ishigatsubo Y, Okubo T, Yoshimura T. Transcriptional regulation of the human monocyte chemoattractant protein-1 gene. Cooperation of two NF-kappaB sites and NF-kappaB/Rel subunit specificity. J Biol Chem. 1997;272(49):31092-9.
- Vaidya R, Gangat N, Jimma T, Finke CM, Lasho TL, Pardanani A, Tefferi A. Plasma cytokines in polycythemia vera: phenotypic correlates, prognostic relevance, and comparison with myelofibrosis. Am J Hematol. 2012;87(11):1003-5.
- Vainchenker W, Constantinescu SN. JAK/STAT signaling in hematological malignancies. Oncogene. 2013;32(21):2601-13.
- Vainchenker W, Delhommeau F, Constantinescu SN, Bernard OA. New mutations and pathogenesis of myeloproliferative neoplasms. Blood. 2011;118(7):1723-35.
- Vainchenker W, Kralovics R. Genetic basis and molecular pathophysiology of classical myeloproliferative neoplasms. Blood. 2017;129(6):667-679.

- Van Coillie E, Van Damme J, Opdenakker G. The MCP/eotaxin subfamily of CC chemokines. Cytokine Growth Factor Rev 1999;10:61–86.
- Vande Broek I, Asosingh K, Vanderkerken K, Straetmans N, Van Camp B, Van Riet I. Chemokine receptor CCR2 is expressed by human multiple myeloma cells and mediates migration to bone marrow stromal cell-produced monocyte chemotactic proteins MCP-1, -2 and -3. Br J Cancer. 2003;88(6):855-62.
- Vannucchi AM, Bianchi L, Cellai C, Paoletti F, Rana RA, Lorenzini R, Migliaccio G, Migliaccio AR. Development of myelofibrosis in mice genetically impaired for GATA-1 expression (GATA-1(low) mice). Blood. 2002;100(4):1123-32.
- Vannucchi AM, Lasho TL, Guglielmelli P, Biamonte F, Pardanani A, Pereira A, Finke C, Score J, Gangat N, Mannarelli C, Ketterling RP, Rotunno G, Knudson RA, Susini MC, Laborde RR, Spolverini A, Pancrazzi A, Pieri L, Manfredini R, Tagliafico E, Zini R, Jones A, Zoi K, Reiter A, Duncombe A, Pietra D, Rumi E, Cervantes F, Barosi G, Cazzola M, Cross NC, Tefferi A. Mutations and prognosis in primary myelofibrosis. Leukemia. 2013;27(9):1861-9.
- Vannucchi AM, Lasho TL, Guglielmelli P, Biamonte F, Pardanani A, Pereira A, Finke C, Score J, Gangat N, Mannarelli C, Ketterling RP, Rotunno G, Knudson RA, Susini MC, Laborde RR, Spolverini A, Pancrazzi A, Pieri L, Manfredini R, Tagliafico E, Zini R, Jones A, Zoi K, Reiter A, Duncombe A, Pietra D, Rumi E, Cervantes F, Barosi G, Cazzola M, Cross NC, Tefferi A. Mutations and prognosis in primary myelofibrosis. Leukemia. 2013 Sep;27(9):1861-9.
- Vannucchi AM, Migliaccio AR, Paoletti F, Chagraoui H, Wendling F. Pathogenesis of myelofibrosis with myeloid metaplasia: lessons from mouse models of the disease. Semin Oncol. 2005;32(4):365-72.
- Vannucchi AM, Pancrazzi A, Guglielmelli P, Di Lollo S, Bogani C, Baroni G, Bianchi L, Migliaccio AR, Bosi A, Paoletti F. Abnormalities of GATA-1 in megakaryocytes from patients with idiopathic myelofibrosis. Am J Pathol. 2005;167(3):849-58.
- Varricchio L, Masselli E, Alfani E, Battistini A, Migliaccio G, Vannucchi AM, Zhang W, Rondelli D, Godbold J, Ghinassi B, Whitsett C, Hoffman R, Migliaccio AR. The dominant negative β isoform of the glucocorticoid receptor is uniquely expressed in erythroid cells expanded from polycythemia vera patients. Blood. 2011;118(2):425-36.
- Varricchio L, Migliaccio AR. The role of glucocorticoid receptor (GR) polymorphisms in human erythropoiesis. Am J Blood Res. 2014;4(2):53-72.
- Verstovsek S, Kantarjian H, Mesa RA, Pardanani AD, Cortes-Franco J, Thomas DA et al. Safety and efficacy of INCB018424, a JAK1 and JAK2 inhibitor, in myelofibrosis. N Engl J Med 2010; 363: 1117–1127.
- Wang F, Fu P, Pang Y, Liu C, Shao Z, Zhu J, Li J, Wang T, Zhang X, Liu J. TERT rs2736100T/G polymorphism upregulates interleukin 6 expression in non-small cell lung cancer especially in adenocarcinoma. Tumour Biol. 2014;35(5):4667-72.
- Werle M, Schmal U, Hanna K, Kreuzer J. MCP-1 induces activation of MAP-kinases ERK, JNK and p38 MAPK in human endothelial cells. Cardiovasc Res. 2002;56(2):284-92.
- Wong WJ, Baltay M, Getz A, Fuhrman K, Aster JC, Hasserjian RP, Pozdnyakova O. Gene expression profiling distinguishes prefibrotic from overtly fibrotic myeloproliferative neoplasms and identifies disease subsets with distinct inflammatory signatures. PLoS One. 2019;14(5):e0216810.
- Wu VY, Walz DA, McCoy LE. Purification and characterization of human and bovine platelet factor 4. Prep Biochem. 1977;7(6):479-93.
- Xu M, Bruno E, Chao J, Huang S, Finazzi G, Fruchtman SM, Popat U, Prchal JT, Barosi G, Hoffman R; MPD Research Consortium. Constitutive mobilization of CD34+ cells into the peripheral blood in idiopathic myelofibrosis may be due to the action of a number of proteases. Blood. 2005;105(11):4508-15.
- Xu N, Lao Y, Zhang Y, Gillespie DA. Akt: a double-edged sword in cell proliferation and genome stability. J Oncol. 2012;2012: 951724.

- Xue M, Guo Z, Cai C, Sun B, Wang H. Evaluation of the Diagnostic Efficacies of Serological Markers KL-6, SP-A, SP-D, CCL2, and CXCL13 in Idiopathic Interstitial Pneumonia. Respiration. 2019;98(6):534-545.
- Yamamoto K, Takeshima H, Hamada K, Nakao M, Kino T, Nishi T, Kochi M, Kuratsu J, Yoshimura T, Ushio Y. Cloning and functional characterization of the 5'-flanking region of the human monocyte chemoattractant protein-1 receptor (CCR2) gene. Essential role of 5'-untranslated region in tissue-specific expression. J Biol Chem. 1999;274(8):4646-54.
- Yamaoka A, Suzuki M, Katayama S, Orihara D, Engel JD, Yamamoto M. EVI1 and GATA2 misexpression induced by inv(3)(q21q26) contribute to megakaryocyte-lineage skewing and leukemogenesis. Blood Adv. 2020;4(8):1722-1736.
- Yamazaki H, Suzuki M, Otsuki A, Shimizu R, Bresnick EH, Engel JD, Yamamoto M. A remote GATA2 hematopoietic enhancer drives leukemogenesis in inv(3)(q21;q26) by activating EVI1 expression. Cancer Cell. 2014;25(4):415-27.
- Yang C, Przyborski S, Cooke MJ, Zhang X, Stewart R, Anyfantis G, Atkinson SP, Saretzki G, Armstrong L, Lako M. A key role for telomerase reverse transcriptase unit in modulating human embryonic stem cell proliferation, cell cycle dynamics, and in vitro differentiation. Stem Cells. 2008;26(4):850-63.
- Yoshimura T, Robinson EA, Tanaka S, Appella E, Leonard EJ. Purification and amino acid analysis of two human monocyte chemoattractants produced by phytohemagglutinin-stimulated human blood mononuclear leukocytes. J Immunol. 1989;142(6):1956-62.
- Zahr AA, Salama ME, Carreau N, Tremblay D, Verstovsek S, Mesa R, Hoffman R, Mascarenhas J. Bone marrow fibrosis in myelofibrosis: pathogenesis, prognosis and targeted strategies. Haematologica. 2016;101(6):660-71.
- Zhao W, Du Y, Ho WT, Fu X, Zhao ZJ. JAK2V617F and p53 mutations coexist in erythroleukemia and megakaryoblastic leukemic cell lines. Exp Hematol Oncol. 2012;1(1):15.
- Zhou J, Cidlowski JA. The human glucocorticoid receptor: one gene, multiple proteins and diverse responses. Steroids. 2005;70(5-7):407-17.
- Zhou YJ, Chen M, Cusack NA, Kimmel LH, Magnuson KS, Boyd JG, Lin W, Roberts JL, Lengi A, Buckley RH, Geahlen RL, Candotti F, Gadina M, Changelian PS, O'Shea JJ. Unexpected effects of FERM domain mutations on catalytic activity of Jak3: structural implication for Janus kinases. Mol Cell. 2001;8(5):959-69.
- Zingariello M, Martelli F, Ciaffoni F, Masiello F, Ghinassi B, D'Amore E, Massa M, Barosi G, Sancillo L, Li X, Goldberg JD, Rana RA, Migliaccio AR. Characterization of the TGF-β1 signaling abnormalities in the Gata1low mouse model of myelofibrosis. Blood. 2013;121(17):3345-63
- Zingariello M, Martelli F, Verachi P, Bardelli C, Gobbo F, Mazzarini M, Migliaccio AR. Novel targets to cure primary myelofibrosis from studies on Gata1^{low} mice. IUBMB Life. 2020;72(1):131-141.
- Zingariello M, Ruggeri A, Martelli F, Marra M, Sancillo L, Ceglia I, Rana RA, Migliaccio AR. A novel interaction between megakaryocytes and activated fibrocytes increases TGF-β bioavailability in the Gata1(low) mouse model of myelofibrosis. Am J Blood Res. 2015;5(2):34-61.